ZooKeys 909: 1–24 (2020)
doi: 10.3897/zookeys.909.35278
http://zookeys.pensoft.net

RESEARCH ARTICLE

A peer-reviewed open-access journal
ZooKeys
Launched to accelerate biodiversity research

Phestilla subodiosus sp. nov. (Nudibranchia, Trinchesiidae), a corallivorous pest species in the aquarium trade

Adam Wang[1], Inga Elizabeth Conti-Jerpe[2,3], John Lawrence Richards[3], David Michael Baker[2,3]

1 *Chinese International School, Hau Yuen Path, Braemar Hill, Hong Kong SAR* **2** *Swire Institute of Marine Science, School of Biological Sciences, The University of Hong Kong, Pok Fu Lam Road, Hong Kong SAR* **3** *School of Biological Sciences, University of Hong Kong, Pok Fu Lam Road, Hong Kong SAR*

Corresponding author: *David Michael Baker* (dmbaker@hku.hk)

Academic editor: *N. Yonow* | Received 8 April 2019 | Accepted 23 December 2019 | Published 5 February 2020

http://zoobank.org/202D2B19-4952-431D-A076-80D6110971CA

Citation: Wang A, Conti-Jerpe IE, Richards JL, Baker DM (2020) *Phestilla subodiosus* sp. nov. (Nudibranchia, Trinchesiidae), a corallivorous pest species in the aquarium trade. ZooKeys 909: 1–24. https://doi.org/10.3897/zookeys.909.35278

Abstract

Phestilla subodiosus **sp. nov.** (Nudibranchia: Trinchesiidae) is a novel species that feeds on corals in the genus *Montipora* (Scleractinia: Acroporidae) which are economically important in the aquarium industry. Nuclear-encoded H3, 28SC1-C2, and mitochondrial-encoded COI and 16S markers were sequenced. Phylogenetic analysis, Automatic Barcode Gap Discovery (ABGD), morphological data, and feeding specialization all support the designation of *Phestilla subodiosus* **sp. nov.** as a distinct species. Although new to science, *Phestilla subodiosus* **sp. nov.** had been extensively reported by aquarium hobbyists as a prolific pest over the past two decades. The species fell into a well-studied genus, which could facilitate research into its control in reef aquaria. Our phylogenetic analysis also revealed *Tenellia chaetopterana* formed a well-supported clade with *Phestilla*. Based upon a literature review, its original morphological description, and our phylogenetic hypothesis, we reclassified this species as *Phestilla chaetopterana* **comb. nov.**

Keywords

Nudibranchs, aquaculture, corallivore

Introduction

While many Nudibranchia species and genera have yet to be described (Gosliner et al. 2015), the deeper relationships in the systematics of several superfamilies and families within this group have been repeatedly investigated and revised in taxonomic and systematic studies employing both morphological and molecular techniques (Wägele and Willan 2000; Carmona et al. 2013; Cella et al. 2016; Korshunova et al. 2017a, b, c, 2018a, b, 2019a, b; Martynov et al. 2019). The superfamily Fionoidea is one of these groups that was recently investigated phylogenetically with genetic markers (Wägele and Willan 2000; Cella et al. 2016). Based on a phylogenetic hypothesis and morphological reasoning, Cella et al. (2016) combined several families (Calmidae, Tergipedidae, Eubranchidae, Cuthonidae, and Trinchesiidae) into the family Fionidae, and several genera (*Catriona*, *Phestilla*, and *Trinchesia*) along with several species from *Cuthona* into the genus *Tenellia*. However, strong defining morphological characteristics were not suggested and "beyond the scope" of the study. Furthermore, one of the phylogenetic arguments put forward by Cella et al. (2016) was that because several genera formed a strongly supported clade, they should be grouped as a single genus; despite this, there were three other strongly supported early diverging subclades within this clade that were not discussed. Korshunova et al. (2017c) studied the synapomorphies of the group and determined the changes proposed by Cella et al. (2016) were under-representing ontogenetic, morphological, and ecological diversity. They resurrected several families under Fionoidea (Calmidae, Cuthonellidae, Cuthonidae, Eubranchidae, Tergipedidae, and Trinchesiidae) and several genera (*Catriona*, *Diaphoreolis*, *Phestilla*, and *Trinchesia*) under the family Trinchesiidae, which matched the subclades within the phylogeny published by Cella et al. (2016). However, even with the thorough taxonomic work being conducted, the globally distributed superfamily (Debelius and Kuiter 2007) still contains dozens of undescribed species (Gosliner et al. 2015) and at least one species, *Tenellia chaetopterana* Ekimova, Deart and Schepetov 2017, that was not incorporated in the systematic study by Korshunova et al. (2017c).

Phestilla (Fionidae: Trinchesiidae) was one of the genera reinstated by Korshunova et al. (2017c). The group is characterized by corallivory (Rudman 1979, 1981; Ritson-Williams et al. 2003; Faucci et al. 2007) and "the modified cerata, lacking cnidosacs but with large glandular ceratal tips" (Rudman 1981: 387). *Phestilla* represents the largest group of Nudibranchia that feed only on scleractinian corals (Ritson-Williams et al. 2003; Goodheart et al. 2017). Studies that combined morphological and molecular approaches have examined the phylogenetic relationships within *Phestilla* (Faucci et al. 2007; Cella et al. 2016; Korshunova et al. 2017c) and several *Phestilla* species have been used as model organisms for studying pharmaceutical drug targets (Kimberly 2003), larval development (Harris 1975; Haramaty 1991; Pasquinelli et al. 2000), invertebrate metamorphosis (Hadfield and Pennington 1990; Hadfield et al. 2001; Hadfield et al. 2006; Ritson-Williams et al. 2009), and predatory control of corallivores *in situ* (Gochfeld and Aeby 1997). Due to their diet, *Phestilla* nudibranchs present a challenge to coral aquaculture (D Hui, J McNelley pers. comm.

2018; Borneman 2007; Riddle 2012; Henschen 2018), often evading detection and eradication due to their small size and effective camouflage (Rudman 1979, 1982; Gochfeld and Aeby 1997).

From 2017 to 2018 we observed nudibranchs feeding on *Montipora* spp. fragments obtained from the aquarium trade in several closed system aquaria in Hong Kong. Morphological, behavioral, and genomic analysis determined that the species was previously undescribed. Later, a single specimen was obtained from the wild in Koh Tao, Thailand that was used for morphological analysis. Here, we describe this novel species of nudibranch as *Phestilla subodiosus* sp. nov. and resolve inconsistencies in the systematics of its family Trinchesiidae. *Phestilla subodiosus* sp. nov. is a corallivorous nudibranch commonly found preying on cultured corals in the genus *Montipora* (Scleractinia: Acroporidae). Aquarists report that damages caused by this species can cost hundreds of dollars (USD) per outbreak (D Hui, J McNelley pers. comm. 2018). Despite the economic and environmental importance of coral aquaculture, little information is available on the eradication and control of pest species (Borneman 2007; Riddle 2012). In the case of *Phestilla subodiosus* sp. nov. the species has not even been described despite online reports of it from as early as 2001 (Gray 2001).

Materials and methods

Collection and preservation

Sexually mature nudibranchs and their egg masses were collected from *Montipora* spp. fragments ($N > 10$) between November 2017 and March 2018 (Figs 1, 2). The *Montipora* spp. fragments were either purchased from aquarium stores or obtained from other hobbyists between 2015 and 2018. A single 3 mm specimen *Phestilla subodiosus* sp. nov. was obtained from a wild locality in Koh Tao, Thailand on 22 April 2019. Adults and juveniles were relaxed for morphological analysis by the dropwise addition of 10 % magnesium chloride and fixed in formalin for 24 hours before being preserved in 95 % ethanol. Egg masses and specimens for DNA extraction were fixed in 95% ethanol directly after collection.

DNA extraction and amplification

Total genomic DNA was extracted from six specimens using the DNeasy blood and tissue extraction kit (Qiagen, Germany), following the manufacturer's protocol. Four loci were amplified with Polymerase Chain Reaction (PCR): mitochondrial Cytochrome *c* oxidase subunit I (COI), mitochondrial 16S structural rRNA subunit (16S), nuclear Histone H3 (H3), and nuclear 28S structural rRNA subunit (28S). Primers used are listed in Table 1. PCR reactions were conducted in 20 µl volume reactions, containing 2 µl of the forward and reverse primers (10 µM concentration) and extracted DNA, 6 µl of

Table 1. Primers used for PCR and sequencing of *Phestilla subodiosus* sp. nov.

LCO 1490	5'-GGTCAACAAATCATAAA-GATATTGG-3'	(Folmer et al. 1994)	5 min at 94 °C, 35× [1min at 94 °C, 30s at 42.5 °C, 1min at 72 °C], 7 min at 72 °C
COIH-2	5'-TAYACYTCRGGATGMC-CAAAAATCA-3'	(Cella et al. 2016)	
H3AF	5'-ATGGCTCGTAC-CAAGCAGACVGC-3'	(Colgan et al. 1998)	3min at 94 °C, 35× [35s at 94 °C, 1min at 50 °C, 1min at 72 °C], 7min at 72 °C
H3AR	5'-ATATCCTTRGGCATRATRGT-GAC-3'	(Colgan et al. 1998)	
16S arL	5'-CGCCTGTTTAACAAAAA-CAT-3'	(Palumbi et al. 2002)	3min at 94 °C, 39× [30s at 94 °C, 30s at 50–55 °C, 1min at 72 °C], 5min at 72 °C
16S R	5'-CCGRTYTGAACTCAGCT-CACG-3'	(Puslednik and Serb 2008)	
28SC1	5'-ACCCGCTGAATTTAAGCAT-3'	(Dayrat et al. 2001)	5min at 94 °C, 35× [1min at 94 °C, 30s at 45 °C, 1min at 72 °C], 7min at 72 °C
28SC2	5'-TGAACTCTCTCTTCAAAGTT CTTTTC-3'	(Le et al. 1993)	

nuclease-free water, and 8 µl of PCR MasterMix (Sigma-Aldrich) or Hot Start Taq DNA Polymerase (BiotechRabbit). Amplification of the COI and 28S markers was performed with an initial denaturation of 5 minutes at 94 °C, followed by 35 cycles of denaturing for 1 minute at 94 °C, annealing for 30 seconds at 42.5 °C for COI and 45 °C for 28S, and elongation for 1 minute at 72 °C, with the final elongation for 7 minutes at 72 °C. Amplification for H3 was performed with an initial denaturation for 3 minutes at 94 °C, followed by 35 cycles of denaturation for 35 seconds at 94 °C, annealing for 1 minute at 50 °C, and elongation for 1 minute at 72 °C, with the final elongation for 7 minutes at 72 °C. Amplification for 16S was performed with an initial denaturation of 3 minutes for 94 °C, 39 cycles of denaturation for 30 seconds at 94 °C, annealing for 30 seconds at 52.5 °C, and elongation for 1 minute at 72 °C, with the final elongation for 5 minutes at 72 °C. All reactions were performed on a Veriti Thermal Cycler (Applied Biosystems, USA). Amplified products were visualized on a 2% agarose gel prior to sequencing.

PCR products for COI, 28S, and H3 were purified with ExoSAP-IT™ PCR Product Cleanup Reagent (ThermoFisher, USA) and cycle sequenced using the BigDye Terminator v3.1 Cycle Sequencing Kit (ThermoFisher, USA), both in accordance with the manufacturer's instructions. Sequencing was performed on an ABI 3130xl Genetic Analyzer (ThermoFisher, USA). 16S PCR products were sequenced externally by the Beijing Genomics Institute (Shenzhen, China).

Phylogeny

Raw reads obtained from *Phestilla subodiosus* sp. nov. were assembled and edited visually with Geneious 11.1.4 (Kearse et al. 2012). nBLAST (Altschul et al. 1990) searches revealed that significantly similar H3, 16S, and COI sequences were available, while few were available for 28S. Due to the lack of similar 28S sequences, this locus was ultimately not used in the phylogenetic analysis. COI, 16S, and H3 sequences ($N = 141$) of 47 species, including 9 undescribed species, from eight Fionoidea families (Suppl. material 1:

Table S1), were downloaded from NCBI's GenBank (Clark et al. 2016). COI, 16S, and H3 sequences were aligned using MUSCLE (Edgar 2004) and trimmed to 658 bp, 492 bp, and 328 bp, respectively, using MEGA X (Kumar et al. 2018). GUIDANCE-2 (Sela et al. 2015) was employed to identify offending sequences in alignments. Hypervariable indel-rich regions in the 16S gene were not removed from the analysis (Cella et al. 2016). Sequences were concatenated manually using MEGA X (Kumar et al. 2018).

IQ-Tree (Nguyen et al. 2015) was used to infer evolutionary histories using the Maximum Likelihood (ML) method with a partitioned analysis (Chernomor et al. 2016) and 1500 pseudoreplicates using the bootstrap method to estimate the ML support values (BS). IQ-Tree's ModelFinder tool (Kalyaanamoorthy et al. 2017) invoked a full tree search of every model for each partition to calculate the Bayesian Information Criterion (BIC), Akaike Information Criteria (AIC), and Corrected Akaike Information Criteria (CAIC) of each substitution model. Based upon BIC, TVM+F+I+G4 for COI and 16S, and TIM2+F+I+G4 for H3 were used for the phylogenetic analysis. MrBayes (Ronquist et al. 2012) was used to infer another evolutionary history using Bayesian Inference (BI) with the GTR+I+G model. Two simultaneous Metropolis-Coupled Monte Carlo Markov Chains (MCMCMC) were run with four chains – one cold and three hot (temp = 0.1) – for 6,000,000 generations. The prior was flat Dirichlet. Diagnostics were calculated every 5000 generations with a 25% burn-in to calculate Posterior Probability (PP). Cold chains were sampled every 1000 generations. Raw newick files were reformatted using MEGA X (Kumar et al. 2018). Final trees were edited and annotated using Photoshop CC 2017 (Adobe, USA).

Trees for each individual gene were computed to gain a better understanding of the systematics of the group. ML trees were estimated using IQ-Tree (Nguyen et al. 2015) with 10,000 bootstrap pseudoreplicates using the UFBoot2 Method (Hoang and Chernomor 2017) and models were automatically found using IQ-Tree's ModelFinder tool (Kalyaanamoorthy et al. 2017). The models utilized were TVM+F+I+G4 for COI and 16S, and TIM2+F+I+G4 for H3. BI trees were estimated using MrBayes (Ronquist et al. 2012) with the GTR+I+G model. Two simultaneous MCMCMC with a flat Dirichlet prior were run for 3,000,000 generations using three hot (temp = 0.1) and one cold chain, with diagnostics being calculated every 1000 generations, a 25% burn-in and cold chain sampling every 500 generations.

Species delineation

An online version of the Automatic Barcode Gap Discovery (ABGD) program (Puillandre et al. 2012) was employed to delineate species using a dataset of 15 *Phestilla* COI sequences from eleven species (Suppl. material 1: Table S1). The ABGD settings were: P_{min} = 0.001, P_{max} = 0.1, Steps = 10, X = 1.5, Nb bins = 20. Three different distance models, Jukes-Cantor (JC69), Kimura (K80) TS/TV 2.0, and Simple Distance, were run (Puillandre et al. 2012). Uncorrected pairwise distances (*p*-distance) for COI were calculated in MEGA X (Kumar et al. 2018) with the nucleotide substitution type using the same *Phestilla* COI dataset. The

rate variation among sites was modelled with a gamma distribution (shape parameter = 4) with invariant sites (G+I). All ambiguous positions were removed for each sequence pair. The bootstrap method with 10,000 pseudoreplicates was used to estimate variance.

Morphological analysis

Live adult (4 mm paratype) and juvenile individuals (1–3 mm paratypes) were photographed using a Nikon D5100 camera (Nikon, Japan) with AF-S Nikkor 18–55 mm 1:3.5–5.6G lens (Nikon, Japan). The holotype (2 mm) and a paratype (egg mass) were imaged using a Leica DFC295 microscope camera (Germany) with a 0.63X Stereo Microscope C-Mount (Leica, Germany) to examine external structures. The holotype obtained from captive *Montipora* spp. (2 mm) and the paratype collected from Thailand (3 mm) were dissected to isolate the buccal mass and reproductive system. Buccal mass was dissolved in dilute bleach (~ 1:30) to review radula and jaw plates. Radula, jaw plates, and reproductive system were imaged and examined under a Meiji Techno M1510 Trinocular Compound Microscope (Meiji Techno Co., Japan). Images were edited and annotated using Photoshop CC 2017 (Adobe, US). All type material was deposited at the Museum of The Swire Institute of Marine Science at The University of Hong Kong.

Observed host species

To elucidate the possible coral hosts of *Phestilla subodiosus* sp. nov., preliminary data of observed hosts were recorded. Individuals of *Phestilla subodiosus* sp. nov. ($5 \geq N \geq 10$) and a single fragment of one of eight species of coral (Table 2) were isolated in a glass beaker (50 ml) for a week. Coral species were identified according to Veron (2000), Chan et al. (2005), and Wallace et al. (2012), and several species representing a diverse selection of colony morphologies and coenosteum phenotypes were chosen (Table 2). Temperature was maintained constant by partially submerging the jars into a water bath 24–27 °C, and approximately 75% of the water was changed daily. A coral species was counted as a host species if they fulfilled two criteria: firstly, *Phestilla subodiosus* sp. nov. had to form an aggregation (see Fig. 1) within 3–4 cm of the coral (Morton et al. 2002); and secondly, the coral had to show evidence of tissue loss from predation surrounding the aggregations (Figs 1, 2B; Ritson-Williams et al. 2003, Dalton and Godwin 2006).

Results

Sequence analysis

In total, 17 of 24 sequences obtained from six sexually mature individuals were used for the final analysis: five from COI, two from 16S, four from 28S, and six from H3.

Table 2. Observational data of the feeding preference of *Phestilla subodiosus* sp. nov. Abbreviations: N indicates that this species of coral did not satisfy the two conditions needed to be counted as a host coral; Y indicates that the species did satisfy both conditions needed to be counted as a host coral.

Family	Genus	Species	Growth form	Host species
Acroporidae	*Acropora*	*samoensis*	Digitate corymbose. Thick branches.	N
		pruinosa	Digitate arborescent. Thin branches.	N
	Montipora	sp. 1	Encrusting.	Y
		sp. 2	Digitate arborescent. Thin branches.	Y
		sp. 3	Laminar scrolling.	Y
		sp. 4	Laminar scrolling or encrusting.	Y
Lobophylliidae	*Echinophyllia*	*aspera*	Laminar scrolling or encrusting.	N
Poritidae	*Porites*	sp. 1	Encrusting.	N

GUIDANCE-2 revealed that the 16S sequence of *Eubranchus rustyus* was low quality and thus it was removed from the alignment. The concatenated dataset used in the phylogenetic analysis was 1255 bp (549 bp for COI, 379 bp for 16S, 327 bp for H3) long, including indels. Trees generated for each individual gene dataset (Suppl. material 2: S2) support the resolution hierarchy proposed by Cella et al. (2016).

The ML and BI phylogenic hypotheses (Fig. 3) and the tree published in Cella et al. (2016) resolved with similar topologies; however, none of the trees were congruent on the relationship between *Rubroamoena*, *Tergipes*, and *Tergiposacca*. These differences could be attributed to the fact that the ML and BI analyses used different models. While in theory the general topology of the trees produced should be the same since the search space of GTR encompasses the spaces of TVM and TIM2, algorithms that maximize likelihoods are prone to getting stuck on a local optimum, especially with constrained parameters or small sample sizes (Hillis et al. 1996). Further research is required for the field of nudibranch systematics to decide which model to trust. However, this does not explain the recovery of *Trinchesia* as polyphyletic in both trees, with *Tr. speciosa* forming a clade with *Diaphoreolis* (BS = 54%, PP = 0.99). The families Trinchesiidae, Fionidae and Tergipedidae were also recovered as paraphyletic and polyphyletic in both trees. Further research is required to identify whether these were artefacts of unbalanced taxon sampling or indicative of flawed taxonomic grouping. However, both trees did recover described *Phestilla* species and *P.* sp. 3 as monophyletic (BS = 54%, PP = 0.78), forming clades with *Phestilla subodiosus* sp. nov. and *P.* sp. L (BS = 64%, PP = 0.65), and with *Te. chaetopterana* and *P.* sp. A (BS = 70%, PP = 1). The clade containing *Phestilla subodiosus* sp. nov. and *P.* sp. L had very short branch lengths and had high support values (BS = 100%, PP = 1), suggesting that *Phestilla subodiosus* sp. nov. and *P.* sp. L are the same species. Both trees also recovered *Tenellia* as polyphyletic, with *Te. chaetopterana* in the same clade as *Phestilla*. To solve this issue, *Te. chaetopterana* should be transferred to *Phestilla*, or to a new genus with *Phestilla* sp. A.

Pairwise distances (Table 3) based on the COI dataset revealed that all *Phestilla subodiosus* sp. nov. samples had virtually identical COI sequences (p = 0.0% ± 0.0 %). *Phestilla*

Table 3. Uncorrected COI *p*-distances (%) among all species of described *Phestilla* with available sequences. Percentages all rounded to one decimal place. Standard error (%) estimates rounded to one decimal place generated from bootstrapping (N = 10,000) are shown above the diagonal.

		1	2	3	4	5	6	7	8	9	10	11	12	13	14	15
1	*Phestilla minor*		1.6	1.4	1.4	1.4	1.4	1.4	1.4	1.6	1.6	1.4	1.4	1.4	1.3	1.4
2	*P. sibogae*	20		1.5	1.5	1.5	1.5	1.5	1.5	1.7	0.6	1.6	1.6	1.5	1.5	1.5
3	*P.* sp. 2	15.2	18.9		1.4	1.4	1.4	1.4	1.4	1.6	1.5	1.3	1.5	1.4	1.4	1.3
4	*P. subodiosus* sp. nov. PS1	14.6	17.5	13.7		0.0	0.0	0.0	0.0	1.5	1.4	1.4	1.4	0.4	1.3	0.4
5	*P. subodiosus* sp. nov. PS3	14.6	17.5	13.7	0.0		0.0	0.0	0.0	1.5	1.4	1.4	1.4	0.4	1.3	0.4
6	*P. subodiosus* sp. nov. PS4	14.6	17.5	13.7	0.0	0.0		0.0	0.0	1.5	1.4	1.4	1.4	0.4	1.3	0.4
7	*P. subodiosus* sp. nov. PS5	14.6	17.5	13.7	0.0	0.0	0.0		0.0	1.5	1.4	1.4	1.4	0.4	1.3	0.4
8	*P. subodiosus* sp. nov. PS6	14.6	17.5	13.7	0.0	0.0	0.0	0.0		1.5	1.4	1.4	1.4	0.4	1.3	0.4
9	*P. chaetopterana* comb. nov.	17.1	18.4	17.1	14.9	14.9	14.9	14.9	14.9		1.6	1.6	1.5	1.5	1.5	1.5
10	*P. lugubris*	19.9	2.2	18.7	16.7	16.7	16.7	16.7	16.7	17.8		1.6	1.5	1.4	1.5	1.4
11	*P. melanobrachia*	14.6	19.7	12.6	15.9	15.9	15.9	15.9	15.9	19.3	19.6		1.5	1.4	1.4	1.4
12	*P. poritophages*	14.2	18.5	16.7	14.2	14.2	14.2	14.2	14.2	15.8	17.7	17.6		1.4	1.4	1.4
13	*Phestilla* sp. L	14.1	16.9	13.6	1.0	1.0	1.0	1.0	1.0	14.7	16.1	15.9	14.1		1.3	0.5
14	*Phestilla* sp. 1	12.9	18	14.6	11.8	11.8	11.8	11.8	11.8	15.5	17.7	14.9	15.1	11.8		1.3
15	*Phestilla* sp. 3	13.7	17.4	13.2	1.2	1.2	1.2	1.2	1.2	14.5	16.9	15.8	14.1	1.5	11.6	

subodiosus sp. nov. was most closely related to *P.* sp. L (p = 1.0% ± 1.4%) and *P.* sp. 3 (p = 1.2% ± 1.4%). All other species had p > 11.0%, providing more evidence that *P.* sp. L is the same species as *Phestilla subodiosus* sp. nov. The next closest species to *Phestilla subodiosus* sp. nov. were *P.* sp. 1 (p = 11.8% ± 1.3%), *P. poritophages* (p = 14.2% ± 1.4%), and *P. minor* (p = 14.6% ± 0.4%). The analysis revealed that *P. lugubris* and *P. sibogae* had very similar COI sequences (p = 2.2% ± 1.6%), providing evidence for their synonymy.

All three ABGD models elucidated ten partitions: simple distance found ten partitions with eight groups; while JC69 and K80 found five partitions with eight groups and five partitions with ten groups. In the partitions with eight groups, *Phestilla subodiosus* sp. nov., *P.* sp. L, and *P.* sp. 3 as well as *P. lugubris* and *P. sibogae* were grouped together. This provides additional evidence that *Phestilla subodiosus* sp. nov., *P.* sp. L, and *P.* sp. 3 are the same species and that *P. lugubris* and *P. sibogae* are synonymous. However, in the partitions with ten groups, while *P. lugubris* and *P. sibogae* were grouped together, *Phestilla subodiosus* sp. nov. was distinct to *P.* sp. L and *P.* sp. 3. These partitions are likely statistical anomalies due to the oversampling of virtually identical *Phestilla subodiosus* sp. nov. sequences.

Observed host species

Of all the coral species examined (Table 2), only *Montipora* species qualified as a suitable host. In all the other trials, *Phestilla subodiosus* sp. nov. wandered across the containment capsules and neither host criteria were met. These results indicate that prey choice is independent to host coral colony morphology. However, it is worthwhile to note that the *Acropora samoensis* specimen did suffer tissue loss towards the base and began re-encrusting within a week after the experiment ended, indicating that the specimen was in fact healthy. It is unclear if the tissue loss was due to predation from *Phestilla subodiosus* sp. nov, or an adverse reaction to another factor.

Taxonomic account

Order Nudibranchia
Superfamily Fionoidea Gray, 1857
Family Trinchesiidae Nordsieck, 1972

Genus *Phestilla* Bergh, 1874

Diagnosis. "Physical form quite depressed. An edge anterior to the head, wing-like, attached to [...]; oral tentacles short, rhinophores simple. Cerata arranged on singular slanting rows, lacking cnidosacs. [...] Masticatory edge contains mandibles behind teeth (round, with irregular serration). Radula uniserial." – Bergh, 1874: 1, partially translated.

Included species. *Phestilla chaetopterana* (Ekimova, Deart & Schepetov, 2017)**,** comb. nov., *Phestilla lugubris* (Bergh, 1870), *Phestilla melanobrachia* (Bergh, 1874), *Phestilla minor* (Rudman, 1981), *Phestilla panamica* (Rudman, 1982), *Phestilla poritophages* (Rudman, 1979), *Phestilla subodiosus* sp. nov.

Remarks. Historically, *Phestilla* was placed in the family Tergipedidae. This family contained a large "unnecessary and unnatural" number of genera (Rudman 1979: 344). Phylogenetic analysis revealed that this grouping was polyphyletic and a "radical solution" (Cella et al. 2016: title) was proposed: several families were combined into the family Fionidae, and several genera, including *Phestilla*, into the genus *Tenellia* (Cella et al. 2016). However, a study into the ontogeny of these groups elucidated that Cella et al.'s (2016) taxonomic decisions were underrepresenting the molecular, ecological, morphological, and ontogenetic diversity of the clades; thus, the families and genera that were combined into Fionidae and *Tenellia* were reinstated (Korshunova et al. 2017c). While there is controversy surrounding which interpretation is the taxonomic truth, we have designated *Phestilla* as a separate genus to *Tenellia* based on the arguments presented by Korshunova et al. (2017c). However, given the results of the *p*-distance and ABGD analysis, we follow Cella et al. (2016) and Rudman's (1981) decisions to synonymize *P. sibogae* with *P. lugubris*.

At the same time that Korshunova et al. (2017c) published their findings, Ekimova et al. (2017) published a paper describing *Tenellia chaetopterana*, a species that clusters phylogenetically and morphologically with *Phestilla*. As both papers were released on the same date (26 September 2019), Ekimova et al. (2017) were unable to incorporate the revised designations from Korshunova et al. (2017c) into their description. However, there are considerable differences between *Te. chaetopterana* and the other *Phestilla* species. Firstly, the radular cusp and lateral denticle proportions are unique in the entire family (Korshunova et al. 2017c), but the general pattern is similar. Secondly, the species lacks penile glands or bulbs. Thirdly each ceratal row only has a single cerata (Ekimova et al. 2017). Finally, *Te. chaetopterana* would represent the first *Phestilla* species that does not feed on scleractinian corals (Rudman 1979, 1981, 1982; Goodheart et al. 2017). Further research is required to determine whether *Te. chaetopterana* should represent a new genus or another species of *Phestilla*. Based on our independent phylogenetic analysis and the synapomorphies shared by *Te. chaetopterana* and *Phestilla*, we propose transferring *Te. chaetopterana* to the genus *Phestilla* as the most parsimonious solution.

***Phestilla subodiosus* sp. nov.**

http://zoobank.org/F5F4BF04-1295-4A66-87F9-F09BC61590EB
Figures 1–4

Tenellia sp. L: Cella et al. 2016: 9, 14, fig. 2, table 5 (locality unlisted).
Tenellia sp.: Cho et al. 2018: GenBank Accession number MG878397 (Jeju Island, South Korea).

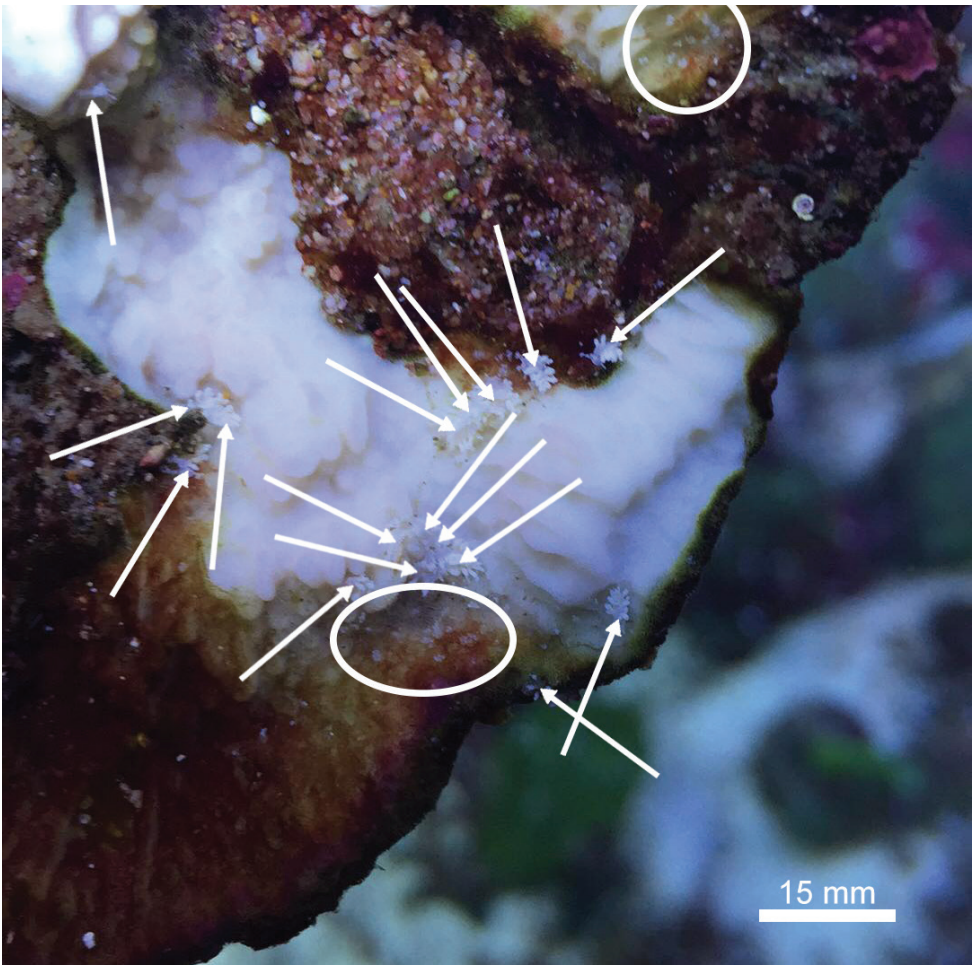

Figure 1. An aggregation of living individuals of *Phestilla subodiosus* sp. nov. on *Montipora* sp. White arrows indicate metamorphosed individuals; white circles indicate clusters of egg masses.

Type Material. ***Holotype:*** [SWIMS-MOL-17-001]. 1 specimen 2 mm long in 95% ethanol, dissected, Hong Kong SAR: *Montipora* spp., cultured in aquaria, coll. A. Wang, 19 Nov. 2017 (Figs 4a, b, 5c).

Paratypes: [SWIMS-MOL-17-002]. 1 egg case 1 mm long in 95% ethanol. Hong Kong SAR: *Montipora* spp., cultured in aquaria, coll. A. Wang, 25 Nov. 2017 (Figs 2c, 4c).[SWIMS-MOL-18-001]. 1 specimen 1.2 mm long in 95% ethanol. Hong Kong SAR: *Montipora* spp., cultured in aquaria, coll. A. Wang, 8 Mar. 2018 (live specimen in Fig. 1). [SWIMS-MOL-19-008]. 1 specimen 3.0 mm long in 95% ethanol, dissected, Thailand: Koh Tao, Taa Chaa, depth 5 m, coll. R. Mehrotra, 22 Apr. 2019 (Fig. 5b) [SWIMS-MOL-17-003]. DNA extract from whole specimen 4mm long in 100% ethanol. Hong Kong SAR: *Montipora* spp., cultured in aquaria, coll. A. Wang, 19 Nov. 2017 (Fig. 2a) [SWIMS-MOL-18-002], [SWIMS-MOL-18-003], [SWIMS-MOL-18-004], [SWIMS-MOL-18-005], [SWIMS-

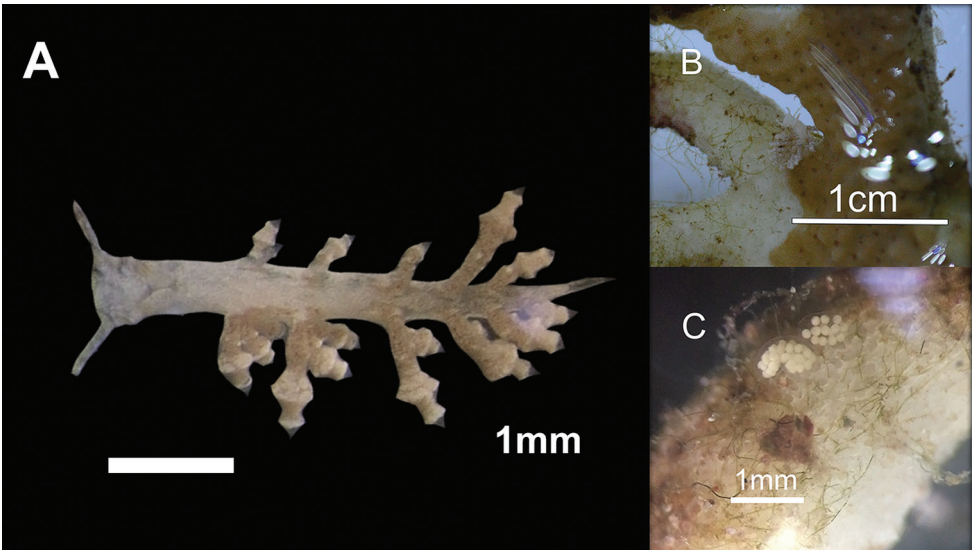

Figure 2. Specimens of *Phestilla subodiosus* sp. nov.: **A** adult (4 mm paratype) **B** adult feeding on *Montipora* sp. **C** paratype egg mass on *Montipora* sp. fragment.

MOL-18-006], [SWIMS-MOL-18-007]. DNA extracts from whole specimens 1–3.5 mm long in 100% ethanol. GenBank, respectively, Hong Kong SAR: *Montipora* spp., cultured in aquaria, coll. A. Wang, 8 Mar. 2018 (live specimens in Fig. 1).

Etymology. The specific epithet, *subodiosus*, Latin for odious and vexatious, is symbolic of its status as a pest in the aquarium trade, and also a homage to the time and prized *Montipora* colonies the first author lost to in an outbreak of this species.

Distribution. Specimen collected from Koh Tao, Thailand (this paper). Reported from Jeju Island, Korea (Cho et al. 2018 as *Tenellia* sp.) and confirmed using molecular methods. A similar species reported from Singapore according to a personal communication with Harris published by Robertson (1987: 3), unconfirmed. The type locality of the material from Cella et al. (2016) was not listed.

Description. ***External morphology*** (Figs 1, 2, 4). Thin elongate body. Sexually mature adults 1.5 mm to 4 mm in length, 0.5 mm to 1 mm in width. Oral tentacles connected to oral veil arising from edge approximately under rhinophores, brown band near the distal third. Rhinophores rounded distally, not distinct and lacking lamellae, with brown band near middle. Oral tentacles and rhinophores approximately same length. Eyes slightly posterior to each rhinophore. Body lacking obvious rhinophoral sheaths. First ceratal row slightly posterior to rhinophores. Fully developed rows contain three cerata. Cerata unbranching and arranged regularly in sloping transverse rows with two to three rows adjoining pericardium. One to three rows of cerata anterior to pericardium with no precardiac rows. Cerata lacking cnidosacs and always swollen terminally. Two to three additional swollen bulbs on fully developed cerata (Fig. 2). Pericardium hump thick in relation to rest of body, nearly 1 mm thick, beginning at first cerata row and ending between second and third row (Fig. 2). Body tapers strongly

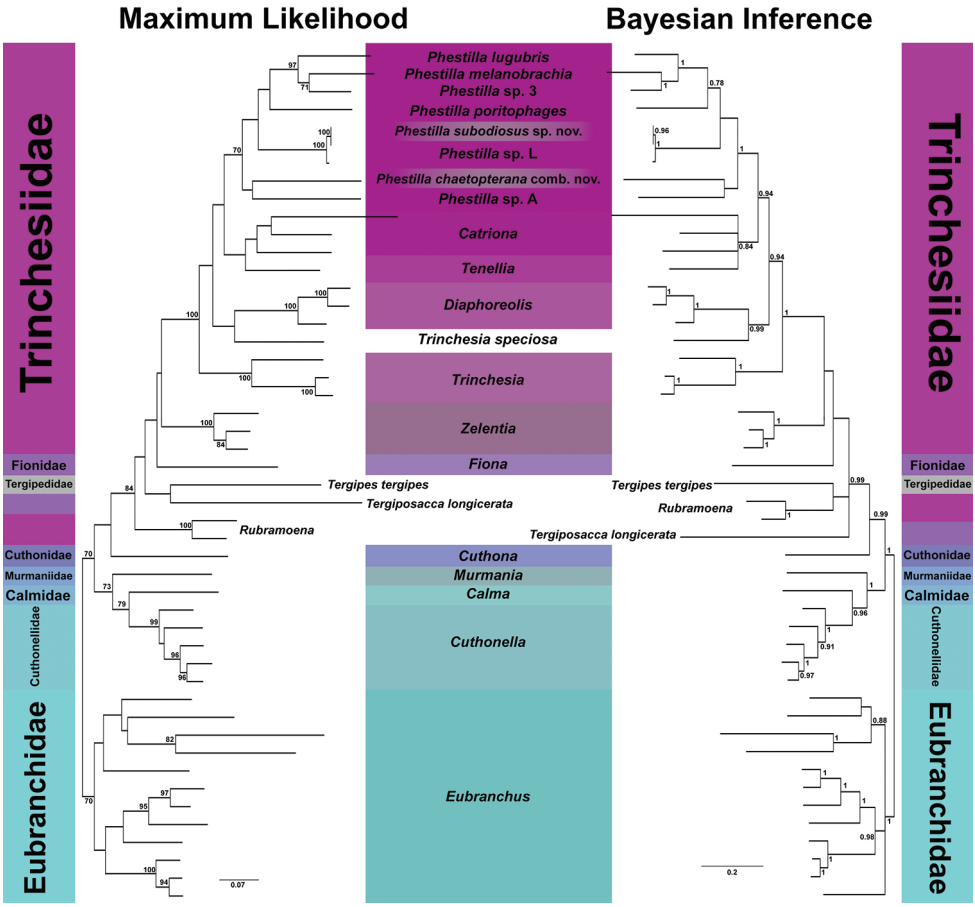

Figure 3. Combined COI-16S-H3 Maximum Likelihood and Bayesian Inference phylogenetic hypotheses. Support values indicate Bootstrap (BS) and Posterior Probability (PP) rounded to two significant digits on the ML and BI trees. *Phestilla subodiosus* sp. nov. and *P. chaetopterana* comb. nov. are highlighted. Trees rooted on *Eubranchus*.

in thickness (<< 1 mm) after pericardium hump. Gonopore below and anterior to first cerata row, approx. at same height as the second cerata on the first row. Mouth large, diameter nearly equal to width of body, and clearly separated from foot.

Internal morphology (Fig. 5). Jaws translucent and thin, smaller than 0.5 mm in 3 mm individual. Radular formula 12 × 0.1.0 in 3 mm individual, uniseriate. Teeth with central cusp and five to seven denticles on each side. Denticles and cusp arranged on curved edge. All denticles approx. same length. Central cusp longer and reaching slightly further than innermost denticles. Lacking secondary denticles. Reproductive system diaulic and spread throughout body. Penile bulb curved, connected to genital opening by short prostate, and adheres to wall of nudibranch. Female gland mass diameter 1.5 times size of penile bulb. Ampulla long and winding, diameter slightly

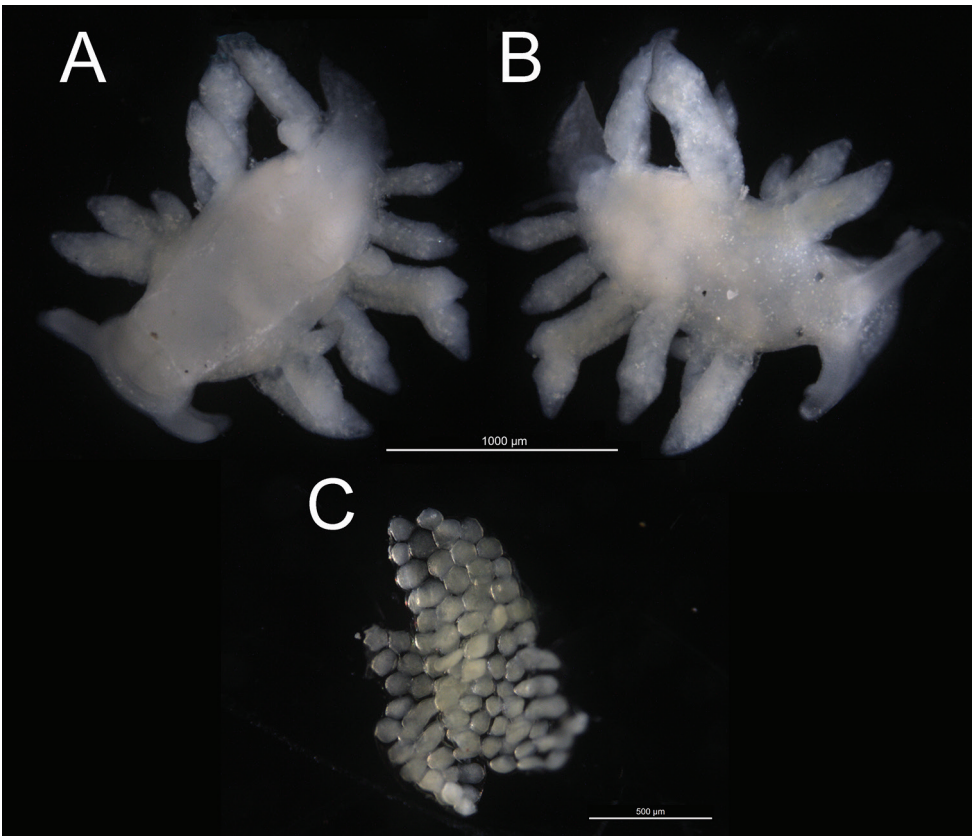

Figure 4. Preserved holotype 2 mm and eggs of *Phestilla subodiosus* sp. nov.: **A** ventral view of holotype **B** dorsal view of holotype **C** preserved egg cluster paratype collected from *Montipora* sp. fragment.

larger than that of penile bulb, connected to vagina and appressed onto female gland mass, leading to hermaphrodite system. Lacks vas deferens. Penile bulb, female gland mass, and ampulla 0.5 mm to 1 mm combined.

Color. Two ontogenetic color forms. Juvenile animals with white epidermal pigment throughout entire body. Adults with white epidermal pigment and translucent ceratal epidermis. Cerata speckled with brown clots, possibly from internal fluids or dinoflagellates of Symbiodiniaceae from coral hosts. Swollen regions on cerata lack speckles. Speckle density decreases towards the posterior of the cerata.

Defense mechanisms. Cerata observed to autotomize and secrete viscous adhesive mucus, usually encapsulating abscised ceras, when animal is disturbed tacitly.

Observed prey items. Preys on coral species in the genus *Montipora*. Does not feed on corals of genera *Porites*, *Acropora*, and *Echinophyllia*. Reports of feeding on corals in genus *Anacropora* (Henschen 2018), a sister genus to *Montipora* (Fukami et al. 2000); however, this observation is unconfirmed by the authors.

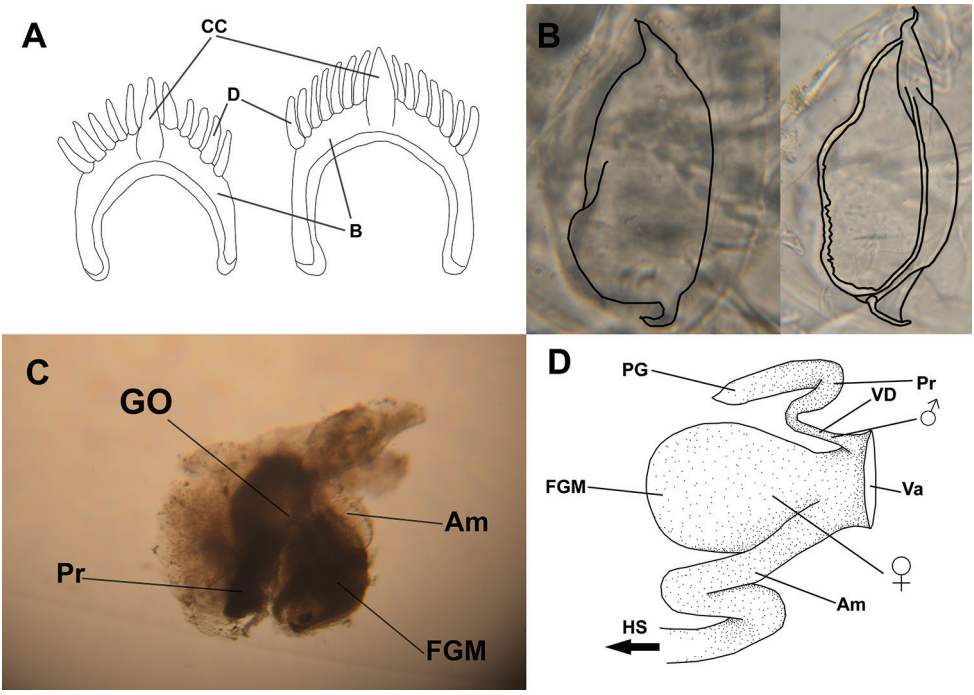

Figure 5. Internal morphology of *Phestilla subodiosus* sp. nov.: **A** schematic of rachidian tooth. Abbreviations: B, base; D, denticles; CC, central cusp **B** schematic of jaw plates overlaid onto microscope imagery **C** microscope imagery of reproductive system. Abbreviations: GO, genital opening; Pr, prostate; FGM, female gland mass; Am, ampulla **D** schematic of reproductive system. Abbreviations: PG, penile gland; Pr, prostate; VD, vas deferens; Va, vagina; FGM, female gland mass; Am, ampulla; HS, hermaphrodite system.

Taxonomic remarks

Based solely on the morphological key given in Korshunova et al. (2017c), *Phestilla subodiosus* sp. nov. does not fit in any of the genera of Trinchesiidae. They defined *Phestilla* as lacking an oral veil, while it was evident that *Phestilla subodiosus* sp. nov. had one. However, in both the original descriptions and redescriptions of various *Phestilla* species in Rudman (1979, 1981, 1982), oral veils were present. Bergh's (1874: 1) original description of *Phestilla* also referred to an "edge anterior to the head", which is likely an oral veil. It is therefore appropriate to place *Phestilla subodiosus* sp. nov. in this genus.

Morphologically, *Phestilla subodiosus* sp. nov. is most similar to *P. minor* and *P. poritophages* in color forms and swollen cerata, but is distinguished by several characters: firstly, *adult Phestilla subodiosis* sp. nov. we observed averaged 3.5 mm in length, approximately half of the size *P. minor* (Rudman 1981) and *Phestilla poritophages* (Rudman 1979); secondly, *Phestilla subodiosus* sp. nov. only has three cerata per row, while *P. minor* has four to five (Rudman 1981) and *Phestilla poritophages* has four (Rudman 1979); thirdly, *Phestilla subodiosus* sp. nov. has only two rows of cerata anterior to its pericardium, while both *P. minor* and *P.*

poritophages have three (Rudman 1979, 1981); fourthly, *Phestilla subodiosus* sp. nov. is the only known nudibranch species to feed on corals of the genus *Montipora*. Although Rudman (1981: 387) argued feeding on corals cannot count as a true distinguishing feature, evidence suggests prey specialization played a strong role in speciation within Cladobranchia (Goodheart et al. 2017) and the genus *Phestilla* itself (Faucci et al. 2007).

One species, *P. panamica*, did not have any sequences available online so a molecular comparison was infeasible. However, it is clear that *P. panamica* and *Phestilla subodiosus* sp. nov. are not the same species. *P. panamica* grows up to 24 mm, has 18 cerata per row, five precardiac rows, and eight postcardiac rows (Rudman 1982), while the largest observed specimen of *Phestilla subodiosus* sp. nov. was 4 mm (Fig. 2a), had three cerata per row, no precardiac rows, and two postcardiac rows. *Phestilla subodiosus* sp. nov. is also not a juvenile of *P. panamica*, as a 3 mm individual analyzed by Rudman (1982) had three precardiac rows. Furthermore, *P. panamica* and *Phestilla subodiosus* sp. nov. have different coral hosts and live on opposite sides of the Pacific Ocean to our current knowledge Rudman (1982).

There were considerable differences in the reproductive system and radula of *Phestilla subodiosus* sp. nov. and the rest of the genus, notably in the presence of a female gland mass. This arrangement is surprisingly similar to the reproductive system of the Chromodorididae. While it possible that the "female gland mass" is a bursa copulatrix, this would be extremely large for the genus, with a diameter 1.5 times the penile bulb's length, and directly attached to the female genital opening. In all other species of *Phestilla*, with the exception of *P. chaetopterana* comb. nov., the bursa copulatrix is much smaller than the penile bulb and attached to the oviduct. In *P. chaetopterana* comb. nov., the bursa copulatrix is small, but attached directly to the female genital opening. As the function of the bursa copulatrix' is to store sperm and/or digest it when needed, a larger one would allow a nudibranch to store more sperm longer thus explaining the phenomena reported by aquarists where the introduction of a single nudibranch can result in an outbreak and their ability to survive long periods without food (D Hui pers. comm. 2018). However, while the specimens dissected for the internal morphology analysis were sexually mature, they were only 2 mm and 3 mm in length. As previously shown, internal morphology has high ontogenetic plasticity throughout development (Ekimova et al. 2019), and further research is required to determine whether the structures recovered represent the final stages of development. Furthermore, in all other *Phestilla* species with the exception of *P. chaetopterana* comb. nov., the denticles extend further than the central cusp, but the cusp of *Phestilla subodiosus* sp. nov. reaches farther than the denticles. The radula of the new species is also the shortest in the genus, with an adult specimen only having 12 teeth, while the next smallest species, *P. minor*, had 30 (Rudman 1981).

Discussion

While several molecular studies have investigated the phylogenetic relationships within Fionoidae, taxonomic assignment of groups has resulted in debate, including the placement and composition of some genera in Trinchesiidae such as *Phestilla*. Several genera

were combined due to their close relationships recovered in a molecular phylogenetic analysis (Cella et al. 2016); however, the absence of synapomorphies led to the reversal of this new classification (Korshunova et al. 2017c). On the same date of the publication as Korshunova et al. (2017c), According to its original description, *Te. chaetopterana* fits within with *Phestilla* morphologically; additionally, our phylogenetic hypothesis found that *Te. chaetopterana* formed a strongly supported clade (96%) with all other *Phestilla* species. We therefore propose reclassifying *Te. chaetopterana* as *Phestilla chaetopterana* comb. nov. Together, *Phestilla subodiosus* sp. nov. and *P. chaetopterana* comb. nov. represent new species that provide clues towards the incomplete puzzle of Fionoidae systematics.

In recent decades, the introduction of coral aquaculture has reshaped both the aquarium industry and coral reef conservation efforts (Cato and Brown 2008; Livengood and Chapman 2007). The ability to culture corals in captivity has fueled the multi-billion-dollar hobbyist industry (Cato and Brown 2008) while relieving collection pressure on natural coral populations (Jones 2011). However, challenges to this technology still exist, including the proliferation of various pests that can damage or kill cultured corals, and are difficult or impossible to eliminate (Bakus 1966; Gochfeld and Aeby 1997; Scott et al. 2017). In particular, *Phestilla* nudibranchs are a problematic group due to their small size and effective camouflage, often evading detection and eradication (Rudman 1979, 1982; Gochfeld and Aeby 1997).

Despite being a prolific pest in aquaria, we were only able to find two reports of nudibranchs that resemble *Phestilla subodiosus* sp. nov. *in situ* (Roberston 1987:3; Cho et al. 2018). However, this seems to be characteristic of *Phestilla* species: their fecundity allows them to decimate entire coral colonies in several days *in vitro* (Fig. 1; Harris 1975; Rudman 1979, 1981, 1982; Haramaty 1991), but their populations are heavily suppressed by predators *in situ* (Gochfeld and Aeby 1997; Mehrotra et al. 2019). It is likely that *Phestilla subodiosus* sp. nov. populations exhibit similar dynamics, and thus are hard to find under natural conditions, likely preventing detection. If this hypothesis is supported, populations of *Phestilla subodiosus* sp. nov. could be controlled in reef tanks through the use of natural predators. Gochfeld and Aeby (1997) identified several fish and crustacean species that preyed on *P. sibogae*. However, further research is required to identify whether these species are also predators of *Phestilla subodiosus* sp. nov. and if they are suitable for a reef aquarium setting. Worthy of note, the outbreak of *Phestilla subodiosus* sp. nov. that led to this description occurred shortly after the death of a *Macropharyngodon meleagris* (Actinopterygii: Labridae) in the aquarium, and another labrid species (*Thalassoma duperrey*) was identified by Gochfeld and Aeby (1997) to feed on *P. sibogae*. *Ma. meleagris* and other labrids may well be suitable candidates for biocontrol of *Phestilla subodiosus* sp. nov.

Phestilla subodiosus sp. nov. displayed prey selectivity in our preliminary tests; however, the underlying mechanism is unclear. It has been established that other *Phestilla* species rely on chemical cues to differentiate host corals (Hadfield and Pennington 1990; Kimberly 2003; Ritson-Williams et al. 2009). The extrapolation of this conclusion to *Phestilla subodiosus* sp. nov. is supported by our observations. As *Phestilla subodiosus* sp. nov. ignored all corals except *Montipora* spp. (Table 2), including several that

shared the same colony morphology or coenosteum phenotype (Veron 2000; Wallace et al. 2012). We therefore speculate that *Phestilla subodiosus* sp. nov. relies on a non-visual and non-tactile system to identify host colonies, likely chemical cues. Determining how *Phestilla subodiosus* sp. nov. identifies suitable hosts could lead to the development of chemical pest control measures that inhibit these cues.

The description of *Phestilla subodiosus* sp. nov. is a key step that will allow for research to be conducted on its ecology and biology, and eventual control within reef aquaria. Given the wide number of common names in use to describe nudibranchs that feed on *Montipora* spp. (D Hui, J McNelley pers. comm. 2018), it is unclear whether several species exist or whether these names all refer to *Phestilla subodiosus* sp. nov. By formally describing *Phestilla subodiosus* sp. nov., further research can be conducted with confidence in the identity of the species being examined, allowing for clear collaboration and communication while a basic biological and ecological understanding of this species is developed. Furthermore, *Phestilla subodiosus* sp. nov. has been placed on the taxonomic tree of life within a well-understood genus containing several model organisms. Previous studies have described the proteins involved in *Phestilla* metamorphosis and drugs have been discovered that inhibit this vital process (Pires et al. 1997, 2000), providing a potential avenue to control this pest species. However, more research is required to determine if this is a safe and effective method for combating *Phestilla subodiosus* sp. nov. in a reef-aquarium setting.

Despite the scientific advances enabled by the aquarium industry (Veron 2000), this exchange of information and technology has not been reciprocated; hobbyist needs are frequently overlooked by researchers, including research into the control of pests. The earliest digital appearance of the term "*Montipora*-eating nudibranchs" appeared in 2001 (Gray 2001), and it has taken nearly two decades for it to be addressed by the scientific community, illustrating the disconnection between the two groups. The diagnosis of *Phestilla subodiosus* sp. nov. will hopefully pave the way to the control and eradication of a costly pest species in the aquarium industry, and this description presents an example of how collaboration between researchers and aquarists can further both fields.

Acknowledgments

We thank the reviewers for their time and effort to review this paper and provide insightful comments and suggestions. The authors gratefully acknowledge Dr. Moriaki Yasuhara and Ms. Maria Lo Gar Yee of the University of Hong Kong for allowing us to use their microscope and microscopy assistance, Kerry Samantha Hsu from the University of Pennsylvania and Dr. Han Guo Hong from the Fourth Military Medical University for manuscript comments, Jeffrey Chan for the design of feeding experiments, and Vriko Yu of the University of Hong Kong for aiding the sequencing and other slug-related work. We are also extremely thankful to Marcus Hibbins from Indiana University Bloomington for his help on phylogenetic analysis, as well as James Townsend and Alejandro Damián Serrano from the University of Pennsylvania, and

everybody else from our science meme page admin group chat for their advice on Latin translations, stylistic elements, and providing moral support. Last but not least, the first author is also extremely grateful and indebted to Dr. Theodore Faunce for helping him receive this opportunity to conduct research for the first time. This project was funded by the Environment and Conservation Fund (# 67/2016) and is manuscript number 48 of MarineGEO-Hong Kong.

References

Altschul SF, Gish W, Miller W, Myers EW, Lipman DJ (1990) Basic local alignment search tool. Journal of Molecular Biology 215(3): 403–410. https://doi.org/10.1016/S0022-2836(05)80360-2

Bakus GJ (1966) Some relationships of fishes to benthic organisms on coral reefs. Nature 210(3): 280–284. https://doi.org/10.1038/210280a0

Bergh LSR (1874) Neue Nacktschnecken der Südsee, Malacologische Untersuchungen II. Journal des Museum Godeffroy 2: 91–116. [pls 1–4] https://biodiversitylibrary.org/page/10860988 [accessed 2 August 2018]

Borneman E (2007) Two potential molluscicides useful against pest aeolid nudibranchs common on species of *Montipora* in aquariums. Reefkeeping 6(8). http://reefkeeping.com/issues/2007-09/eb/ [accessed 1 July 2018]

Carmona L, Pola M, Gosliner TM, Cervera JL (2013) A tale that morphology fails to tell: A molecular phylogeny of Aeolidiidae (Aeolidida, Nudibranchia, Gastropoda). PLoS ONE 8 (5): e63000. https://doi.org/10.1371/journal.pone.0063000

Cato J, Brown C (2008) Marine Ornamental Species: Collection, Culture & Conservation. Wiley, Iowa, 395 pp.

Cella K, Carmona L, Ekimova I, Chichvarkhin A, Schepetov D, Gosliner T (2016) A radical solution: The phylogeny of the nudibranch family Fionidae. PLoS ONE 11(23): e0167800. https://doi.org/10.1371/journal.pone.0167800

Chan L, Choi L, McCorry D, Chan K, Lee M (2005) Field guide to hard corals of Hong Kong. 郊野公园之友会天地图书有限公司, Hong Kong, 373 pp.

Chernomor O, von Haeseler A, Minh BQ (2016) Terrace aware data structure for phylogenomic inference from supermatrices. Systematic Biology 65(6): 997–1008. https://doi.org/10.1093/sysbio/syw037

Cho YG, Kang HS, Choi JH, Choi KS (2018) *Tenellia* sp. YGC-2018 cytochrome c oxidase subunit I gene, partial cds; mitochondrial. GenBank Sequence. http://www.ncbi.nlm.nih.gov/nuccore/MG878397.1 [accessed 2 September 2019]

Clark K, Karsch-Mizrachi I, Lipman DJ, Ostell J, Sayers EW (2016) GenBank. Nucleic Acids Research 44 (Database issue): D67–D72. https://doi.org/10.1093/nar/gkv1276

Colgan DJ, McLauchlan A, Wilson GDF, Livingston SP, Edgecombe GD, Macaranas J, Cassis G, Gray MR (1998) Histone H3 and U2 snRNA DNA sequences and arthropod molecular evolution. Australian Journal of Zoology 46(5): 419. https://doi.org/10.1071/ZO98048

Dalton SJ, Godwin S (2006) Progressive coral tissue mortality following predation by a corallivorous nudibranch (*Phestilla* sp.). Coral Reefs 25(4): 529–529. https://doi.org/10.1007/s00338-006-0139-0

Dayrat B, Tillier A, Lecointre G, Tillier S (2001) New clades of euthyneuran gastropods (Mollusca) from 28S rRNA sequences. Molecular Phylogenetics and Evolution 19(2): 225–235. https://doi.org/10.1006/mpev.2001.0926

Debelius H, Kuiter RH (2007) Nudibranchs of the world: 1,200 nudibranchs from around the world, 1st ed. Ikan, Frankfurt, 360 pp.

Edgar RC (2004) MUSCLE: multiple sequence alignment with high accuracy and high throughput. Nucleic Acids Research 32(5): 1792–1797. https://doi.org/10.1093/nar/gkh340

Ekimova I, Deart Y, Schepetov D (2017) Living with a giant parchment tube worm: a description of a new nudibranch species (Gastropoda: Heterobranchia) associated with the annelid *Chaetopterus*. Marine Biodiversity 49(1): 289–300. https://doi.org/10.1007/s12526-017-0795-z

Ekimova I, Valdés Á, Chichvarkhin A, Antokhina T, Lindsay T, Schepetov D (2019) Diet-driven ecological radiation and allopatric speciation result in high species diversity in a temperate-cold water marine genus *Dendronotus* (Gastropoda: Nudibranchia). Molecular Phylogenetics and Evolution 141(1): 106609. https://doi.org/10.1016/j.ympev.2019.106609

Faucci A, Toonen RJ, Hadfield MG (2007) Host shift and speciation in a coral-feeding nudibranch. Proceedings of the Royal Society B: Biological Sciences 274(1606): 111–119. https://doi.org/10.1098/rspb.2006.3685

Folmer O, Black M, Hoeh W, Lutz R, Vrijenhoek R (1994) DNA primers for amplification of mitochondrial cytochrome c oxidase subunit I from diverse metazoan invertebrates. Molecular Marine Biology and Biotechnology 3(5): 294–299.

Fukami H, Omori M, Hatta M (2000) Phylogenetic relationships in the coral family Acroporidae, reassessed by inference from mitochondrial genes. Zoological Science 17(5): 689–696. https://doi.org/10.2108/zsj.17.689

Gochfeld DJ, Aeby GS (1997) Control of populations of the coral-feeding nudibranch *Phestilla sibogae* by fish and crustacean predators. Marine Biology 130(1): 63–69. https://doi.org/10.1007/s002270050225

Goodheart JA, Bazinet AL, Valdés Á, Collins AG, Cummings MP (2017) Prey preference follows phylogeny: evolutionary dietary patterns within the marine gastropod group Cladobranchia (Gastropoda: Heterobranchia: Nudibranchia). BMC Evolutionary Biology 17(1): 221. https://doi.org/10.1186/s12862-017-1066-0

Gosliner TM, Valdes A, Behrens D (2015) Nudibranch and Sea Slug Identification: Indo-Pacific, 1st ed. New World Publications, Jacksonville, FL, 408 pp.

Gray T (2001) Elimination of a predatory nudibranch. Reeffarmers Articles. http://www.reeffarmers.com/tracygraynudi01.htm [accessed 24 November 2018]

Hadfield MG, Pennington JT (1990) Nature of the metamorphic signal and its internal transduction in larvae of the nudibranch Phestilla sibogae. Bulletin of Marine Science 46(2): 455–464.

Hadfield MG, Faucci A, Koehl MAR (2006) Measuring recruitment of minute larvae in a complex field environment: The corallivorous nudibranch *Phestilla sibogae* (Bergh). Journal of Experimental Marine Biology and Ecology 338(1): 57–72. https://doi.org/10.1016/j.jembe.2006.06.034

Hadfield MG, Carpizo-Ituarte EJ, Carmen KD, Nedved BT (2001) Metamorphic competence, a major adaptive convergence in marine invertebrate larvae. American Zoologist 41(5): 9. https://doi.org/10.1093/icb/41.5.1123

Haramaty L (1991) Reproduction effort in the nudibranch *Phestilla sibogae*: Calorimetric analysis of food and eggs. Pacific Science 45(3): 257–262.

Harris LG (1975) Studes on the life history of two coral-eating nudibranchs of the genus *Phestilla*. The Biological Bulletin 149 (3): 539–550. https://doi.org/10.2307/1540385

Henschen B (2018) *Montipora* Eating Nudibranchs | Coral Rx Don't Risk It Dip It! https://coralrx.com/2018/12/28/montipora-eating-nudibranchs/ [accessed 10 March 2019]

Hillis DM, Moritz C, Mable BK (1996) Molecular Systematics, 2nd ed. Sinauer Associates, Inc., Sunderland, Mass, 655 pp. https://doi.org/10.2307/1447682

Hoang DT, Chernomor O (2017) UFBoot2: Improving the ultrafast bootstrap approximation. Molecular Biology and Evolution 35(2): 518–522. https://doi.org/10.1093/molbev/msx281

Jones AM (2011) Raiding the coral nurseries? Diversity 3(3): 466–482. https://doi.org/10.3390/d3030466

Kalyaanamoorthy S, Minh BQ, Wong TKF, von Haeseler A, Jermiin LS (2017) ModelFinder: fast model selection for accurate phylogenetic estimates. Nature Methods 14(6): 587–589. https://doi.org/10.1038/nmeth.4285

Kearse M, Moir R, Wilson A, Stones-Havas S, Cheung M, Sturrock S, Buxton S, Cooper A, Markowitz S, Duran C, Thierer T, Ashton B, Meintjes P, Drummond A (2012) Geneious Basic: An integrated and extendable desktop software platform for the organization and analysis of sequence data. Bioinformatics 28(12): 1647–1649. https://doi.org/10.1093/bioinformatics/bts199

Kimberly C (2003) Pharmacological and molecular investigations of mechanisms of metamorphosis in the marine gastropod *Phestilla sibogae*. PhD Thesis. University of Hawai'i at Mānoa. http://hdl.handle.net/10125/3052

Korshunova T, Martynov A, Picton B (2017a) Ontogeny as an important part of integrative taxonomy in tergipedid aeolidaceans (Gastropoda: Nudibranchia) with a description of a new genus and species from the Barents Sea. Zootaxa 4324(1): 1. https://doi.org/10.11646/zootaxa.4324.1.1

Korshunova T, Martynov A, Bakken T, Picton B (2017b) External diversity is restrained by internal conservatism: New nudibranch mollusc contributes to the cryptic species problem. Zoologica Scripta 46(6): 683–692. https://doi.org/10.1111/zsc.12253

Korshunova T, Lundin K, Malmberg K, Picton B, Martynov A (2018a) First true brackish-water nudibranch mollusk provides new insights for phylogeny and biogeography and reveals paedomorphosis-driven evolution. PLoS ONE 13(3): e0192177. https://doi.org/10.1371/journal.pone.0192177

Korshunova T, Fletcher K, Lundin K, Picton B, Martynov A (2018b) The genus *Zelentia* is an amphi-boreal taxon expanded to include three new species from the North Pacific and Atlantic oceans (Gastropoda: Nudibranchia: Trinchesiidae). Zootaxa 4482(2): 297–321. https://doi.org/10.11646/zootaxa.4482.2.4

Korshunova T, Mehrotra R, Arnold S, Lundin K, Picton B, Martynov A (2019a) The formerly enigmatic Unidentiidae in the limelight again: A new species of the genus *Unidentia*

from Thailand (Gastropoda: Nudibranchia). Zootaxa 4551(5): 556–570. https://doi.org/10.11646/zootaxa.4551.5.4

Korshunova T, Martynov A, Bakken T, Evertsen J, Fletcher K, Mudianta IW, Saito H, Lundin K, Schrödl M, Picton B (2017c) Polyphyly of the traditional family Flabellinidae affects a major group of Nudibranchia: aeolidacean taxonomic reassessment with descriptions of several new families, genera, and species (Mollusca, Gastropoda). ZooKeys 717(1): 1–139. https://doi.org/10.3897/zookeys.717.21885

Korshunova T, Picton B, Furfaro G, Mariottini P, Pontes M, Prkić J, Fletcher K, Malmberg K, Lundin K, Martynov A (2019b) Multilevel fine-scale diversity challenges the "cryptic species" concept. Scientific Reports 9(1): 1–23. https://doi.org/10.1038/s41598-019-42297-5

Kumar S, Stecher G, Li M, Knyaz C, Tamura K (2018) MEGA X: Molecular Evolutionary Genetics Analysis across computing platforms. Molecular Biology and Evolution 35(6): 1547–1549. https://doi.org/10.1093/molbev/msy096

Le LV, Lecointre G, Perasso R (1993) A 28S rRNA-based phylogeny of the gnathostomes: First steps in the analysis of conflict and congruence with morphologically based cladograms. Molecular Phylogenetics and Evolution 2(1): 31–51. https://doi.org/10.1006/mpev.1993.1005

Livengood EJ, Chapman FA (2007) The ornamental fish trade: An introduction with perspectives for responsible aquarium fish ownership. Department of Fisheries and Aquatic Sciences; University of Florida/Institute of Food and Agricultural Sciences: FA123. https://agrilifecdn.tamu.edu/fisheries2/files/2013/10/The-Ornamental-Fish-Trade-An-Introduction-with-Perspectives-for-Responsible-Aquarium-Fish-Ownership.pdf

Martynov A, Mehrotra R, Chavanich S, Nakano R, Kashio S, Lundin K, Picton B, Korshunova T (2019) The extraordinary genus *Myja* is not a tergipedid, but related to the Facelinidae s. str. With the addition of two new species from Japan (Mollusca, Nudibranchia). ZooKeys 818(1): 89–116. https://doi.org/10.3897/zookeys.818.30477

Mehrotra R, Monchanin C, Scott C, Phongsuwan N, Caballer Gutiérrez M, Chavanich S, Hoeksema B (2019) Selective consumption of sacoglossan sea slugs (Mollusca: Gastropoda) by scleractinian corals (Cnidaria: Anthozoa). PLoS ONE 14(4): e0215063. https://doi.org/10.1371/journal.pone.0215063

Morton B, Blackmore G, Kwok CT (2002) Corallivory and prey choice by *Drupella rugosa* (Gastropoda: Muricidae) in Hong Kong. Journal of Molluscan Studies 68(3): 217–223. https://doi.org/10.1093/mollus/68.3.217

Nguyen L-T, Schmidt HA, von Haeseler A, Minh BQ (2015) IQ-TREE: A Fast and Effective Stochastic Algorithm for Estimating Maximum-Likelihood Phylogenies. Molecular Biology and Evolution 32(1): 268–274. https://doi.org/10.1093/molbev/msu300

Palumbi SR, Martin A, Romano S, McMillan WO, Stice L, Grabowski G (2002) The Simple Fool's Guide to PCR V2.0. Dept. of Zoology and Kewalo Marine Laboratory, University of Hawaii, Hawaii, 45 pp.

Pasquinelli AE, Reinhart BJ, Slack F, Martindale MQ, Kuroda MI, Maller B, Hayward DC, Ball EE, Degnan B, ller PM, Srinivasan A, Fishman M, Finnerty J, Corbo J, Levine M, Leahy P, Davidson E, Ruvkun G (2000) Conservation of the sequence and temporal expression of let-7 heterochronic regulatory RNA. Nature 408(6808): 86–89. https://doi.org/10.1038/35040556

Pires A, Coon SL, Hadfield MG (1997) Catecholamines and dihydroxyphenylalanine in metamorphosing larvae of the nudibranch *Phestilla sibogae* Bergh (Gastropoda: Opisthobranchia). Journal of Comparative Physiology. A, Sensory, Neural, and Behavioral Physiology 181(1): 187–194. https://doi.org/10.1007/s003590050105

Pires A, Croll R, Hadfield M (2000) Catecholamines modulate metamorphosis in the opisthobranch gastropod *Phestilla sibogae*. The Biological Bulletin 198(3): 319–331. https://doi.org/10.2307/1542688

Puillandre N, Lambert A, Brouillet S, Achaz G (2012) ABGD, Automatic Barcode Gap Discovery for primary species delimitation. Molecular Ecology 21(8): 1864–1877. https://doi.org/10.1111/j.1365-294X.2011.05239.x

Puslednik L, Serb JM (2008) Molecular phylogenetics of the Pectinidae (Mollusca: Bivalvia) and effect of increased taxon sampling and outgroup selection on tree topology. Molecular Phylogenetics and Evolution 48(3): 1178–1188. https://doi.org/10.1016/j.ympev.2008.05.006

Riddle D (2012) Aquarium Invertebrates: *Phestilla* Nudibranchs: Cryptic Enemies of *Porites*, *Goniopora*, *Tubastrea* and *Dendrophyllia* Corals and an Identification of '*Montipora*-eating Nudibranchs. Advanced Aquarist 11(6). https://www.advancedaquarist.com/2012/6/inverts

Ritson-Williams R, Shjegstad S, Paul V (2003) Host specificity of four corallivorous *Phestilla* nudibranchs (Gastropoda: Opisthobranchia). Marine Ecology Progress Series 255(1): 207–218. https://doi.org/10.3354/meps255207

Ritson-Williams R, Shjegstad SM, Paul VJ (2009) Larval metamorphosis of *Phestilla* spp. in response to waterborne cues from corals. Journal of Experimental Marine Biology and Ecology 375(1): 84–88. https://doi.org/10.1016/j.jembe.2009.05.010

Robertson R (1970) Review of the Predators and Parasites of Stony Corals, with Special Reference to Symbiotic Prosobranch Gastropods. Pacific Science 24(1): 43–54.

Ronquist F, Teslenko M, van der Mark P, Ayres DL, Darling A, Höhna S, Larget B, Liu L, Suchard MA, Huelsenbeck JP (2012) MrBayes 3.2: Efficient bayesian phylogenetic inference and model choice across a large model space. Systematic Biology 61(3): 539–542. https://doi.org/10.1093/sysbio/sys029

Rudman WB (1979) The ecology and anatomy of a new species of aeolid opisthobranch mollusc; a predator of the scleractinian coral *Porites*. Zoological Journal of the Linnean Society 65(4): 339–350. https://doi.org/10.1111/j.1096-3642.1979.tb01099.x

Rudman WB (1981) Further studies on the anatomy and ecology of opisthobranch molluscs feeding on the scleractinian coral *Porites*. Zoological Journal of the Linnean Society 71(4): 373–412. https://doi.org/10.1111/j.1096-3642.1981.tb01136.x

Rudman WB (1982) A new species of *Phestilla*; the first record of a corallivorous aeolid nudibranch from tropical America. Journal of Zoology 198(4): 465–471. https://doi.org/10.1111/jzo.1982.198.4.465

Scott C, Mehrotra R, Hoeksema B (2017) In-situ egg deposition by corallivorous snails on mushroom corals at Koh Tao (Gulf of Thailand). Journal of Molluscan Studies 83(3): 360–362. https://doi.org/10.1093/mollus/eyx020

Sela I, Ashkenazy H, Katoh K, Pupko T (2015) GUIDANCE2: accurate detection of unreliable alignment regions accounting for the uncertainty of multiple parameters. Nucleic Acids Research 43(W1): W7–W14. https://doi.org/10.1093/nar/gkv318

Veron C (2000) Corals of the World. Australian Institute of Marine Science, 1382 pp.
Wägele H, Willan RC (2000) Phylogeny of the Nudibranchia. Zoological Journal of the Linnean Society 130(1): 83–181. https://doi.org/10.1111/j.1096-3642.2000.tb02196.x
Wallace CC, Done BJ, Paul RM (2012) Revision and catalogue of world-wide staghorn corals *Acropora* and *Isopora* (Scleractinia:Acroporidae) in the Museum of Tropical Queensland. Memoirs of the Queensland Museum Nature 57: 255.

Supplementary material 1

Table S1: List of sequences used for molecular analysis

Authors: Adam Wang, Inga Elizabeth Conti-Jerpe, John Lawrence Richards, David Michael Baker

Data type: GenBank Accession Numbers

Explanation note: The species name and GenBank accessions of sequences we obtained and used for phylogenetic inference, ABGD analysis, p-distance are included within this table.

Link: https://doi.org/10.3897/zookeys.909.35278.suppl1

Supplementary material 2

S2: Phylogenetic hypotheses based upon individual COI, 16s, and H3 partial gene sequences

Authors: Adam Wang, Inga Elizabeth Conti-Jerpe, John Lawrence Richards, David Michael Baker

Data type: Newick Trees

Explanation note: The compressed file contains 6 newick tree files and are named based upon the partial gene and phylogenetic inference method that were used to generate that tree. BI = Bayesian Inference, ML = Maximum Likelihood.

Link: https://doi.org/10.3897/zookeys.909.35278.suppl2

ZooKeys 909: 25–57 (2020)
doi: 10.3897/zookeys.909.47137
http://zookeys.pensoft.net

RESEARCH ARTICLE

A peer-reviewed open-access journal
ZooKeys
Launched to accelerate biodiversity research

On eight species of jumping spiders from Xishuangbanna, Yunnan, China (Araneae, Salticidae)

Cheng Wang[1], Shuqiang Li[2]

1 *College of Agriculture and Forestry Engineering and Planning, Tongren University, Tongren 554300, Guizhou, China* **2** *Institute of Zoology, Chinese Academy of Sciences, Beijing 100101, China*

Corresponding author: *Shuqiang Li* (lisq@ioz.ac.cn)

Academic editor: *Yuri Marusik* | Received 8 October 2019 | Accepted 8 January 2020 | Published 5 February 2020

http://zoobank.org/C5846B70-4E14-4500-AF7C-751C863B0580

Citation: Wang C, Li S (2020) On eight species of jumping spiders from Xishuangbanna, Yunnan, China (Araneae, Salticidae). ZooKeys 909: 25–57. https://doi.org/10.3897/zookeys.909.47137

Abstract

Seven new species of jumping spiders collected from Xishuangbanna Tropical Botanical Garden, China are diagnosed and described: *Cytaea tongi* **sp. nov.** (♂♀), *Dexippus pengi* **sp. nov.** (♂♀), *Euophrys subwanyan* **sp. nov.** (♂♀), *Gelotia liuae* **sp. nov.** (♂♀), *Irura lvshilinensis* **sp. nov.** (♂♀), *Rhene menglunensis* **sp. nov.** (♂♀), and *Siler zhangae* **sp. nov.** (♂). The female of *Gelotia zhengi* Cao & Li, 2016 is described for the first time.

Keywords

Morphology, new species, salticid, South China, taxonomy

Introduction

Of the 6173 jumping spider species known worldwide (WSC 2020), more than 500 species and nearly 125 genera have been recorded from China (Metzner 2020). Of these, at least 30 species in 26 genera have been described as new from Xishuangbanna in Yunnan, South China (Peng and Yin 1991; Song 1991; Peng 1995; Xie and Peng

1995; Peng and Kim 1997; Song and Zhu 1998; Xiao 2002; Xiao and Wang 2004; Cao and Li 2016). Despite the collecting conducted in the region, new species, typically known by only a single sex, are frequently discovered, which indicates that jumping spider fauna in Xishuangbanna is understudied, with the true diversity remaining elusive.

Recently, several expeditions to Xishuangbanna Tropical Botanical Garden (XTBG) were carried out by colleagues from the Chinese Academy of Sciences, and more jumping spiders were collected. In this paper, seven new species are described in addition to the female of *Gelotia zhengi* Cao & Li, 2016 for the first time.

Material and methods

Specimens were mainly collected by fogging, beating shrubs, and hand collecting from the tree canopy, tree trunks, and leaf litter in the tropical rainforest of Xishuangbanna, Yunnan, China. All specimens were preserved in 75% ethanol. All specimens are deposited in the Institute of Zoology, Chinese Academy of Sciences (IZCAS) in Beijing, China.

The specimens were examined with an Olympus SZX16 stereomicroscope. After dissection, the epigyne was cleared in trypsin enzyme solution before examination and imaging. Left male palps were used for the description and illustration. Photos of the copulatory organs and habitus were taken with a Kuy Nice CCD mounted on an Olympus BX53 compound microscope. Compound focus images were generated using Helicon Focus v. 6.7.1.

All measurements are given in millimeters. Leg measurements are given as: total length (femur, patella + tibia, metatarsus, tarsus). References to figures in the cited papers are listed in lowercase type (fig. or figs); figures in this paper are noted with an initial capital (Fig. or Figs). Abbreviations used in the text and figures are as follows:

AERW anterior eye row width;
ALE anterior lateral eye;
AME anterior median eye;
AR anterior chamber of receptacle;
BR body of receptacle;
C conductor;
CD copulatory duct;
CO copulatory opening;
CP cymbial process;
E embolus;
EFL eye field length;
FD fertilization duct;
F fold;
ICR intermediate canal of receptacle;
H hood;
HR head of receptacle;
PERW posterior eye row width;
PLE posterior lateral eye;
PME posterior median eye;
PR posterior chamber of receptacle;
PTA prolateral tibial apophysis;
RPA retrolateral patella apophysis;
RTA retrolateral tibial apophysis;
R receptacle;
S septum;
SD sperm duct;
VTA ventral tibial apophysis;
W window.

Taxonomy

Family Salticidae Blackwall, 1841

Genus *Cytaea* Keyserling, 1882

Type species. *Cytaea alburna* Keyserling, 1882 from Australia.

Comments. The genus *Cytaea* contains 41 nominal species and is currently known from the Asia and Oceania. It is rather poorly studied, as more than half (22) of its species are only known from a single sex and some species have no diagnostic illustrations and can not be confidently identified.

***Cytaea tongi* sp. nov.**

http://zoobank.org/38F11BF9-1DFA-4059-AD56-76522CB34B79

Figs 1, 2, 17A, 18A, 19A

Type material. ***Holotype*** ♂ (IZCAS Ar 39756) CHINA: Yunnan: Xishuangbanna, Mengla County, Menglun Town, Menglun Nature Reserve, Xishuangbanna Tropical Botanical Garden, tropical rainforest (21°55.20'N, 101°16.21'E, ca 550 m), 26.04.2019, Y.F. Tong et al. leg. ***Paratypes*****:** 2♂ 4♀ (IZCAS Ar 39757–39762), same data as holotype; 1♀ (IZCAS Ar 39763), garbage dump, secondary tropical rainforest (21°54.33'N, 101°16.79'E, ca 620 m), 7.05.2019, Y.F. Tong et al. leg; 1♂ (IZCAS Ar 39764), Leprosy Village (21°53.62'N, 101°18.25'E, ca 520 m), 29.04.2019, Y.F. Tong et al. leg; 1♀ (IZCAS Ar 39765), Leprosy Village (21°53.59'N, 101°17.30'E, ca 550 m), 4.05.2019, Y.F. Tong et al. leg.

Etymology. The specific name is a patronym after Yanfeng Tong (Shenyang, China), one of the collectors of the new species.

Diagnosis. *Cytaea tongi* sp. nov. resembles *C. oreophila* Simon, 1902 known from Indonesia and Singapore by the shape of the copulatory organs and habitus but differs in the following: 1) the RTA is curved towards the bulb medially in ventral view (Fig. 1C), whereas it is curved towards the bulb terminally in *C. oreophila* (Zhang and Maddison 2015, fig. 554); 2) the RTA is S-shaped and tapering in retrolateral view (Fig. 1B), whereas it is straight and broadening in *C. oreophila* (Zhang and Maddison 2015, fig. 555); 3) the epigynal window occupies about two-thirds of the epigynal plate (Fig. 2A, B), whereas it occupies more than nine-tenths of the plate in *C. oreophila* (Zhang and Maddison 2015, fig. 557). The male of *C. tongi* sp. nov. also resembles those of *C. carolinensis* Berry, Beatty & Prószyński, 1998, known from Caroline Island, by the shape of male palp but differs by the following: 1) the RTA is strongly curved medially in ventral view (Fig. 1C), whereas it is straight in *C. carolinensis* (Berry et al. 1998, fig. 8); 2) the tip of the RTA is blunt in retrolateral view (Fig. 1B), whereas it is pointed in *C. carolinensis* (Berry et al. 1998, fig. 9).

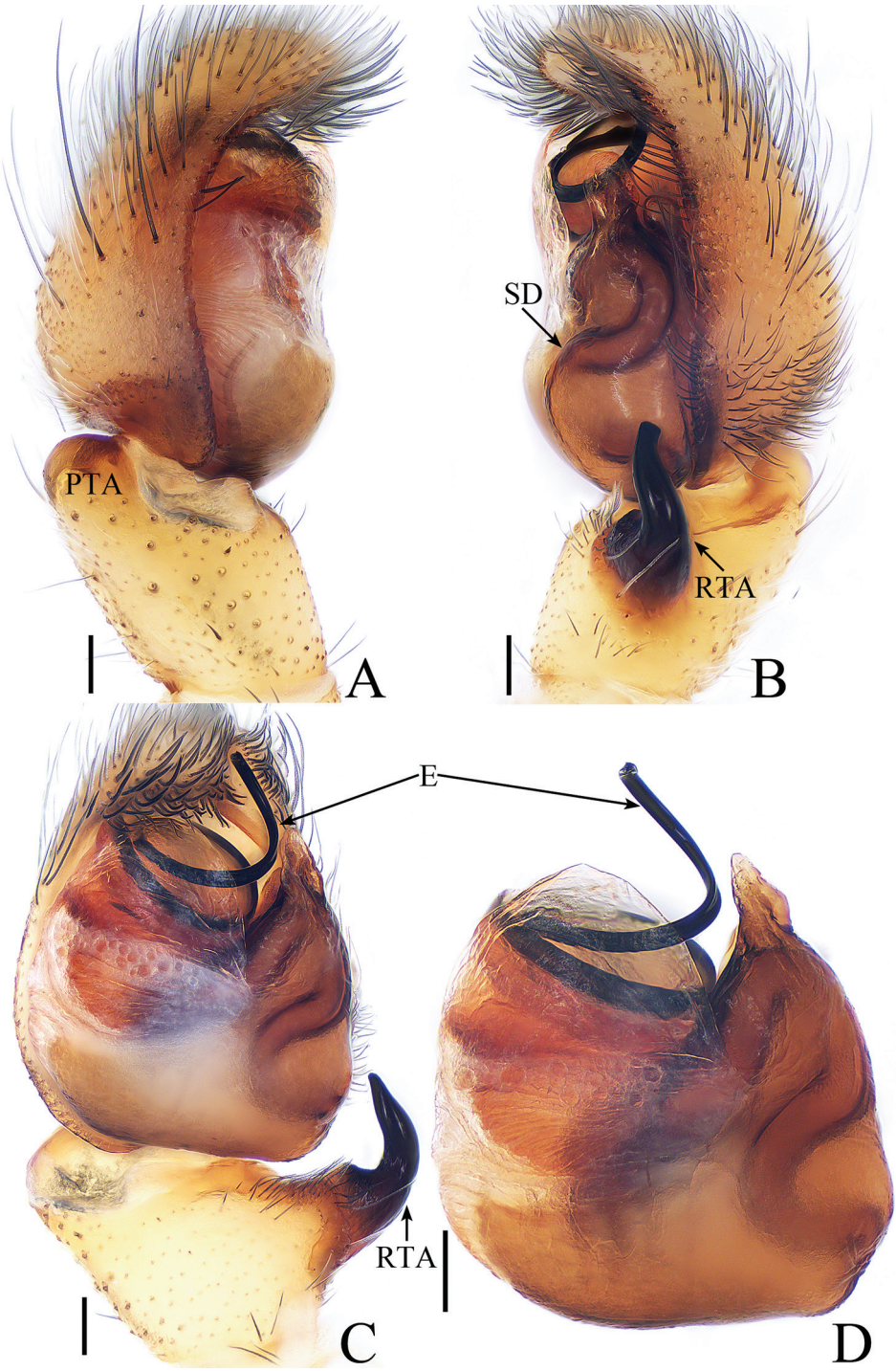

Figure 1. Male palp of *Cytaea tongi* sp. nov., **A**–**C** holotype; **D** paratype. **A** prolateral **B** retrolateral **C** ventral **D** bulb, ventral. Scale bars: 0.1.

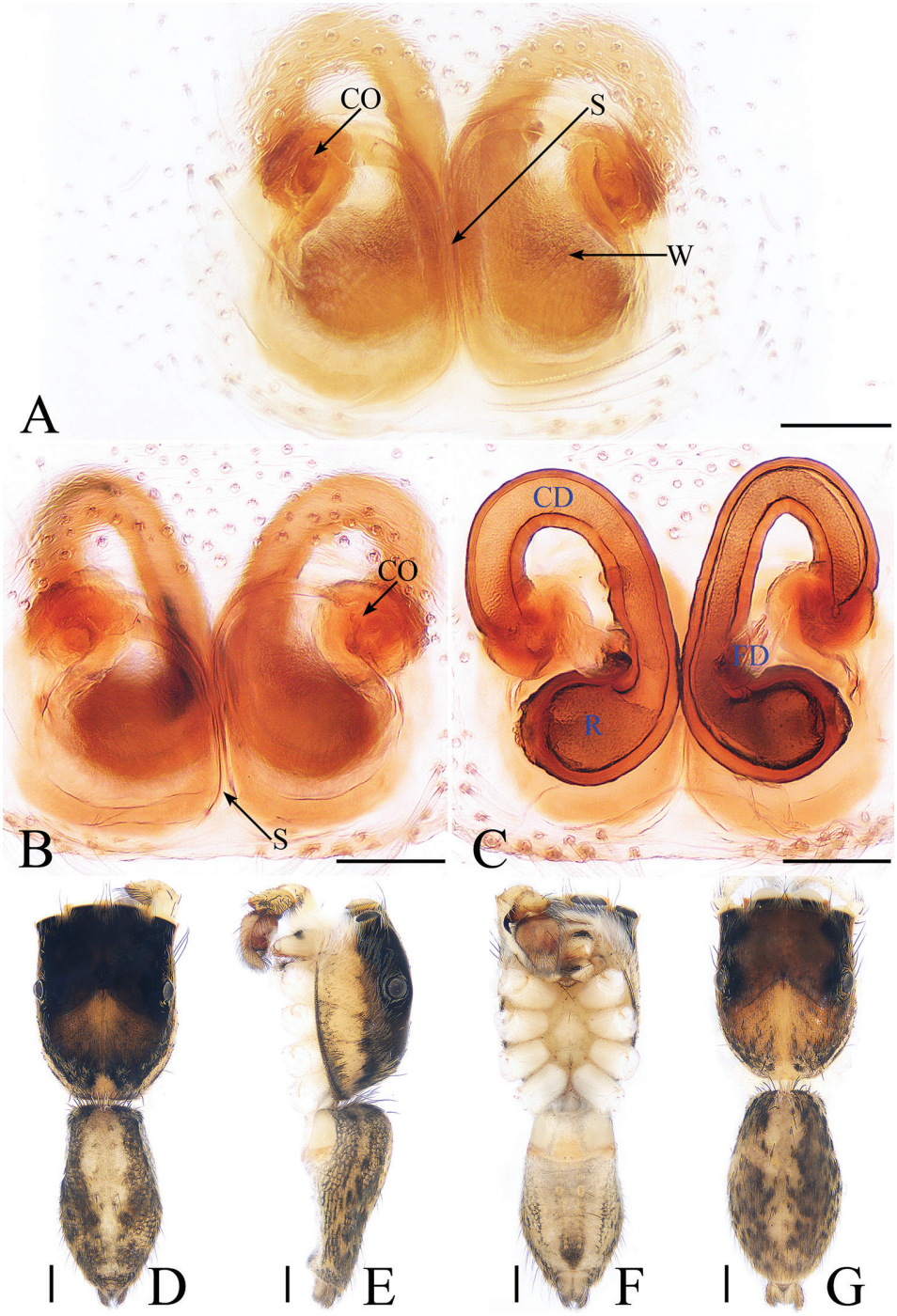

Figure 2. *Cytaea tongi* sp. nov., female paratype and male holotype. **A**, **B** epigyne, ventral **C** epigyne, dorsal **D** holotype habitus, dorsal **E** holotype habitus, lateral **F** holotype habitus, ventral **G** female paratype habitus, dorsal. Scale bars: 0.1 (**A**–**C**); 0.5 (**D**–**G**).

Description. ***Male*****.** Total length 5.09. Carapace 2.46 long, 1.87 wide. Abdomen 2.52 long, 1.37 wide. Clypeus 0.14 high. Eye sizes and inter-distances: AME 0.46, ALE 0.32, PLE 0.28, AERW 1.83, PERW 1.87, EFL 1.15. Legs: I 6.11 (1.63, 2.66, 1.22, 0.60), II 5.55 (1.63, 2.15, 1.22, 0.55), III 5.81 (1.80, 1.95, 1.46, 0.60), IV 6.04 (1.90, 2.05, 1.49, 0.60). Carapace (Figs 2D–F, 17A) yellow-brown to dark-brown, with dense white and yellow scale-like setae around eyes, stripes of yellow setae posteriorly. Fovea longitudinal, situated between PLEs. Clypeus yellow, covered with dense white setae. Chelicerae (Fig. 18A) pale yellow with 5 promarginal teeth and 1 retromarginal fissident with 2 cusps. Endites, labium, and sternum colored as chelicerae. Legs pale yellow except dorsum of femora green. Spination of leg I: femur d1-1-5; patella p0-1-1, r0-1-0; tibia d1-0-0, p1-2-0, r1-2-0, v2-2-2; metatarsus p2-0-2, v2-0-2. Abdomen (Fig. 2D–F) elongated oval, dorsum with 2 pairs of muscle depressions medially, irregular pale yellow stripe nearly extending across the entire surface and bifurcated posteriorly, covered with dense brown setae and sparse, long setae; venter pale brown, with 2 rows of spots medially and a large dark spot close to the spinnerets. Palp (Fig. 1A–D): femur yellow, about 2.5 times longer than wide, covered with setae; patella colored as femur, almost as long as wide, covered with white setae; tibia stocky, slightly wider than long, with lobe-shaped prolateral apophysis and sclerotized, hook-shaped RTA curved towards bulb medially; cymbium longer than wide, covered with dense setae; bulb approximately as long as wide, retrolatero-terminally with 2 round processes; embolus long, completing nearly full flattened coil at base, the base of the embolus mostly hidden by membranous structure on bulb, with blunt tip that reaches cymbial tip.

Female**.** Total length 5.26. Carapace 2.41 long, 1.91 wide. Abdomen 2.63 long, 1.54 wide. Clypeus 0.15 high. Eye sizes and inter-distances: AME 0.46, ALE 0.32, PLE 0.27, AERW 1.83, PERW 1.87, EFL 1.15. Legs: I 5.31 (1.59, 2.12, 1.05, 0.55), II 4.75 (1.59, 1.66, 0.95, 0.55), III 5.33 (1.63, 1.88, 1.27, 0.55), IV 5.50 (1.71, 1.90, 1.34, 0.55). Habitus (Fig. 2G) similar to those of male except paler. Epigyne (Fig. 2A–C) almost as long as wide, windows large, separated by narrow septum; copulatory openings almost round, situated latero-medially; copulatory ducts extremely short, inverse U-shaped; receptacles oval, about 1.5 times the diameter of the copulatory ducts; fertilization ducts membranous, lamellar.

Distribution. China (Yunnan).

Comments. Although differing greatly from the type species of the genus, we place the new species in *Cytaea* because it is similar to *C. oreophila* and *C. carolinensis*, two species already placed in this genus.

Dexippus Thorell, 1891

Type species. *Dexippus kleini* Thorell, 1891 from Indonesia.

Comments. The poorly known genus *Dexippus* contains three species, one endemic each to Indonesia, India, and China. Two are known from males, and *D. to-*

pali Prószyński, 1992 is known from both sexes. There are three papers that provide diagnostic illustrations of the type species and descriptions of the two other species (Prószyński 1984, 1992; Peng and Li 2002).

***Dexippus pengi* sp. nov.**
http://zoobank.org/06321D4E-4D79-4385-AC9A-0AFFA338983F
Figs 3, 4, 17C, 18C, 19C

Type material. ***Holotype*** ♂ (IZCAS Ar 39771) CHINA: Yunnan: Xishuangbanna, Mengla County, Menglun Town, Menglun Nature Reserve, Mannanxing Village (21°53.49'N, 101°17.12'E, ca 560 m), 9.08.2018, C. Wang et al. leg. ***Paratypes*****:** 2♂ 2♀ (IZCAS Ar 39772–39775), same data as holotype; 2♀ (IZCAS Ar 39776–39777), same locality, tropical rainforest (21°55.35'N, 101°16.36'E, ca 610 m), 7.08.2018, C. Wang et al. leg; 1♂ 1♀ (IZCAS Ar 39778–39779), same locality, tropical rainforest (21°55.05'N, 101°16.24'E, ca 570 m), 26.07.2018, X.Q. Mi et al. leg; 1♂ (IZCAS Ar 38780), Leprosy Village (21°53.59'N, 101°17.30'E, ca 550 m), 4.05.2019, Y.F. Tong et al. leg; 2♂ (IZCAS Ar 39781–39782), same locality, Vine Garden (21°55.80'N, 101°45.41'E, ca 550 m), 2.08.2018, C. Wang et al. leg; 1♂ 3♀ (IZCAS Ar 39783–39786), same locality, tropical rainforest (21°55.20'N, 101°16.21'E, ca 550 m), 30.04.2019, Y.F. Tong et al. leg.

Etymology. The specific name is a patronym in honor of Dr Xianjin Peng (Changsha, China), who has produced many important works on the taxonomy of Chinese jumping spiders.

Diagnosis. *Dexippus pengi* sp. nov. resembles *D. topali* Prószyński, 1992 from India by the shape of the copulatory organs and habitus but differs in the following: 1) palpal tibia is longer than wide (Fig. 3B–C), whereas it is wider than long in *D. topali* (Prószyński 1992, figs 12, 13); 2) the dorsal ramus of the RTA is thorn-like in retrolateral view (Fig. 3C), whereas it is not developed in *D. topali* (Prószyński 1992, fig. 13); 3) in the female, the copulatory openings are separated by a septum (Fig. 4A), whereas they are covered by a bell-shaped structure in *D. topali* (Prószyński 1992, fig. 14).

Description. ***Male*****.** Total length 5.37. Carapace 2.76 long, 2.17 wide. Abdomen 2.41 long, 1.61 wide. Clypeus 0.09 high. Eye sizes and inter-distances: AME 0.57, ALE 0.37, PLE 0.35, AERW 2.07, PERW 2.07, EFL 1.30. Legs: I 5.10 (1.63, 2.05, 0.83, 0.59), II 4.62 (1.24, 2.01, 0.78, 0.59), III 5.25 (1.73, 1.88, 1.05, 0.59), IV 5.69 (1.90, 1.93, 1.27, 0.59). Carapace (Figs 4C–E, 17C) orange-brown, cephalic part darker, clothed with dense setae antero-bilaterally, thoracic part sloping abruptly, clothed with orange-brown and dark setae around eyes. Fovea longitudinal. Clypeus orange-brown to dark brown, covered with thin setae. Chelicerae (Fig. 18C) red-brown, with 1 retromarginal tooth and 2 promarginal teeth. Endites red-brown, inner tip pale. Labium dark brown, tip pale and covered with dark setae. Sternum yellow, covered with dark and grey-white setae. Legs red-brown, patella and tibia I with scopulae, legs III, IV paler. Spination of leg I: femur d0-1-5; patella p0-1-0; tibia

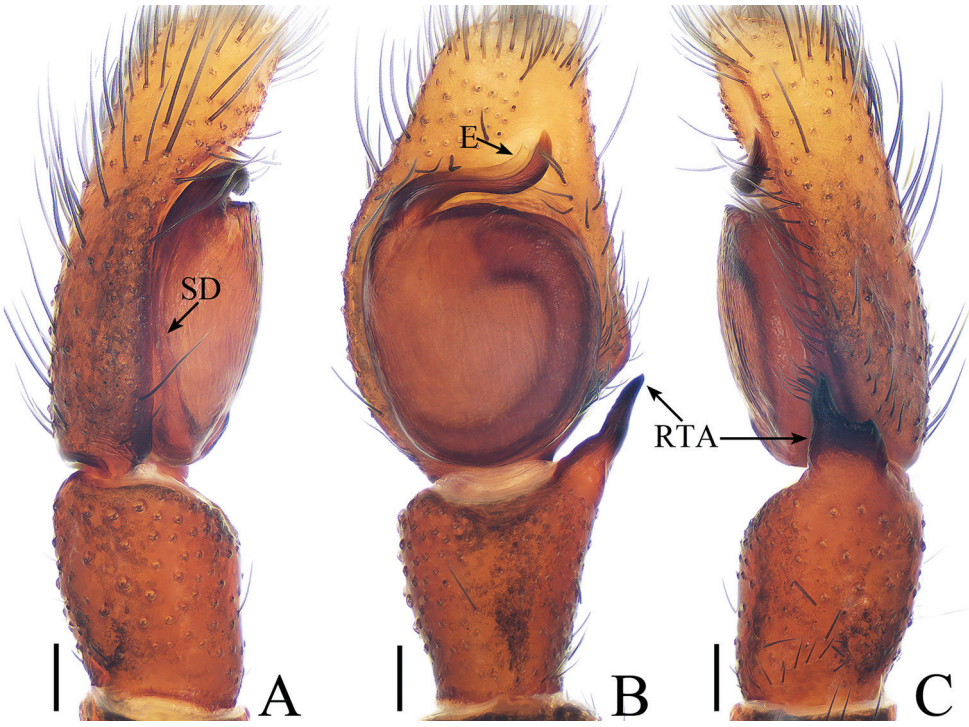

Figure 3. Male palp of *Dexippus pengi* sp. nov., holotype. **A** prolateral **B** ventral **C** retrolateral. Scale bars: 0.1.

d1-0-0, p1-1-0, r1-1-0, v2-2-2; metatarsus p0-0-1, v2-0-2. Abdomen (Fig. 4C–E) elongated oval, dorsum with 2 pairs of muscle depressions, irregular black-brown stripes, several chevrons postero-medially; venter pale brown, with dark spots. Palp (Fig. 3A–C): femur red-brown, about 3.3 times longer than wide, covered with dense setae; patella red-brown, slightly longer than wide; tibia distinctly longer than wide, RTA bifurcated with ventral ramus well-developed, tapering to a pointed tip, dorsal ramus thorn-like; cymbium flattened, covered with long setae; bulb almost round, with sperm duct extending along margin; embolus stout, originating near 10 o'clock position of bulb.

***Female*.** Total length 4.77. Carapace 2.21 long, 1.75 wide. Abdomen 2.60 long, 1.87 wide. Clypeus 0.09 high. Eye sizes and inter-distances: AME 0.55, ALE 0.31, PLE 0.27, AERW 1.69, PERW 1.69, EFL 1.06. Legs: I 3.78 (1.17, 1.56, 0.61, 0.44), II 3.76 (1.22, 1.49, 0.61, 0.44), III 4.60 (1.59, 1.54, 0.93, 0.54), IV 4.91 (1.59, 1.76, 1.02, 0.54). Habitus (Fig. 4F) similar to those of male except paler. Epigyne (Fig. 4A, B) wider than long, with pair of hoods near epigastral furrow; copulatory openings situated medially, separated by anchor-shaped septum; copulatory ducts relatively stout, ascending before extending almost transversely to connect with receptacles; receptacles divided into oval head and body.

Distribution. China (Yunnan).

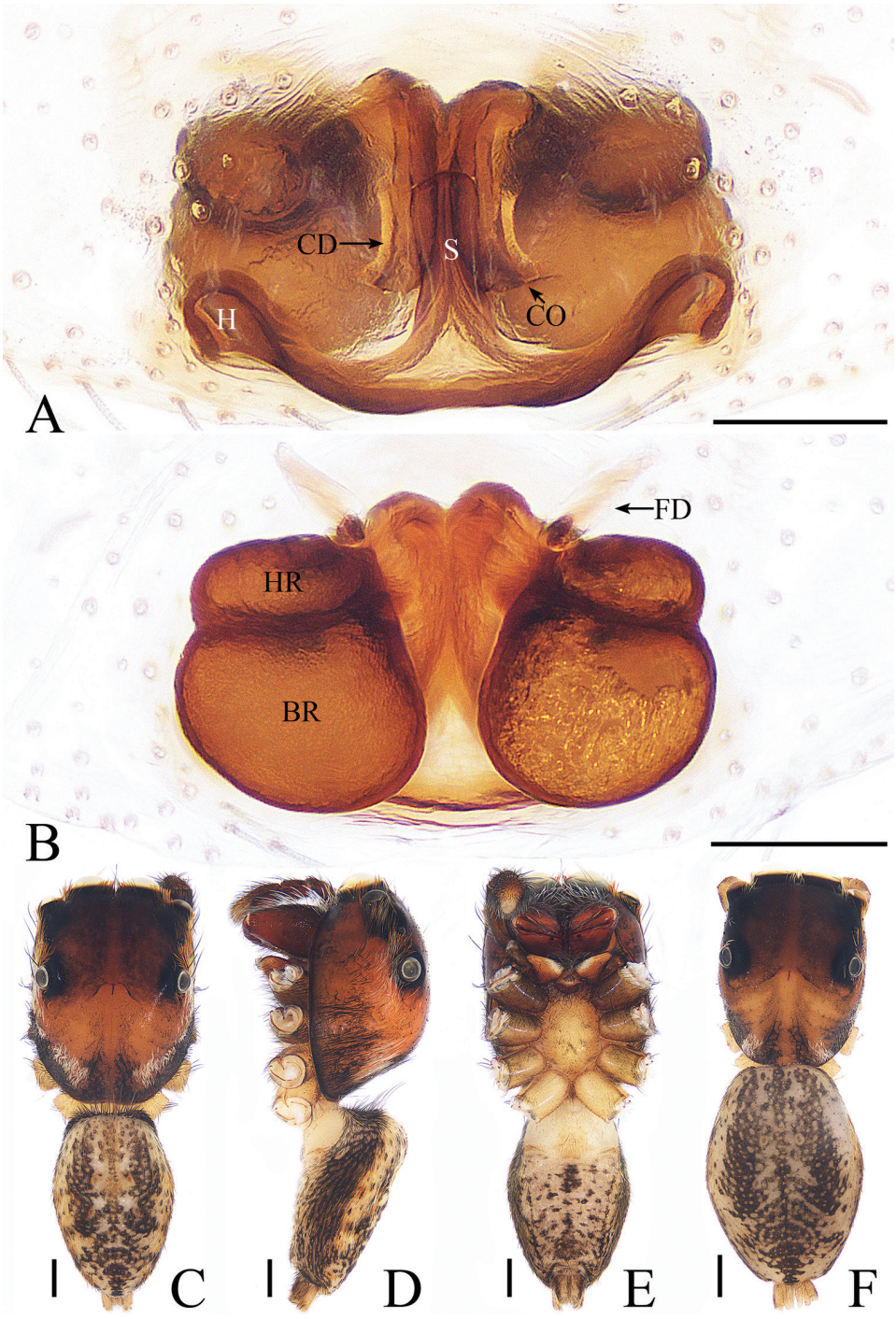

Figure 4. *Dexippus pengi* sp. nov., female paratype and male holotype. **A** epigyne, ventral **B** epigyne, dorsal **C** holotype habitus, dorsal **D** holotype habitus, lateral **E** holotype habitus, ventral **F** female paratype habitus, dorsal. Scale bars: 0.1 (**A**–**B**); 0.5 (**C**–**F**).

Euophrys C.L. Koch, 1834

Type species. *Aranea frontalis* Walckenaer, 1802 from France.

Comments. The genus *Euophrys* is one of the largest genera of the family Salticidae, currently containing 108 nominal species from the Holarctic, Afrotropical, and Neotropical realms (Prószyński et al. 2018; WSC 2020). The genus is rather poorly studied with 57 species only known from a single sex; some poorly known species have no diagnostic illustrations, and many species are pending re-classification (Prószyński et al. 2018; WSC 2020). To date, 34 species have been recorded from Asia. Of these, 19 species are known from only a single sex: eight males and 11 females. Seven species lack diagnostic illustrations, and one species is known from a description of a juvenile specimen. Presently, 12 species from China have diagnostic illustrations, including seven endemics. Five of these are known from only a single sex (WSC 2020).

Euophrys subwanyan sp. nov.

http://zoobank.org/7F4D8CE5-556C-4781-B226-D6017DB7BF7B
Figs 5, 6, 17B, 18B, 19B

Type material. ***Holotype*** ♂ (IZCAS Ar 39766) CHINA: Yunnan: Xishuangbanna, Mengla County, Menglun Town, Menglun Nature Reserve, Xishuangbanna Tropical Botanical Garden, Vine Garden (21°55.80'N, 101°45.41'E, ca 550 m), 2.08.2018, C. Wang et al. leg. ***Paratypes*****:** 1♂ 3♀ (IZCAS Ar 39767–39770), same data as holotype.

Etymology. The specific epithet is referring to the similarity with *E. wanyan* Berry, Beatty & Prószyński, 1996, substantive.

Diagnosis. *Euophrys subwanyan* sp. nov. resembles *E. wanyan* known from Caroline Island in the Eastern Pacific by the shape of the copulatory organs and habitus but differs by the following: 1) the embolus is directed anteriorly (Fig. 5C), whereas it is directed towards the cymbial prolateral margin in *E. wanyan* (Berry et al. 1996, fig. 55); 2) the tip of the RTA is directed anteriorly (Fig. 5C), whereas it is directed prolaterally in *E. wanyan* (Berry et al. 1996, fig. 55); 3) the copulatory ducts are coiled in a 360° spiral (Fig. 6C), whereas they are coiled in a 150° spiral in *E. wanyan* (Berry et al. 1996, fig. 58).

Description. ***Male*****.** Total length 3.46. Carapace 1.86 long, 1.38 wide. Abdomen 1.67 long, 1.11 wide. Clypeus 0.07 high. Eye sizes and inter-distances: AME 0.43, ALE 0.29, PLE 0.25, AERW 1.48, PERW 1.33, EFL 0.92. Legs: I 3.61 (1.10, 1.37, 0.63, 0.51), II 3.05 (0.93, 1.12, 0.54, 0.46), III 3.49 (1.10, 1.15, 0.73, 0.51), IV 3.74 (1.20, 1.27, 0.76, 0.51). Carapace (Figs 6D–F, 17B) dark brown, cephalic part almost square, thoracic part sloping abruptly, bilaterally with scattered white setae. Fovea longitudinal, bar-shaped. Clypeus dark. Chelicerae (Fig. 18B) red-brown, with 2 promarginal teeth and 1 retromarginal tooth. Endites, labium and sternum colored as chelicerae. Sternum slightly longer than wide, covered with dark setae. Legs yellow to brown. Spination of leg I: femur d1-1-1; tibia v2-2-2; metatarsus p1-0-0, v2-0-2.

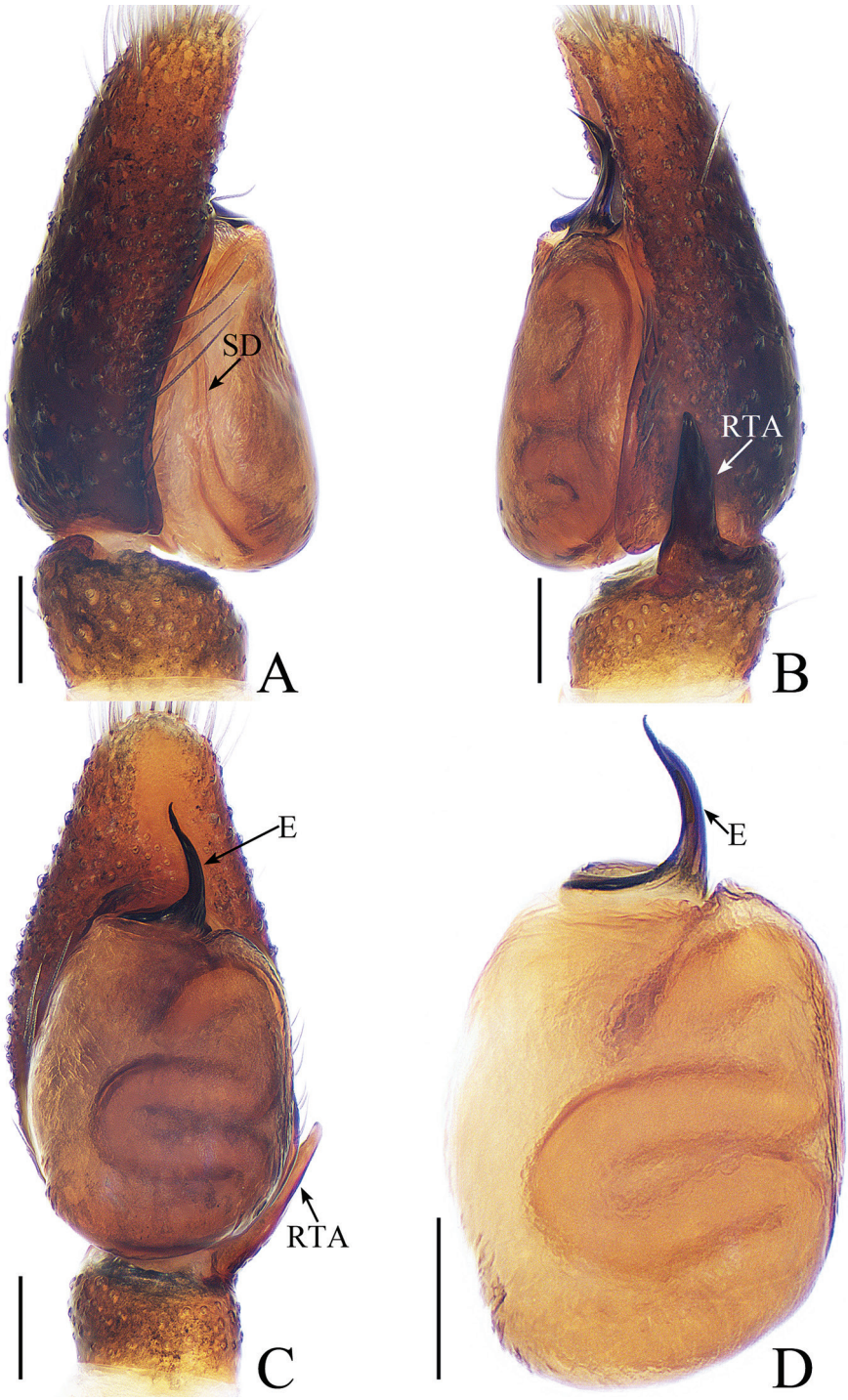

Figure 5. Male palp of *Euophrys subwanyan* sp. nov., **A**–**C** holotype **D** paratype **A** prolateral **B** retrolateral **C** ventral **D** bulb, ventral. Scale bars: 0.1.

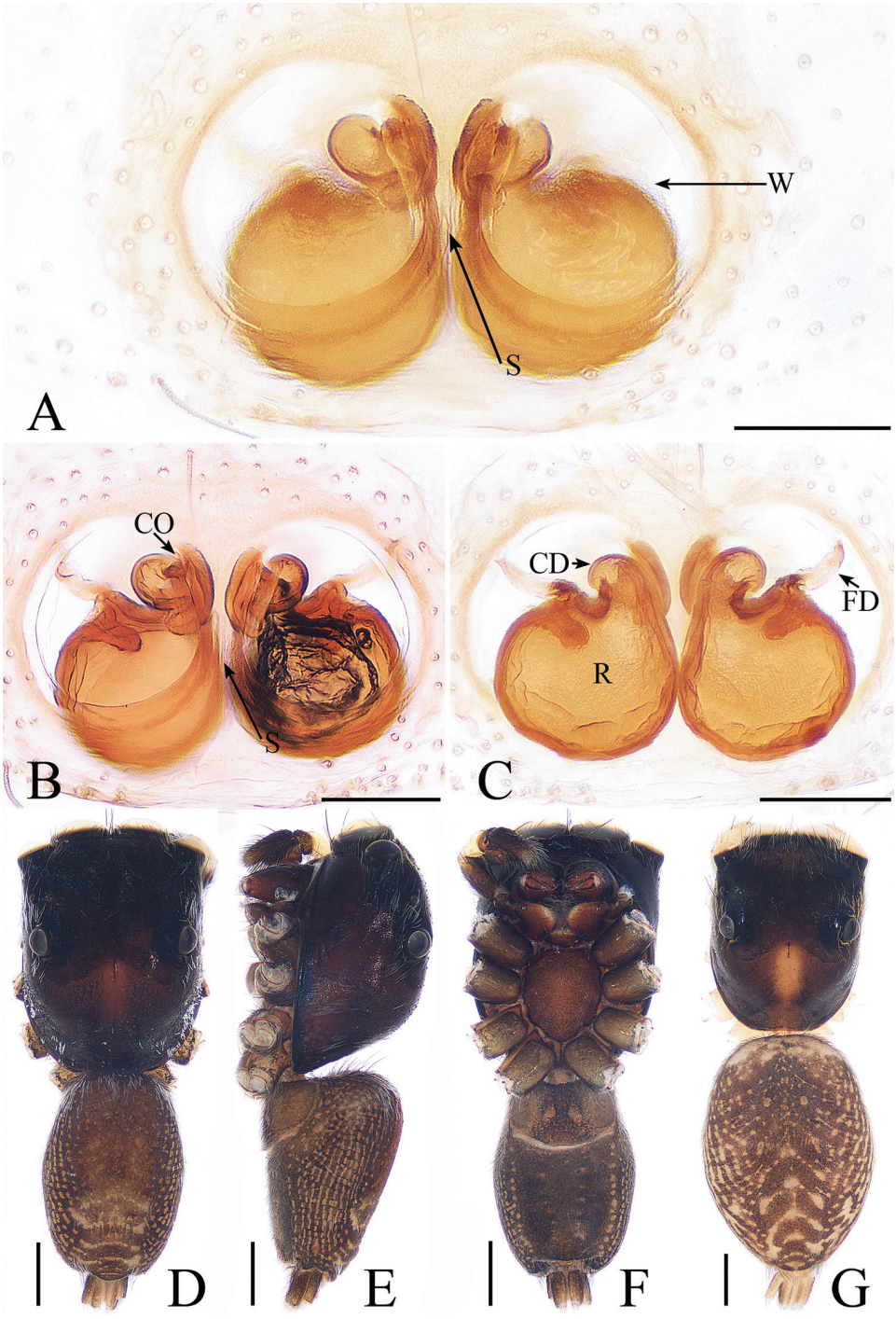

Figure 6. *Euophrys subwanyan* sp. nov., female paratype and male holotype. **A**, **B** epigyne, ventral **C** epigyne, dorsal **D** holotype habitus, dorsal **E** holotype habitus, lateral **F** holotype habitus, ventral **G** female paratype habitus, dorsal. Scale bars: 0.1 (**A**–**C**); 0.5 (**D**–**G**).

Abdomen (Fig. 6D–F) elongated oval, speckled bilaterally, dorsum with a scutum covering anterior half, 2 pairs of muscle depressions located medially, and several chevrons posteriorly, covered with white setae, denser at anterior margin; venter dark brown, with 4 rows of spots. Palp (Fig. 5A–D): femur red-brown, about 3 times longer than wide; patella yellow, slightly longer than wide; tibia wider than long, with relatively long RTA slightly longer than tibia in retrolateral view, tapering to a slightly pointed tip; cymbium red-brown, longer than wide, widest medially; bulb longer than wide, with sperm duct relatively stout, meandering retrolaterally and tapering prolaterally; embolus with a coiled base that is perpendicular to the long axis of the palp, slightly curved medially, tip of embolus directed anteriorly.

Female. Total length 4.18. Carapace 1.82 long, 1.43 wide. Abdomen 2.29 long, 1.63 wide. Clypeus 0.07 high. Eye sizes and inter-distances: AME 0.47, ALE 0.33, PLE 0.28, AERW 1.83, PERW 1.87, EFL 1.15. Legs: I 3.70 (1.10, 1.41, 0.63, 0.56), II 3.39 (1.12, 1.17, 0.59, 0.51), III 3.93 (1.24, 1.34, 0.83, 0.52), IV 4.34 (1.32, 1.46, 1.02, 0.54). Habitus (Fig. 6G) similar to that of male except paler. Epigyne (Fig. 6A–C) slightly wider than long, windows large, separated by narrow septum; copulatory openings on each side of septum located anteriorly; copulatory ducts curved anteriorly, then coiled 360° to connect with anterior edge of the receptacles; receptacles spherical, touching medially; fertilization ducts originating from the median anterior edge of receptacles, extending almost transversely.

Distribution. China (Yunnan).

Comments. The new species has been assigned to this genus due to similarity to *E. wanyan*. However, both species differ from the type species, *E. frontalis* (Walckenaer, 1802) (i.e. the face without coloured eyebrows, versus distinct eyebrows in *E. frontalis*; embolic base perpendicular to the long axis of the palp, versus parallel to the long axis of the palp in *E. frontalis*; RTA is not needle-shaped). Prószyński et al. (2018) doubted the placement *E. wanyan* in *Euophrys* and listed it as "*Euophrys*[?] *wanyan*". Therefore, the generic placement of the new species is provisional.

Gelotia Thorell, 1890

Type species. *Gelotia frenata* Thorell, 1890 from Indonesia.

Comments. The genus *Gelotia* contains nine nominal species currently known from East and South Asia, peninsular Malaysia through the Indonesian archipelago to New Guinea (Wijesinghe 1991; WSC 2020). All species are endemic and each is known from a single country, except for *G. syringopalpis* Wanless, 1984, which is distributed in China, Malaysia, and Borneo. Although the genus was revised by Wanless (1984) and all species have diagnostic illustrations, six species, including the generotype, are known from only a single sex, indicating that *Gelotia* remains inadequately studied. To date, six species are recorded from Southeast Asia and only two, *G. syringopalpis* and *G. zhengi* Cao & Li, 2016, from China (WSC 2020).

***Gelotia liuae* sp. nov.**
http://zoobank.org/DFE83826-81FE-49AF-8AA1-1C07AE506308
Figs 7, 8, 17D, 18D, 19D

Gelotia sp.: Maddison et al. 2014: 68, fig. 7 (♂).

Type material. ***Holotype*** ♂ (IZCAS Ar 39787) CHINA: Yunnan: Xishuangbanna, Mengla County, Menglun Town, Menglun Nature Reserve, Xishuangbanna Tropical Botanical Garden, tropical rainforest (21°55.20'N, 101°16.21'E, ca 550 m), 30.04.2019, Y.F. Tong et al. leg. ***Paratypes*****:** 3♂ 2♀ (IZCAS Ar 39788–39792), same data as holotype; 1♀ (IZCAS Ar 39793), tropical rainforest (21°55.20'N, 101°16.21'E, ca 550 m), 5.08.2018, C. Wang et al. leg; 1♀ (IZCAS Ar 39794), tropical rainforest (21°55.05'N, 101°16.24'E, ca 570 m), 26.07.2018, X.Q. Mi et al. leg.

Etymology. The specific name is a patronym after Shijia Liu (Shenyang, China), one of the collectors of the new species.

Diagnosis. The male of *G. liuae* sp. nov. resembles *G. syringopalpis*, known from Southeast Asia, in having 3 palpal tibial apophyses, a slender embolus, and a flattened tegulum but differs in the following: 1) the RTA is directed towards 7:30 o'clock in retrolateral view (Fig. 7B), whereas it is directed towards about 6 o'clock in *G. syringopalpis* (Wanless 1984, fig. 21D); 2) the dorsal tibial apophysis is obscured in ventral view and directed towards 3 o'clock in retrolateral view (Fig. 7B, C), whereas it is conspicuous and directed towards 1 o'clock in *G. syringopalpis* (Wanless 1984, fig. 21D, I). The female of the new species resembles *G. frenata* from Indonesia by the epigyne having a similar anterior sclerotized fold but differs in the following: 1) the receptacle is distant from the epigastral fold, the distance between them about half the length of the receptacle in dorsal view (Fig. 8B), whereas they are near the epigastral fold in *G. frenata*, with the distance between them less than one-tenth the length of the receptacle (Prószyński 1969, fig. 7); 2) the copulatory ducts width are about one-third the width of the receptacle (Fig. 8B), whereas the ducts are less than one-eighth the width of the receptacle in *G. frenata* (Prószyński 1969, fig. 7).

Description. ***Male*****.** Total length 4.04. Carapace 2.08 long, 1.67 wide. Abdomen 2.12 long, 1.27 wide. Clypeus 0.10 high. Eye sizes and inter-distances: AME 0.49, ALE 0.29, PLE 0.25, AERW 1.62, PERW 1.59, EFL 1.08. Legs: I 5.13 (1.49, 1.88, 1.15, 0.61), II 4.78 (1.41, 1.68, 1.10, 0.59), III 4.59 (1.34, 1.56, 1.10, 0.59), IV 6.33 (1.80, 2.12, 1.80, 0.61). Carapace (Figs 8C–E, 17D) brown, darker in eye field, cephalic area almost square, covered with setae around eyes, thoracic part sloping acutely, with posterior marginal cambered stripes of white and black setae. Fovea longitudinal. Clypeus yellow, the anterior margin with long setae. Chelicerae (Fig. 18D) yellow, with 3 promarginal and 5 retromarginal teeth. Endites yellow. Labium brown. Sternum colored as endites, covered with sparse setae. Legs yellow to brown. Spination of leg I: femur d1-1-4; patella p0-1-0, r0-1-0; tibia d1-0-0, p0-1-1, r0-1-1, v2-2-2; metatarsus p1-1-0, r1-1-0, v2-0-2. Abdomen (Fig. 8C–E) elongated oval, dorsum speckled, with 2 pairs of muscle depressions medially, 2 transverse

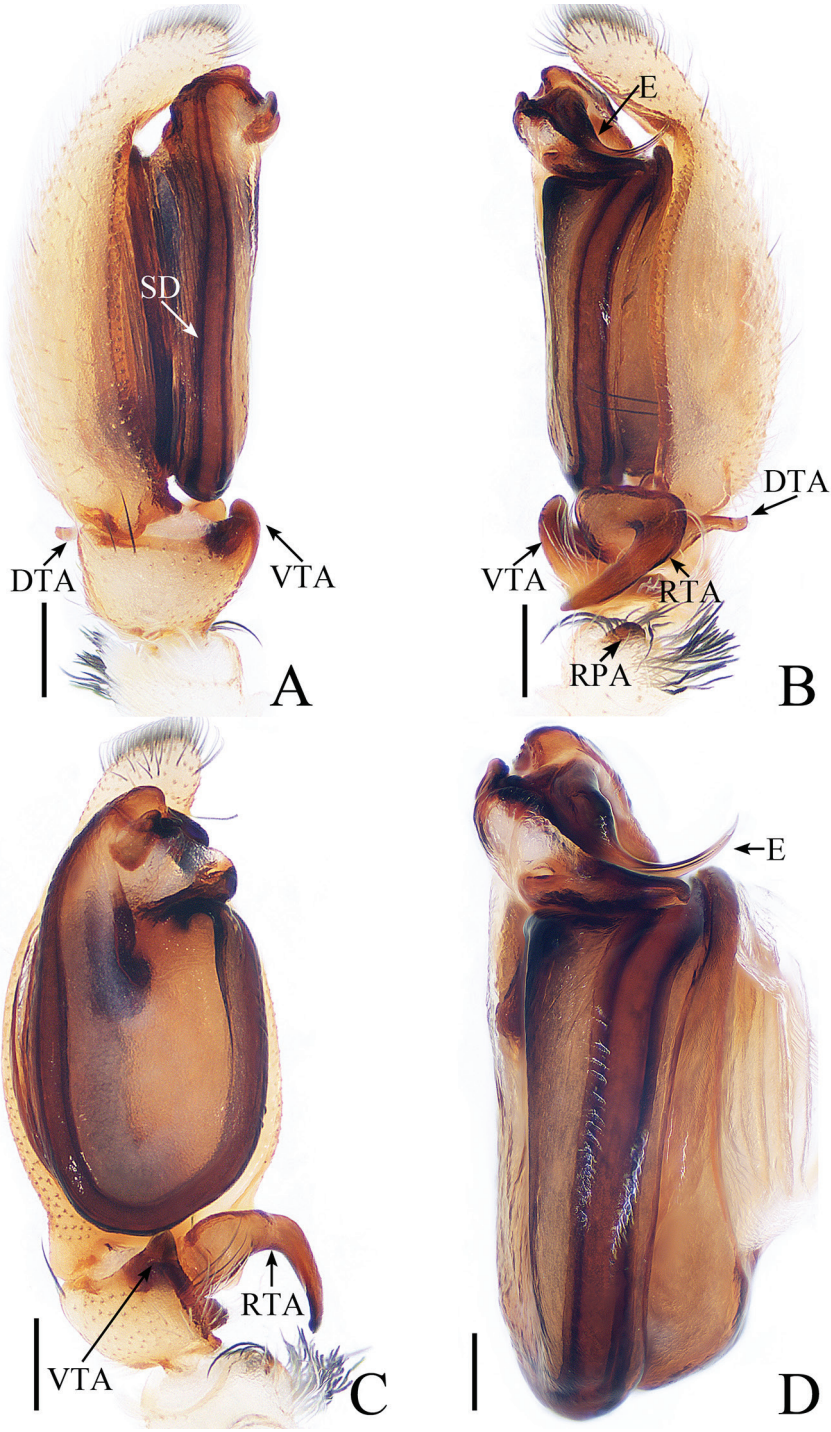

Figure 7. Male palp of *Gelotia liuae* sp. nov., **A**–**C** male holotype; **D** male paratype. **A** prolateral **B** retrolateral **C** ventral **D** bulb, retrolateral. Scale bars: 0.2 (**A**–**C**) ; 0.1 (**D**).

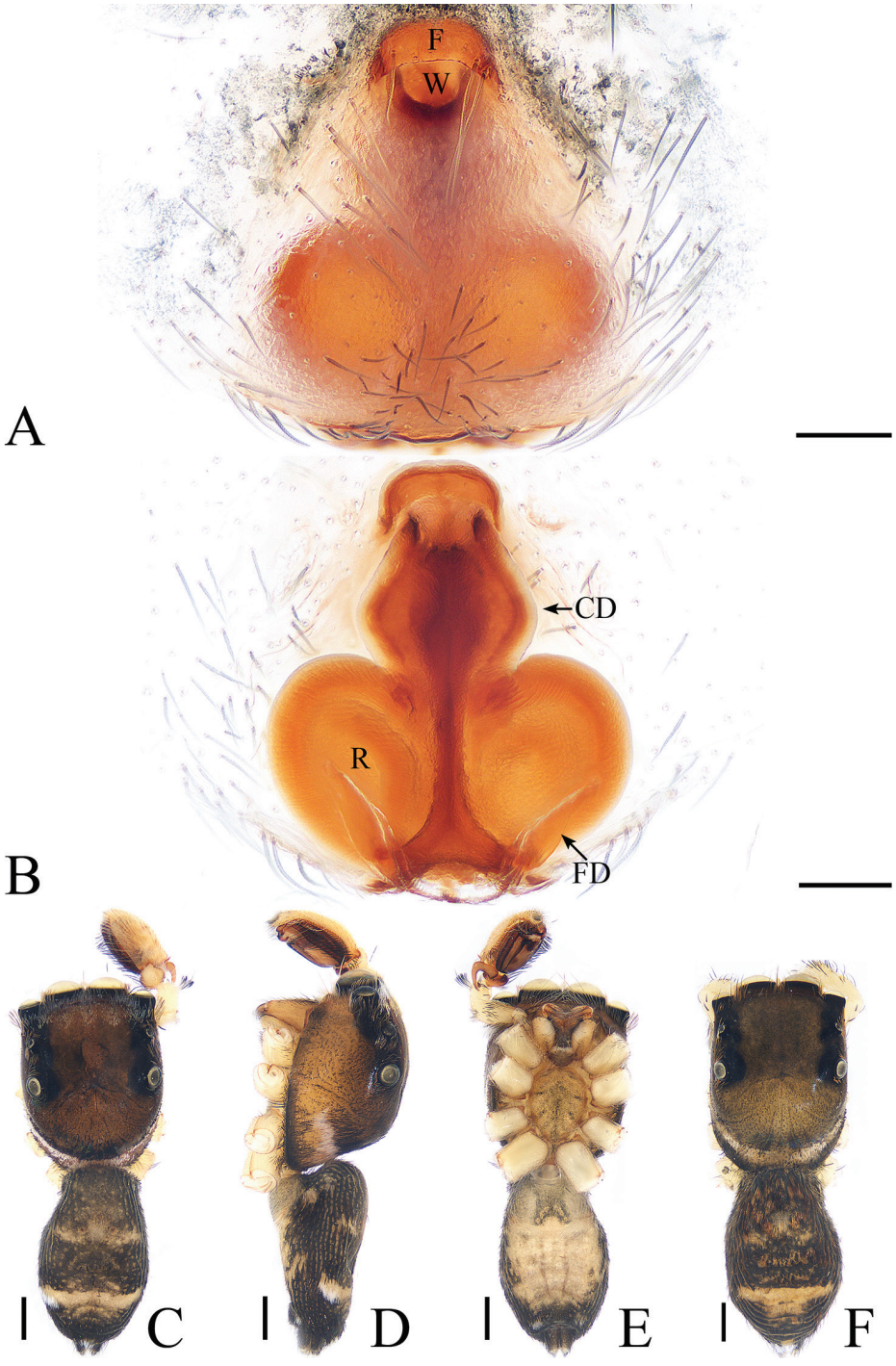

Figure 8. *Gelotia liuae* sp. nov., female paratype and male holotype. **A** epigyne, ventral **B** epigyne, dorsal **C** holotype habitus, dorsal **D** holotype habitus, lateral **E** holotype habitus, ventral **F** female paratype habitus, dorsal. Scale bars: 0.1 (**A**, **B**); 0.5 (**C**–**F**).

yellow stripes postero-medially; venter pale yellow, with 2 white dots close to the spinnerets. Palp (Fig. 7A–D): femur yellow, about 3 times longer than wide, covered with dense setae; patella pale yellow, with dense setae dorsally, tubelike retrolateral apophysis bearing long curved setae; tibia almost as long as wide, with ventral apophysis subtriangular in ventral view, RTA curved medially, directed towards 7 o'clock apically in retrolateral view, dorsal apophysis widest at base, extending transversely, blunt distally; cymbium flattened, narrowed posteriorly; bulb flattened, distally with well-developed lobe, sperm duct extending along margin, almost U-shaped; embolus originating from anterior edge of bulb, broadening at base, curved towards alveolus and pointed apically.

Female. Total length 4.61. Carapace 2.39 long, 1.78 wide. Abdomen 2.33 long, 1.52 wide. Clypeus 0.11 high. Eye sizes and inter-distances: AME 0.50, ALE 0.30, PLE 0.25, AERW 1.74, PERW 1.75, EFL 1.15. Legs: I 5.35 (1.63, 2.01, 1.10, 0.61), II 5.02 (1.63, 1.76, 1.02, 0.61), III 4.82 (1.63, 1.56, 1.02, 0.61), IV 6.32 (1.83, 2.17, 1.71, 0.61). Habitus (Fig. 8F) similar to those of male except paler. Epigyne (Fig. 8A, B) longer than wide, with broad fold anteriorly; epigynal window almost round, located posterior to the fold; copulatory ducts relatively short (less than the length of the receptacles), stout, expanding medially, connected to the inner anterior edge of the receptacles; receptacles oval, touching each other.

Distribution. China (Yunnan, Guangxi).

Comments. Although "*Gelotia* sp. [Guangxi] (from China)" of Maddison et al. (2014) is known by the figure of only the male palpal tibia, the structure is identical to *G. liuae* sp. nov. Thus, they are determined to be the same species, and the distribution of the new species includes Guangxi Province.

Gelotia zhengi Cao & Li, 2016

Figs 9, 10, 17G, 18G, 19G

Gelotia zhengi Cao & Li, in Cao et al. 2016: 78, figs 24A–D, 25A, B (♂).

Material examined. 1♂ 1♀ (IZCAS Ar 39795–39796), CHINA: Yunnan: Xishuangbanna, Mengla County, Menglun Town, Menglun Nature Reserve, Lvshilin Rainforest Park, limestone tropical seasonal rainforest (21°54.58'N, 101°16.50'E, ca 570 m), 27.04.2019, C. Wang leg; 1♀ (IZCAS Ar 39797), Leprosy Village (21°53.62'N, 101°18.25'E, ca 520m), 4.05.2019, Y.F. Tong et al. leg.

Diagnosis. The male has been diagnosed by Cao and Li (2016). The female resembles. *G. bimaculata* Thorell, 1890 from Borneo but differs by the following: 1) the receptacles are widest medially (Fig. 10C), whereas they are widest basally in *G. bimaculata* (Prószyński and Deeleman-Reinhold 2012, fig. 54); 2) the copulatory openings are situated medially (Fig. 10A, B), whereas they are situated anteriorly in *G. bimaculata* (Prószyński and Deeleman-Reinhold 2012, fig. 53).

Description. ***Male.*** Described by Cao and Li (2016).

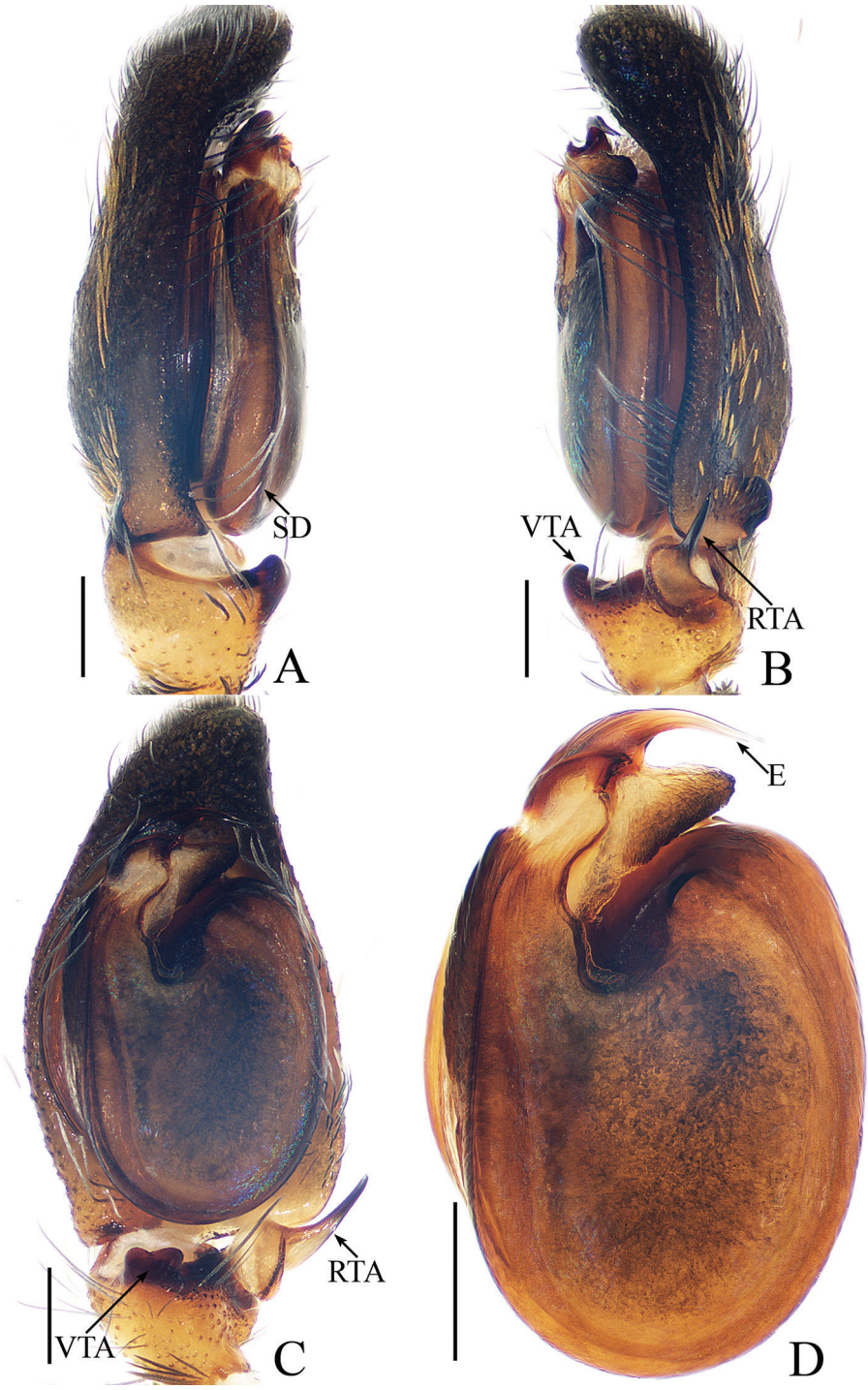

Figure 9. Male palp of *Gelotia zhengi* Cao & Li, 2016. **A** prolateral **B** retrolateral **C** ventral **D** bulb, retrolateral. Scale bars: 0.2.

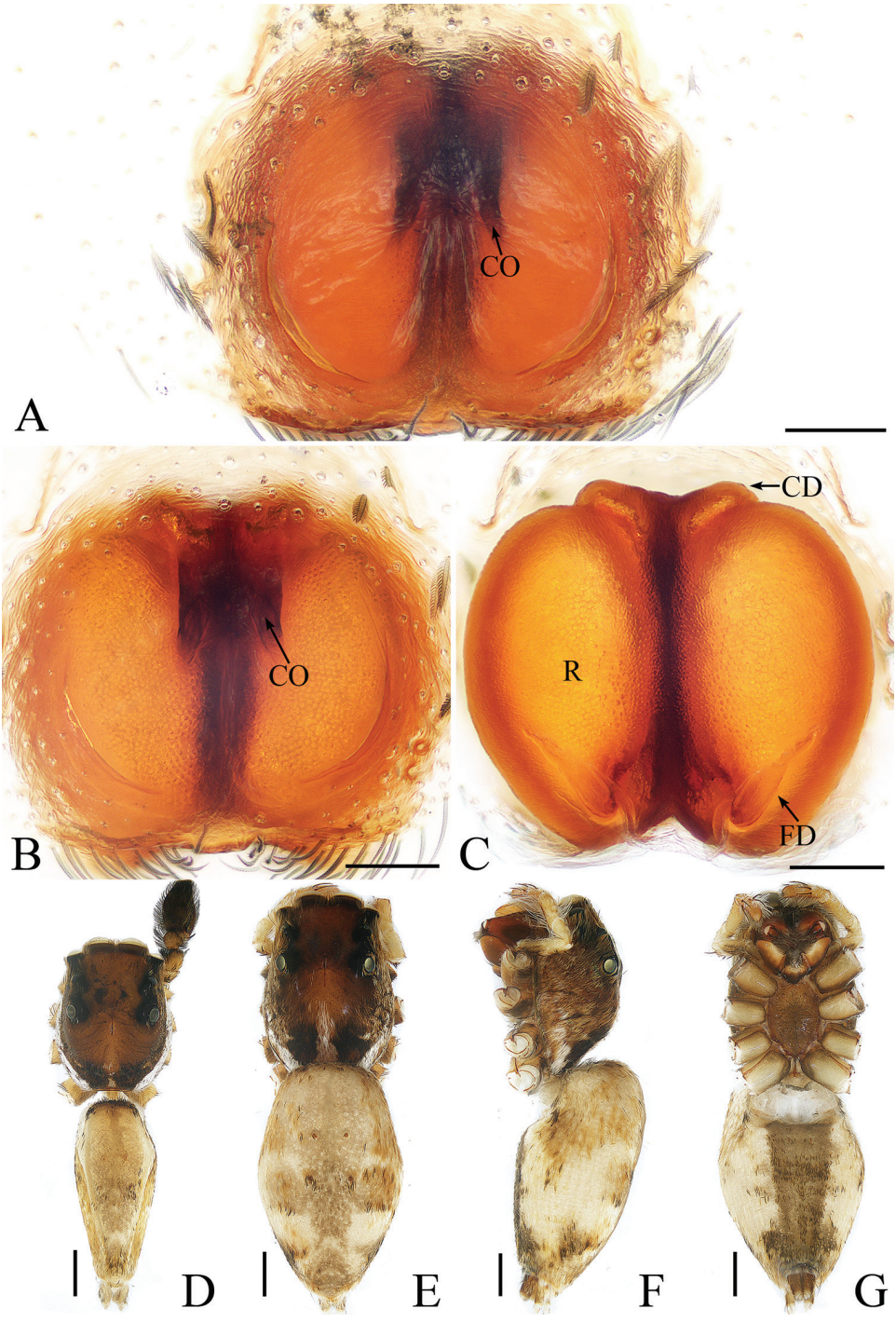

Figure 10. *Gelotia zhengi* Cao & Li, 2016. **A**, **B** epigyne, ventral **C** epigyne, dorsal **D** male habitus, dorsal **E** female habitus, dorsal **F** female habitus, lateral **G** female habitus, ventral. Scale bars: 0.1 (**A**–**C**); 1.0 (**D**–**G**).

***Female*.** Total length 9.13. Carapace 4.12 long, 2.97 wide. Abdomen 5.56 long, 3.38 wide. Clypeus 0.14 high. Eye sizes and inter-distances: AME 0.70, ALE 0.41, PLE 0.38, AERW 2.38, PERW 2.25, EFL 1.63. Legs: I 8.39 (2.39, 3.12, 1.90, 0.98), II 7.42 (2.12, 2.71, 1.71, 0.88), III 6.95 (1.95, 2.39, 1.78, 0.83), IV 8.29 (2.39, 3.12, 2.80, 0.98). Carapace (Figs 10E–G, 17G) red-brown, covered with dense brown setae, posteriorly with white stripes of setae. Clypeus yellow to brown, covered with several long setae. Chelicerae (Fig. 18G) red-brown, with 3 promarginal and 6 retromarginal teeth. Endites brown. Labium covered with dark setae. Sternum colored as endites, covered with brown setae. Legs yellow to brown, tibia of legs I with long, dark, dense setae ventrally. Spination of leg I: femur d1-1-3; tibia v2-2-2; metatarsus v2-0-2. Abdomen (Fig. 10E–G) elongated oval, dorsum with 2 pairs of muscle depressions medially, covered with dense yellow-brown setae, transverse white stripes postero-medially; venter with broad longitudinal brown stripe extending over the entire length, covered with brown setae. Epigyne (Fig. 10A–C) slightly wider than long; windows large, almost round; copulatory openings separated from each other by about 2 times their width, located medially; copulatory ducts stout, ascending before extending transversely to connect with long, oval receptacles; fertilization ducts lamellar.

Distribution. China (Yunnan).

Irura Peckham & Peckham, 1901

Type species. *Irura pulchra* Peckham & Peckham, 1901 from Sri Lanka.

Comments. The genus *Irura* is represented by 16 nominal species that are endemic to Vietnam (2), Malaysia (1), Sri Lanka (1), and China (11). The type locality of *I. mandarina* Simon, 1903 is unknown other than "Southeast Asia" (WSC 2020). The genus is rather poorly studied. Five species, including the generotype, are known from only females and two species from only males. The generotype, *I. pulchra*, is the westernmost species, and all other species are known from more than 2000 km east. The concept of the genus suggested by Peng et al. (1993) is followed here.

Irura lvshilinensis sp. nov.

http://zoobank.org/23C20C31-C56C-439C-8DC2-E696834ACDE7
Figs 11, 12, 17E, 18E, 19E

Type material. ***Holotype*** ♂ (IZCAS Ar 39798), CHINA: Yunnan: Xishuangbanna, Mengla County, Menglun Town, Menglun Nature Reserve, Lvshilin Rainforest Park, limestone tropical seasonal rainforest (21°54.58'N, 101°16.50'E, ca 570 m), 27.04.2019, C. Wang leg. ***Paratypes*:** 2♂ 1♀ (IZCAS Ar 39799–39801), same data as holotype.

Etymology. The species name is derived from the name of the type locality; adjective.

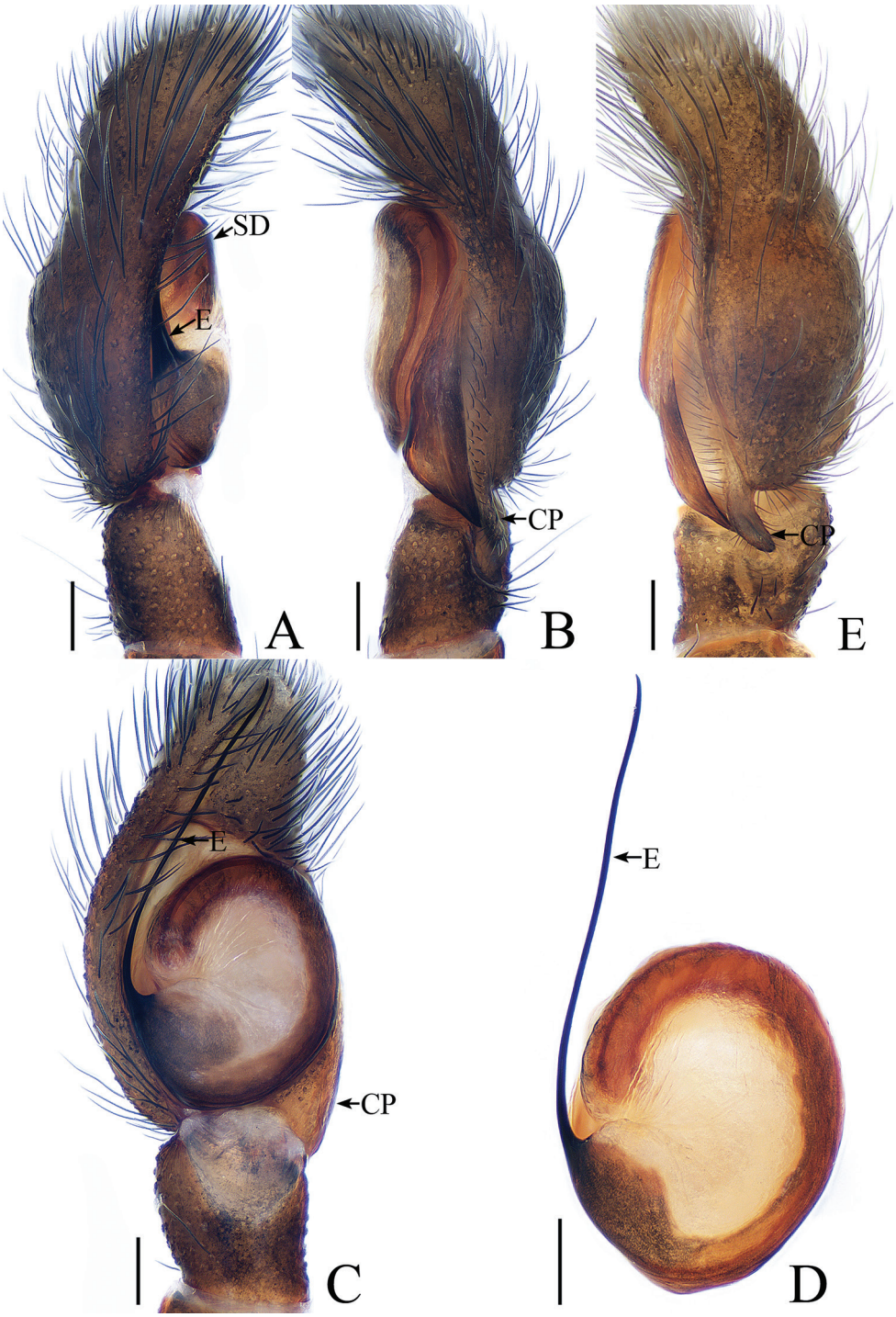

Figure 11. Male palp of *Irura lvshilinensis* sp. nov., **A**–**C**, **E** male holotype; **D** male paratype. **A** prolateral **B** retrolateral **C** ventral **D** bulb, ventral **E** dorsal. Scale bars: 0.1.

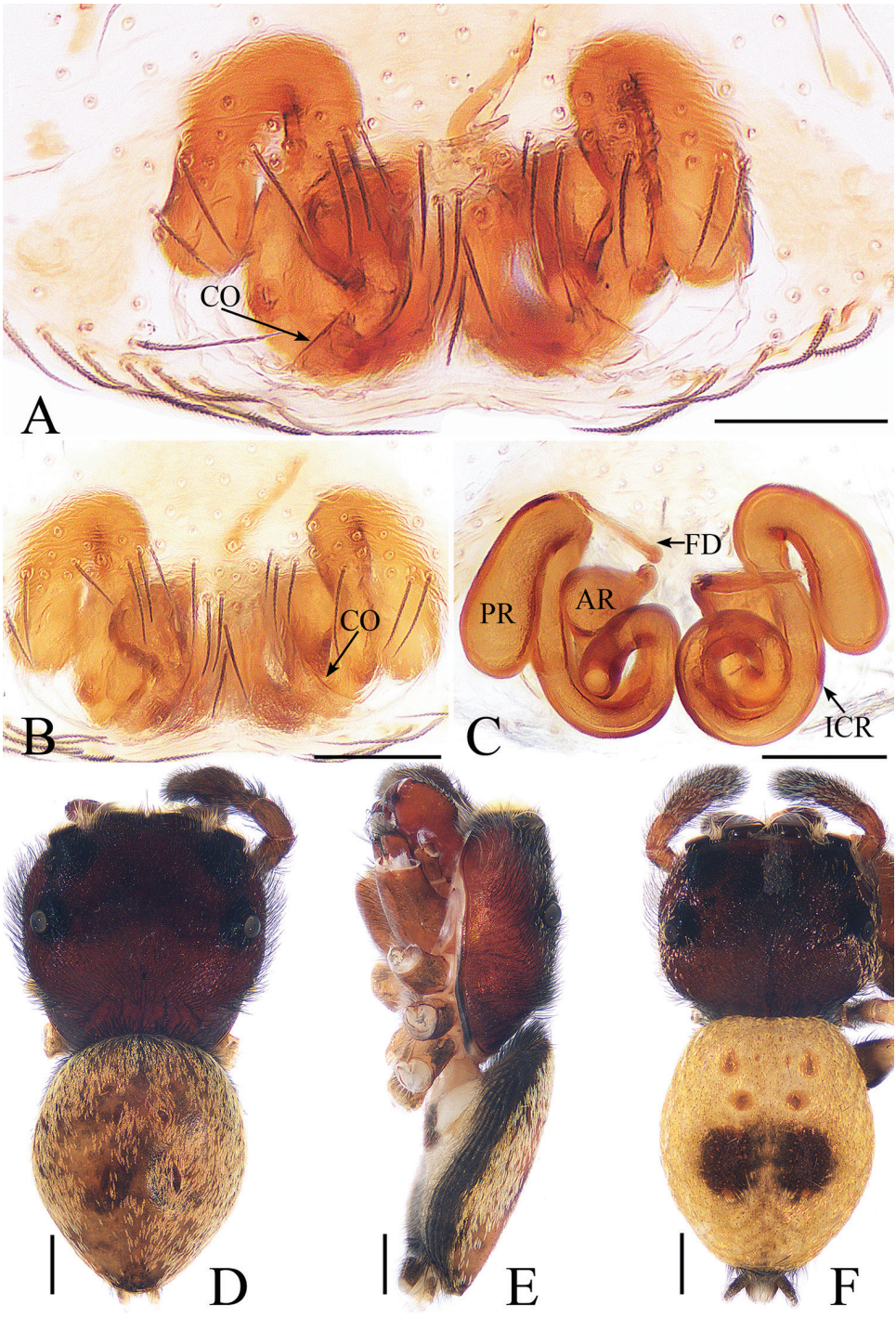

Figure 12. *Irura lvshilinensis* sp. nov., female paratype and male holotype. **A**, **B** epigyne, ventral **C** epigyne, dorsal **D** holotype habitus, dorsal **E** holotype habitus, lateral **F** female paratype habitus, dorsal. Scale bars: 0.1 (**A**–**C**); 0.5 (**D**–**F**).

Diagnosis. The male of *I. lvshilinensis* sp. nov. can be easily distinguished from other species considered in this genus except for *I. uniprocessa* Mi & Wang, 2016 from China by lacking a RTA. It can be distinguished from *I. uniprocessa* by the following: 1) the embolus is about one and a third times the bulb length (Fig. 11C, D), whereas it is almost equal to the bulb length in *I. uniprocessa* (Mi and Wang 2016, figs 1c, 2a); 2) the cymbial process extends distally above the tibia (Fig. 11B), whereas it does not extend beyond the tibia-cymbium joint in *I. uniprocessa* (Mi and Wang 2016, figs 1d, 2b). The female of the new species resembles *I. yunnanensis* (Peng & Yin, 1991,) known from China, in the general shape of the epigyne but differs in the following: 1) the intermediate canal of the receptacles is coiled and forms a loop medially (Fig. 12C), whereas the intermediate canal of the receptacles is only curved in *I. yunnanensis* (Peng and Yin 1991, fig. 3H); 2) the fertilization ducts are located medially (Fig. 12C), whereas they are located posteriorly in *I. yunnanensis* (Peng and Yin 1991, fig. 3H).

Description. ***Male.*** Total length 3.98. Carapace 1.96 long, 2.05 wide. Abdomen 2.20 long, 1.82 wide. Clypeus 0.03 high. Eye sizes and inter-distances: AME 0.45, ALE 0.29, PLE 0.21, AERW 1.68, PERW 1.95, EFL 0.96. Legs: I 5.00 (1.59, 2.24, 0.71, 0.46), II 2.99 (0.98, 1.07, 0.54, 0.40), III 2.73 (0.93, 0.90, 0.50, 0.40), IV 3.11 (1.02, 1.07, 0.61, 0.41). Carapace (Figs 12D, E, 17E) red-brown, covered with dense black setae, cephalic part with irregular dark stripe medially, thoracic part sloping acutely, with pair of dark stripes. Clypeus brown, with long setae. Fovea indistinct. Chelicerae (Fig. 18E) red-brown, with 2 promarginal teeth and 1 retromarginal fissident with 4 cusps. Endites yellow-brown, labium colored as endites, tip covered with dense, dark setae. Sternum yellow. Legs brown to red-brown; legs I stronger than others. Spination of leg I: tibia v0-2-2; metatarsus v2-0-2. Abdomen (Fig. 12D, E) oval, dorsum with 3 pairs of muscle depressions medially, covered with setae; venter pale, with large, brown markings posteriorly. Palp (Fig. 11A–E): femur red-brown, about 3.5 times longer than wide; patella colored as femur, slightly longer than wide; tibia slightly longer than wide, lacking apophysis; cymbium flattened, longer than wide, proximo-retrolaterally with well-developed process extending above tibia about 1/5 tibial length in retrolateral view; bulb almost round, with sperm duct extending along margin; embolus slender, about 1.3 times bulb length, arising at almost 9 o'clock, with a pointed tip that reaches cymbial tip.

Female. Total length 3.65. Carapace 1.54 long, 1.67 wide. Abdomen 2.14 long, 1.79 wide. Clypeus 0.03 high. Eye sizes and inter-distances: AME 0.37, ALE 0.21, PLE 0.19, AERW 1.39, PERW 1.74, EFL 0.88. Legs: I 3.63 (0.98, 1.63, 0.61, 0.41), II 2.64 (0.85, 0.95, 0.44, 0.40), III 2.34 (0.76, 0.78, 0.40, 0.40), IV 2.91 (0.95, 1.10, 0.46, 0.40). Habitus (Fig. 12F) similar to that of male except paler, with pair of dark round patches on the dorsum of the abdomen. Epigyne (Fig. 12A–C) slightly wider than long; copulatory openings located posteriorly; copulatory ducts indistinct; receptacle divided into 2 chambers interconnected by an intermediate canal, anterior chamber almost pyriform, posterior chamber elongated oval; intermediate canal of receptacles long, coiling into complete circle medially; fertilization ducts slender, situated medially.

Distribution. China (Yunnan).

Rhene Thorell, 1869

Type species. *Rhanis flavigera* C.L. Koch, 1846 from Indonesia.

Comments. The genus *Rhene* with 64 named species has never been revised. Both sexes are not yet known for more than two-thirds (42) of the species, and some are known from juvenile specimens. To date, 19 species have been recorded from Southeast Asia. Of these, 10 are known from only a single sex: seven from males and three from females, and two species are known from juvenile specimens. Presently, 10 species, including five endemics, are known from China (WSC 2020).

Rhene menglunensis sp. nov.

http://zoobank.org/8132458E-6CCE-498C-BA89-11BF797FB534
Figs 13, 14, 17F, 18F, 19F

Type material. ***Holotype*** ♂ (IZCAS Ar 39802) CHINA: Yunnan: Xishuangbanna, Mengla County, Menglun Town, Menglun Nature Reserve, garbage dump, secondary tropical rainforest (21°54.30'N, 101°16.78'E, ca 620 m), 26.04.2019, Y.F. Tong et al. leg. ***Paratypes*****:** 3♀ (IZCAS Ar 39803–39805), same data as holotype; 2♂ 1♀ (IZCAS Ar 39806–39808), same locality, Vine Garden (21°55.80'N, 101°45.41'E, ca 550 m), 2.08.2018, C. Wang et al. leg; 1♂ (IZCAS Ar 39809), Lvshilin Rainforest Park, limestone tropical seasonal rainforest (21°54.58'N, 101°16.50'E, ca 570 m), 27.04.2019, C. Wang leg; 1♂ (IZCAS Ar 39810), same locality, tropical rainforest (21°55.20'N, 101°16.21'E, ca 550 m), 30.04.2019, Y.F. Tong et al. leg; 1♂ (IZCAS Ar 39811), riverside near the suspension bridge (21°56.02'N, 101°15.06'E, ca 550 m), 1.05.2019, C. Wang leg.

Etymology. The species name is derived from the name of the type locality; adjective.

Diagnosis. The male of *R. menglunensis* sp. nov. can be easily distinguished from other species of the genus by the conductor having several spinose processes. The female of the new species resembles *R. atrata* Karsch, 1881 known from Far East Asia in the general shape of the epigyne but differs by the following: 1) the epigynal hood is wider than long (Fig. 14A), whereas it is longer than wide in *R. atrata* (Logunov 1993, fig. 3C); 2) the fertilization ducts originate from the anterior part of the receptacles (Fig. 14B), whereas they originate from the posterior part of the receptacles in *R. atrata* (Logunov 1993, fig. 3D).

Description. ***Male*****.** Total length 3.15. Carapace 1.47 long, 1.55 wide. Abdomen 1.82 long, 1.43 wide. Clypeus 0.04 high. Eye sizes and inter-distances: AME 0.36, ALE 0.20, PLE 0.15, AERW 1.22, PERW 1.58, EFL 0.99. Legs: I 3.14 (1.10, 1.20, 0.44, 0.40), II 2.38 (0.76, 0.80, 0.42, 0.40), III 2.19 (0.68, 0.71, 0.40, 0.40), IV 2.74 (0.88, 0.95, 0.51, 0.40). Carapace (Figs 14C–E, 17F) red-brown, with irregular dark stripe antero-medially, covered with dense grey-white setae. Clypeus red-brown, covered with dark, long setae. Chelicerae (Fig. 18F) red-brown, with 1 retromarginal tooth and 2 promarginal teeth. Endites, labium, and sternum colored as chelicerae.

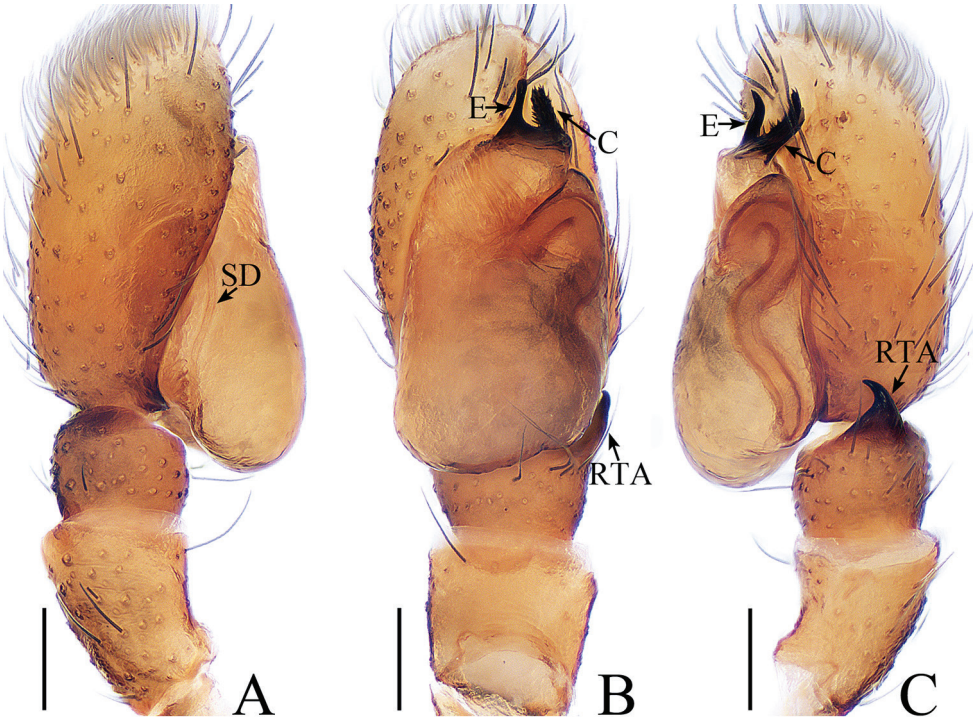

Figure 13. Male palp of *Rhene menglunensis* sp. nov., male holotype. **A** prolateral **B** ventral **C** retrolateral. Scale bars: 0.1.

Legs I robust, red-brown, other legs pale yellow. Spination of leg I: femur d0-0-1, p0-0-3; tibia v0-0-2; metatarsus v2-0-2. Abdomen (Fig. 14C–E) elongated oval, with a pattern of darker setae medially, covered with dense setae; venter red to dark brown, without distinct markings. Palp (Fig. 13A–C): femur yellow, about 3 times longer than wide; patella colored as femur, almost as long as wide; tibia wider than long, with claw-shaped RTA shorter than tibia, tapering distally and curved towards bulb medially; cymbium longer than wide, slightly longer than the length of the bulb in retrolateral view; bulb longer than wide, with sperm duct extending along margin; embolus short, blunt apically in ventral view; conductor relatively thick, with spinose processes.

Female. Total length 3.74. Carapace 1.53 long, 1.65 wide. Abdomen 2.32 long, 1.62 wide. Clypeus 0.04 high. Eye sizes and inter-distances: AME 0.35, ALE 0.19, PLE 0.15, AERW 1.19, PERW 1.58, EFL 0.96. Legs: I 2.84 (1.15, 1.05, 0.32, 0.32), II 2.34 (0.80, 0.88, 0.34, 0.32), III 2.18 (0.71, 0.73, 0.42, 0.32), IV 2.96 (0.98, 1.12, 0.54, 0.32). Habitus (Fig. 14F) similar to that of male except paler and lacking a clear pattern. Epigyne (Fig. 14A, B) with distinct posterior hood wider than long; copulatory openings almost cambered, situated anteriorly; copulatory ducts long, widest at base; fertilization ducts knife-shaped.

Distribution. China (Yunnan).

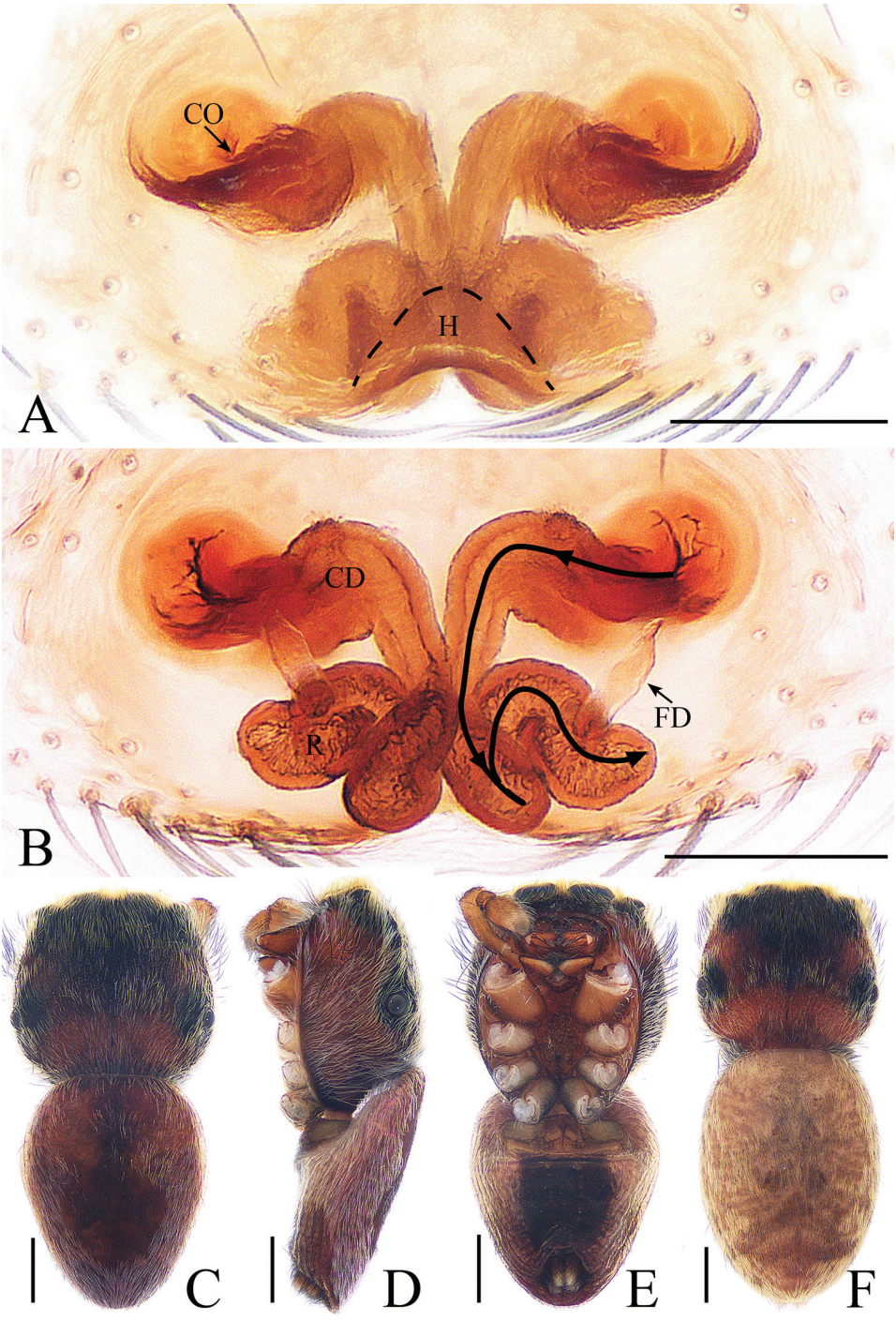

Figure 14. *Rhene menglunensis* sp. nov., female paratype and male holotype. **A** epigyne, ventral **B** epigyne, dorsal **C** holotype habitus, dorsal **D** holotype habitus, lateral **E** holotype habitus, ventral **F** female paratype habitus, dorsal. Scale bars: 0.1 (**A**, **B**); 0.5 (**C**–**F**).

Siler Simon, 1889

Type species. *Siler cupreus* Simon, 1889 from Japan.

Comments. The genus *Siler* contains 10 nominal species currently known from East, South, and Southeast Asia. It is rather poorly studied and has not been revised. More than half (six) of the species are known from only a single sex: four from males and two from females. Additionally, one species has never been illustrated. Five species, including an endemic, occur in China (WSC 2020).

Siler zhangae sp. nov.

http://zoobank.org/C6DDC2DE-468F-4CF2-BE43-D1AA19FB82CC
Figs 15, 16, 17H, 18H, 19H

Type material. ***Holotype*** ♂ (IZCAS Ar 39819), CHINA: Yunnan: Xishuangbanna, Mengla County, Menglun Town, Menglun Nature Reserve, Lvshilin Rainforest Park, limestone tropical seasonal rainforest (21°54.58'N, 101°16.50'E, ca 570 m), 6.08.2018, C. Wang et al. leg. **Paratypes:** 2♂ (IZCAS Ar 39820–39821), same locality, Grapefruit Garden (21°54.07'N，101°16.36'E, ca 540 m), 25.07.2018, X.Q. Mi et al. leg; 1♂ (IZCAS Ar 39822), same locality, tropical rainforest (21°55.40'N, 101°16.32'E, ca 580 m), 11.08.2018, C. Wang et H. Liu leg.

Etymology. The specific name is a patronym in honor of Dr Junxia Zhang (Baoding, China), who has contributed greatly to the taxonomy of jumping spiders worldwide.

Diagnosis. *Siler zhangae* sp. nov. resembles *S. semiglaucus* (Simon, 1901) from Southeast Asia by having a relatively long bulb but differs by the following: 1) the embolus is directed anteriorly (Fig. 15B), whereas it is directed antero-prolaterally in *S. semiglaucus* (Peng et al. 1993, fig. 747); 2) the posterior lobe of the bulb is blunt (Fig. 15B), whereas it is pointed in *S. semiglaucus* (Peng et al. 1993, fig. 747); 3) the embolus is twisted (Fig. 15B, C), whereas it is not twisted in *S. semiglaucus* (Peng et al. 1993, figs 747, 748).

Description. ***Male.*** Total length 3.76. Carapace 1.68 long, 1.27 wide. Abdomen 1.98 long, 1.19 wide. Clypeus 0.04 high. Eye sizes and inter-distances: AME 0.36, ALE 0.21, PLE 0.16, AERW 1.08, PERW 1.19, EFL 0.86. Legs: I 3.82 (1.32, 1.41, 0.68, 0.41), II 2.91 (0.93, 1.02, 0.56, 0.40), III 3.29 (1.02, 1.10, 0.73, 0.44), IV 4.31 (1.29, 1.51, 1.07, 0.44). Carapace (Figs 16A–C, 17H) red-brown, widest between coxae II and III, covered with white scale-like setae. Clypeus dark brown. Fovea longitudinal. Chelicerae (Fig. 18H) yellow, with 2 promarginal teeth and 1 retromarginal fissident. Endites widest at tip. Sternum brown, covered with thin setae. Tibia of legs I with characteristic brushes of long, dark, dense setae ventrally and dorsally. Spination of leg I: femur d1-1-3; tibia v2-0-2; metatarsus v0-2-2. Abdomen (Fig. 16A–C) elongated oval, dorsum with 2 pairs of muscle depressions, and scale-shaped setae bilaterally and posteriorly; venter pale brown, also with scale-shaped setae. Palp (Fig. 15A–C): femur yellow, about 3 times longer than wide, covered with dense white setae; patella colored as femur, almost as long as wide; tibia wider than long, with RTA tapering toward the tip, slightly longer

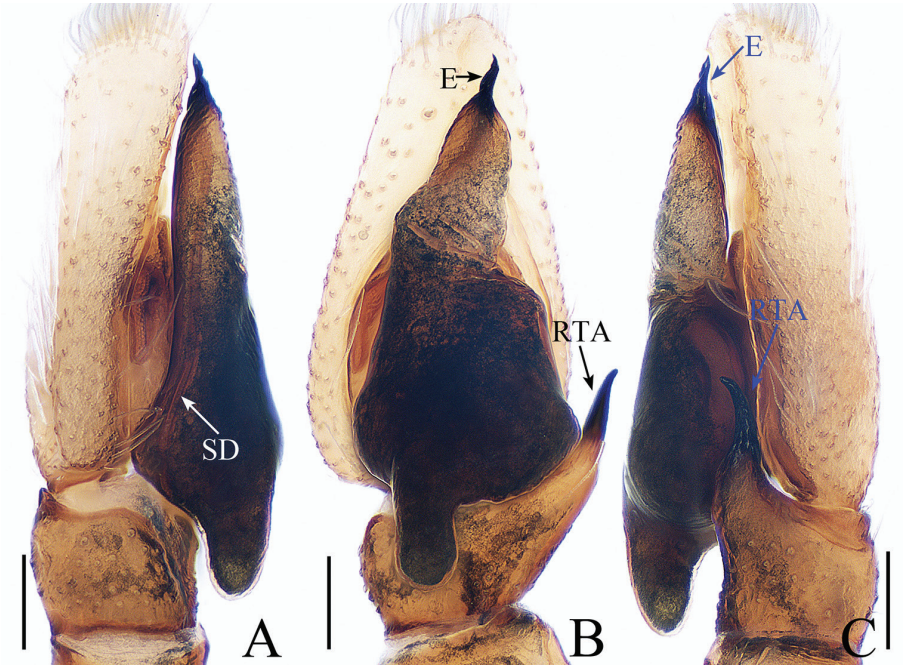

Figure 15. Male palp of *Siler zhangae* sp. nov., male holotype. **A** prolateral **B** ventral **C** retrolateral. Scale bars: 0.1.

Figure 16. Habitus of *Siler zhangae* sp. nov., male holotype. **A** dorsal **B** lateral **C** ventral. Scale bars: 0.5.

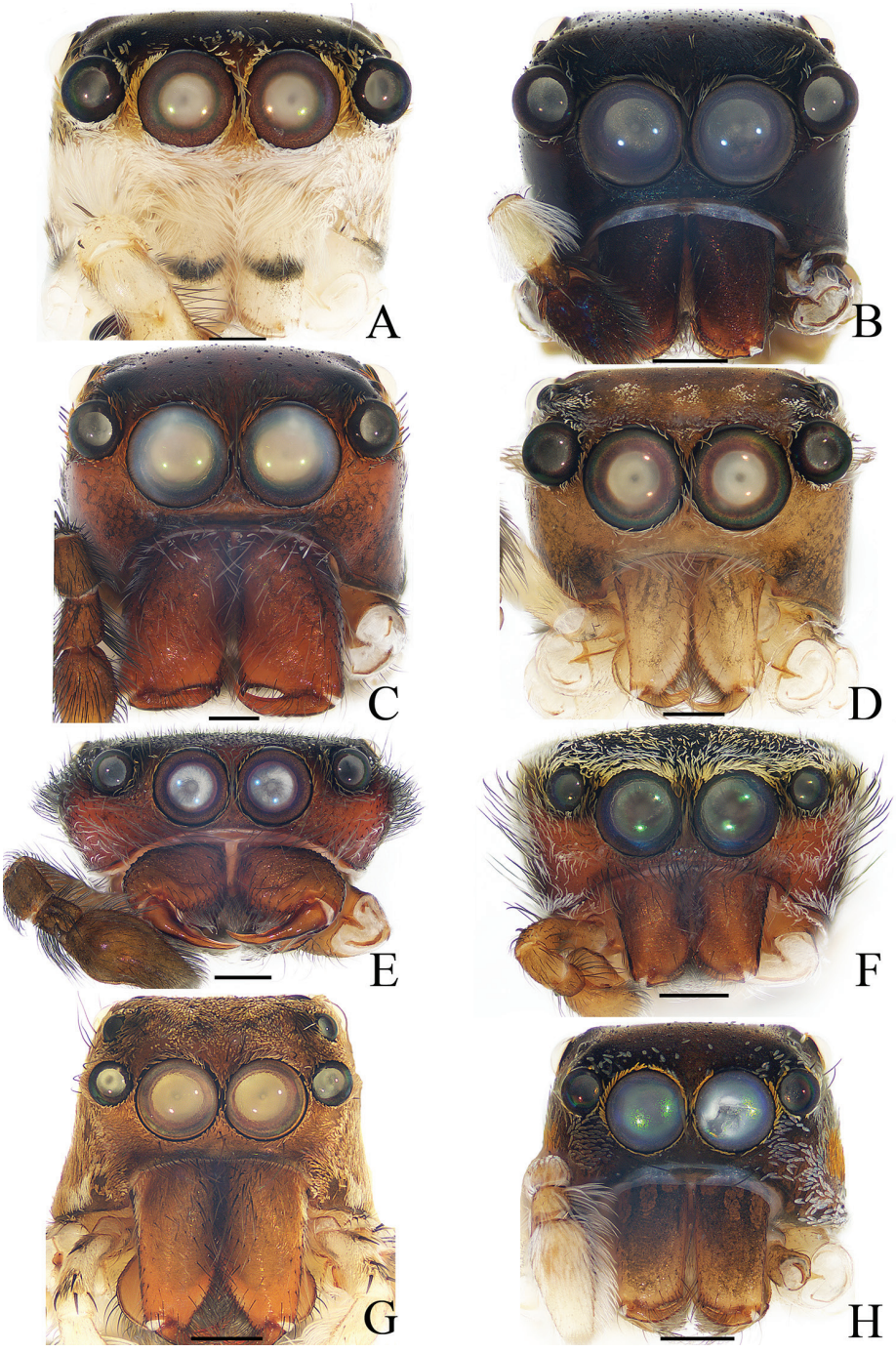

Figure 17. Frontal view of Carapace, **A–F, H** male holotype; **G** female. **A** *Cytaea tongi* sp. nov. **B** *Euophrys subwanyan* sp. nov. **C** *Dexippus pengi* sp. nov. **D** *Gelotia liuae* sp. nov. **E** *Irura lvshilinensis* sp. nov. **F** *Rhene menglunensis* sp. nov. **G** *Gelotia zhengi* Cao & Li, 2016 **H** *Siler zhangae* sp. nov. Scale bars: 0.3 (A–F, H); 0.5 G.

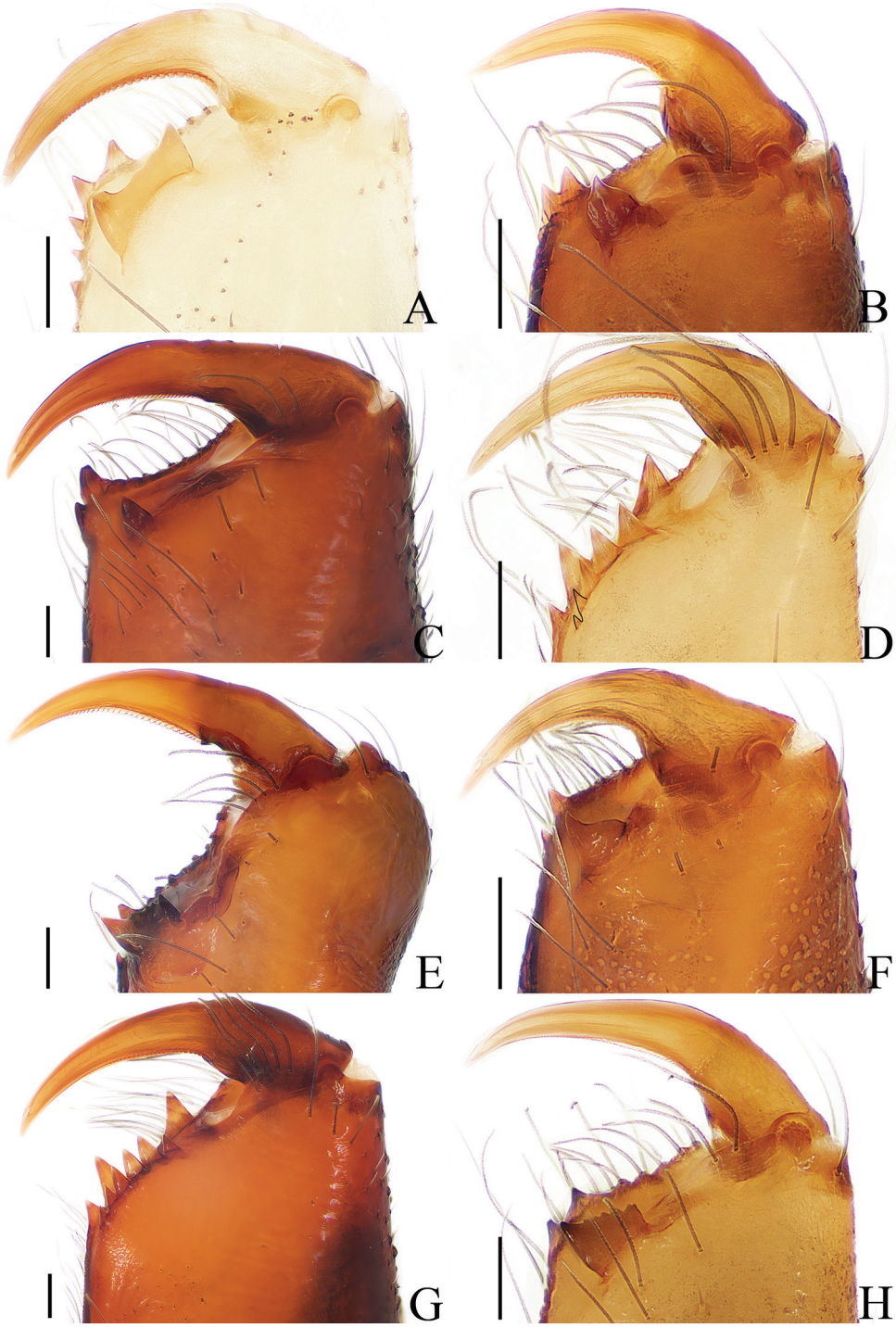

Figure 18. Dorsal view of chelicerae, **A**–**F**, **H** male holotype; **G** female. **A** *Cytaea tongi* sp. nov. **B** *Euophrys subwanyan* sp. nov. **C** *Dexippus pengi* sp. nov. **D** *Gelotia liuae* sp. nov. **E** *Irura lvshilinensis* sp. nov. **F** *Rhene menglunensis* sp. nov. **G** *Gelotia zhengi* Cao & Li, 2016 **H** *Siler zhangae* sp. nov. Scale bars: 0.1.

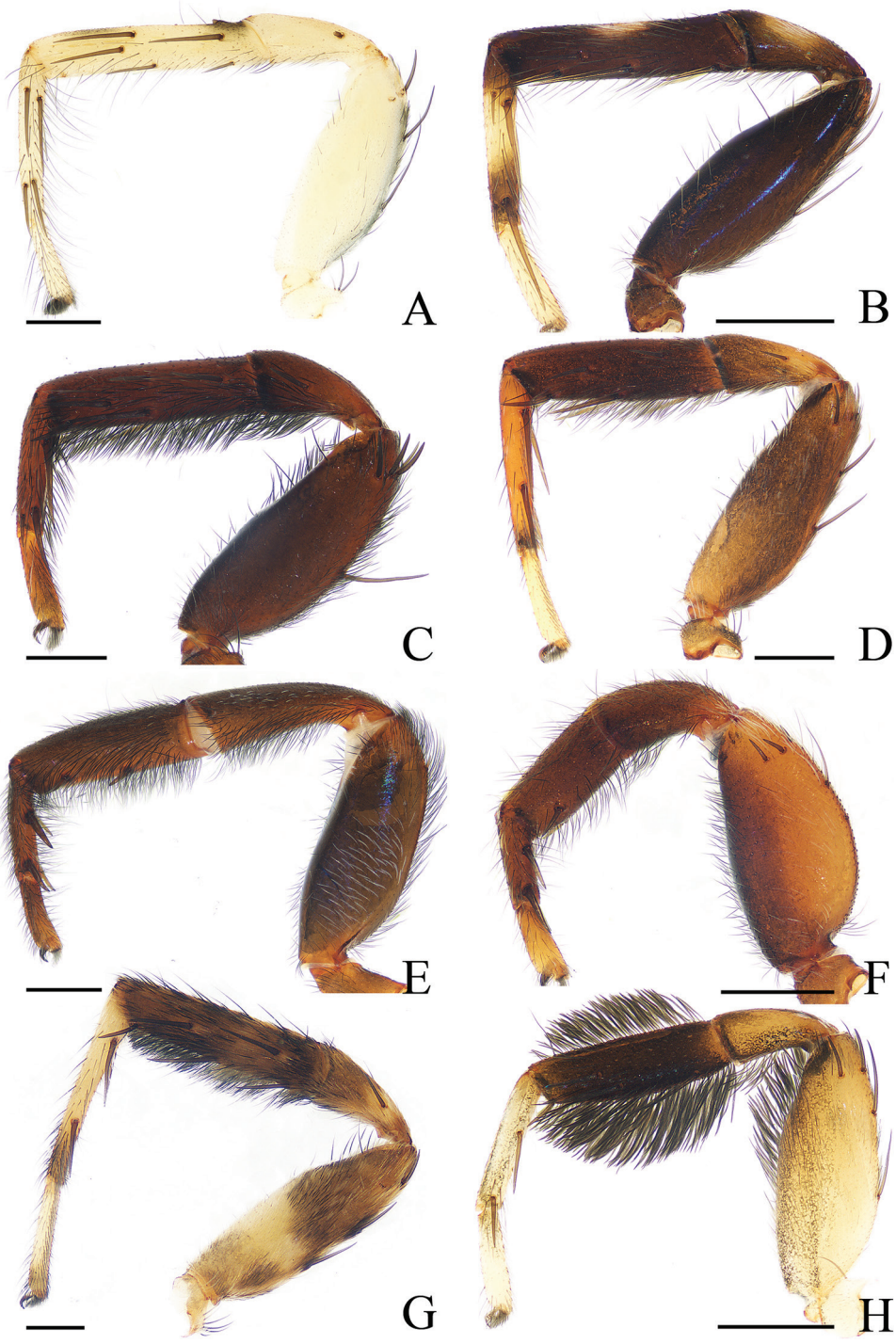

Figure 19. Prolateral view of right leg I, **A**–**F**, **H** male holotype; **G** female. **A** *Cytaea tongi* sp. nov. **B** *Euophrys subwanyan* sp. nov. **C** *Dexippus pengi* sp. nov. **D** *Gelotia liuae* sp. nov. **E** *Irura lvshilinensis* sp. nov. **F** *Rhene menglunensis* sp. nov. **G** *Gelotia zhengi* Cao & Li, 2016 **H** *Siler zhangae* sp. nov. Scale bars: 0.5.

than tibia, tip slightly bent ventrally; cymbium flattened, widest at base, tapering in ventral view; bulb elongated, widest at base, with well-developed, blunt posterior lobe extending above tibia about half the length of the tibia in ventral view; embolus longer than RTA with long, subconical base, and relatively short, twisted tip directed anteriorly.

***Female*.** Unknown.

Distribution. China (Yunnan).

Comments. This species is described based on males only, and so there is a possibility it is conspecific to one of the two species (*S. flavocinctus* (Simon, 1901), *S. bielawskii* Zabka, 1985) known from only females.

Acknowledgments

The manuscript benefited greatly from comments by Yuri Marusik (Magadan, Russia), Dmitri Logunov (Manchester, UK), Peter Koomen (Leeuwarden, Holland), Galina N. Azarkina (Novosibirsk, Russia), and Wayne Maddison (Vancouver, Canada). Sarah Crews (San Francisco, USA) kindly checked the English of the earlier draft. Yanfeng Tong (Shenyang), Hao Yu (Guiyang), Zhigang Chen (Beijing), Zilong Bai (Beijing), Shijia Liu (Shenyang), Xiaoqi Mi (Tongren), Jiahui Gan (Tongren), Yuanfa Yang (Tongren) and Hong Liu (Tongren) kindly helped in collecting the specimens. This research was supported by the National Natural Science Foundation of China to Shuqiang Li (NSFC-31530067) and Xiaoqi Mi (NSFC-31660609), Science and Technology Cooperation Project Foundation of Guizhou Province (LH-2016/7303), Natural Science Research Project Foundation of Guizhou Province of Education (KY-2018-345).

References

Berry JW, Beatty JA, Prószyński J (1996) Salticidae of the Pacific Islands. I. Distributions of twelve genera, with descriptions of eighteen new species. Journal of Arachnology 24: 214–253.

Berry JW, Beatty JA, Prószyński J (1998) Salticidae of the Pacific Islands. III. Distribution of seven genera with descriptions of nineteen new species and two new genera. Journal of Arachnology 26: 149–189.

Cao Q, Li S, Żabka M (2016) The jumping spiders from Xishuangbanna, Yunnan, China (Araneae, Salticidae). ZooKeys 630: 43–104. https://doi.org/10.3897/zookeys.630.8466

Logunov DV (1993) Notes on two salticid collections from China (Araneae: Salticidae). Arthropoda Selecta 2 (1): 49–59.

Metzner H (2020) Jumping spiders (Arachnida: Araneae: Salticidae) of the world. https://www.jumping-spiders.com [Accessed on: 2020-1-6]

Mi XQ, Wang C (2016) A new species of *Irura* Peckham et Peckham, 1901 (Araneae: Salticidae) from Yunnan Province, China. Sichuan Journal of Zoology 35 (3): 400–403.

Peng XJ, Yin CM (1991) Five new species of the genus *Kinhia* from China (Araneae: Salticidae). Acta Zootaxonomica Sinica 16: 35–47.

Peng XJ, Xie LP, Xiao XQ, Yin CM (1993) Salticids in China (Arachnida: Araneae). Hunan Normal University Press, Changsha, China, 270 pp.

Peng XJ (1995) Two new species of jumping spiders from China (Araneae: Salticidae). Acta Zootaxonomica Sinica 20: 35–38.

Peng XJ, Kim JP (1997) Three new species of the genus *Eupoa* from China (Araneae: Salticidae). Korean Journal of Systematic Zoology 13: 193–198.

Peng XJ, Li S (2002) Four new and two newly recorded species of Taiwanese jumping spiders (Araneae: Salticidae) deposited in the United States. Zoological Studies 41: 337–345.

Prószyński J (1969) Redescriptions of type-species of genera of Salticidae (Araneida). III—remarks on the genera *Gelotia* Thorell, 1890 and *Policha* Thorell, 1892. Annali del Museo Civico di Storia Naturale Giacomo Doria 77: 12–20.

Prószyński J (1984) Atlas rysunków diagnostycznych mniej znanych Salticidae (Araneae). Wyższa Szkola Rolniczo-Pedagogiczna, Siedlcach 2: 1–177.

Prószyński J (1992) Salticidae (Araneae) of India in the collection of the Hungarian National Natural History Museum in Budapest. Annales Zoologici, Warszawa 44: 165–277.

Prószyński J, Deeleman-Reinhold CL (2012) Description of some Salticidae (Aranei) from the Malay archipelago. II. Salticidae of Java and Sumatra, with comments on related species. Arthropoda Selecta 21: 29–60. https://doi.org/10.15298/arthsel.21.1.04

Prószyński J, Lissner J, Schäfer M (2018) Taxonomic survey of the genera *Euophrys*, *Pseudeuophrys* and *Talavera*, with description of *Euochin* gen. n. (Araneae: Salticidae) and with proposals of a new research protocol. Ecologica Montenegrina 18: 26–74.

Song DX (1991) Three new species of the genus *Ptocasius* from China (Araneae: Salticidae). Sinozoologia 8: 163–168.

Song DX, Zhu MS (1998) Two new species of the family Salticidae (Araneae) from China. Acta Arachnologica Sinica 7: 26–29.

Wanless FR (1984) A review of the spider subfamily Spartaeinae nom. n. (Araneae: Salticidae) with descriptions of six new genera. Bulletin of the British Museum of Natural History (Zoology) 46: 135–205. https://doi.org/10.5962/bhl.part.15964

Wijesinghe DP (1991) A new species of *Gelotia* (Araneae: Salticidae) from Sri Lanka. Journal of the New York Entomological Society 99: 274–277.

WSC (2020) World Spider Catalog, version 20.5. Natural History Museum Bern. http://wsc.nmbe.ch [2020-1-6]

Xiao XQ (2002) A new species of the genus *Myrmarachne* from China (Araneae: Salticidae). Acta Zootaxonomica Sinica 27: 477–478.

Xiao XQ, Wang SP (2004) Description of the genus *Myrmarachne* from Yunnan, China (Araneae, Salticidae). Acta Zootaxonomica Sinica 29: 263–265.

Xie LP, Peng XJ (1995) Spiders of the genus *Thyene* Simon (Araneae: Salticidae) from China. Bulletin of the British Arachnological Society 10: 104–108.

Żabka M (1985) Systematic and zoogeographic study on the family Salticidae (Araneae) from Viet-Nam. Annales Zoologici, Warszawa 39: 197–485.

Zhang JX, Maddison WP (2015) Genera of euophryine jumping spiders (Araneae: Salticidae), with a combined molecular-morphological phylogeny. Zootaxa 3938(1): 1–147. https://doi.org/10.11646/zootaxa.3938.1.1

ZooKeys 909: 59–66 (2020)
doi: 10.3897/zookeys.909.46488
http://zookeys.pensoft.net

SHORT COMMUNICATION

A peer-reviewed open-access journal
ZooKeys
Launched to accelerate biodiversity research

First record on the biology of *Sarcophaga* (Bulbostyla) (Diptera, Sarcophagidae)

Pierre-Marc Brousseau[1], Marjolaine Giroux[2], I. Tanya Handa[1]

1 *Département des sciences biologiques, Université du Québec à Montréal, 141, avenue du Président-Kennedy, Montréal, QC, H2X 1Y4, Canada* **2** *Montréal Insectarium / Space for life, 4581, rue Sherbrooke Est, Montréal, QC, H1X 2B2, Canada*

Corresponding author: *Marjolaine Giroux* (marjolaine.giroux@elf.mcgill.ca)

Academic editor: *M. Hauser* | Received 12 September 2019 | Accepted 18 November 2019 | Published 5 February 2020

http://zoobank.org/80AA62AC-300C-40DC-932A-03736D3E9954

Citation: Brousseau P-M, Giroux M, Handa IT (2020) First record on the biology of *Sarcophaga* (Bulbostyla) (Diptera, Sarcophagidae). ZooKeys 909: 59–66. https://doi.org/10.3897/zookeys.909.46488

Abstract

A first breeding record for *Sarcophaga* (*Bulbostyla*) *cadyi* Giroux & Wheeler on the American giant millipede *Narceus americanus* (de Beauvois) (Spirobolida, Spirobolidae) is reported. Digital photographs of the terminalia of *S.* (*B.*) *cadyi* and of *Sarcophaga* (*Bulbostyla*) *yorkii* Parker are also provided.

Keywords

feeding behaviour, flies, host, millipedes, Nearctic Region, Spirobolidae

Introduction

Sarcophaga Meigen is a large and diverse genus comprising about 890 valid species worldwide (Buenaventura et al. 2017). In Canada, 39 species are currently known including 21 species recorded in Quebec (Pape 1996; Dahlem and Naczi 2006; Giroux and Wheeler 2010). Adult flies of *Sarcophaga* feed on various resources including sugar, carrion and dung. The main resources of the larvae are dead arthropods, snails and small vertebrates which they can use as scavengers, parasitoids or predators (Pape 1996; Coupland and Barker 2004; Mello-Patiu 2016). Within this genus, the recently described subgenus *Bulbostyla* Giroux & Wheeler comprises nine species restricted to North and South America. It differs from other *Sarcophaga* mainly by characters of the

male genitalia (Giroux and Wheeler 2010). The ecology of *Bulbostyla* species remains little known, although most specimens were collected on hilltops (Giroux and Wheeler 2010). No feeding records have previously been documented for larvae.

Here, we present the first observation of an interaction between the flesh fly *S.* (*Bulbostyla*) *cadyi* Giroux & Wheeler and the American giant millipede *Narceus americanus* (de Beauvois) (Spirobolida, Spirobolidae). We also present digital photographs of the male terminalia of both species of *Bulbostyla* found in the province of Quebec (*S.* (*B.*) *cadyi* and *S.* (*B.*) *yorkii* Parker) and photographs of the female external terminalia of *S.* (*B.*) *cadyi*.

Materials and methods

A dead *N. americanus* colonized by eight sarcophagid larvae was collected on August 20, 2017. The millipede was found on the forest floor (45°33.18'N, 73°18.30'W) at Mont-Saint-Bruno National Park in southern Quebec. The millipede and the larvae of *S. cadyi* were brought to the laboratory and kept at constant room temperature (~20 °C) in a small plastic container with garden soil. Once adult flies emerged, they were killed in the freezer and preserved in 70% alcohol. In order to be morphologically identified, they were rinsed twice in 100% ethyl acetate, then dried and pinned.

The specimens of *S.* (*B.*) *yorkii* were collected using a hand-held entomological net at the summit of Mont Rigaud (45°27.96'N, 74°19.56'W, summers of 2007 and 2017) and of Mont-Saint-Bruno (45°33.12'N, 73°19.68'W, summer 2010). Those specimens were killed using ethyl acetate fumes and pinned shortly afterwards.

The habitus photographs (Figs 1–4) were taken using a Nikon D810 DSLR camera with Nikon Micro-Nikkor 200 mm f/4 lens on a Manfrotto 454 micrometric positioning sliding plate. Lighting was provided by two Nikon SB-25 flash units with a Cameron Digital diffusion photo box. Adobe Photoshop Elements 13 was used as post-processing software. Photographs of the terminalia and genitalia were taken with an Olympus DP27 camera mounted with stereoscope SZX16. Images were captured and stacked using Helicon Focus 7 before being enhanced using Adobe Photoshop CC (version 20.0) (Adobe Systems, Mountain View, CA).

To solidify species identity, a leg of some specimens of *S.* (*B.*) *cadyi* and *S.* (*B.*) *yorkii* were submitted to LifeScanner (http://lifescanner.net/) and others to the Canadian Centre for DNA Barcoding for DNA barcoding. It was only possible to obtain sequences for *S.* (*B.*) *cadyi*. Those sequences were compared and analysed using the Barcode of Life Data (BOLD: http://boldsystems.org/) System ID Engine (Ratnasingham and Hebert 2007). Individual sequences from the successful specimens are publicly available via GenBank accession codes MK585627–MK585630. They can also be retrieved from BOLD in the public dataset DS-SARCOPH (https://doi.org/10.5883/DS-SARCOPH).

The terminology of the terminalia follows Buenaventura and Pape (2017). All voucher specimens are deposited in Insectarium de Montréal's scientific collection (IMQC).

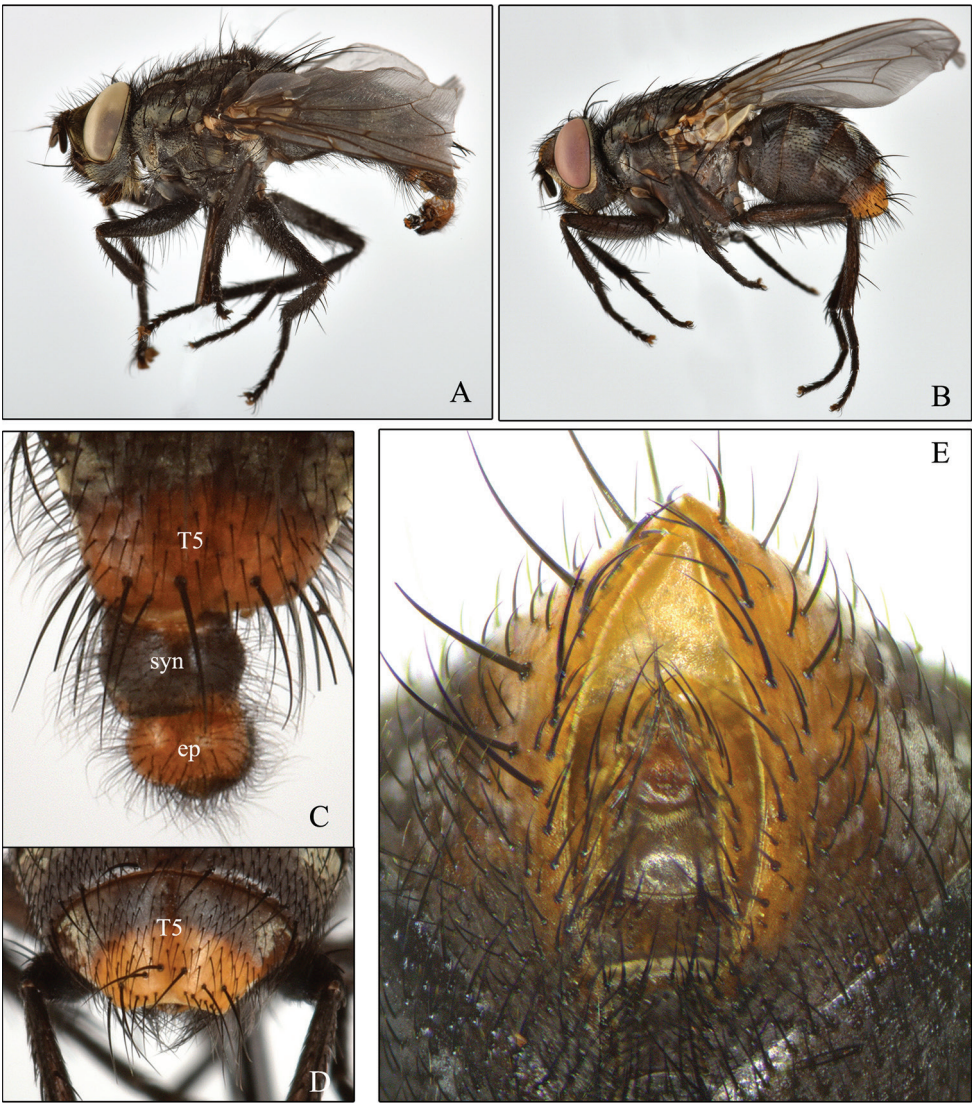

Figure 1. *Sarcophaga* (*Bulbostyla*) *cadyi* **A** male habitus **B** female habitus **C** male tergite 5 (T5), syntergosternite 7+8 (syn) and epandrium (ep), dorsal **D** female tergite 5 (T5), dorsal **E** female postabdomen, ventral.

Results and discussion

We present the first breeding record for a species of *Bulbostyla* and the first mention of their larvae developing in a spirobolid millipede. We also present the first mention of a *Sarcophaga* species showing a feeding interaction with a millipede in North America, and the second worldwide after the European species *Sarcophaga* (*Myorhina*) *iulicida* Pape (Pape 1990a).

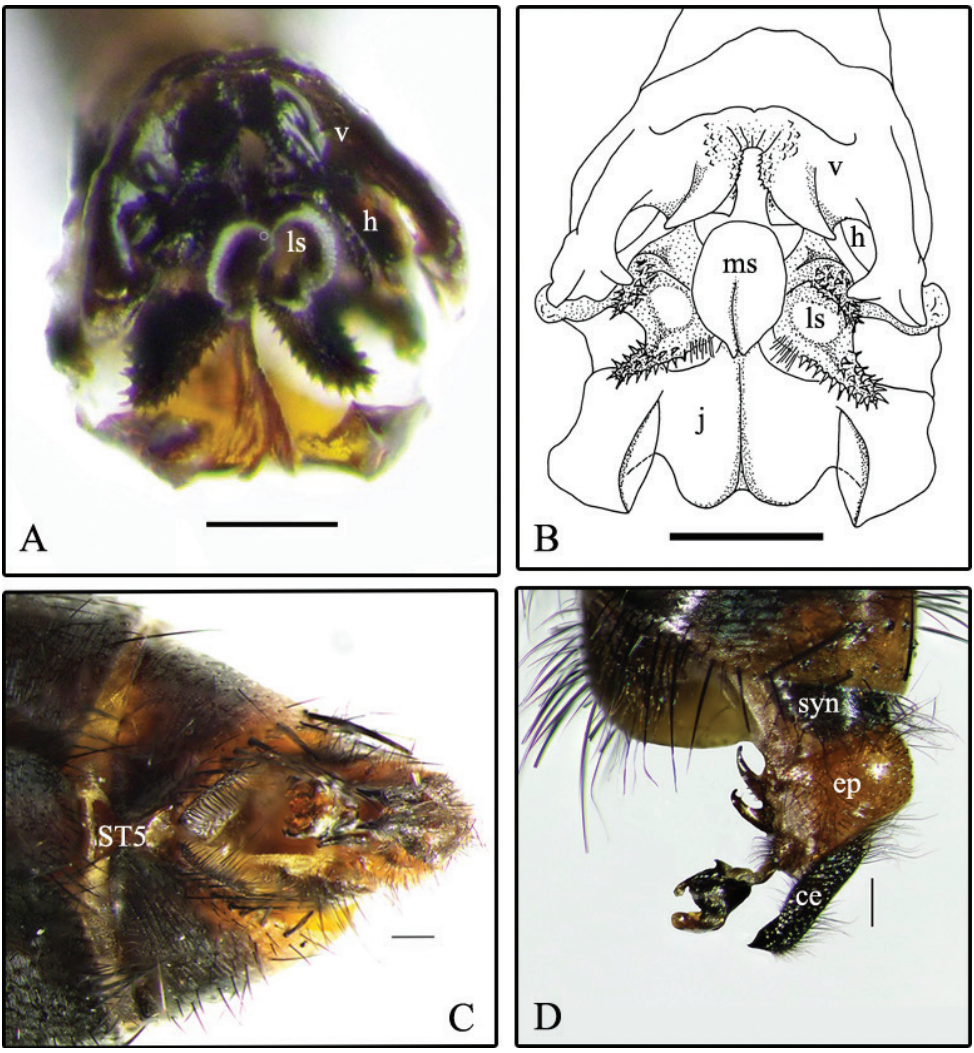

Figure 2. *Sarcophaga* (*Bulbostyla*) *cadyi* **A** distiphallus, anterior **B** distiphallus, anterior (from Giroux and Wheeler 2010) **C** male postabdomen, ventral **D** male postabdomen, left lateral. Abbreviations: j, juxta; ls, lateral stylus; ms, median stylus; h, harpes; v, vesica; syn, syntergosternite 7+8; ep, epandrium; ce, cercus; ST5, sternite 5. Scale bars: 0.2 mm (**A–B**), 0.5 mm (**C–D**).

Only three dipteran families (Sarcophagidae, Phoridae, Sciomyzidae) have been reported as parasitoids of diplopods (Hash et al. 2017). Within the Sarcophagidae, the species *Blaesoxipha beameri* Hall (Pape 1994) and species of the genus *Spirobolomyia* Townsend have been bred exclusively from spirobolid millipedes (Aldrich 1916; Pape 1990b, 1996) in North America. However, it is likely that species of this genus are not true millipede parasitoids. All observations of larviposition by *Spirobolomyia* species were on injured hosts with wounds large enough for the larva to enter (Hash et al. 2017).

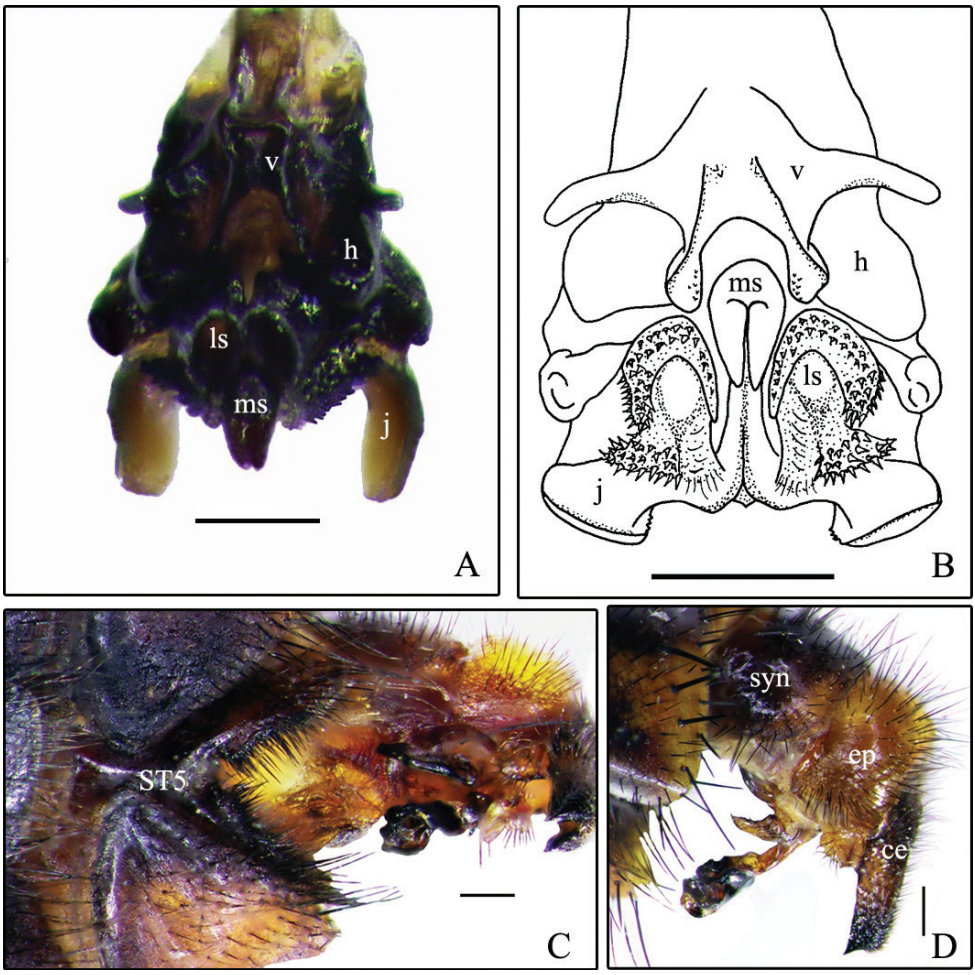

Figure 3. *Sarcophaga* (*Bulbostyla*) *yorkii* **A** distiphallus, anterior **B** distiphallus, anterior (from Giroux and Wheeler 2010) **C** male postabdomen, ventral **D** male postabdomen, left lateral. Abbreviations: j, juxta; ls, lateral stylus; ms, median stylus; h, harpes; v, vesica; syn, syntergosternite 7+8; ep, epandrium; ce, cercus; ST5, sternite 5. Scale bars: 0.2 mm (**A–B**), 0.5 mm (**C–D**).

We did not observe the larviposition of *S.* (*B.*) *cadyi* on *N. americanus*, which was already dead and colonized by the last instar larvae when we found it. Thus, we do not know if the spirobolid millipede was healthy, injured or already dead upon arrival of the female sarcophagid fly. In this sense, further investigations are needed to be able to determine the larval feeding habits of *S.* (*B.*) *cadyi*. The larvae pupated around August 25th. They pupated inside the millipede rather than exiting and pupating in the surrounding soil. It is unclear if this behaviour was due to laboratory conditions, or if it is also displayed in nature. Four males and four females emerged two weeks later, between 7 and 11 September 2017.

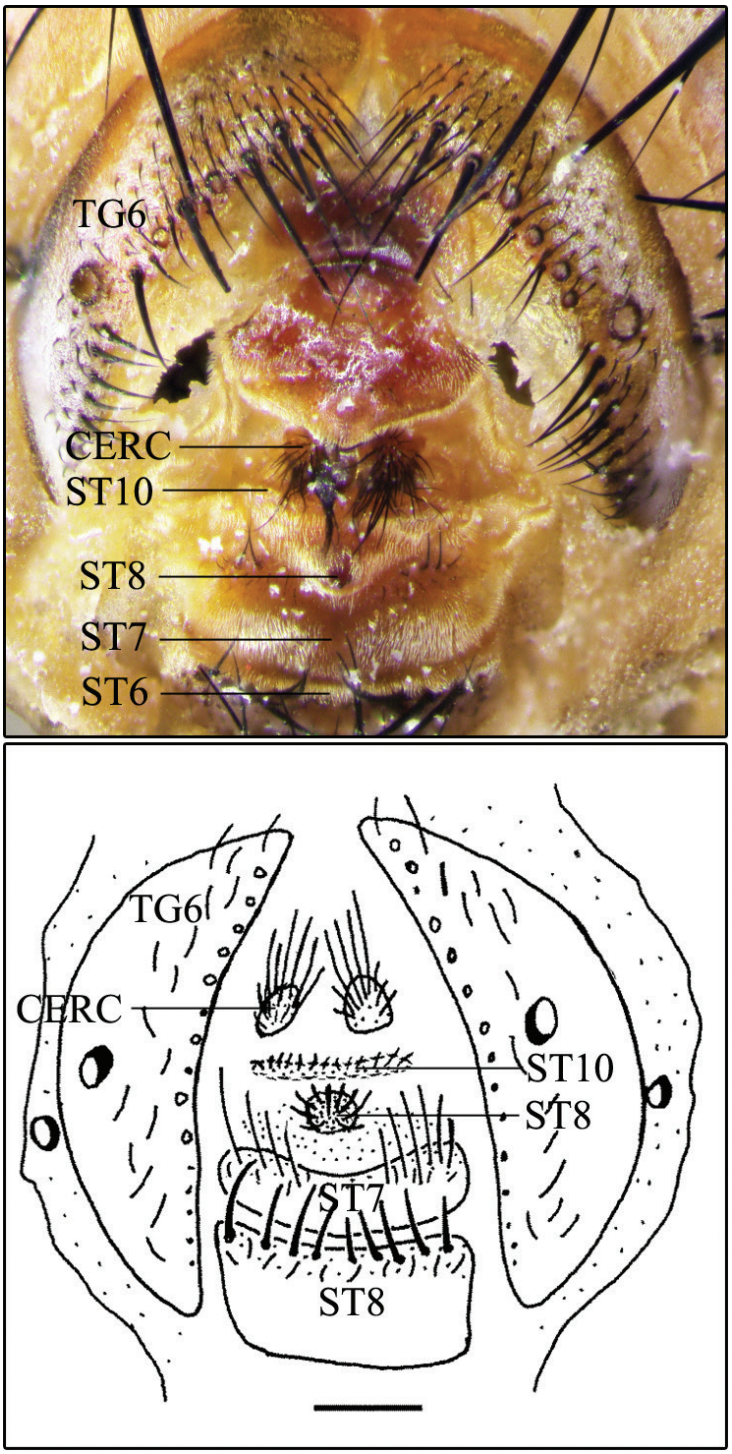

Figure 4. *Sarcophaga* (*Bulbostyla*) *cadyi* **A** female external terminalia, dorsoventral **B** female external terminalia, dorsoventral (from Giroux and Wheeler 2010). Abbreviations: cerc, cerci; st, sternite; tg, tergite. Scale bars: 0.5 mm (**A–B**).

Descriptions and an identification key for males of *S.* (*B.*) *cadyi* and *S.* (*B.*) *yorkii* can be found in Giroux and Wheeler (2010). However, in order to help in the identification of these species, some digital photographs are provided here: the habitus of *S.* (*B.*) *cadyi*, male and female (Fig. 1A, B); the postabdomen of a *S.* (*B.*) *cadyi* male (Figs 1C, 2C, D) and female (Fig. 1E) as well as the one of a *S.* (*B.*) *yorkii* male (Fig. 3C, D). Male and female specimens of both species have tergite 5 with an orange-yellow posterior half or third (sometimes entirely yellow) and a row of strong setae forming a semi circle that spreads on the apical third (Fig. 1C–E). The male cerci and syntergosternite 7+8 are darker than the epandrium (Figs 1C, 2D, 3D). The window on male sternite 5 is almost even with the rest of the base (Figs 2C, 3C). The male distiphallus of both species as well as the external terminalia of female *S.* (*B.*) *cadyi* were digitally photographed (Figs 2A, 3A, 4A) and illustrations (Figs 2B, 3B, 4B) were added for a better understanding of their structural morphology.

Acknowledgments

We thank Maxim Larrivée for support and René Limoges (Insectarium de Montréal) for the habitus photographs, Alexandra Cecan and Karine Thivierge (Laboratoire de Santé Publique du Québec) for training and access to the stereomicroscope and photography equipment and Jade Savage (Bishop's University) for the sequencing of some specimens. We also thank Emilie Desjardins for collecting various *N. americanus* samples and Nathalie Rivard for permission to collect in the Parc national du Mont-Saint-Bruno. This research was funded by a Natural Sciences and Engineering Research Council of Canada Discovery Grant to ITH and by the Insectarium de Montréal to MG.

References

Aldrich JM (1916) *Sarcophaga* and allies in North America. The Thomas Say Foundation of the Entomological Society of America 1: 1–301. https://doi.org/10.5962/bhl.title.8573

Buenaventura E, Pape T (2017) Phylogeny, evolution and male terminalia functionality of Sarcophaginae (Diptera: Sarcophagidae). Zoological Journal of the Linnean Society 183 (4): 808–906. https://doi.org/10.1093/zoolinnean/zlx070

Buenaventura E, Whitmore D, Pape T (2017) Molecular phylogeny of the hyperdiverse genus *Sarcophaga* (Diptera: Sarcophagidae), and comparison between algorithms for identification of rogue taxa. Cladistics 33(2): 109–133. https://doi.org/10.1111/cla.12161

Coupland JB, Barker GM (2004) Diptera as predators and parasitoids of terrestrial gastropods, with emphasis on Phoridae, Calliphoridae, Sarcophagidae, Muscidae and Fanniidae. In: Barker GM (Ed.) Natural Enemies of Terrestrial Molluscs. CAB International, Wallingford, 85–158. https://doi.org/10.1079/9780851993195.0085

Dahlem GA, Naczi RFC (2006) Flesh flies (Diptera: Sarcophagidae) associated with North American pitcher plants (Sarraceniaceae), with description of three new species. Annals

of the Entomological Society of America 99(2): 218–240. https://doi.org/10.1603/0013-8746(2006)099[0218:FFDSAW]2.0.CO;2

Giroux M, Wheeler TA (2010) Systematics of *Bulbostyla*, a new subgenus of *Sarcophaga* Meigen, and change of status for *Robackina* Lopes (Diptera: Sarcophagidae). Zootaxa 2553(1):35–59. https://doi.org/10.11646/zootaxa.2553.1.2

Hash JM, Millar JG, Heraty JM, Harwood JF, Brown BV (2017) Millipede defensive compounds are a double-edged sword: natural history of the millipede-parasitic genus *Myriophora* Brown (Diptera: Phoridae). Journal of Chemical Ecology 43(2): 198–206. https://doi.org/10.1007/s10886-016-0815-7

Mello-Patiu CA (2016) Family Sarcophagidae. Zootaxa 4122(1): 884–903. https://doi.org/10.11646/zootaxa.4122.1.75

Pape T (1990a) Two new species of *Sarcophaga* Meigen from Madeira and mainland Portugal (Diptera: Sarcophagidae). Tijdschrift voor Entomologie 133(1): 39–42. http://biostor.org/reference/49964

Pape T (1990b) Revisionary notes on American Sarcophaginae (Diptera: Sarcophagidae). Tijdschrift voor Entomologie 133(1): 43–74. https://archive.org/details/cbarchive_48786_revisionarynotesonamericansarc1990/page/n2

Pape T (1994) The world *Blaesoxipha* Loew, 1861 (Diptera: Sarcophagidae). Entomologica Scandinavica, Supplement 45: 1–247.

Pape T (1996) Catalogue of the Sarcophagidae of the world (Insecta: Diptera). Memoirs on Entomology 8: 1–557.

Ratnasingham S, Hebert PDN (2007) The Barcode of Life Data System (http://www.barcodinglife.org). Molecular Ecology Notes 7(3): 355–364. https://doi.org/10.1111/j.1471-8286.2007.01678.x

ZooKeys 909: 67–77 (2020)
doi: 10.3897/zookeys.909.39347
http://zookeys.pensoft.net

RESEARCH ARTICLE

A peer-reviewed open-access journal
ZooKeys
Launched to accelerate biodiversity research

Morphology lies: a case-in-point with a new non-biting midge species from Oriental China (Diptera, Chironomidae)

Chao Song[1], Xinhua Wang[2], Wenjun Bu[2], Xin Qi[1]

1 *College of Life Sciences, Taizhou University, Taizhou, Zhejiang 318000, China* **2** *College of Life Sciences, Nankai University, Tianjin, 300071, China*

Corresponding author: *Xin Qi* (qixin0612@tzc.edu.cn)

Academic editor: *F.L. da Silva* | Received 22 August 2019 | Accepted 17 December 2019 | Published 5 February 2020

http://zoobank.org/2D411E81-F5CB-4906-9845-BA82E04F5616

Citation: Song C, Wang X, Bu W, Qi X (2020) Morphology lies: a case-in-point with a new non-biting midge species from Oriental China (Diptera, Chironomidae). ZooKeys 909: 67–77. https://doi.org/10.3897/zookeys.909.39347

Abstract

Morphological traits are generally indicative of specific taxa, and particularly function as keys in taxonomy and species delimitation. In this study, a non-biting midge species with an *Einfeldia*-like superior volsella makes it hard to accurately determined based on its morphological characteristics. Molecular genes of two ribosomal genes and three protein-encoding genes were compiled to construct a related genera phylogeny and to address the taxonomic issues. Phylogenetic inference clearly supports the undetermined species as belonging to *Kiefferulus*. Therefore, a new species classified in the genus *Kiefferulus* is described and figured as an adult male from Oriental China. The species could be easily distinguished from other species in having an *Einfeldia*-like superior volsella and a triangular tergite IX.

Keywords

COI, CAD, *Kiefferulus*, morphology, phylogeny, PGD, taxonomy

Introduction

For hundreds of years, taxonomists have been mainly focused on morphological characteristics for classification, taxonomy, and species identification. The most essential part of traditional taxonomy is based on similarities and differences to create systematics. Linnaeus (1753) simplified and standardized the nomenclature into the binomial system

of genus and species. However, the system created is mainly based on visible characteristics by taxonomists' own professional experience, which is unstable and difficult to test. Discoveries and naming of new organisms aim to seek natural groupings with different proxies, such as morphology, genes, ecology, and behavior (Holstein and Luebert 2017). Nevertheless, classification of insects has been based on morphological characteristics to a great extent, which means that one species is deemed to be related with another based on shared characteristics of the same origin (synapomorphies).

With the burgeoning of molecular technology, there have been heated debates among scientists on whether the traditional system should be retained (Garnett and Christidis 2017; Thomson et al. 2018). Some think that the classification of complex organisms is in chaos and hampers species conservation, while others argue that taxonomy is necessary for global species conservation. After more than 250 years of the predominance of comparative morphology in species discovery, advanced methods and technology, especially molecular data, are rapidly expanding the realm of taxonomy (Padial et al. 2010). In addition, molecular information of certain species is increasingly registered or recorded and made available via several global initiatives, such as National Center for Biotechnology Information (NCBI), Barcode of Life Data System (BOLD), and different local barcode libraries (Ratnasingham and Hebert 2007). However, integrative taxonomy requires both detailed morphology description and molecular inference, which is time-consuming. Recently, regarding new species description, it is preferable to provide both morphology and COI barcodes, but COI-based phylogeny inference is unstable and not always convincing. Consequently, with the acceleration of new species descriptions, there would be much likely the peril of erroneous species hypotheses and unstable names (Padial et al. 2010)

Chironomidae is a large family of diverse flies and commonly called non-biting midges. It is the most widely distributed of all aquatic insect families occurring in all zoogeographical region of the world, including Antarctica (Cranston et al. 1989). It also shows adaptions to different extreme niches, surviving at elevations of 5,600 m of Himalaya Mountains (Kohshima 1984) and at more than 1,000 m depth in Lake Baikal (Linnevich 1971).

Kiefferulus was described by Goetghebuer (1922) to accommodate *Tanytarsus tedipediformis* from Belgium (Chaudhuri and Ghosh 1986). However, it was later recognized as a subgenus of *Pentapedilum* Kiefer by Edwards (1929) and of *Chironomus* Meigen by Townes (1945), after which Hamilton et al. (1969) restored its generic status. The male *Kiefferulus* is easily recognized by its characteristic hypopygium, such as the broadly sickle-shaped superior volsella with numerous long setae on the inner margin and long microtrichia reaching the distal part, and the distal inferior volsella being strongly expanded (Cranston et al. 1989).

Herein, we used sequences from two ribosomal genes (18S and 28S ribosomal DNA), three protein-encoding genes [cytochrome oxidase I (COI), CPSase region of carbamol-phosphate synthase-aspartate transcarbamolylase-dihydroorotase (CAD), and phosphogluconate dehydrogenase (PGD)] to explore the undetermined chirono-

mid species' systemic position. Through phylogenetic relationships, it is recognized as a new species of *Kiefferulus* based on molecular phylogeny analysis. We also discuss whether morphological traits can be independently used to define species within non-biting midges. Finally, *Kiefferulus trigonum* sp. nov. is presented and described.

Materials and methods

Taxon sampling

The morphological nomenclature follows Sæther (1980). The examined specimens were mounted on slides following the procedure by Sæther (1969). Measurements are given as ranges followed by the mean when there are four or more specimens examined. All types are deposited in College of Life Science, Nankai University.

Digital photographs were captured with a Leica DFC420 camera using a Leica DM6000 B compound microscope and under the application of the software Leica Suite at the NTNU university Museum, NTNU (Trondheim, Norway). Photograph post-processing were done in Adobe photoshop and Illustrator (Adobe Inc., California, USA).

DNA extraction, PCR amplification, sequencing, and alignment

Tissues for total genome DNA extraction were removed from the thorax, heads of adult, and abdomen of larvae. The extraction procedure followed the Qiagen DNeasy Blood and Tissue kit except for elusion buffer ranging from 100–150 µl according to different body sizes. After extraction, the exoskeletons were cleared and mounted to corresponding voucher numbers. We amplified two ribosomal genes (18S and 28S) and four protein coding gene segments including fragments of one mitochondrial gene (COI-3P), two sections of the CPSase region of carbamoylphosphate synthase-aspartate transcarbamoylase-dihydroorotase (CAD1 and CAD4), and phosphogluconate dehydrogenase (PGD). Besides, universal primers LCO1490 and HCO2198 were used for the standard COI barcode sequences.

Polymerase Chain Reaction (PCR) amplifications were done in a 25 µl volume including 12.5 µl 2 × Es Taq MasterMix (CoWin Biotech Co., Beijing, China), 0.625 µl of each primer, 2 µl of template DNA and 9.25 µl deionized H_2O, or 2.5 µl 10× Takara ExTaq buffer (CL), 2 µl 2.5 mM dNTP mix, 2 µl 25 mM MgCl2, 0.2 µl Takara Ex Taq HS, 1 µl 10 µM of each primer, 2 µl template DNA and 14.3 µl ddH_2O. PCR was performed on a PowerCylcer Gradient SL (Biometra Gmbh, Göttingen, Germany). For the mitochondrial gene, the program was set as follows: an initial denaturation step of 95 °C for 5 min, then followed by 34 cycles of 94 °C for 30 s, 51 °C for 30 s, 72 °C for 1 min and final extension at 72 °C for 3 min. The program of ribosomal genes and nuclear protein coding genes were referred to Cranston et al. (2012), alternatively for the protein coding genes that a touchdown program: initial denaturation step of 98 °C

for 10 s, then 94 °C for 1 min followed by five cycles of 94 °C for 30 s, 52 °C for 30 s, 72 °C for 2 min and 7 cycles of 94 °C for 30 s, 51 °C for 1 min, 72 °C for 2 min and 37 cycles of 94 °C for 30 s, 45 °C for 20 s, 72 °C for 2 min 30 s and one final extension at 72 °C for 3 min. PCR product were confirmed on a 1 % agarose gel and sequenced in both directions with ABI 3730 or ABI 3730XL capillary sequencers at Beijing Genomics Institute Co., Ltd, Beijing, China.

DNA sequences were edited and assembled with BioEdit 7.0.1 (Hall 1999). We applied the appropriate IUPAC code when editing the raw sequences in case of ambiguous bases but use "?" instead of the ambiguity symbol "N" in the matrix. Sequence matrix of protein coding genes were aligned by their amino acid sequences using Muscle (Edgar 2004) in MEGA7 (Kumar et al. 2016). Introns in CAD and PGD were recognized and deleted according to refence sequences and "GT-AG" rule before analysis. For two ribosomal genes sequences were aligned by muscle and then removed the poorly aligned positions using Glocks online server (http://phylogeny.lirmm.fr/phylo_cgi/one_task.cgi?task_type=gblocks) (Castresana 2000; Dereeper et al. 2008).

Phylogenetic analysis

Maximum likelihood (ML) trees were constructed in raxml-GUI v1.5b2 (Silvestro and Michalak 2012), with 1000 bootstrap replicates in a rapid bootstrap analysis, using GTR+G+I substitution model with partitions. Bayesian inference analysis (BI) was performed in two parallel runs in MrBayes (Nylander et al. 2004), consisting each of four chains of six million generations with a sampling frequency 1000 generation for one tree and burin of 25%. Partitions were in PartionFinder using greedy search and selected according to aicc (Lanfear et al. 2012). Result was as follows: TRN+I+G for 18S, COI3_ 2; GTR+I+G for COI3p_p1, 28S; GTR+I+G for CAD4_P1, CAD1_P1, PGD_P1; GTR+I+G for CAD1_P2, CAD4_P2, PGD_P2; GTR+I+G for CAD4_P3, PGD_P3; HKY+G for COI3p_P3; HKY+I+G for CAD1_P3. The convergence was checked in Tracer v1.7 (Rambaut et al. 2014) and terminated when ESS were superior to 200 with the initial 25% trees as burn in.

Results

The initial sequences of genes are CAD1 909bp, CAD4 846 bp, PGD 747 bp, 18S 933 bp, COI3P 826 bp, and 28S 743 bp (DOI: dx.doi.org/10.5883/DS-KIFFER). To reduce the effects of missing data, we trimmed the beginning and end of the protein coding genes and delete highly variable regions of 18S and 28S and finally concatenated to 4335 bp (CAD1 828 bp, CAD4 760 bp, PGD 747 bp, COI3P 662 bp, 18S 852 bp, 28S 455 bp) (SI). Both ML and BI inference show the same topology (Fig. 1) and agree on the simple phylogenetic scenario: the odd species conflict with the morphotype genus of *Einfeldia* but are clearly supported as species of *Kiefferulus*.

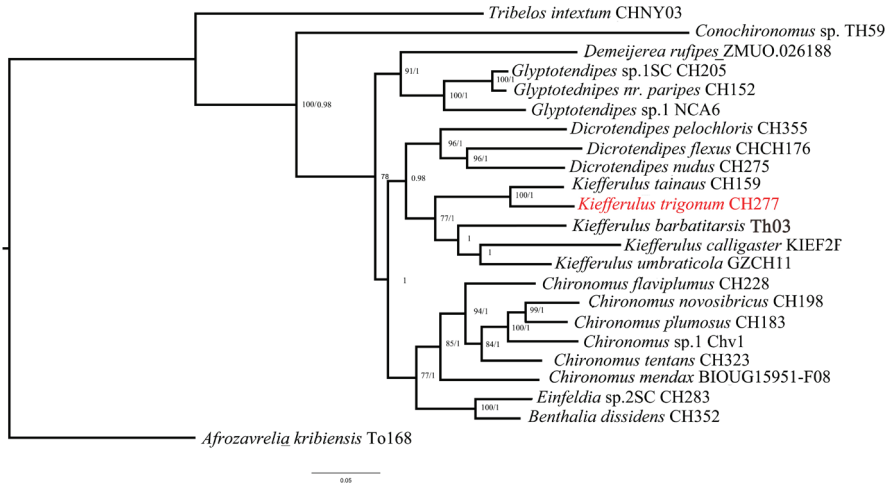

Figure 1. Bayes Inference tree (BI) tree based on the concatenated DNA dataset (18S, 28S, COI3P, CAD1, CAD4, PGD) of *Kiefferulus* and its related genera; *Afrozavrelia* was used as the outgroup. Numbers on branches refer to ML bootstrap values over 75 % and posterior probabilities over 0.95.

The new species was not identified using morphological taxonomic keys for adult Chironomidae (Cranston et al. 1989). The superior volsella with a large hairy base and a digitiform bare projection was recognized as an important and diagnostic definition of *Einfeldia* sensu lato, which makes it a pre-identification as an *Einfeldia* sp. Nevertheless, the typical superior volsella is not exclusive, and also occurs in *Benthalia*, *Chironomus* (including its subgenera *Chironomus* and *Lobochironomus*), *Conochironomus*, *Glyptotendipes*, and *Tribelos*. From morphological parsimony analysis, these genera sharing similar superior volsella are not closely related (Andersen et al. 2017). Molecular phylogeny of the related genera in this study, and in Cranston et al. (2012) show that *Conochironomus* and *Glyptotendipes* are not closely related to *Einfeldia*. Consequently, generic complexes or species groups with *Einfeldia*-like superior volsella are not genetically monophyletic clades (Fig. 1). Such cases of convergent characters are likely to causes serious problems in phylogenetic analysis, and lead to misplacement of species or genus. The hypothesis of generic diagnosis has raised great confusion within adult taxonomy. The case is not unique in Chironomidae: the marine species *Dicrotendipes sinicus* Qi & Lin was suggested as a new genus within the subfamily Chironominae. However, the analysis of genetic data revealed that the marine species nested within the genus *Dicrotendipes* (Qi et al. 2019).

To clearly illustrate the species' systemic position, it was included in the molecular phylogeny of related genera. Surprisingly, the morphologically identified species fall within the clade of *Kiefferulus* (Fig 1). Obviously, morphology-based identification conflicts with the molecular phylogeny. Considering the morphological homoplasy and phenotypic changes, we clarified the *Einfeldia*-like species within the genus

Kiefferulus. While the *Einfeldia*-type superior volsella is unique in *Kiefferulus*, the new species is named as *Kiefferulus trigonum* sp. nov.

When defining a species new to science, almost no taxonomists would test its systemic position, which would be time-consuming and costly. Hierarchical classifications based on appropriate morphological characters provide a main backbone of the life tree, while molecular data provide corroboration, resolution, and support (Scotland et al. 2003). Genera defined and recognized by clear morphological characters as in Chironomidae, such as Wiederholm (1989) for adults, Andersen et al. (2013) for larvae, and Wiederholm (1986) for pupae have not been tested with a full molecular phylogeny. Morphology alone was not enough to make a correct placement especially for some hyper diverse genera or monotypic genera and the traditional taxonomy needs revisions according to molecular phylogeny.

Taxonomy

***Kiefferulus trigonum* sp. nov.**
http://zoobank.org/E880611F-E713-4FCC-9F82-1696F96008A5
Figs 2, 3, BIN: ADG9680

Type material. ***Holotype*** (BDN No. 041685) 1♂, China, Fujian Province**:** Longyan City, Shanghang County, Buyun Town, Qiushan, 25.03N, 116.24E, 6.V.1993, Wang XH, light trap. Paratypes: 1♂ same as holotype; 3♂, Fujian Province: Sanming City, Jianning County, 25. IX.2002, Liu Z, light trap; 1♂, Guangxi Zhuang Autonomous Region: Nanning City, 9. V.1986, Wang XH; 2♂, Guizhou Province: Libo County, 7.VIII.1995, Bu WJ, light trap; 1♂, Hainan Province: Ledong City, Jianfengling National Forest Park, Song C, light trap.

Etymology. From Latin, *trigonum* means triangle, referring to the triangular tergite IX.

Diagnostic characters. The male adults could be obviously distinguished from other *Kiefferulus* species by the triangular IX tergite, superior volsella with projection and basal part of inferior volsella wider than distal part.

Description. Male imago (*N* = 9). Total length 4.78–5.90, 5.30 mm; wing length 2.13–2.85, 2.46 mm; total length/ wing length 1.95–2.38, 2.16; wing length / length of profemur 1.98–2.33, 2.12.

Coloration. Head, thorax and abdomen brown, legs yellowish except distal fore femur and tarsus I light brown.

Head. Frontal tubercle absent. AR 3.07–3.69, 3.25. Temporal setae 15–25, 20; Clypeus with 20–33, 26 setae;

Palpomere lengths (in μm): 38–55; 47; 115–153, 128; 123–163,141; 170–245, 208. Length of 5th palpomere / 3rd palpomere 1.42–2.04, 1.61.

Wing (Fig. 2A) VR 1.07–1.14, 1.10; Brachiolum with 2–3 setae; R with 20–29, 25 setae; R_1 with 13–21, 17 setae; R_{4+5} with 12–18, 15 setae; squama with 9–19, 15 setae. Anal lobe developed.

Thorax. Dorsocentrals 8–13, 12; acorstichals 20–28, 23; prealars 5–7, 6; scutellum 10–18, 12 setae.

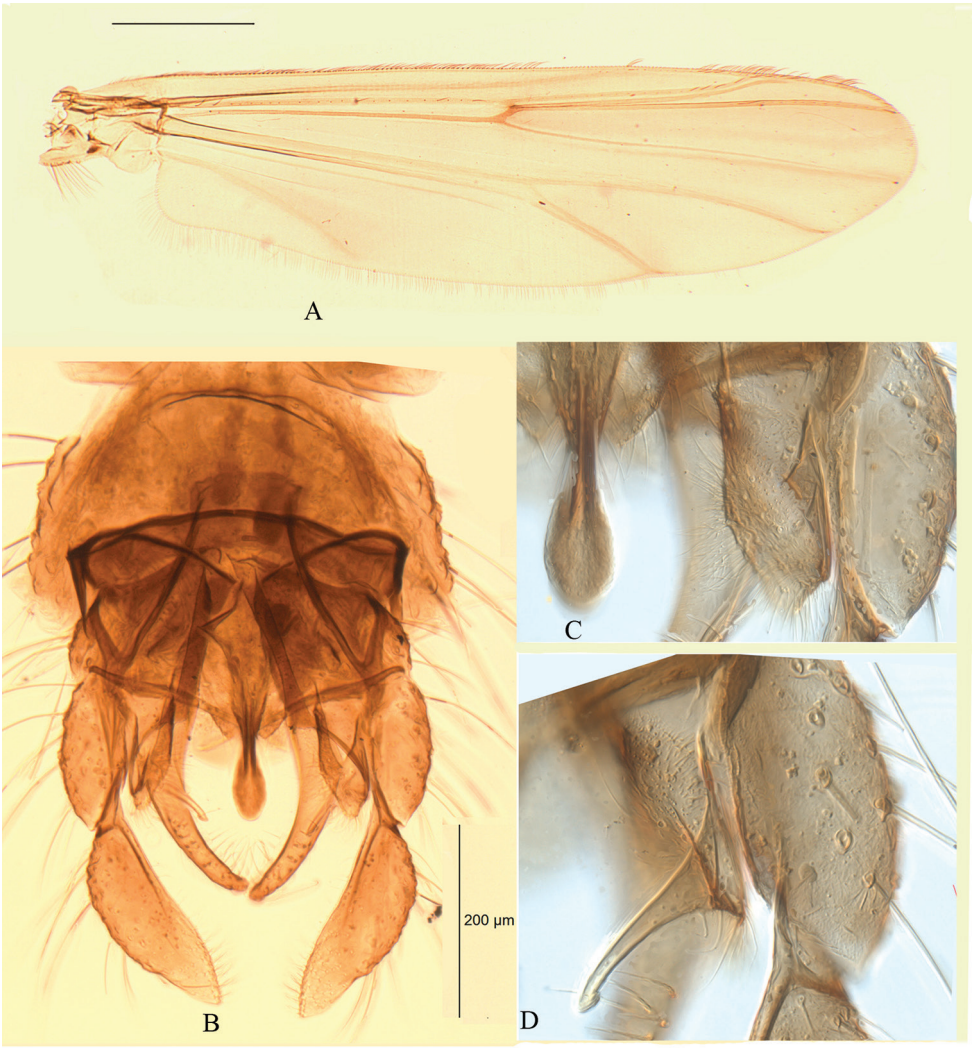

Figure 2. *Kiefferulus trigonum* sp. nov. male **A** wing **B** hypopygium in dorsal view **C** anal point and base of superior volsella **D** projection of superior volsella.

Legs. Tarsomere 1 of Mid and hind leg with 9–20, 14 and 6–17, 10 sensilla chaetica respectively. Front scale bluntly rounded; Spurs of mid tibia 23–38, 29 μm, and 25–33, 29 μm long, of hind tibia 28–38, 32 μm, and 25–35, 29 μm. Width at apex of front tibia 75–98, 85 μm, of mid tibia 83–95, 89 μm, of hind tibia 90–110, 98 μm. Lengths and proportions of legs as the Table 1.

Hypopygium (Figs 2B–D, 3). Anal tergite bands medially fused, and median anal tergite seta absent. Anal point basically narrow and apically broaden. Superior volsella with pad-like microchichiose and setose base, with long finger like projection inward to the apex of anal point. Inferior volsella slender, with strong distal setae. Gonocoxite 270–310, 293 μm long, gonostylus 180–210, 198 μm, with numerous

Table 1. Length (in μm) and proportions of legs of *Kiefferulus trigonum* sp. nov.

	fe	ti	ta_1	ta_2	ta_3	ta_4
p_1	1050–1325, 1161	825–1050, 919	1150–1500, 1322	720–860, 779	630–800, 712	540–690, 611
p_2	950–1250, 1078	820–1100, 956	520–650, 582	300–380, 337	230–300, 263	160–200, 180
p_3	1075–1350, 1203	1050–1375, 1194	470–940, 777	420–540, 472	360–480, 418	220–280, 251
	ta_5	LR	BV	SV	BR	
p_1	230–300, 262	1.38–1.52,1.44	1.37–1.49, 1.44	1.53–1.63, 1.57	3.67–6.89, 5.44	
p_2	110–130, 119	0.58–0.65, 0.61	2.80–3.06, 2.93	3.32–3.67, 3.49	2.32–4.86, 3.53	
p_3	140–170, 154	0.66–0.69, 0.68	2.35–2.58, 2.47	2.87–3.10, 2. 97	3.24–6.50, 4.09	

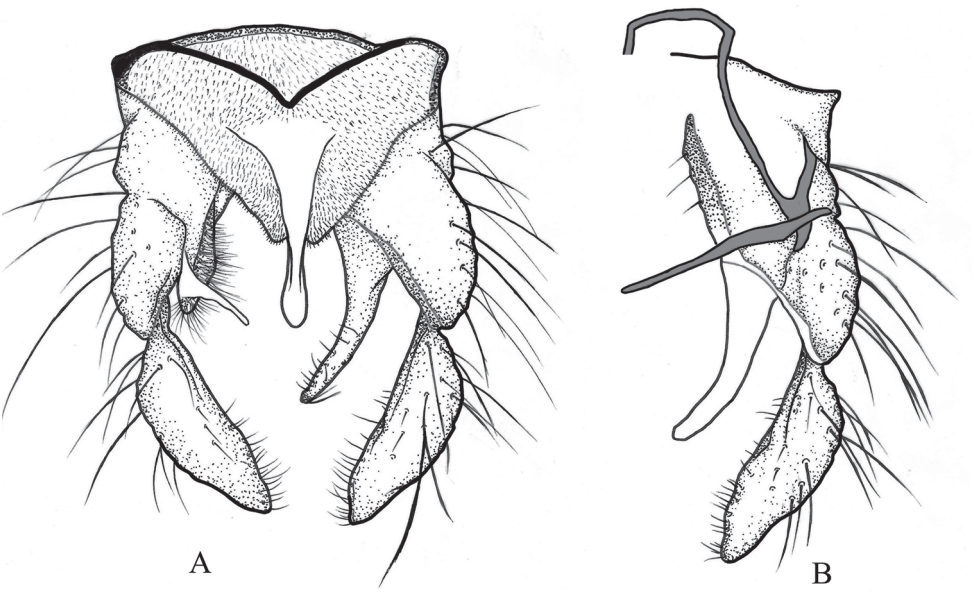

Figure 3. *Kiefferulus trigonum* sp. nov. male **A** hypopygium in dorsal view **B** hypopygium in ventral view.

distal microtrichia. Phallapodeme 220–250, 232 μm; transverse sternapodeme 100–113, 108 μm. HR 1.42–1.61, 1.49; HV 1.95–2.88, 2.59.

Larva and female unknown.

Distribution. Fujian Province, Guizhou Province, Guangxi Zhuang Autonomous Region, and Hainan Province (Oriental China).

Remarks

Morphological characters such as the anal point narrow basally, distally broad, the superior volsella with microtrichia, and the gonostylus distally constricted positively and molecular phylogeny provide clues indicating the genus *Kiefferulus*. Morphologically, the new species shows great similarity with *Einfeldia* species with pad-like microtrichose and setose bases and a finger-like projection inwards to the apex of the anal point that clearly distinguishes them from species of *Kiefferulus*.

Acknowledgements

This paper forms part of the project "Phylogeny of the subfamily Chironominae". The first author is indebted to Elisabeth Stur and Torbjørn Ekrem (NTNU University Museum, Trondheim, Norway) when studying in Trondheim. Many thanks to Yu Xue, who did a lot of work on *Kiefferulus* and Mingxuan Hong for figures drawing in preparing the manuscript. Financial support is acknowledged from Zhejiang Provincial Natural Science Foundation of China (LY17C040001) and the National Natural Science Foundation of China (31672264).

References

Andersen T, Cranston PS, Epler JH (2013) The larvae of Chironomidae (Diptera) of the Holarctic Region – Keys and diagnoses. Insect Systematics & Evolution Supplement 66:1–571.

Andersen T, Mendes HF, Pinho LC (2017) Two new Neotropical Chironominae genera (Diptera: Chironomidae). CHIRONOMUS Journal of Chironomidae Research 30: 26–54. https://doi.org/10.5324/cjcr.v0i30.2029

Castresana J (2000) Selection of conserved blocks from multiple alignments for their use in phylogenetic analysis. Molecular Biology and Evolution 17(4): 540–552. https://doi.org/10.1093/oxfordjournals.molbev.a026334

Cranston PS, Dillon ME, Pinder LCV, Reiss F (1989) The adult males of Chironominae (Diptera, Chironomidae) of the Holarctic region. Keys and diagnoses. In: Wiederholm T (Ed.) The adult males of Chironomidae (Diptera) of the Holarctic region – Keys and diagnoses. Entomologica scandinavica Supplement 34: 353–502.

Cranston PS, Hardy NB, Morse GE (2012) A dated molecular phylogeny for the Chironomidae (Diptera). Systematic Entomology 37(1): 172–188. https://doi.org/10.1111/j.1365-3113.2011.00603.x

Cranston PS, Martin J, Mulder M, Spies M (2016) Clarification of *Einfeldia* Kieffer, 1922 (Diptera: Chironomidae) with *E. australiensis* (Freeman, 1961), comb. n. based on immature stages. Zootaxa 4158(4): 491–506. https://doi.org/10.11646/zootaxa.4158.4.3

Dereeper A, Guignon V, Blanc G, Audic S, Buffet S, Chevenet F, Dufayard JF, Guindon S, Lefort V, Lescot M, Claverie JM, Gascuel O (2008) Phylogeny.fr: robust phylogenetic analysis for the non-specialist. Nucleic Acids Research 36 (Web Server issue): W465–469. https://doi.org/10.1093/nar/gkn180

Edgar RC (2004) MUSCLE: multiple sequence alignment with high accuracy and high throughput. Nucleic Acids Research 32(5): 1792–1797. https://doi.org/10.1093/nar/gkh340

Folmer O, Black M, Hoeh W, Lutz R, Vrijenhoek R (1994) DNA primers for amplification of mitochondrial cytochrome c oxidase subunit I from diverse metazoan invertebrates. Molecular Marine Biology and Biotechnology 3(5): 294–299.

Garnett ST, Christidis L (2017) Taxonomy anarchy hampers conservation Taxonomy anarchy hampers conservation. Nature 546(7656): 25–27. https://doi.org/10.1038/546025a

Hall TA (1999) BioEdit: a user-friendly biological sequence alignment editor and analysis program for Windows 95/98/NT. Nucleic acids symposium series 41: 95–98.

Hamilton AL, Saether OA, Oliver DR (1969) A Classification of the Nearctic Chironomidae. Fisheries research board of canada technical report 124: 1–42.

Holstein N, Luebert F (2017) Taxonomy: stable taxon boundaries. Nature 548(7666): 158–158. https://doi.org/10.1038/548158d

Kohshima S (1984) A novel cold-tolerant insect found in a Himalayan glacier. Nature 310(5974): 225–227. https://doi.org/10.1038/310225a0

Kumar S, Stecher G, Tamura K (2016) MEGA7: Molecular Evolutionary Genetics Analysis Version 7.0 for Bigger Datasets. Molecular Biology and Evolution 33(7): 1870–1874.

Lanfear R, Calcott B, Ho SYW, Guindon S (2012) PartitionFinder: combined selection of partitioning schemes and substitution models for phylogenetic analyses. Molecular Biology and Evolution 29(6): 1695–1701.

Linnaeus C (1753) Species plantarum (Vol. 2). Stockholm: Laurentius Salvius.

Linnevich AA (1971) The Chironomidae of Lake Baikal. Limnologica (Berlin) 8: 51–52.

Nylander JAA, Ronquist F, Huelsenbeck JP, Nieves-Aldrey JL (2004) Bayesian phylogenetic analysis of combined data. Systematic Biology 53(1): 47–67. https://doi.org/10.1080/10635150490264699

Padial JM, Miralles A, De la Riva I, Vences M (2010) The integrative future of taxonomy. Frontiers in Zoology 7: 16. https://doi.org/10.1186/1742-9994-7-16

Qi X, Lin XL, Ekrem T, Beutel RG, Song C, Orlov I, Chen CT, Wang XH (2019) A new surface gliding species of Chironomidae: An independent invasion of marine environments and its evolutionary implications. Zoologica Scripta 48(1): 81–92.

Rambaut A, Suchard MA, Xie D, Drummond AJ (2014) Tracerv1.6. http://beast.bio.ed.ac.uk/Tracer.2014

Ratnasingham S, Hebert PDN (2007) BOLD: The Barcode of Life Data System (www.barcodinglife.org). Molecular Ecology Notes 7(3): 355–364. https://doi.org/10.1111/j.1471-8286.2007.01678.x

Sæther OA (1969) Some Nearctic Pondonominae, Diamesinae, and Orthocladiinae (Diptera: Chironomidae). Bulletin of the Fisheries Research Board of Canada 170: 1–154.

Sæther OA (1980) Glossary of chironomid morphology terminology (Diptera: Chironomidae). Entomologica scandinavica Supplement 14: 1–51.

Scotland RW, Olmstead RG, Bennett JR (2003) Phylogeny reconstruction: the role of morphology. Systematic Biology 52(4): 539–548. https://doi.org/10.1080/10635150309309

Silvestro D, Michalak I (2012) raxmlGUI: a graphical front-end for RAxML. Organisms Diversity & Evolution 12(4): 335–337. https://doi.org/10.1007/s13127-011-0056-0

Thomson SA, Pyle RL, Ahyong ST, Alonso-Zarazaga M, Ammirati J, Araya JF, et al. (2018) Taxonomy based on science is necessary for global conservation. Plos Biology 16(3).

Townes HK (1945) The Nearctic Species of Tendipedini – Diptera, Tendipedidae (= Chironomidae). American Midland Naturalist 34(1): 1–206. https://doi.org/10.2307/2421112

Wiederholm T (1986) The pupae of Chironomidae of the Holarctic region – Keys and diagnoses. Entomologica scandinavica Supplement 28: 1–482.

Wiederholm T (1989) The adult males of Chironomidae of the Holarctic region – Keys and diagnoses. Entomologica scandinavica Supplement 34:1–532.

Supplementary material 1

The concatenated DNA dataset used for phylogenetic analyses.

Authors: Chao Song, Xinhua Wang, Wenjun Bu, Xin Qi

Data type: NEX file

Link: https://doi.org/10.3897/zookeys.909.39347.suppl1

ZooKeys 909: 79–158 (2020)
doi: 10.3897/zookeys.909.46838
http://zookeys.pensoft.net

RESEARCH ARTICLE

A peer-reviewed open-access journal
ZooKeys
Launched to accelerate biodiversity research

Revision of the *Merodon serrulatus* group (Diptera, Syrphidae)

Ante Vujić[1], Laura Likov[1], Snežana Radenković[1], Nataša Kočiš Tubić[1], Mihajla Djan[1], Anja Šebić[1], Celeste Pérez-Bañón[2], Anatolij Barkalov[3], Rüstem Hayat[4], Santos Rojo[2], Andrijana Andrić[5], Gunilla Ståhls[6]

1 *University of Novi Sad, Department of Biology and Ecology, Trg Dositeja Obradovića 2, Novi Sad, Serbia* **2** *Department of Environmental Sciences and Natural Resources, Faculty of Sciences III, Campus of San Vicente, University of Alicante, Spain* **3** *Institute of Systematics and Ecology of Animals, Russian Academy of Sciences, Siberian Branch, Novosibirsk, Russia* **4** *Department of Plant Protection, Faculty of Agriculture, Akdeniz University, Antalya, Turkey* **5** *University of Novi Sad, BioSense Institute, Dr Zorana Đinđića 1, Novi Sad, Serbia* **6** *Zoology Unit, Finnish Museum of Natural History Luomus, University of Helsinki, Finland*

Corresponding author: *Laura Likov* (laura.likov@dbe.uns.ac.rs)

Academic editor: *X. Mengual* | Received 27 September 2019 | Accepted 11 December 2019 | Published 5 February 2020

http://zoobank.org/22B7FF16-D0A2-40F9-B20E-F7C6E0AF1842

Citation: Vujić A, Likov L, Radenković S, Kočiš Tubić N, Djan M, Šebić A, Pérez-Bañón C, Barkalov A, Hayat R, Rojo S, Andrić A, Ståhls G (2020) Revision of the *Merodon serrulatus* group (Diptera, Syrphidae). ZooKeys 909: 79–158. https://doi.org/10.3897/zookeys.909.46838

Abstract

The phytophagous hoverfly genus *Merodon* Meigen, 1803 (Diptera, Syrphidae), which comprises more than 160 species distributed in Palaearctic and Afrotropical regions, can be differentiated into multiple groups of species that harbor high levels of hidden diversity. In this work, the *serrulatus* species group of *Merodon* is revised, providing an illustrated key to species, a detailed discussion on the taxonomic characters and a morphological diagnosis, including also the first data about the preimaginal morphology of this species group. The study includes characteristics of the 13 species of the *M. serrulatus* group, along with the available distributional data. Moreover, descriptions are provided for seven new species, namely *M. defectus* Vujić, Likov & Radenković **sp. nov.**, *M. disjunctus* Vujić, Likov & Radenković **sp. nov.**, *M. medium* Vujić, Likov & Radenković **sp. nov.**, *M. nigrocapillatus* Vujić, Likov & Radenković **sp. nov.**, *M. nigropunctum* Vujić, Likov & Radenković **sp. nov.**, *M. opacus* Vujić, Likov & Radenković **sp. nov.**, and *M. trianguloculus* Vujić, Likov & Radenković **sp. nov.** In addition, the taxa *M. serrulatus* (Wiedemann in Meigen, 1822), *M. bequaerti* Hurkmans, 1993, *M. hirsutus* Sack, 1913, *M. kawamurae* Matsumura, 1916, *M. sacki* (Paramonov, 1936) and *M. sophron* Hurkmans, 1993 are redefined and redescribed. Following a detailed study of the type material sourced from different entomological collections, the status of all avail-

able taxa related to *M. serrulatus* is revised and a new synonymy is proposed: *M. tener* Sack, 1913 **syn. nov.** (junior synonym of *M. serrulatus*). The identity of *M. trizonus* (Szilády, 1940) could not be assessed as the type specimens are lost. Thus, the name *M. trizonus* is considered as *nomen dubium*. The monophyly and composition of this species group are assessed through Maximum Parsimony and Maximum Likelihood analyses of the mitochondrial COI and nuclear 28S rRNA gene sequences.

Keywords
28S rRNA, COI, immature stages, lectotype, morphology, new species, new synonyms, taxonomy

Table of contents

Introduction

The phytophagous hoverfly genus *Merodon* Meigen, 1803 contains more than 160 species distributed across the Palaearctic and Afrotropical regions (Ståhls et al. 2009). Adults mimic bees and bumblebees (Hymenoptera: Apidae) and feed on pollen and nectar from early spring to autumn (Hurkmans 1993; Speight 2018). Based on the immature stages of *Merodon* found to date, underground storage organs (bulbs, corms and rhizomes) of geophytes of the families Asparagaceae, Amaryllidaceae and Iridaceae are larval microhabitats of this taxon and phytophagy is its feeding mode (Ricarte et al. 2017; Preradović et al. 2018). The immature stages of only eight *Merodon* species have been described to date (Heiss 1938; Stuckenberg 1956; Ricarte et al. 2008, 2017; Andrić et al. 2014; Preradović et al. 2018) and a detailed literature review on the immature stages of *Merodon*, including host plants, has recently been published by Ricarte et al. (2017).

The taxonomic status and identification of many *Merodon* species requires further investigation, as the genus contains a high number of species groups consisting of morphologically cryptic taxa with very subtle morphological differences. In various recent publications, an integrative taxonomic approach combining morphological and molecular information has been adopted and resulted useful in resolving taxonomic ambiguities in hoverflies, e.g., in *Merodon equestris* species complex (Marcos-García et al. 2011), *Merodon avidus* complex (Popović et al. 2015; Ačanski et al. 2016), *Merodon aureus* species group (Šašić et al. 2016), genus *Chrysotoxum* Meigen, 1803 (Nedeljković et al. 2013, 2015) and *Melanostoma* Schiner, 1860 (Haarto and Ståhls 2014).

Most recent publications pertaining to the genus *Merodon* have focused on particular species groups, within which the authors delimited individual species (Vujić et al. 2012, 2013, 2015; Ačanski et al. 2016; Šašić et al. 2016; Veselić et al. 2017; Kočiš Tubić et al. 2018; Radenković et al. 2018a). The *Merodon avidus-nigritarsis* lineage was confirmed as one of four main lineages in the genus *Merodon*, alongside with three other lineages: *albifrons+desuturinus*, *aureus* and *natans*. Likov et al. (2019) presented a phylogenetic inference where the *Merodon avidus-nigritarsis* lineage was resolved in a similar way as in the studies by Šašić et al. (2016) and Radenković et al. (2018b). In the same study, Likov et al. (2019) divided the *M.*

avidus-nigritarsis lineage into 10 species groups (namely *M. aberrans*, *M. aurifer*, *M. avidus*, *M. clavipes*, *M. fulcratus*, *M. italicus*, *M. nigritarsis*, *M. pruni*, *M. serrulatus*, and *M. tarsatus* groups), and five species were not included in any of these species groups (i.e., *M. clunipes* Sack, 1913, *M. crassifemoris* Paramonov, 1925, *M. eumerusi* Vujić, Radenković & Likov, 2019, *M. murinus* Sack, 1913, and *M. ottomanus* Hurkmans, 1993).

The *Merodon serrulatus* species group includes taxa with a characteristic basolateral protrusion on the posterior surstyle lobe (Fig. 1). Based on recently published data, this group contains six already described species, i.e., *Merodon bequaerti* Hurkmans, 1993, *M. hirsutus* Sack, 1913, *M. kawamurae* Matsumura, 1916, *M. sacki* (Paramonov, 1936), and *M. serrulatus* (Wiedemann in Meigen, 1822) (Likov et al. 2019).

In this study, we present a taxonomic review of the *serrulatus* species group based on a detailed examination of material gathered as a part of our long-term field research in the Palaearctic region, especially in the Mediterranean and the Middle East. Our aims are 1. to review materials stored in several major entomological institutions and private collections holding specimens of this group; 2. to define and describe the taxa within the *serrulatus* species group, including new species; 3. to infer the phylogenetic relationships among the members of this species group using mtDNA COI gene and the 28S rRNA gene; and 4. to present the first data about the preimaginal morphology of the *M. serrulatus* species group.

Materials and methods

Material examined

Most of the recently collected specimens were sampled by sweep net. Further specimens of the *Merodon serrulatus* species group were sourced from collections deposited in museums and universities which are listed below. Consisted total of 1,083 specimens collected from 1837 to 2018 across 22 countries (i.e., Algeria, China, Croatia, France, Greece, Israel, Italy, Kazakhstan, Kyrgyzstan, Libya, Montenegro, Morocco, North Macedonia, Portugal, Russia, Spain, Syria, Tajikistan, Tunisia, Turkey, Turkmenistan, and Uzbekistan) were studied for the present study.

The information on labels of the material examined is provided for each studied specimen in the following order: country name, a bullet point (indicating the beginning of a material citation), number and sex of specimen(s), locality data, geographical coordinates, altitude, collection date, collector(s) followed by "leg.", institutional acronym and specimen codes/unique identifiers ("to" indicates range). The specimens are listed alphabetically by country and subsequently by increasing latitude (south to north) within each country. In the quotations of the type specimens' original label data, double quotation marks were used to indicate separate labels, and the slash was adopted to indicate a new line within a label, with additional details and interpretations provided in square brackets, where applicable.

Institutional acronyms

A. S. coll.	Axel Ssymank collection, Achtberg, Germany (ssymanka@t-online.de)
CEUA	Colección Entomológica de la Universidad de Alicante, Alicante, Spain
D. D. coll.	Dieter Doczkal collection, Munich, Germany (dieter.doczkal@gmail.com)
EMIT	Entomological Museum of Isparta, Isparta, Turkey
FSUNS	Faculty of Sciences, Department of Biology and Ecology, University of Novi Sad, Novi Sad, Serbia
G. V. W. coll.	Guy Van de Weyer collection, Reet (Rumst), Belgium (guido.vandeweyer@skynet.be)
GLAHM	Hunterian Zoology Museum, University of Glasgow, Glasgow, UK
J. T. S. coll.	John T. Smit collection, Utrecht, the Netherlands (John.Smit@naturalis.nl)
J. v. S. coll.	Jeroen van Steenis collection, Amersfoort, the Netherlands (jvansteenis1@gmail.com)
M. B. coll.	Miroslav Barták collection, Prague, Czech Republic (bartak@af.czu.cz)
M. H. coll.	Martin Hauser collection, Sacramento, USA (martin.hauser@cdfa.ca.gov)
MAegean	The Melissotheque of the Aegean, University of the Aegean, Mytilene, Greece
MNHN	Muséum National d'Histoire Naturelle, Paris, France
MZH	Finnish Museum of Natural History, University of Helsinki, Helsinki, Finland
NBCN	Naturalis Biodiversity Center [formerly known as the National Museum of Natural History (RMNH)], Leiden, The Netherlands
NHMUK	Natural History Museum, London, UK
NHMW	Museum of Natural History (Naturhistorisches Museum Wien), Vienna, Austria
NMNH	The Department of Entomology, of the National Museum of Natural History, Smithsonian Institution, Washington, DC, USA
NMPC	National History Museum, Prague, Czech Republic
NMS	National Museums Scotland, Edinburgh, UK
S. K. coll.	Sakari Kerppola collection, Helsinki, Finland (sakari.kerppola@helsinkinet.fi)
S. S. coll.	Süleyman Sarıbıyık collection, Kastamonu, Turkey
SIZK	I.I. Schmalhausen Institute of Zoology of National Academy of Sciences of Ukraine, Kiev, Ukraine
SZMN	Siberian Zoological Museum of the Institute of Systematics and Ecology of Animals, Siberian Branch of the Russian Academy of Sciences, Novosibirsk, Russia
TAUI	Tel Aviv University, Tel Aviv, Israel

WML	World Museum Liverpool, Liverpool, UK
ZHMB	Zoological (Zoologisches) Museum of the Humboldt University, Berlin, Germany
ZMKU	Zoological Museum, State University of Kiev, Kiev, Ukraine
ZMUC	Zoological Museum, Natural History Museum of Denmark, University of Copenhagen, Copenhagen, Denmark

Taxonomic study of adults

The type material of all described species of the *Merodon serrulatus* species group were studied, with the exception of the type material of *Merodon trizonus* (Szilády, 1940) because the type specimens are lost.

To study the male genitalia, dry specimens were relaxed in a closed pot containing water to ensure high humidity levels, and the genitalia were extracted using an insect pin with a hooked tip. Genitalia were cleared by boiling them individually in tubes of water-diluted KOH pellets for 3–5 minutes. This was followed by brief immersion in acetic acid to neutralize the KOH, immersion in ethanol to remove the acid, and storage in microvials containing glycerol. Specimens' measurements were taken in dorsal view with a micrometer and are presented as ranges. Body length was measured from the lunule to the end of the abdomen. Drawings were made using a FSA 25 PE drawing tube attached to a binocular microscope Leica MZ16. Specimens photographs were captured by a Nikon D7100 camera connected to a personal computer, as well as a Leica DFC 320 digital camera attached to a Leica MZ16 binocular microscope. After photographing, CombineZ software (Hadley 2006) was used in order to create composite image with an extended depth of field, created from the in-focus areas of each image.

Terminology adopted in the morphological descriptions follows Thompson (1999) and, for male genitalia, Marcos-García et al. (2007), while the term "fossette" follows Doczkal and Pape (2009).

Localities were geo-referenced in Google Earth (Google Inc, California, USA, https://www.google.com/earth; accessed on 10.02.2019). Geographic coordinates of localities were represented in GenGIS (v 2.5.3) (Parks et al. 2013) in order to create distributional maps.

The study of preimaginal morphology

Sampling

A targeted search for immature *Merodon* hoverflies was conducted in the chestnut forest of Agiassos, Lesvos Island (Greece). Abundant population of *M. serrulatus* and other *Merodon* species were found at this locality. Searches for larvae were carried out during a field trip from February 27 to March 10 2006, as owing to their biological cycle, these *Merodon* species would be in immature stages (larvae or pupae) during

this period. An area of ca. 3m^2, where the presence of many bulb species and adults of *Merodon* were reported the previous year was selected. The whole area was excavated to a depth of approximately 20 cm and the soil was sieved searching for the larvae. Only one larva (third larval stage) was found in the soil surrounding bulbs of different plant genera, such as *Fritillaria* Tourn. ex L., *Gagea* Salisb., *Muscari* Miller, and *Ornithogalum* L. This solitary larva was kept in a plastic container with the soil in which it had been found at room temperature until it pupated two days later. The adult of *M. opacus* sp. nov. emerged on 21 March 2006 after spending 17 days in the pupal stage.

Morphological study

The cephalopharyngeal skeleton was removed from the antero-ventral margin of the puparium using entomological pins. After dissection, the cephalopharyngeal skeleton was soaked in 10% KOH and heated for 15 min in order to remove the remaining tissues attached, after which it was soaked for a few minutes in acetic acid followed by 70% ethanol. Once the tissues had been cleared, the skeleton was preserved in glycerin. Debris adhering to the puparial integument was removed with pins and brushes and by placing the specimens in an ultrasonic cleaner for a few minutes. The cleaned specimen was mounted on stubs and was examined with a scanning electron microscope (S3000N Hitachi) at 20 kV using variable-pressure (or low vacuum) mode, as this technique allows a direct evaluation of the specimens without coating the samples with gold. The stereomicroscope Olympus SZX16 (equipped with Olympus U-TVO.5XC-3 camera) was used for the examination and to capture images of the puparium (general view) and the cephalopharyngeal skeleton. Dimension measurements (in mm) were performed on preserved specimens using a Leica MZ9.5 binocular microscope.

The terminology for immature stages adopted here follows Rotheray (1993) and Rotheray and Gilbert (1999), whereas certain characters of the cephalopharyngeal skeleton are determined in line with Hartley (1963), and our morphological character descriptions are based on *Merodon* puparia descriptions provided by other authors (Heiss 1938; Stuckenberg 1956; Ricarte et al. 2008, 2017; Preradović et al. 2018). The studied material has been deposited at the University of Alicante, Spain (CEUA).

Molecular analysis

The specimens subjected to molecular analysis are presented in Supplementary file 8: Table 1. DNA voucher specimens were deposited in FSUNS, EMIT, SZMN, and MZH. The genomic DNA of each specimen was extracted from two or three legs using a slightly modified SDS extraction protocol (Chen et al. 2010). For this purpose, the D2–3 region of the nuclear 28S ribosomal RNA gene and the mitochondrial protein-coding cytochrome c oxidase subunit I (COI) gene were amplified. Primer pair F2 and 3DR was used for the amplification of 28S rRNA gene region (Belshaw et al. 2001), whereas C1-J-2183 (alias Jerry) and TL2-N-3014 (alias Pat) primer pair

(Simon et al. 1994) was chosen for 3'-end of COI gene, and for 5'-end COI gene, we used LCO1490 and HCO2198 primer pair (Folmer et al. 1994). The PCR reactions were carried out according to Kočiš Tubić et al. (2018). The amplification products were enzymatically purified by Exonuclease I and FastAP Thermosensitive Alkaline Phosphatase enzymes (ThermoScientific, Lithuania) and sequenced using only forward primers on an ABI3730x1 Genetic Analyzer (Applied Biosystems, Foster City, CA, USA) at the Finnish Institute for Molecular Medicine (FIMM), Helsinki, Finland.

Data analysis

In order to establish the systematic position and composition of the *Merodon serrulatus* group, samples representing the four main *Merodon* lineages were analyzed following the approaches described by Šašić et al. (2016) and Radenković et al. (2018b), while two further Merodontini species served as outgroups, i.e., *Platynochaetus macquarti* Loew, 1862 and *Eumerus grandis* Meigen, 1822 (see Supplementary file 8: Table 1 for GB accession numbers of all analyzed species and outgroups). Alignment of the obtained COI sequences was achieved using the Clustal W algorithm (Thompson et al. 1994) implemented in BioEdit (Hall 1999), while rRNA 28S gene was aligned by the multiple alignment using Fast Fourier Transform (MAFFT) program (Katoh et al. 2005, 2009), version 7, which implements iterative refinement methods (Katoh and Standley 2013). The E-INS-i strategy was chosen (Katoh et al. 2009). All sequences in the analyzed two-gene dataset (concatenated COI and 28S rRNA gene sequences) were trimmed to equal lengths. Phylogenetic tree construction was performed by conducting Maximum Parsimony (MP) and Maximum Likelihood (ML) analyses. The parsimony analysis was conducted using NONA (Goloboff 1999), spawned with the aid of ASADO, version 1.85 (Nixon 2008), using the heuristic search algorithm (settings: mult*1,000, hold/100, max trees 100,000, TBR branch swapping). GTRGAMMA model was determined as the best choice model for the analysed dataset using MEGA 7 (Kumar et al. 2016). The dataset was divided into two partitions: COI gene and 28S rRNA gene. The ML tree was constructed by RAxML 8.2.8 (Stamatakis 2014) using the CIPRES Science Gateway (Miller et al. 2010) and applying the general time-reversible (GTR) evolutionary model with a gamma distribution (GTRGAMMA) (Rodríguez et al. 1990). Nodal support was estimated using nonparametric bootstrapping with 1,000 replicates for both MP and ML trees, which were rooted on *Platynochaetus macquarti*.

Results

Merodon serrulatus group

Diagnosis. Member species of the *Merodon serrulatus* species group exhibit a distinctive and characteristic basolateral protrusion (lateral hump) on the posterior surstyle lobe (Fig. 1A, B: bp, 6: bp, 14C: bp). They are relatively large (11–15 mm) species with

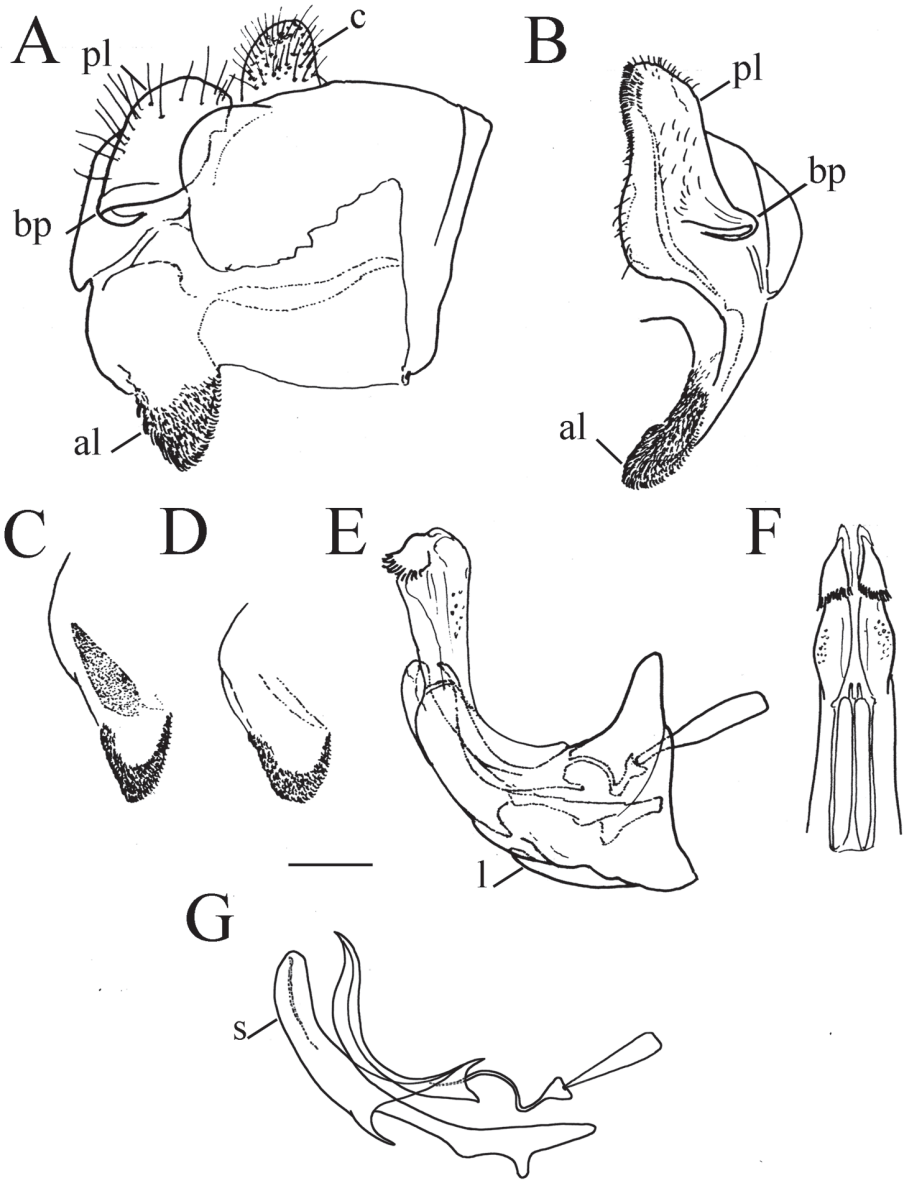

Figure 1. *Merodon serrulatus* male genitalia. **A** Epandrium, lateral view **B** Epandrium, ventral view **C, D** Posterior surstyle lobe, lateral view **E** Hypandrium, lateral view **F** Part of hypandrium, ventral view **G** Aedeagus, lateral view. Abbreviations: al–anterior surstyle lobe, bp–basolateral protrusion, c–cercus, l–lingula, pl–posterior surstyle lobe, s–lateral sclerite of aedeagus. Scale bar: 0.2 mm.

a dark scutum and white microtrichose fasciae (at least in females) on the dark olive brown terga 2–4 (as in Fig. 2); tergum 2 usually with a pair of reddish orange lateral maculae. Antennae dark brown (as in Fig. 5).

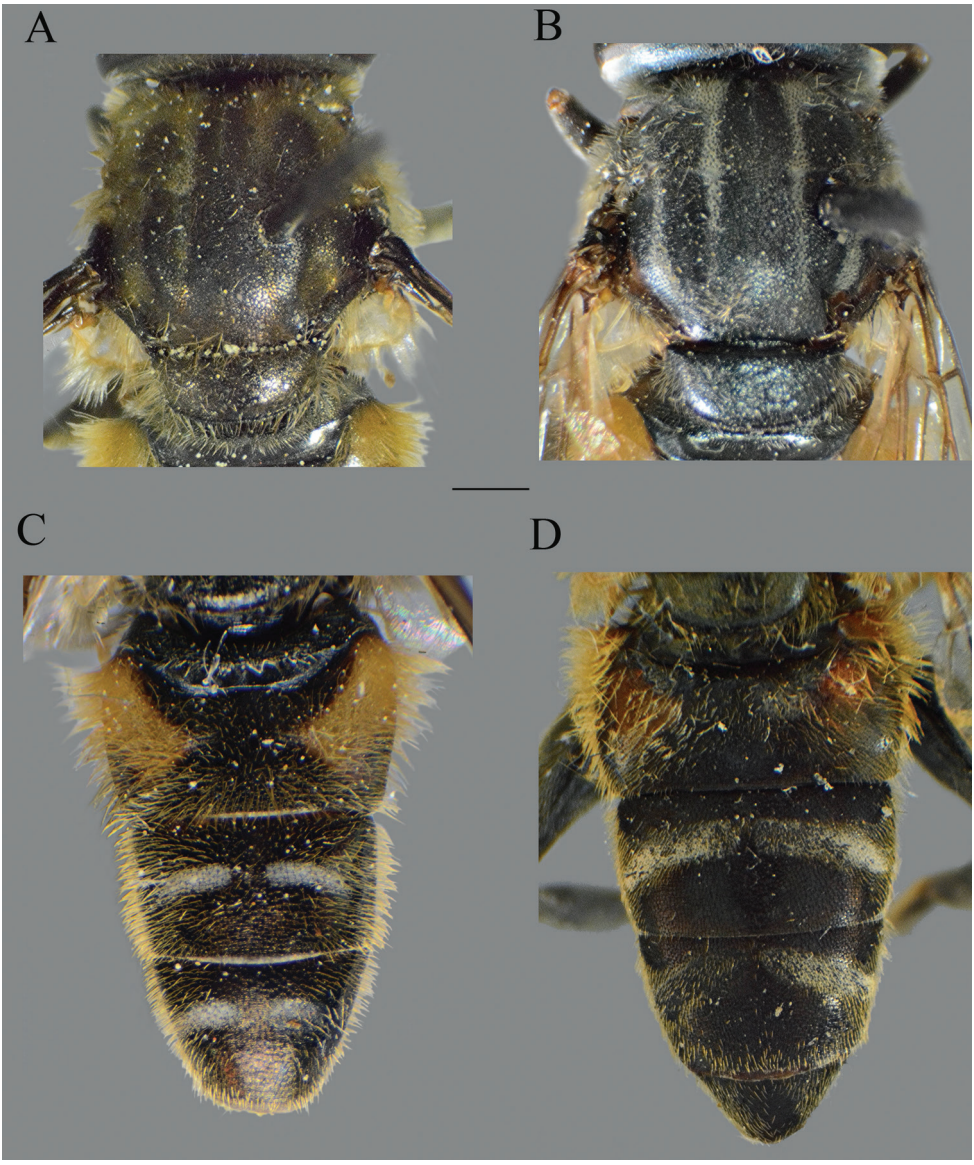

Figure 2. *Merodon serrulatus* body parts, dorsal view. **A** thorax, male **B** thorax, female **C** abdomen, male **D** abdomen, female. Scale bar: 2 mm.

Basoflagellomere 1.5–2.2 times as long as wide, usually obviously concave dorsally (as in Fig. 3A, D, G, J). Scutum covered with erect, usually yellow pile. Pile on metasternum erect, and as long as those on metacoxa. Posterior part of mesocoxa bare, without long pile. Legs mostly black, without spinae or other protuberances (as in Fig. 4). Metafemora incrassate (as on Fig. 4). Tarsi black dorsally and dark brown ventrally. Abdomen elongated, narrow and tapering (as on Fig. 2), slightly longer than scutum

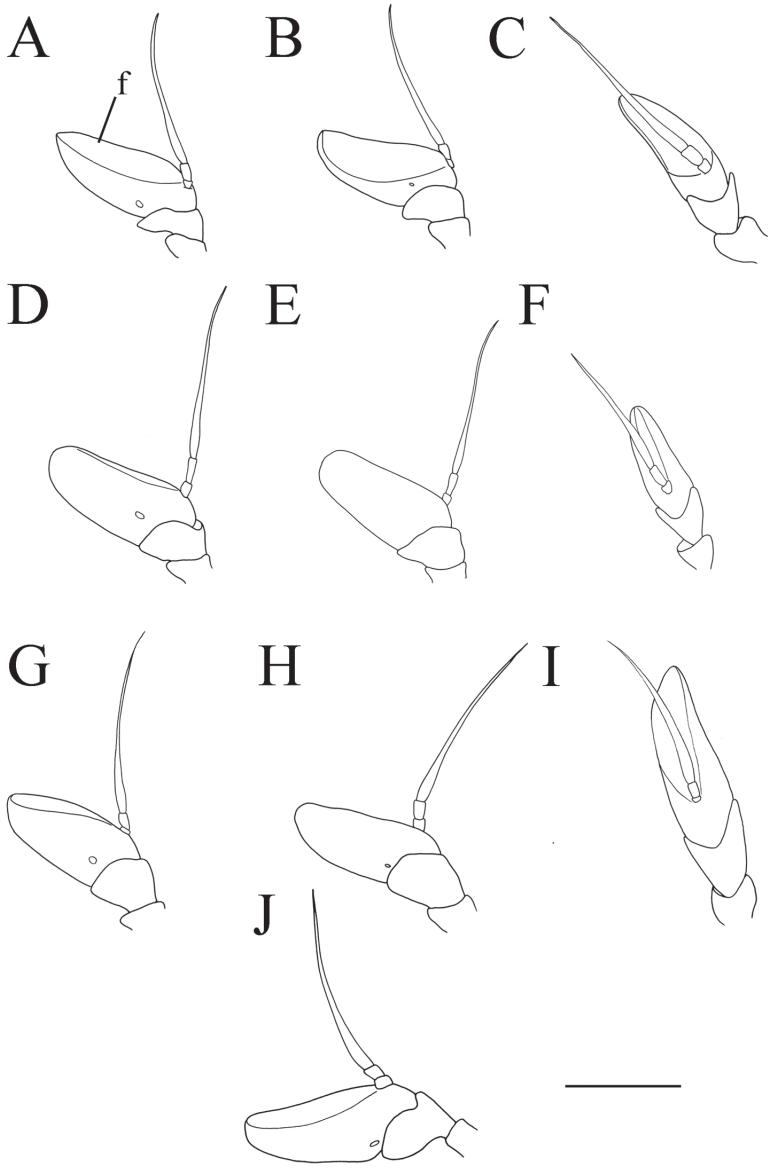

Figure 3. *Merodon serrulatus* antenna. **A** outer side, lateral view, male (Spain) **B** inner side, lateral view, male (Spain) **C** dorsal view, male (Spain) **D** outer side, lateral view, female (Spain) **E** inner side, lateral view, female (Spain) **F** dorsal view, female (Spain) **G** outer side, lateral view, male (Greece) **H** inner side, lateral view, male (Greece) **I** dorsal view, male (Greece) **J** outer side, lateral view, male (Russia). Abbreviation: f–fossette. Scale bar: 1 mm.

and scutellum together. Male genitalia: apical part of anterior surstyle lobe more or less of rhomboid or triangular in shape (as on Fig. 1A: al, C, D), covered with dense short pile; posterior surstyle lobe oval with basolateral protrusion (lateral hump) (Fig. 1A,

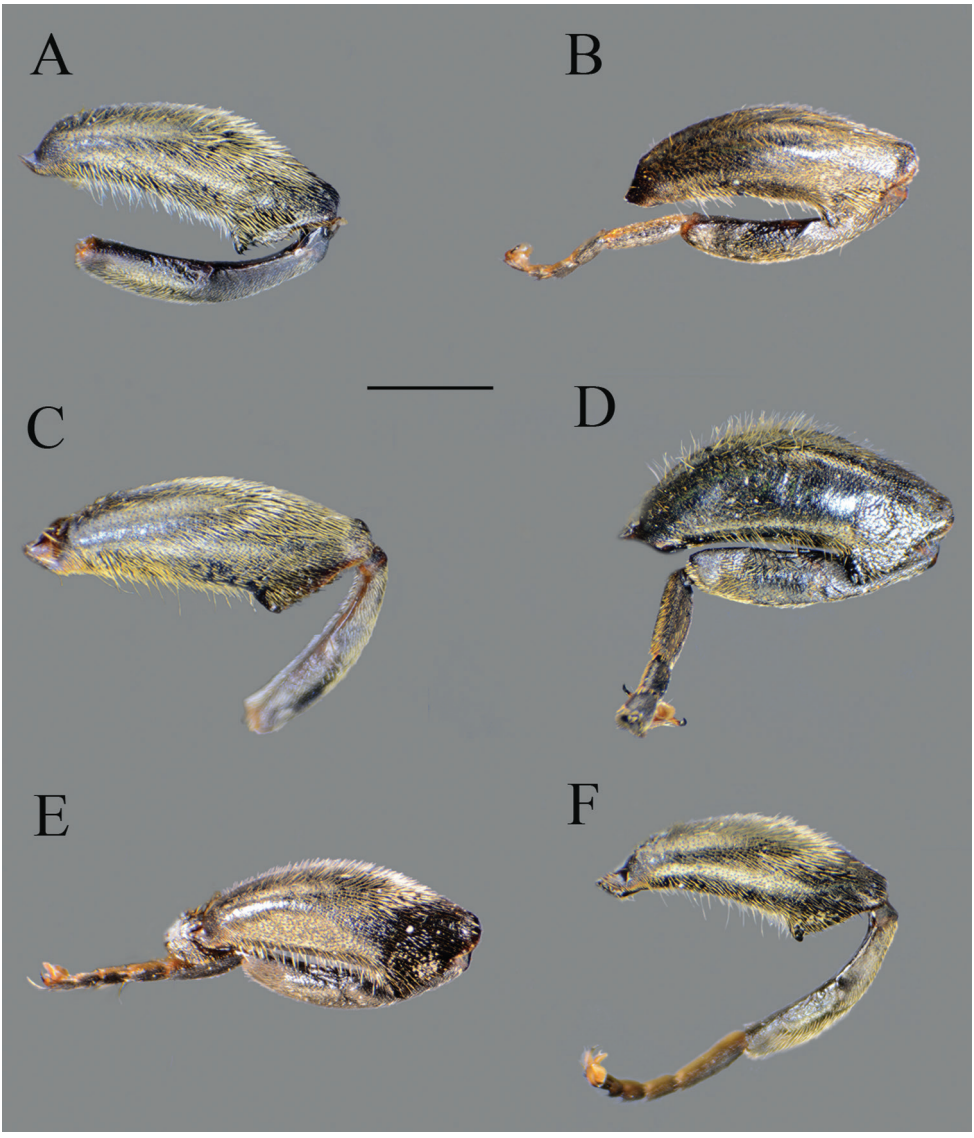

Figure 4. *Merodon serrulatus*, lateral view. **A**, **C** metatrochanter, metafemur and metatibia **B**, **D**–**F** metaleg. **A**–**B** male (Spain) **C** female (Spain) **D** male (France) **E** male (Greece) **F** male (Russia). Scale bar: 2 mm.

B: bp, 14C: bp); cercus rectangular, without prominences (Fig. 1A: c). Hypandrium elongated and sickle shaped (Fig. 1E); lateral sclerite of aedeagus finger-like with basal thorn-like process (Fig. 1G: s); lingula usually present (as on Fig. 1E: l).

Intraspecific variability. In most of the taxa in the *Merodon serrulatus* species group, the length of pile on the metafemur and the presence of microtrichia on the scutum and terga is highly variable among specimens of the same species.

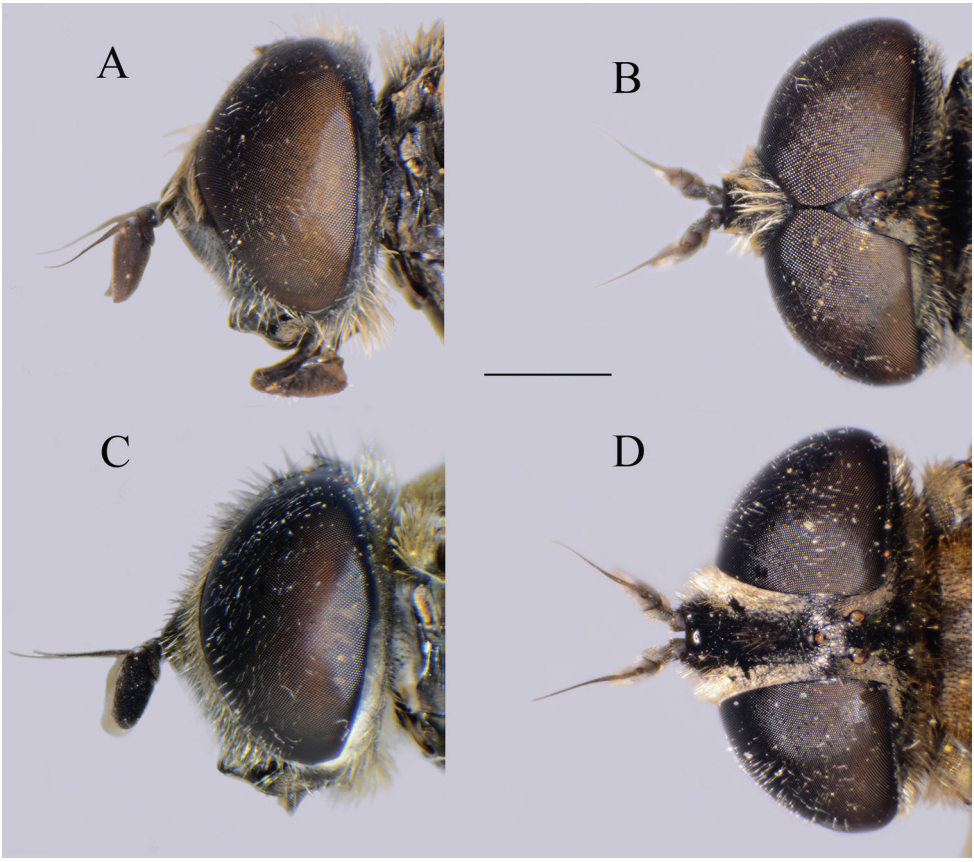

Figure 5. *Merodon serrulatus* head. **A** lateral view, male **B** dorsal view, male **C** lateral view, female **D** dorsal view, female. Scale bar: 2 mm.

The *Merodon serrulatus* species group consists of 13 species, namely *M. bequaerti*, *M. defectus* sp. nov., *M. disjunctus* sp. nov., *M. hirsutus*, *M. kawamurae*, *M. medium* sp. nov., *M. nigrocapillatus* sp. nov., *M. nigropunctum* sp. nov., *M. opacus* sp. nov., *M. sacki*, *M. serrulatus*, *M. sophron* Hurkmans, 1993, and *M. trianguloculus* sp. nov.

Taxonomy and nomenclature of the species belonging to the *Merodon serrulatus* species group

Merodon bequaerti Hurkmans, 1993

Figs 8A, B, 9A–C, J, 10A, B, 11A–C

Diagnosis. Large (8–11.9 mm), dark brown species with pairs of narrow microtrichose fasciae on terga 2–4 in males, in some specimens absent; metafemur with long pile on

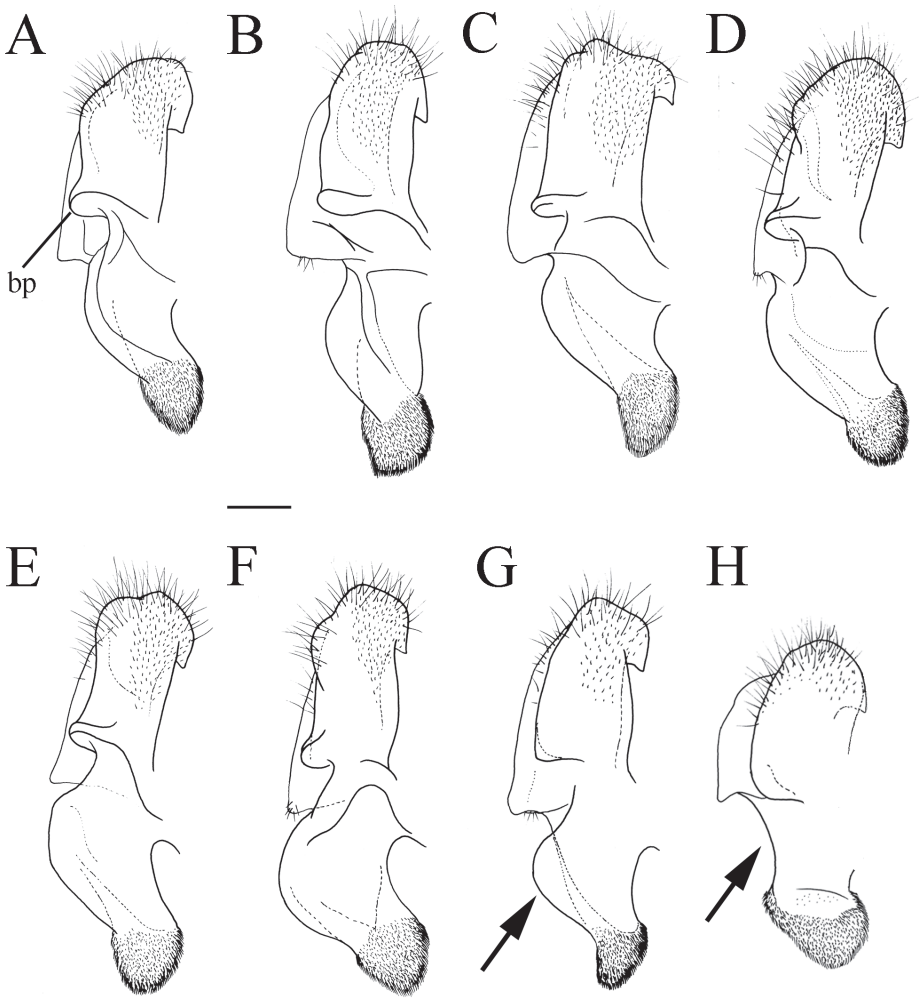

Figure 6. Male genitalia, surstylus, lateral view. **A** *Merodon serrulatus*, Spain **B** *Merodon serrulatus*, France **C** *Merodon serrulatus*, Greece (Pindos) **D** *Merodon serrulatus*, Greece (Olympos) **E** *Merodon serrulatus*, Greece (Peloponnese) **F** *Merodon serrulatus*, Montenegro **G** *Merodon serrulatus*, Russia **H** *Merodon medium* sp. nov. G, **H** margin of anterior surstyle lobe marked with arrow. Abbreviation: bp–basolateral protrusion. Scale bar: 0.2 mm.

ventral margin; the longest pile as long as one third to half of width of metafemur (Fig. 8); apical part of anterior surstyle lobe rhomboid shape, covered with dense, short pile, and strong dark brown marginal pile on posterior surstyle lobe (Fig. 9A: al, J); females with very narrow microtrichose fasciae on terga 2–4 and sparse pilosity on ventral margin of metafemur, only with few longer pile. Similar to *Merodon sacki* but differs in a less curved metafemur and generally shorter body pile in males, clearly visible on tergum 4 (Fig. 10), and by well separated anterior and posterior surstyle lobe (Fig. 9A), almost fused in *M. sacki* (Fig. 9D). Related to *M. sophron*, but differs in more incrassate metafemur (Fig. 8A, D), longer pile on ventral margin of metafemur in both sexes (Fig.

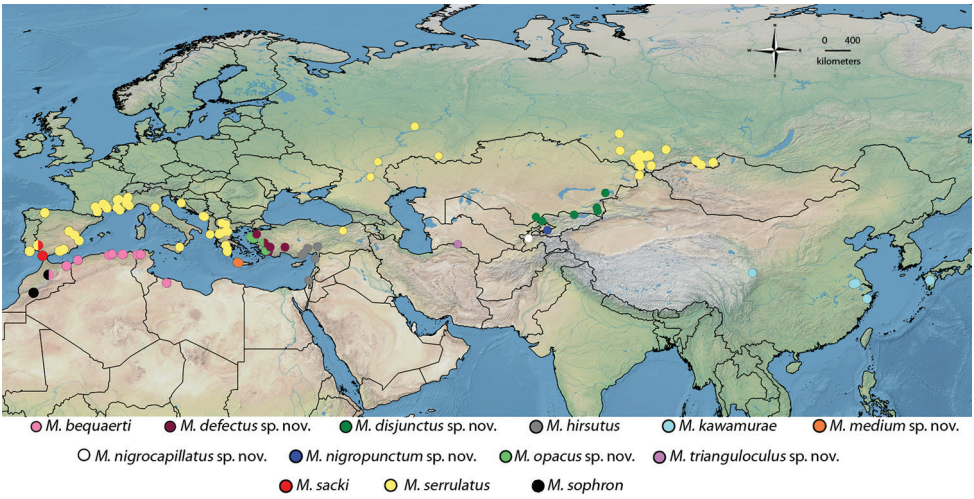

Figure 7. Distribution map of *Merodon serrulatus* species group.

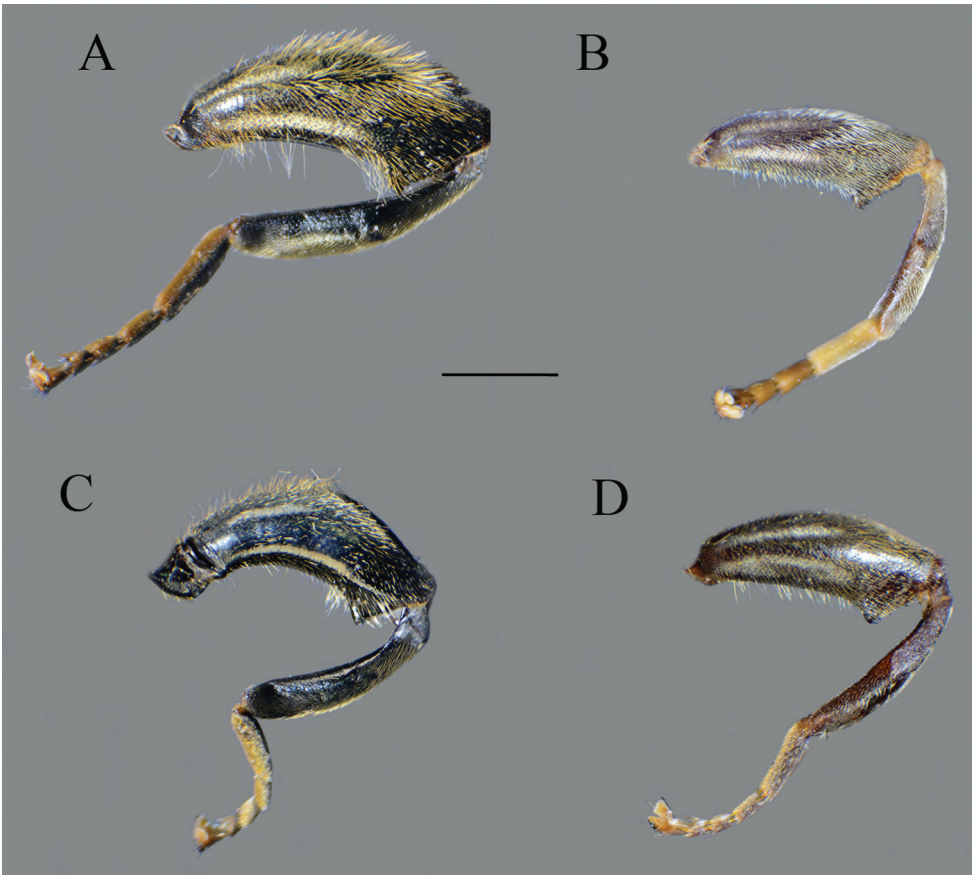

Figure 8. Metaleg, lateral view. **A** *Merodon bequaerti*, male **B** *Merodon bequaerti*, female **C** *Merodon sacki*, male **D** *Merodon sophron*, male. Scale bar: 2 mm.

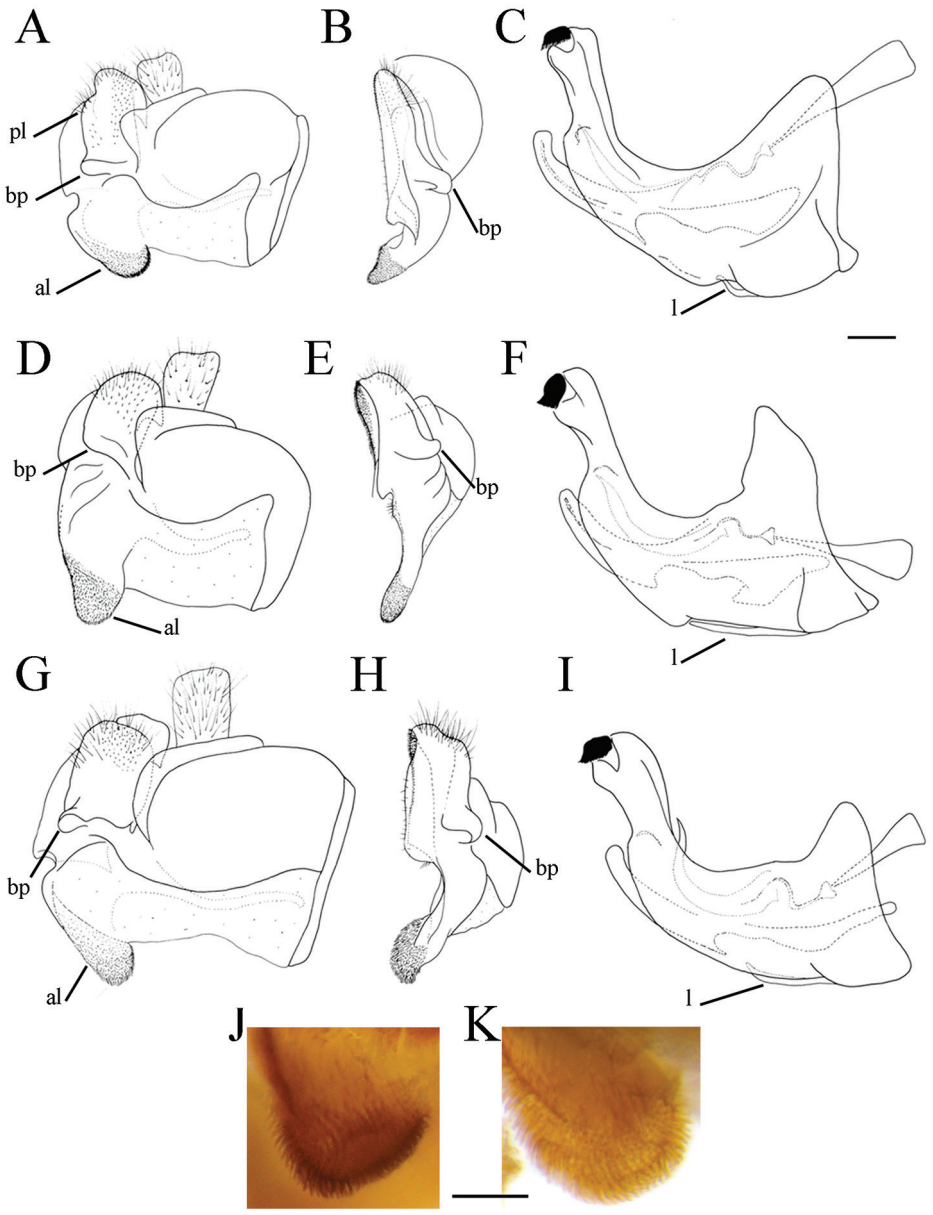

Figure 9. Male genitalia. **A** *Merodon bequaerti*, epandrium, lateral view **B** *Merodon bequaerti*, epandrium, ventral view **C** *Merodon bequaerti*, hypandrium, lateral view **D** *Merodon sacki*, epandrium, lateral view **E** *Merodon sacki*, epandrium, ventral view **F** *Merodon sacki*, hypandrium, lateral view **G** *Merodon sophron*, epandrium, lateral view **H** *Merodon sophron*, epandrium, ventral view **I** *Merodon sophron*, hypandrium, lateral view **J** *Merodon bequaerti*, anterior surstyle lobe, lateral view **K** *Merodon sophron*, anterior surstyle lobe, lateral view. Abbreviations: al–anterior surstyle lobe, bp–basolateral protrusion, l–lingula, pl–posterior surstyle lobe. Scale bar: 0.2 mm.

8), and presence of dense, dark brown marginal pile on apical part of anterior surstyle lobe (Fig. 9A, J), less dense and light yellow in *M. sophron* (Fig. 9G, K).

Redescription (based on the type material and additional specimens). **Male.** Head. Antennae black to dark brown; basoflagellomere 1.7–2.1 times as long as wide, and 2.3 times as long as pedicel, concave dorsally with acute apex; fossette dorsolateral (Fig. 11); arista dark and thickened at basal one third, covered with dense microtrichia; arista 1.4–1.7 times as long as basoflagellomere (Fig. 11A, B); face and frons black with gray microtrichia, face covered with dense whitish gray, and frons with yellowish gray pile; oral margin shiny with microtrichose lateral areas; lunule shiny black, bare; eye contiguity 10–12 facets long; vertex isosceles, shiny covered with golden microtrichia in front of ocellar triangle; vertex with long, pale whitish yellow pile mixed with black pile on the ocellar triangle; ocellar triangle equilateral; occiput shiny, with gray-yellow pile, covered with a dense, gray microtrichia in ventral half; eyes covered with dense pile.

Thorax. Scutum and scutellum black with bronze luster, covered with dense, erect, yellow pile; scutum at wing basis with short black pile, in some specimens with fascia of black pile between wing basis; scutum with two or more microtrichose vittae, anteriorly connected and posteriorly reaching the scutellum; posterodorsal part of anterior anepisternum, posterior anepisternum (except anteroventral angle), anterior anepimeron, dorsomedial anepimeron, and posterodorsal and anteroventral parts of katepisternum with long, pale yellow pile and grayish microtrichia; wings entirely covered with microtrichia; wing veins brown; calypteres and halteres pale yellow; legs without spinae or other protuberances; legs mostly black, except brown tarsi ventrally in some specimens; pile on legs pale yellow, except black pile at apical one fourth of metafemur; metafemur curved and incrassate, ca. three times longer than wide; pile on postero- and anteroventral surface long, and ca. one third to half of width of metafemur, slightly longer than pile on dorsal margin (Fig. 8A).

Abdomen. Wide, tapering, 1.2 times longer than mesonotum; terga dark brown to black, with or without pairs of narrow microtrichose fasciae; tergum 2 with orange lateral maculae; pile on terga all yellow, except few black pile on medial part of terga 3 and 4 in some specimens (Fig. 10A, B); sterna dark brown, covered with long whitish/yellow pile.

Male genitalia. Apical part of anterior surstyle lobe rhomboid shape, 1.5 times longer than wide, covered with dense, short pile, and strong dark brown marginal pile (Fig. 9A: al, J); posterior surstyle lobe oval (Fig. 9A: pl) with basolateral protrusion (lateral hump) (Fig. 9A, B: bp); hypandrium sickle-shaped, without lateral projections; lingula small (Fig. 9C: l).

Female. Similar to the male except for normal sexual dimorphism and for the following characteristics: antennae with rounded tip, basoflagellomere 1.7–1.9 times longer than wide (Fig. 11C); frons with microtrichose vittae along eye margins; frons covered with pilosity of variable color, from mostly gray-yellow until predominantly black; ocellar triangle covered with black pile; ventral margin of metafemur with sparse pilosity, only few pile longer (Fig. 8B); lateral side of terga, anterior two third of tergum 2 and all tergum 5 with yellow pile; terga 2–4 with short adpressed black pile and with very narrow microtrichose fascia.

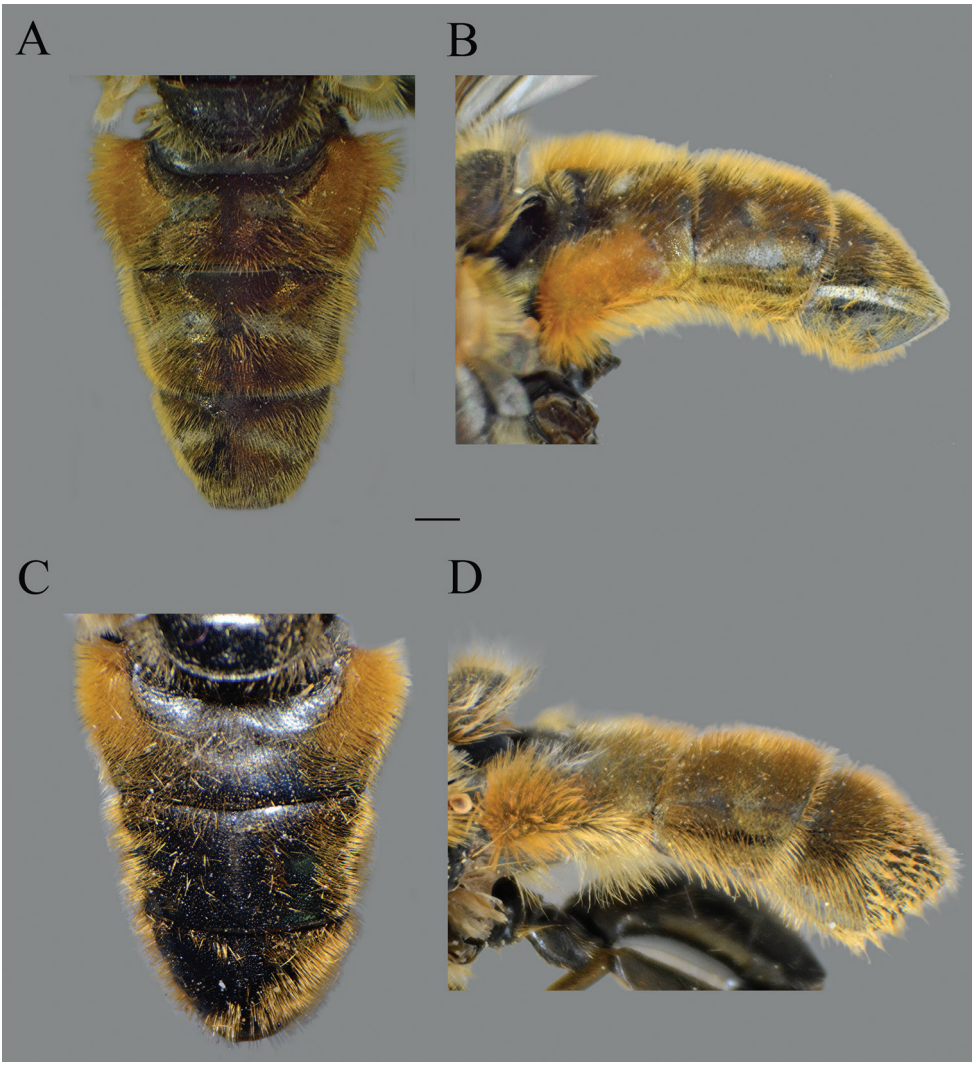

Figure 10. Abdomen of males. **A** *Merodon bequaerti*, dorsal view **B** *Merodon bequaerti*, lateral view **C** *Merodon sacki*, dorsal view **D** *Merodon sacki*, lateral view. Scale bar: 2 mm.

Distribution. *Merodon bequaerti* is distributed in north-western Africa (Algeria, Libya, Morocco, and Tunisia) (Fig. 7).

Ecology. Preferred environment: unimproved montane grassland, including open, grassy areas in pine forest or Mediterranean scrub. Flowers visited: no data. Flight period: February-June.

Type material. Holotype [original designation by Hurkmans (1993: 194)]: male. Original label: "*Merodon bequaerti* / *spec. nov. HOLOTYPE* / ♂. *W. Hurkmans 1988*." [red label handwritten], "*Merodon* / *parietum* / *Mg* ♂" [label handwritten], "Noiseux Oran / Algeria / Dr. J. Bequaert" "23-IV-l0" [handwritten on the back side] (MNHN) (See Supplementary file 1: Figure 1A). **Paratype**: female. Same label data as holotype (MNHN) (studied).

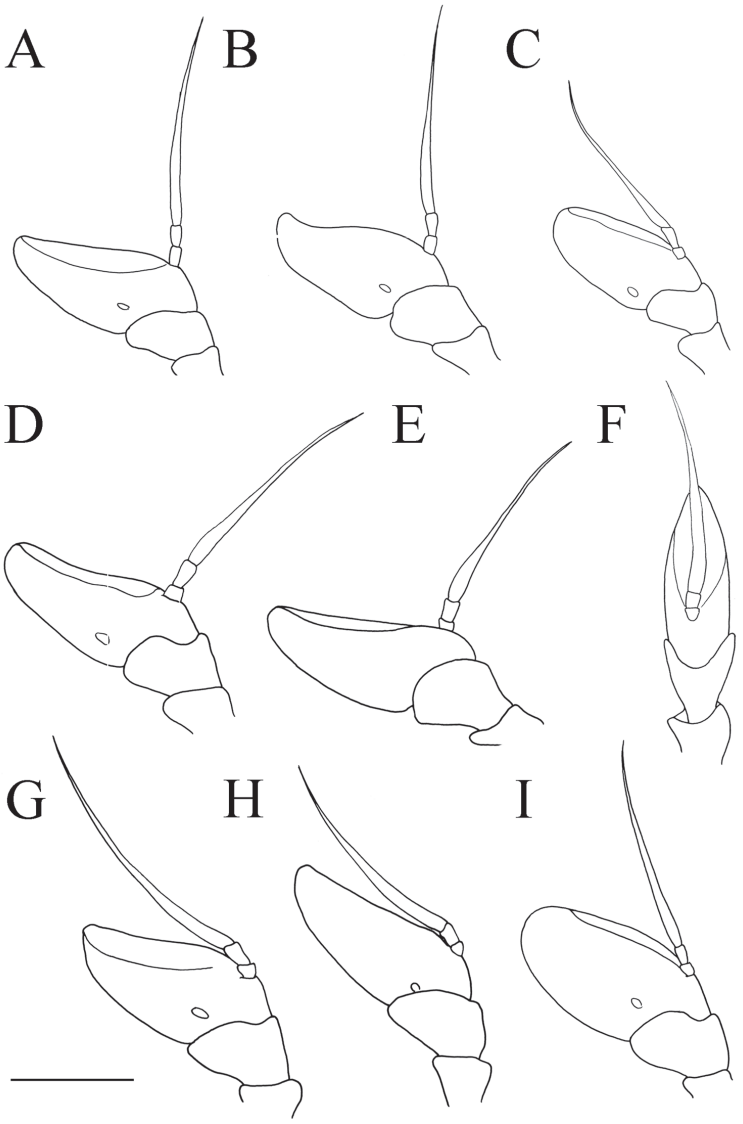

Figure 11. Antenna. **A** *Merodon bequaerti*, outer side, lateral view, male **B** *Merodon bequaerti*, inner side, lateral view, male **C** *Merodon bequaerti*, outer side, lateral view, female **D** *Merodon sacki*, outer side, lateral view, male **E** *Merodon sacki*, inner side, lateral view, male **F** *Merodon sacki*, dorsal view, male **G** *Merodon sophron*, outer side, lateral view, male **H** *Merodon sophron*, inner side, lateral view, male **I** *Merodon sophron*, outer side, lateral view, female. Scale bar: 1 mm.

Other material. Algeria • 1 ♂; Kabylie, Tikjda; 36°27'00"N, 4°07'60"E; 28 Jun. 1954; NBCN • 1 ♂; Jijel, Oued el Kebir; 36°35'22"N, 6°16'16"E; 20 May 1981; NBCN • 1 ♂; Jijel, Foce Oued El Kebir; 36°35'45"N, 6°15'29"E; 20 May 1981; I. Aslan leg.; NBCN 05636 • 1 ♀; El Kseur, Akfadou; 36°37'60"N, 4°36'00"E; 22–23 May 1981; NBCN 04079.

Libya • 1 ♀; Tripolitania, Garian; 32°10'46"N, 13°01'53"E; "2.500 feet" [760 m a.s.l.]; 22 Feb. 1954; K. M. Guichard leg.; NHMUK 04353.

Morocco • 1 ♂; Moyen Atlas, Azrou; 33°25'48"N, 5°12'36"W; 15 Jun. 1928; R. Benoist leg.; MNHN 22623 • 8 ♂♂; Mountain de Beni-Snassen 2; 34°48'43"N, 2°24'08"W; 29 Apr. 2013; A. Vujić, S. Radenković leg.; FSUNS Đ13, Đ14, Đ16 to Đ21.

Tunisia • 1 ♂; Jundubah, 40 km W from Jendouba; 36°31'54"N, 8°28'25"E; 17 May 1988; ZMUC 02497 • 1 ♂; same data as for preceding; 36°34'33"N, 9°02'12"E; ZMUC 02498.

***Merodon defectus* Vujić, Likov & Radenković sp. nov.**
http://zoobank.org/7EDC43D1-8B17-46D0-8C28-B18485482741
Figs 12J, K, 13E, 14A, B, D, 15B, 16C

Diagnosis. Medium sized (7.6–10.9 mm), dark species with olive-brown reflection; antennae dark brown; legs mostly black; basoflagellomere elongated (in males 1.8 times as long as wide) obviously concave dorsally; arista short, 1.6–1.8 times as long as basoflagellomere (Fig. 12J, K); terga dark brown to black, except pale yellow-orange lateral maculae on tergum 2; metafemur incrassate, ventrally covered with pilosity of medium length (Fig. 13E); male genitalia: posterior surstyle lobe with very small lateral hump (Fig. 14A, B: bp); apical part of anterior surstyle lobe triangular (Fig. 14A: al); lingula medium sized (Fig. 14D: l). Similar to *Merodon serrulatus* from which differs in reduced lateral hump on posterior surstyle lobe (Fig. 14A, B: bp) (in *M. serrulatus* distinct, Fig. 1A, B: bp, 14C: bp). Morphologically related to *M. opacus* sp. nov. and *M. hirsutus* from which can be distinguished by the presence of yellow-orange lateral maculae on tergum 2 (in *M. opacus* sp. nov. and *M. hirsutus* tergum 2 dark). Additionally, differing from *M. hirsutus* by shorter dorsolateral pile on metafemur (Fig. 13E) and posterior surstyle lobe with very small lateral hump (Fig. 14A, B: bp), well developed in *M. hirsutus* (Fig. 14E, F: bp) and *M. opacus* sp. nov. (14H, I: bp).

Description. Male. Head. Antennae black to dark brown; basoflagellomere elongated, 1.8 times as long as wide, and 2.3 times as long as pedicel, concave dorsally with acute apex; dorsolateral fossette large; arista dark brown and thickened at basal one third, covered with dense microtrichia, 1.6–1.8 times as long as basoflagellomere (Fig. 12J); face black with gray microtrichia, covered with whitish pile; oral margin microtrichose, with small, shiny, lateral bare area; lunule shiny black; frons microtrichose, with yellowish gray pile; eye contiguity ca. eight facets long; vertex isosceles, with long, pale whitish yellow pile, mixed with black pile on the ocellar triangle; ocellar triangle isosceles (Fig. 16C); occiput shiny, with gray-yellow pile; eyes covered with dense pile; vertical triangle: eye contiguity: frons = 3 : 1 : 3.

Thorax. Scutum and scutellum black with bronze luster, covered with dense, erect, yellow pile; scutum at wing basis with short black pile and some black pile between wing basis, from few ones to fascia of black pilosity in some specimens; scutum usually with two or more microtrichose vittae, anteriorly connected and posteriorly reaching

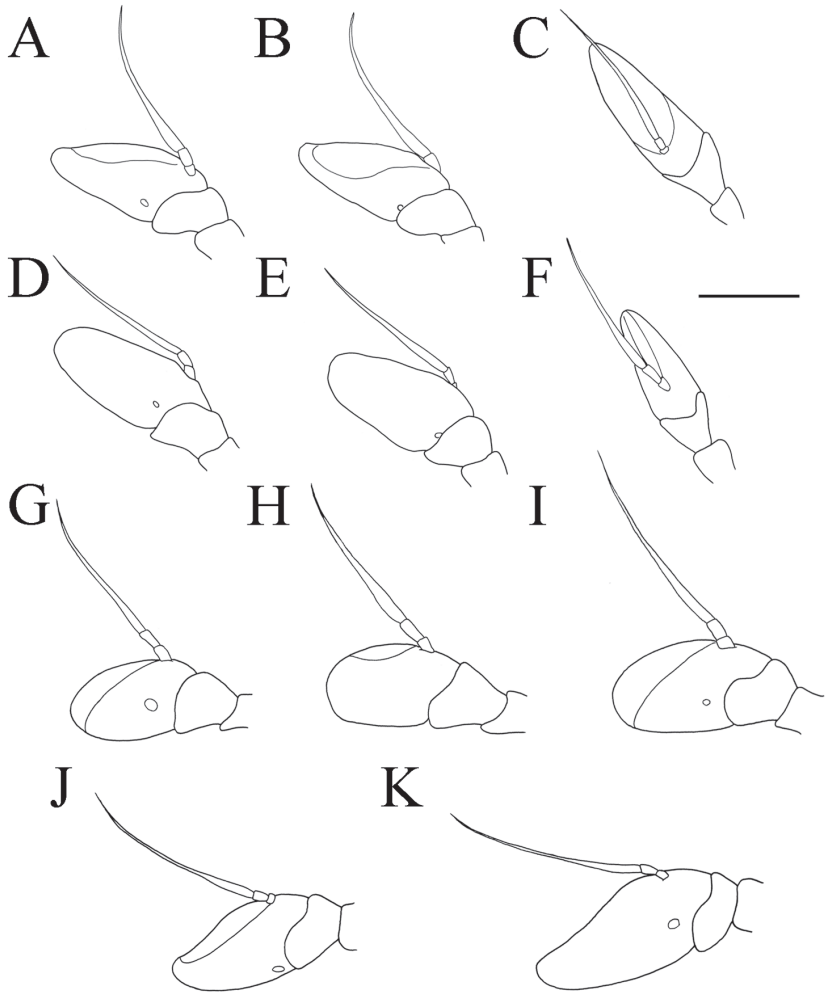

Figure 12. Antenna. **A** *Merodon opacus* sp. nov., outer side, lateral view, male **B** *Merodon opacus* sp. nov., inner side, lateral view, male **C** *Merodon opacus* sp. nov., dorsal view, male **D** *Merodon opacus* sp. nov., outer side, lateral view, female **E** *Merodon opacus* sp. nov., inner side, lateral view, female **F** *Merodon opacus* sp. nov., dorsal view, female **G** *Merodon disjunctus* sp. nov., outer side, lateral view, male **H** *Merodon disjunctus* sp. nov., inner side, lateral view, male **I** *Merodon disjunctus* sp. nov., outer side, lateral view, female **J** *Merodon defectus* sp. nov., outer side, lateral view, male **K** *Merodon defectus* sp. nov., outer side, lateral view, female. Scale bar: 1 mm.

the scutellum; scutum dull; posterodorsal part of anterior anepisternum, posterior anepisternum (except anteroventral angle), anterior anepimeron, dorsomedial anepimeron, and posterodorsal and anteroventral parts of katepisternum with long, pale yellow pile and grayish microtrichia; wings entirely covered with microtrichia; wing veins brown; calypteres yellowish; halteres brown-yellow; legs mostly black, except brown tarsi ventrally in some specimens; pile on legs gray-yellow; metafemur moderately in-

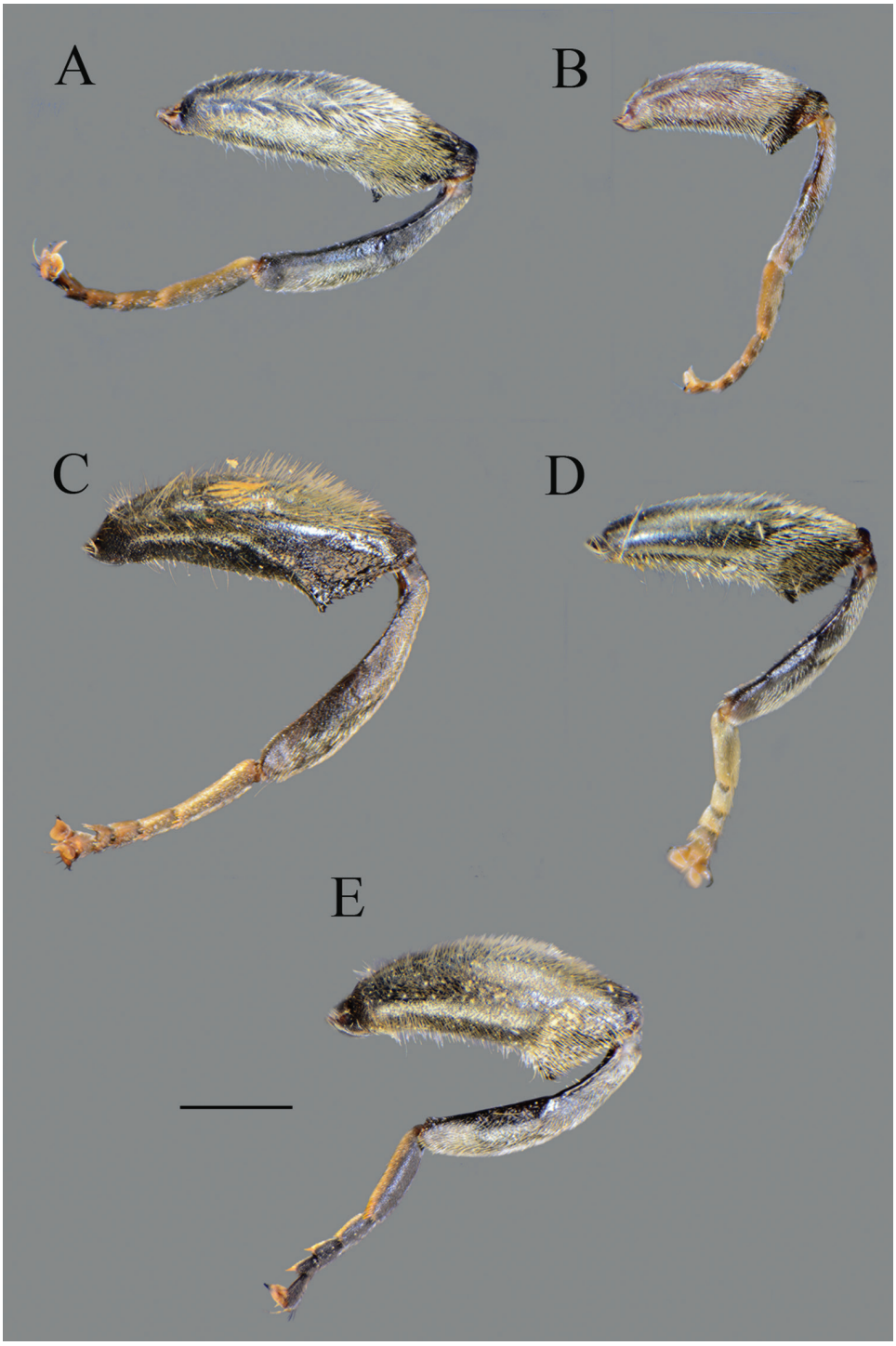

Figure 13. Metaleg, lateral view. **A** *Merodon opacus* sp. nov., male **B** *Merodon opacus* sp. nov., female **C** *Merodon hirsutus*, male **D** *Merodon hirsutus*, female **E** *Merodon defectus* sp. nov., male. Scale bar: 2 mm.

crassate, ca. three times longer than wide; pile on postero- and anteroventral surface of medium length; pile on dorsolateral surface dense and length ca. one third to one fourth of width of metafemur (Fig. 13E).

Abdomen. Tapering, 1.2 times longer than mesonotum; terga dark brown to black, except pale yellow-orange lateral maculae on tergum 2; terga 2–4 each with a pair of white microtrichose, oblique fasciae (on tergum 2 triangular); pile on terga long, yellow, except some black pile on terga 3 and 4 medially; sterna dark brown, covered with long whitish yellow pile.

Male genitalia. Apical part of anterior surstyle lobe triangular, ca. two times longer than wide, covered with dense, short pile (Fig. 14A: al); posterior surstyle lobe with very small basolateral protrusion (Fig. 14A, B: bp); hypandrium sickle-shaped, without lateral projections; lingula medium size (Fig. 14D: l).

Female. Similar to the male except for normal sexual dimorphism and for the following characteristics: basoflagellomere ca. two times longer than wide (Fig. 12K), fossette dorsal; frons with broad microtrichose vittae along eye margins; frons covered with pilosity of variable color, from mostly gray-yellow to predominantly black; ocellar triangle covered with black pile; terga with whitish pile, except terga 2–5 medially with short black pile; microtrichose fasciae on terga 3 and 4 conspicuous (Fig. 15C).

Etymology. Latin adjective *defectus* (reduced in size, smaller) refers to small basolateral protrusion (lateral hump) on posterior surstyle lobe.

Distribution. *Merodon defectus* sp. nov. has been identified in western Turkey (Fig. 7).

Ecology. Preferred environment: forest/open ground; thermophilous and evergreen *Quercus* forest; *Castanea* forest, dry *Pinus* forest; unimproved grassland and tracksides; coniferous forest with some yellow flowers along a stream [Reemer and Smit (2007) refer to this last observation as being *Merodon alexeji* Paramonov, 1925]. Flowers visited: *Ornithogalum* spp., *Potentilla* spp., and *Thymus* spp. Flight period: May-July.

Type material. Holotype. Turkey • ♂; Bozdağ mountain, Near Bozdağ; 38°22'28"N, 28°04'38"E; 1140 m a.s.l.; 7 Jun. 2014; A. Vujić, J. Ačanski leg.; FSUNS 06950. Original label: "HOLOTYPE of *Merodon* / *defectus* Vujić, Likov et / Radenković sp.n. 2019" [red label], "Turkey, Bozdağ Mountain, / near Bozdağ 7/6/2014 / 38.374523 28.077339 1140m / Leg. Vujić, Ačanski", "AU305", "06950" (See Supplementary file 2: Figure 2A). **Paratypes**. Turkey • 1 ♂; Muğla, 14 km NE from Ağla, Lake Kartar; 37°01'50"N, 28°45'09"E; 1600 m a.s.l.; 31 May 2000; J. T. Smit leg.; J. T. S. coll. 04066 [published in Reemer and Smit (2007) under name *Merodon alexeji*] • 1 ♀; Muğla, 14 km NE from Ağla, Lake Kartar; 37°01'50"N, 28°45'09"E; 1600 m a.s.l.; 31 May 2000; J. T. Smit leg.; J. T. S. coll. 04067 [published in Reemer and Smit (2007) under name *Merodon alexeji*] • 4 ♀♀; Isparta, Yenişarbademli, Melikler Yaylası 2; 37°41'38"N, 31°17'56"E; 1770 m a.s.l.; 21 Jun. 2016; R. Hayat, A. Vujić, O. Demirözer, J. Ačanski leg.; EMIT 12301 to 12304 • 1 ♂; Babadağ, Near Denizli valley I; 37°41'43"N, 28°59'35"E; 1870 m a.s.l.; 5 Jul. 2015; A. Vujić, S. Radenković, J. Ačanski, S. Gökhan, N. Veličković leg.; FSUNS 09774 • 2 ♀♀; Babadağ, Near Denizli valley I; 37°41'43"N, 28°59'35"E; 1870 m a.s.l.; 5 Jul. 2015; A. Vujić, S. Radenković, J. Ačanski, S. Gökhan, N. Veličković leg.; FSUNS 09773, 09775 • 3 ♂♂;

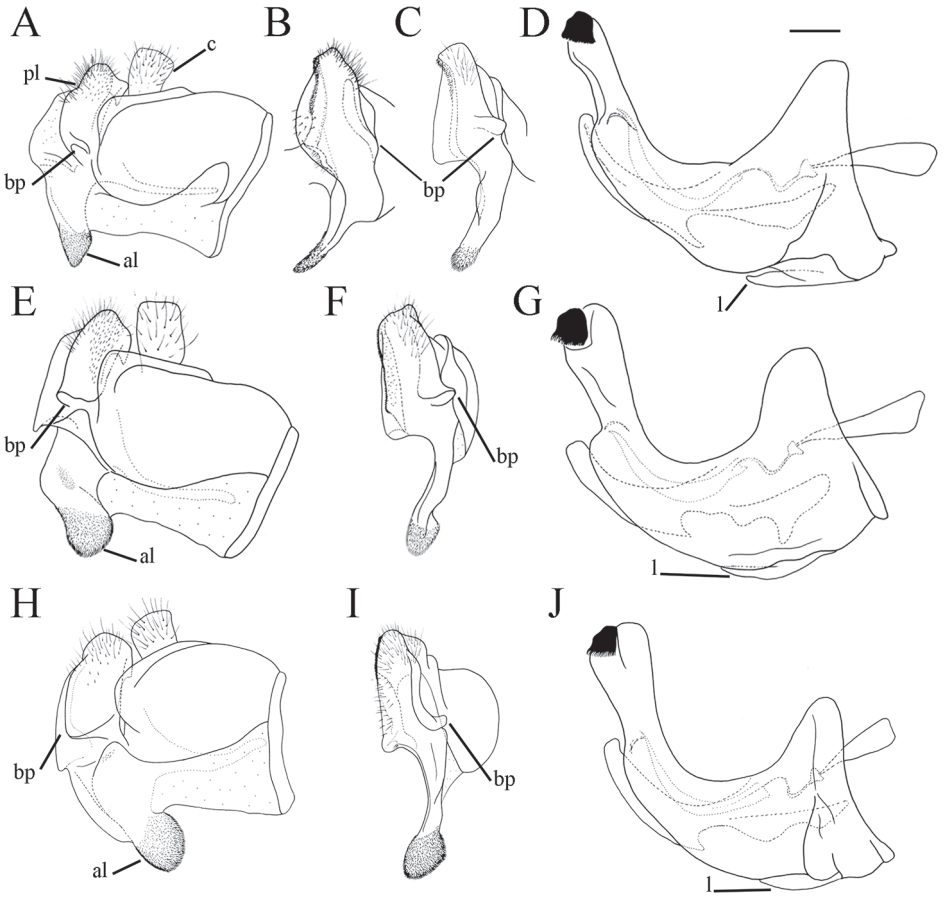

Figure 14. Male genitalia. **A** *Merodon defectus* sp. nov., epandrium, lateral view **B** *Merodon defectus* sp. nov., epandrium, ventral view **C** *Merodon serrulatus*, epandrium, ventral view **D** *Merodon defectus* sp. nov., hypandrium, lateral view **E** *Merodon hirsutus*, epandrium, lateral view **F** *Merodon hirsutus*, epandrium, ventral view **G** *Merodon hirsutus*, hypandrium, lateral view, **H** *Merodon opacus* sp. nov., epandrium, lateral view **I** *Merodon opacus* sp. nov., epandrium, ventral view **J** *Merodon opacus* sp. nov., hypandrium, lateral view. Abbreviations: al–anterior surstyle lobe, bp–basolateral protrusion, c–cercus, l–lingula, pl–posterior surstyle lobe. Scale bar: 0.2 mm.

Isparta, Yenişarbademli, Melikler Yaylası; 37°41'52"N, 31°17'39"E; 1730 m a.s.l.; 30 Jun. 2015; A. Vujić, R. Hayat, O. Dermirözer, A. Uzal leg.; EMIT 09953 to 09955 • 3 ♀♀; Isparta, Yenişarbademli, Melikler Yaylası; 37°41'52"N, 31°17'39"E; 1730 m a.s.l.; 30 Jun. 2015; A. Vujić, R. Hayat, O. Demirözer, A. Uzal leg.; EMIT 09952, 09956, 09957 • 8 ♂♂; Isparta, Yenişarbademli, Melikler Yaylası 1; 37°41'52"N, 31°17'39"E; 1730 m a.s.l.; 21 Jun. 2016; R. Hayat, A. Vujić, O. Demirözer, J. Ačanski leg.; EMIT 12249 to 12251, 12256, 12257, 12260, 12264 • 9 ♀♀; Isparta, Yenişarbademli, Melikler Yaylası 1; 37°41'52"N, 31°17'39"E; 1730 m a.s.l.; 21 Jun. 2016; R. Hayat, A. Vujić, O. Demirözer, J. Ačanski leg.; EMIT 12253 to 12255, 12258, 12259, 12261 to

Figure 15. Abdomen, dorsal view. **A** *Merodon disjunctus* sp. nov., male **B** *Merodon defectus* sp. nov., female. Scale bar: 2 mm.

12263, 12265 • 3 ♀♀; Babadağ, Near Denizli on the top; 37°42'33"N, 28°59'23"E; 2060 m a.s.l.; 5 Jul. 2015; A. Vujić, S. Radenković, J. Ačanski, S. Gökhan, N. Veličković leg.; FSUNS 09769, 09770, 09772 • 1 ♀; Bozdağ mountain, Near Bozdağ; 38°19'58"N, 28°06'35"E; 1570 m a.s.l.; 7 Jun. 2014; A. Vujić, J. Ačanski leg.; FSUNS 06931 • 8 ♂♂; Bozdağ mountain, Near Bozdağ; 38°20'50"N, 28°04'08"E; 1170 m a.s.l.; 7 Jun. 2014; A. Vujić, J. Ačanski leg.; FSUNS 06952, 06953, 06956, 06957, 06959 to 06962 • 6 ♀♀; Bozdağ mountain, Near Bozdağ; 38°20'50"N 28°04'08"E; 1170 m a.s.l.; 7 Jun. 2014; A. Vujić, J. Ačanski leg.; FSUNS 06954, 06955, 06958, 06963 to 06965 • 1 ♂; Balıkesir, Edremit-Akçay; 39°40'40"N, 26°54'09"E; 27 Jul. 2015; J. Devalez leg.; MAegean 10131.

Merodon disjunctus Vujić, Likov & Radenković sp. nov.

http://zoobank.org/2A04080B-F1B9-4CE1-A2B1-42AECB902F65
Figs 12G–I, 15A, 16A, B, 17A–C, 18A–C

Diagnosis. Medium sized (8.5–10.8 mm), dark, olive-brown species, covered with pale yellow pile; males with dichoptic eyes, separated by a distance of 3–5 facets (Fig. 16B); terga 2–4 with pairs of white microtrichose fasciae, differently developed (from conspicuous to vague) (Fig. 15A); in male basoflagellomere short, 1.2 times longer than wide, with large fossette extending to the apex of basoflagellomere (Fig. 12G–I).

Description. Male. Head. Antennae black; basoflagellomere short, 1.2 times as long as wide, and ca. 1.7 times as long as pedicel, and with rounded apex; large fossette

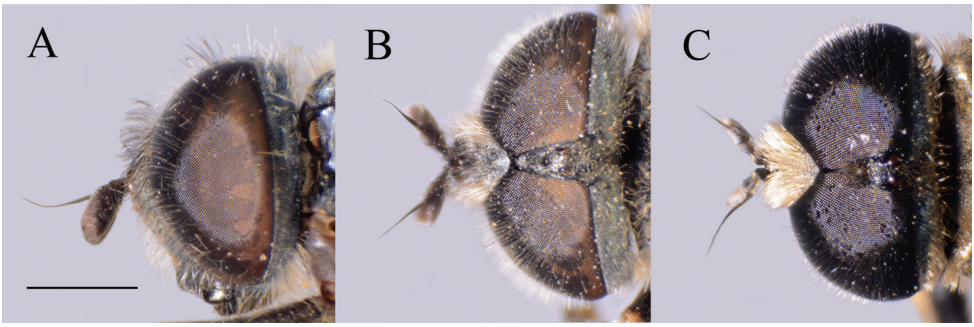

Figure 16. Head of male. **A** *Merodon disjunctus* sp. nov., lateral view **B** *Merodon disjunctus* sp. nov., dorsal view **C** *Merodon defectus* sp. nov., dorsal view. Scale bar: 2 mm.

Figure 17. *Merodon disjunctus* sp. nov. **A** thorax, dorsal view, male **B** metaleg, lateral view, male **C** metaleg, lateral view, female. Scale bar: 2 mm.

dorsomedial and dorsolateral including apex of basoflagellomere (Fig. 12G); arista black and thickened at basal one third, covered with dense microtrichia, 1.5 times as long as basoflagellomere (Fig. 12G–H); face and frons black with gray microtrichia; face covered with dense whitish gray, while frons with mostly black pile (Fig. 16A); oral margin shiny, with lateral microtrichose area; lunule shiny black, bare; eye dichoptic, separated by distance of 3–5 facets (Fig. 16B); vertex isosceles, covered with dark gray microtrichia and long, black pile; ocellar triangle equilateral; occiput shiny covered with black pile in upper half, ventrally with gray-yellow pile and dense, gray microtrichia; eyes covered with dense pile.

Thorax. Scutum and scutellum dull, with bronze luster, covered with dense, erect, yellowish pile, except posterior half medially with few to many black pile intermixed; in some specimens scutellum with few black pile; scutum with indistinct microtrichose vittae (Fig. 17A); posterodorsal part of anterior anepisternum, posterior anepisternum (except anteroventral angle), anterior anepimeron, dorsomedial anepimeron, and posterodorsal and anteroventral parts of katepisternum with long, dark gray pile and gray-

ish microtrichia; wings entirely covered with microtrichia; wing veins yellow-brown; calypteres and halteres whitish yellow; legs black, except yellow-brown tarsi, tip of femora and basal part of tibiae; pile on legs mostly yellowish; metafemur moderate incrassate, ca. five times longer than wide; pile on postero- and anteroventral surface long, ca. half to two thirds of width of metafemur, as same length as pile dorsally (Fig. 17B).

Abdomen. Tapering, ca. 1.2 times longer than mesonotum; terga dark brown to black, except for a pair of yellow-orange, triangular, lateral maculae on tergum 2; terga 2–4 with conspicuous or with trace of white microtrichose pair of fasciae (variable character); pile on terga mostly yellow, except terga 3 and 4 medially with black pile; sterna dark brown to black, covered with long whitish pile.

Male genitalia. Apical part of anterior surstyle lobe rhomboid in shape, ca. 1.5 times longer than wide, covered with dense, short pile (Fig. 18A: al); posterior surstyle lobe oval with basolateral protrusion (lateral hump) (Fig. 18A, B: bp); hypandrium sickle-shaped, without lateral projections; lingula medium sized (Fig. 18C: l).

Female. Similar to the male except for normal sexual dimorphism and for the following characteristics: basoflagellomere 1.6–1.8 times longer than wide, fossette large, dorsolateral (Fig. 12I); frons mostly microtrichose and predominantly covered with black pile; ocellar triangle covered with black pile; microtrichose fasciae on terga 3 and 4 conspicuous.

Etymology. The name derives from the Latin adjective *disjunctus* meaning separated, disconnected which pertains to the dichoptic eyes in the males.

Distribution. *Merodon disjunctus* sp. nov. has so far only been recorded in Kyrgyzstan and Kazakhstan (Fig. 7).

Ecology. Preferred environment: no data. Flowers visited: no data. Flight period: May-July.

Type material. Holotype. Kyrgyzstan • ♂; Talassky Mt.R, Ara Bijik rav., 13 km NNE Majdantal Pass; 42°22'00"N, 70°00'00"E; 2700 m a.s.l.; 4 Jul. 1988; Milko leg.; SZMN 05847. Original label: "HOLOTYPE of *Merodon* / *disjunctus* Vujić, Likov et / Radenković sp.n. 2019" [red label], "NW KIRG., Talassky Mt.R, / Ara Bijik rav., 13 km NNE / Majdantal Pass ~2700 m / 42°22'N 70°57'E / 04.07.1998 *D. Milko leg.*", "05847" (See Supplementary file 2: Figure 2B). **Paratypes**. Kazakhstan • 1 ♂; Ketmen, Mt. Kirgyzsay; 43°16'60"N, 79°31'00"E; 2200 m a.s.l.; 3 Jun. 2001; M. Hauser leg.; M. H. coll. 02470 • 2 ♂♂; Ketmen, Mt. Kirgyzsay; 43°16'60"N, 79°31'00"E; 1800 m a.s.l.; 1–3 Jun. 2001; M. Hauser leg.; M. H. coll. 02467, 02472 • 1 ♀; Almaty, Charyn; 43°46'58"N, 79°23'24"E; 20 May 2003; A. Selin leg.; S. K. coll. 03971 • 2 ♀♀; Kyzyltchy; 46°03'31"N, 80°43'10"E; 21 May 2004; A. Selin leg.; S. K. coll. 03970, 02460 • 1 ♂; Kyzyltchy; 46°03'31"N, 80°43'10"E; 21 May 2004; A. Selin leg.; S. K. coll. 02461 • 1 ♂; Talasskip hr., R. Kara-Bura; 1600 m a.s.l.; 18 Jul. 1968; Pek leg.; SZMN 05815.

Kyrgyzstan • 1 ♂; Tchatkal Valley, 4 SW Ajgyr-Dzhal vill.; 41°42'00"N, 70°57'00"E; 1800 m a.s.l.; 12 Jul. 1998; Milko leg.; SZMN 05848 • 1 ♂; Issyk Kul, Chong Kemin-Tal; 42°40'60"N, 75°55'00"E; 1350 m a.s.l.; 3 Jun. 1998; M. Kraus M. leg.; NBCN 02468 • 1 ♀; Issyk Kul, Chong Kemin-Tal; 42°42'00"N, 75°54'00"E; 1350 m a.s.l.; 3 Jun. 1998; M. Kraus leg.; NBCN 02464 • 1 ♂; Issyk Kul, Chong Kemin-Tal; 42°42'00"N, 75°54'00"E; 1350 m a.s.l.; 3 Jun. 1998; M. Kraus leg.; NBCN 02469.

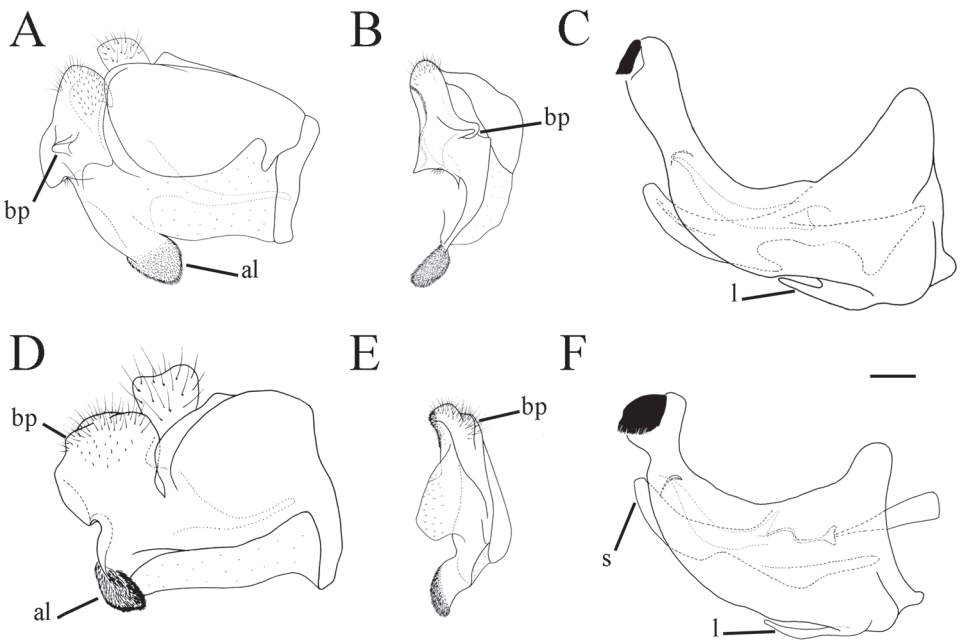

Figure 18. Male genitalia. **A** *Merodon disjunctus* sp. nov., epandrium, lateral view **B** *Merodon disjunctus* sp. nov., epandrium, ventral view **C** *Merodon disjunctus* sp. nov., hypandrium, lateral view **D** *Merodon kawamurae*, epandrium, lateral view **E** *Merodon kawamurae*, epandrium, ventral view **F** *Merodon kawamurae*, hypandrium, lateral view. Abbreviations: al–anterior surstyle lobe, bp–basolateral protrusion, l–lingula, pl–posterior surstyle lobe, s–lateral sclerite of aedeagus. Scale bar: 0.2 mm.

Merodon hirsutus Sack, 1913

Figs 13C, D, 14E–G, 19A–D, 20A, B, 21E–G

Diagnosis. Medium sized (8.1–10.4 mm), dark species with olive-brown reflection; antennae dark brown; legs mostly black; basoflagellomere elongated (ca. two times as long as wide) obviously concave dorsally; arista 1.6–1.7 times as long as basoflagellomere (Fig. 19A–D); terga dark brown to black; metafemur incrassate, covered with short pilosity ventrally, and with long pile on dorsolateral surface (Fig. 13C); male genitalia: posterior surstyle lobe with lateral hump (Fig. 14E, F: bp); apical part of anterior surstyle lobe rhomboid (Fig. 14E: al); lingula large (Fig. 14G: l). Similar to *Merodon serrulatus* from which differs in dark tergum 2 (in *M. serrulatus* with small pale lateral maculae, at least in females). Morphologically related to *M. opacus* sp. nov. from which can be distinguished by longer dorsolateral and ventral pile on metafemur (Fig. 13C) and longer pile on terga (Fig. 21F, G); females with mostly shiny frons (Fig. 20B) (in *M. opacus* sp. nov. dull, covered with dense microtrichia).

Redescription (based on lectotype and additional specimens from the type locality, Syria, and Israel). **Male.** Head. Antennae black to dark brown; basoflagellomere elongated ca. two times as long as wide, and 2.2–2.5 times as long as pedicel, concave

dorsally with acute apex; large fossette dorsolateral and dorsomedial; arista dark and thickened at basal one third, covered with dense microtrichia, 1.6–1.7 times as long as basoflagellomere (Fig. 19A–C); face black with gray microtrichia, covered with whitish pile; frons mostly shiny, with yellowish gray pile; oral margin microtrichose, with small, shiny lateral area; lunule shiny black, bare; eye contiguity 12–14 facets long; vertex isosceles, with long, pale whitish yellow pile, mixed with black pile on the ocellar triangle; ocellar triangle equilateral; occiput with gray-yellow pile; eyes covered with dense pile (Fig. 20A); vertical triangle: eye contiguity: frons = 1.4 : 1 : 2 .

Thorax. Scutum and scutellum black with bronze luster, covered with dense, erect, yellow pile; scutum at wing basis with short black pile; scutum usually with two or more microtrichose vittae, anteriorly connected and posteriorly reaching the scutellum; scutum dull; posterodorsal part of anterior anepisternum, posterior anepisternum (except anteroventral angle), anterior anepimeron, dorsomedial anepimeron, and posterodorsal and anteroventral parts of katepisternum with long, pale yellow pile and grayish microtrichia; wings entirely covered with microtrichia; wing veins brown; calypteres and halteres yellowish; legs mostly black, except brown tarsi ventrally in some specimens; pile on legs pale yellow, except black pile at apical one third of metafemur; metafemur moderately incrassate, ca. three times longer than wide; pile on postero- and anteroventral surface very short; pile on dorsolateral surface long and dense ca. as half of width of metafemur (Fig. 13C).

Abdomen. Tapering, ca. 1.2 times longer than mesonotum; terga dark; terga 2–4 each with a pair of white microtrichose, wide, oblique fasciae (on tergum 2 triangular); pile on terga long, all yellow (Fig. 21F); sterna dark brown, covered with long whitish yellow pile.

Male genitalia. Apical part of anterior surstyle lobe rhomboid shape, ca. two times longer than wide, covered with short pile (Fig. 14E: al); posterior surstyle lobe oval with basolateral protrusion (lateral hump) (Fig. 14E, F: bp); hypandrium sickle-shaped, without lateral projections; lingula large (Fig. 14G: l).

Female. Similar to the male except for normal sexual dimorphism and for the following characteristics: antennae with rounded tip, basoflagellomere 1.8–2 times longer than wide, fossette dorsolateral (Fig. 19D); frons with narrow microtrichose vittae along eye margins; frons covered with variable pilosity, from mostly gray-yellow to predominantly black; ocellar triangle covered with black pile; metafemur with shorter pile on dorsolateral surface (Fig. 13D); terga mostly with yellowish pile on tergum 2 and with whitish pile on terga 3–5, except terga 2–4 medially with short black pile; microtrichose fasciae on terga 3 and 4 narrower (Fig. 21F, G).

Distribution. *Merodon hirsutus* is distributed in Israel, Syria, and south-eastern Turkey (Fig. 7).

Ecology. Preferred environment: no data. Flowers visited: no data. Flight period: March-June.

Type material. Described by Sack (1913: 435) based on unspecified number of specimens. Lectotype [designated by Hurkmans (1993)]: male, "Jebel al Aqra [35° 35' N, 36° 15' E] vi.85 [1885], N. Syria, Dr. E. Leuthner / *Lampetia hirsuta* Sack det. Sack" (NHMW) (studied).

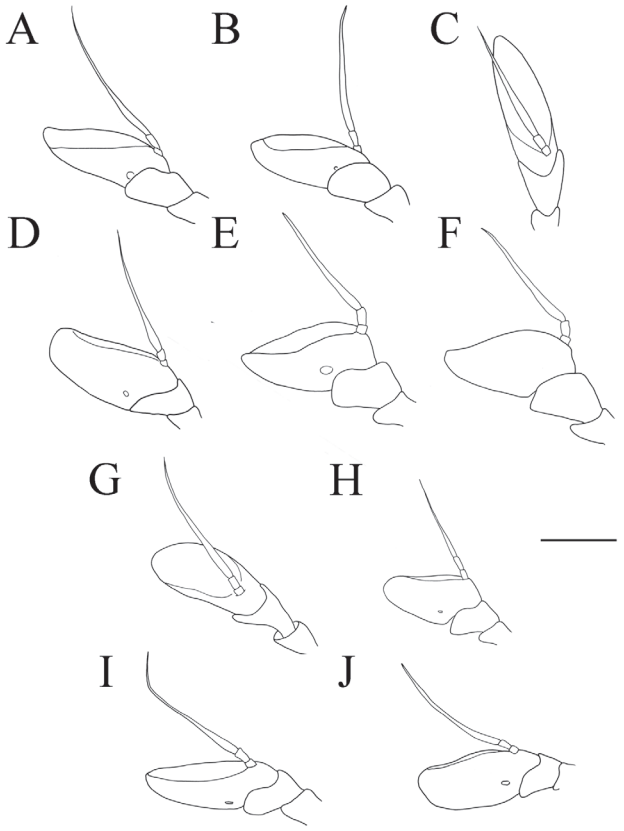

Figure 19. Antenna. **A** *Merodon hirsutus*, outer side, lateral view, male **B** *Merodon hirsutus*, inner side, lateral view, male **C** *Merodon hirsutus*, dorsal view, male **D** *Merodon hirsutus*, outer side, lateral view, female **E** *Merodon kawamurae*, outer side, lateral view, male **F** *Merodon kawamurae*, inner side, lateral view, male **G** *Merodon kawamurae*, dorsal view, male **H** *Merodon kawamurae*, outer side, lateral view, female **I** *Merodon medium* sp. nov., outer side, lateral view, male **J** *Merodon medium* sp. nov., outer side, lateral view, female. Scale bar: 1 mm.

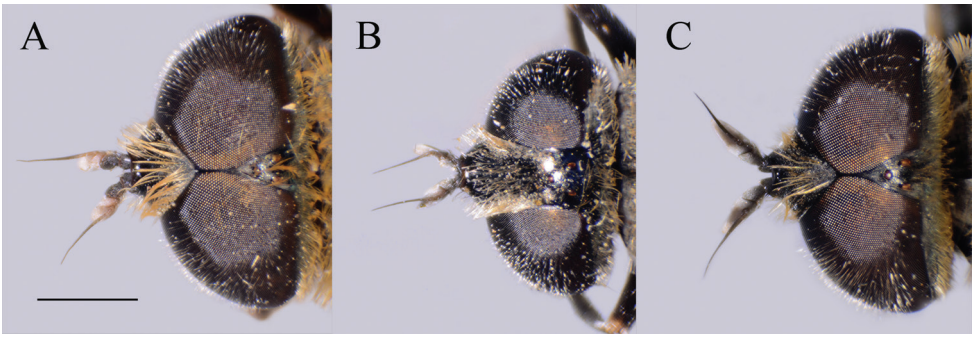

Figure 20. Head, dorsal view. **A** *Merodon hirsutus*, male **B** *Merodon hirsutus*, female **C** *Merodon opacus* sp. nov., male. Scale bar: 2 mm.

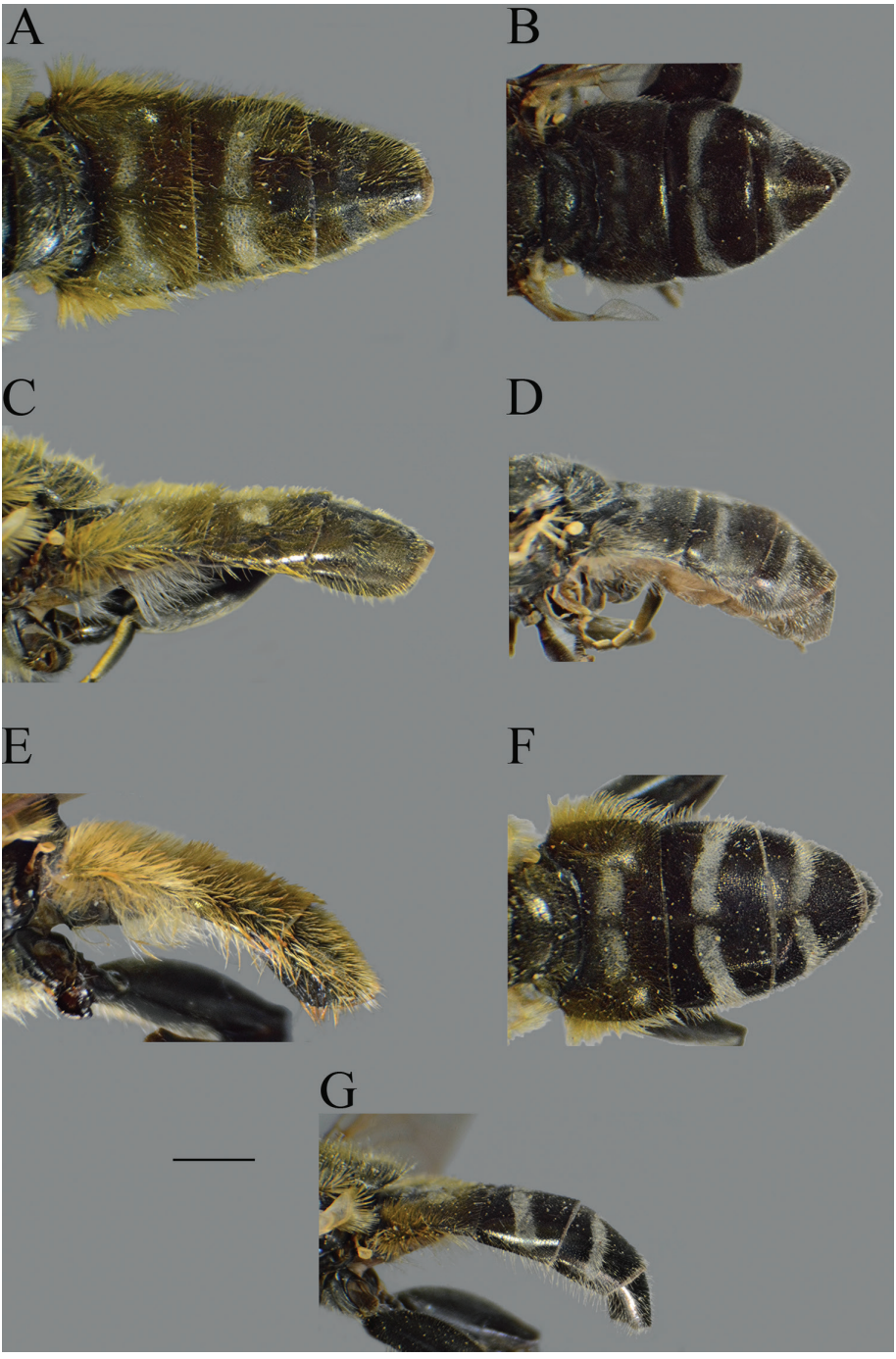

Figure 21. Abdomen. **A** *Merodon opacus* sp. nov., dorsal view, male **B** *Merodon opacus* sp. nov., dorsal view, female **C** *Merodon opacus* sp. nov., lateral view, male **D** *Merodon opacus* sp. nov., lateral view, female **E** *Merodon hirsutus,* lateral view, male **F** *Merodon hirsutus*, dorsal view, female **G** *Merodon hirsutus*, lateral view, female. Scale bar: 2 mm.

Other material. Israel • 1 ♀; Hefa, "Ma`yan Zevi" [Ma Yan Zevi]; 32°34'00"N, 34°55'60"E; 17 Apr. 1980; TAUI 04162.

Syria • 1 ♂; Jebel al Aqra; 35°55'18"N, 35°57'51"E; Jun. 1985; D. F. Leuthner leg.; NHMW 02479.

Turkey • 1 ♂; İçel, İcel-Taşucu, Silifke; 36°22'17"N, 33°54'54"E; 300 m a.s.l.; 17 Mar. 1984; FSUNS 04161 • 1 ♀; Erdemli; 36°44'59"N, 34°11'51"E; 8 Jun. 2008; Skorpik leg.; MNHN 17917 • 3 ♀♀; Pozantı-Tekir; 37°31'05"N, 34°47'42"E; 6 Jun. 2008; M. Kafka leg.; M. B. coll. 17918 to 17920 • 1 ♀; Kahramanmaraş, Andırın, Beyoluğu village; 37°45'00"N, 36°17'00"E; 1400 m a.s.l.; 7 Jun. 2002; S. Sarıbıyık leg.; S. S. coll. 02482 • 3 ♂♂; same data as for preceding; S. S. coll. 17910 to 17912 • 2 ♀♀; Kahramanmaraş, Andırın, Çiğşar village; 37°45'00"N 36°18'00"E; 1400 m a.s.l.; 7 Jun. 2002; S. Sarıbıyık leg.; S. S. coll. 17914, 17916 • 2 ♂♂; same data as for preceding; S. S. coll. 17913, 17915.

Merodon kawamurae Matsumura, 1916

Figs 18D–F, 19E–H, 22A, B, 23E, F

Lampetia micromegas Hervé-Basin, 1929: 111 – syn. published by Hurkmans 1993: 165.

Diagnosis. Medium sized (7.7–11.2 mm), with olive-brown reflection; antennae reddish brown; body pile predominantly pale, except some black pile on vertex and terga 2–4 medially; basoflagellomere short, ca. 1.2 times as long as wide, with large dorsal to dorsolateral fossette, and short arista (Fig. 19E–H); tergum 2 with reddish yellow lateral maculae; tergum 3 laterally reddish or brown; metafemur incrassate with long pilosity as long as half of width of metafemur in male and as one third of width of metafemur in female (Fig. 22A, B); male genitalia: posterior surstyle lobe with small lateral hump (Fig. 18E: bp); apical part of anterior surstyle lobe rhomboid (Fig. 18D: al); lingula large (Fig. 18F: l), lateral sclerite of aedeagus elongated (Fig. 18F: s).

Redescription (based on the types of *Merodon micromegas* and additional material from China). **Male.** Head. Antennae reddish brown; basoflagellomere short, ca. 1.2 times as long as wide, and ca. two times as long as pedicel, straight dorsally with acute apex; dorsal to dorsolateral fossette large; arista reddish brown and thickened at basal one third, covered with dense microtrichia, ca. 1.3 times as long as basoflagellomere (Fig. 19E–G); face and frons black with gray microtrichia, face covered with dense whitish, and frons with yellowish white pile; lunule shiny black, bare; vertex isosceles, dull, in front of anterior ocellus covered with dense microtrichia; vertex with long, pale yellow pile, in some specimens mixed with black or dark gray pile on the ocellar triangle; ocellar triangle isosceles; eyes covered with dense pile; occiput with gray-yellow pile, ventrally covered with a dense, gray microtrichia; eye contiguity ca. ten facets long; vertical triangle: eye contiguity: frons = 2.5 : 1 : 2.5.

Thorax. Scutum and scutellum black with bronze luster, covered with dense, erect yellow pile; scutum usually with indistinct microtrichose vittae; posterodorsal part of

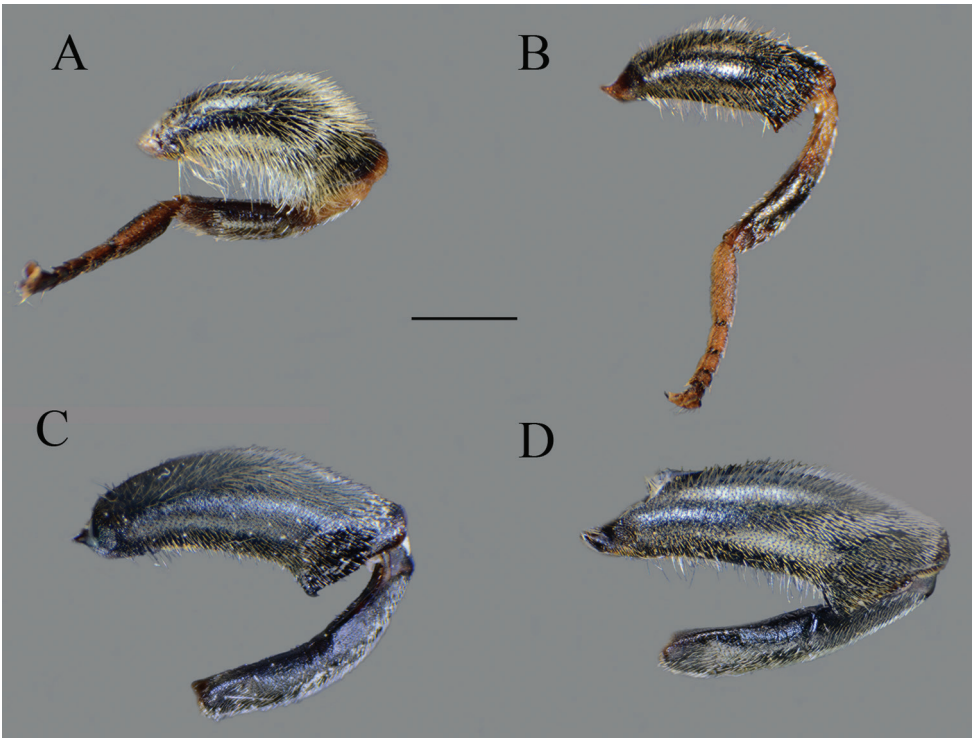

Figure 22. A, B metaleg, **C, D** metatrochanter, metafemur and metatibia, lateral view. **A** *Merodon kawamurae*, male **B** *Merodon kawamurae*, female **C** *Merodon medium* sp. nov., male **D** *Merodon medium* sp. nov., female. Scale bar: 2 mm.

anterior anepisternum, posterior anepisternum (except anteroventral angle), anterior anepimeron, dorsomedial anepimeron, and posterodorsal and anteroventral parts of katepisternum with long, dense pale yellow pile and grayish microtrichia; wings entirely covered with microtrichia; wing veins reddish brown; calypteres and halteres pale yellow; legs mostly black, except tip of femora and basal part of tibiae and brown tarsi ventrally; pile on legs pale yellow; metafemur incrassate and curved, ca. three times longer than wide; long pile on postero- and anteroventral surface ca. as half of width of metafemur, approximately the same length as pile on dorsal surface (Fig. 22A).

Abdomen. Broad, tapering, 1.2 times longer than mesonotum; terga dark, except for a pair of reddish yellow, triangular, lateral maculae on tergum 2 (and in some specimen on 3); terga 2–4 each with a pair of white microtrichose, wide, usually oblique fasciae; pile on terga all yellow, except black pile on tergum 3 medially, and on tergum 2 posteriorly and tergum 4 anteriorly in some specimens (Fig. 23E); sterna dark brown, covered with long whitish yellow pile.

Male genitalia. Apical part of anterior surstyle lobe rhomboid shape, covered with dense, short pile (Fig. 18D: al); posterior surstyle lobe oval with small basolateral protrusion (lateral hump) (Fig. 18E: bp); hypandrium sickle-shaped, without lateral projections; lingula large (Fig. 18F: l); lateral sclerite of aedeagus elongated (Fig. 18F: s).

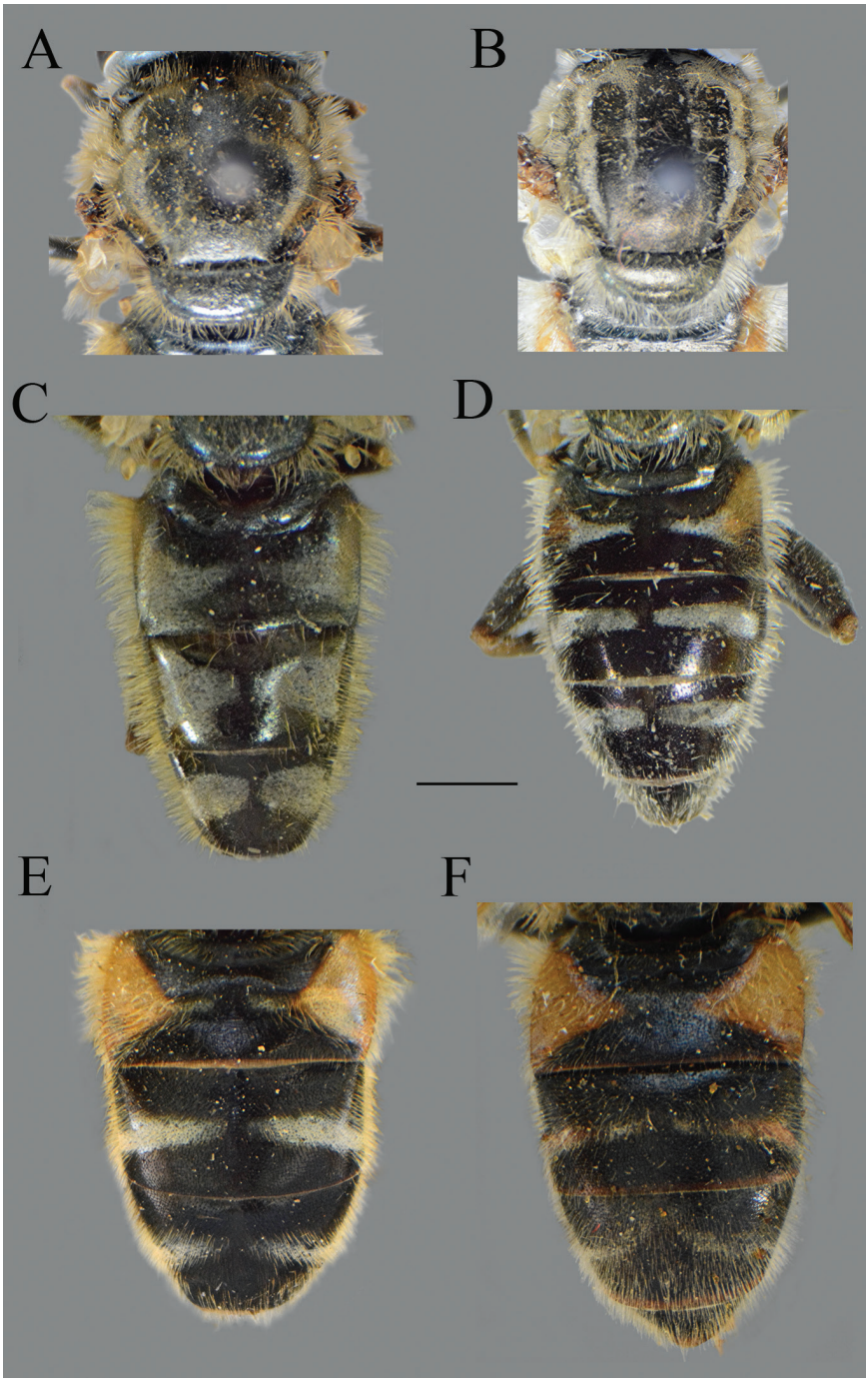

Figure 23. Body parts, dorsal view. **A** *Merodon trianguloculus* sp. nov., thorax, male **B** *Merodon trianguloculus* sp. nov., thorax, female **C** *Merodon trianguloculus* sp. nov., abdomen, male **D** *Merodon trianguloculus* sp. nov., abdomen, female **E** *Merodon kawamurae*, abdomen, male **F** *Merodon kawamurae*, abdomen, female. Scale bar: 2 mm.

Female. Similar to the male except for normal sexual dimorphism and for the following characteristics: antennae with rounded tip, fossette dorsolateral (Fig. 19D); frons microtrichose, covered with mostly gray-yellow pile; ocellar triangle covered with black pile; long pile on postero- and anteroventral surface ca. as half of width of metafemur (Fig. 22B); microtrichose fasciae on terga 2–4 narrower (Fig. 23F).

Distribution. *Merodon kawamurae* is known from Japan and China (Fig. 7). This is the only species of the genus *Merodon* in eastern Palaearctic.

Ecology. Preferred environment: no data. Flowers visited: no data. Flight period: April-May.

Type material. *Merodon kawamurae* was described after an unknown number of specimens from Kumamoto, Kyushu, Japan, leg. Kawamura. Matsumura's type material is held at the Hokkaido University, Department for Systematic Entomology, at Sapporo, Japan, but the type material was inaccessible for this study.

Merodon micromegas Lectotype [designated by Hurkmans (1993)]: "Tchen-Kiang, 13.iv.1918 / *Lampetia micromegas* H. B. type" (MNHN) (studied).

Paralectotypes (*Lampetia micromegas*). CHINA • 1 ♂; Chemo; 33°44'32"N, 103°23'45"E; 25 Apr. 1918; MNHN 02520 • 1 ♂; Chemo; 33°44'32"N, 103°23'45"E; 26 Apr. 1918; MNHN 02521 • 1 ♀; Chemo; 33°44'32"N, 103°23'45"E; 23 Apr. 1918; MNHN 02522 • 1 ♀; Shia-Shu; 10 May 1918; MNHN 02525 • 1 ♀; Jiangsu, Nanking; 32°00'27"N, 118°57'22"E; 6 May 1918; MNHN 02524.

Other material. CHINA • 1 ♀; Ningpo; 29°44'29"N, 121°06'02"E; 29 Apr. 1925; J. T. Chu leg.; NMNH 05118 • 1 ♂; Jiangsu, Nanking; 32°00'27"N, 118°57'22"E; 1981; H. Jettmar leg.; NHMW 02516 • 1 ♀; Jiangsu, Nanking; 32°00'27"N, 118°57'22"E; 15 Apr. 1918; NBCN 02518 • 1 ♀; same data as for preceding; 16 Apr. 1918; MNHN • 16 ♂♂; Chenkiang; 32°08'24"N, 119°23'25"E; 1–13 Apr. 1918; MNHN • 12 ♀♀; same data as for preceding; MNHN • 6 ♂♂; Chemo; 33°44'32"N, 103°23'45"E; 23 Apr. 1918; MNHN • 4 ♀♀; same data as for preceding; MNHN • 1 ♀; Chemo; 33°44'32"N, 103°23'45"E; 23 Apr. 1918; NBCN • 1 ♀; same data as for preceding; 26 Apr. 1918; NBCN • 1 ♂; Hoachan; 16 May 1918; MNHN • 2 ♀♀; same data as for preceding; MNHN • 3 ♂♂; Shia-Shu; 22 Apr. 1918; MNHN.

Merodon medium Vujić, Likov & Radenković sp. nov.

http://zoobank.org/E384B35E-E377-49B6-90CE-DEBDCBCEDDCB

Figs 6H, 19I, J, 22C, D, 24A, B, 25A–C

Diagnosis. Large species (10.3–13 mm) with wide dark brown abdomen and yellow-orange maculae on lateral sides of tergum 2 (Fig. 24A, B); basoflagellomere elongated, ca. 2.5 times longer than broad (Fig. 19 I, J,); metafemur incrassate (Fig. 22C, D); terga 2–4 with conspicuous microtrichose fasciae (Fig. 24A, B). Similar to some populations of *Merodon serrulatus*, but clearly differs in shape of abdomen: relation between maximum width of tergum 2 and its medial length is 3.3 in male and 3.5 in female of *M. medium* sp. nov. compared with 2.3 in *M. serrulatus* male and 2.7 in female; male

genitalia: anterior surstyle lobe with concave margin in *M. medium* sp. nov. (Fig. 6H: marked with arrow), convex in *M. serrulatus* (Fig. 6G: marked with arrow); apical microtrichose area of anterior surstyle lobe 2.5 times broader than long in *M. medium* sp. nov. (Fig. 6G: al), less than one time in *M. serrulatus* (Fig. 6G: al); molecular data and distribution (*M. medium* sp. nov. is an endemic to the island of Crete in Greece).

Description. Male. Head. Antennae black to dark brown; basoflagellomere elongated ca. 2.2 times as long as wide, and ca. 2.5 times as long as pedicel, concave dorsally with acute apex; dorsolateral fossette narrow; arista dark and thickened at basal one third, covered with dense microtrichia, ca. 1.5 times as long as basoflagellomere (Fig. 19I); face and frons black with gray microtrichia, face covered with dense whitish gray, and frons with yellowish gray pile; oral margin microtrichose with shiny lateral areas; lunule shiny black, bare; vertex shiny black, except microtrichose area in front of anterior ocellus; vertex isosceles, with long, pale whitish yellow pile, mixed with few black pile on the ocellar triangle; ocellar triangle equilateral; eyes covered with dense pile; occiput with gray-yellow pile, ventrally covered with a dense, gray microtrichia; eye contiguity 10–12 facets long; vertical triangle: eye contiguity: frons = 1.2 : 1 : 2.

Thorax. Scutum and scutellum black with bronze luster, covered with dense, erect, yellow pile, except sides of scutum at wing basis with patch of short black pile and fascia of black pile between wing basis; scutum with two or more microtrichose vittae, anteriorly connected and posteriorly reaching the scutellum; scutum dull; posterodorsal part of anterior anepisternum, posterior anepisternum (except anteroventral angle), anterior anepimeron, dorsomedial anepimeron, and posterodorsal and anteroventral parts of katepisternum with long, pale yellow pile and grayish microtrichia; wings entirely covered with microtrichia; wing veins brown; calypteres and halteres yellowish; legs mostly black, except brown tarsi ventrally in some specimens; pile on legs pale yellow, except few black pile in apical fifth of metafemur in some specimens; metafemur incrassate, ca. three times longer than wide; pile on postero- and anteroventral surface short, except few sparse pile approximately the same length as pile on dorsal surface (Fig. 22C).

Abdomen. Broad, tapering, 1.2 times longer than mesonotum; terga dark, except for a pair of yellow-orange, triangular, lateral maculae on tergum 2; terga 2–4 each with a pair of white microtrichose, oblique fasciae (on tergum 2 more triangular); pile on terga all yellow (Fig. 24A); sterna dark brown, covered with long whitish yellow pile.

Male genitalia. Apical part of anterior surstyle lobe rhomboid shape, 1.5 times longer than wide, covered with dense, short pile (Fig. 25A: al) and with concave margin (Fig. 6H: marked with arrow); posterior surstyle lobe oval with basolateral protrusion (lateral hump) (Fig. 25B: bp) and basal hook-like extension (Fig. 25A: marked with arrow); hypandrium sickle-shaped, without lateral projections; lingula medium sized (Fig. 25C: l).

Female. Similar to the male except for normal sexual dimorphism and for the following characteristics: antennae with rounded tip, basoflagellomere ca. two times longer than wide, (Fig. 19J); frons with broad microtrichose vittae along eye margins; frons covered with pilosity of variable color, from mostly gray-yellow until predominately black pile; ocellar triangle covered with black pile; metafemur incrassate, pile on

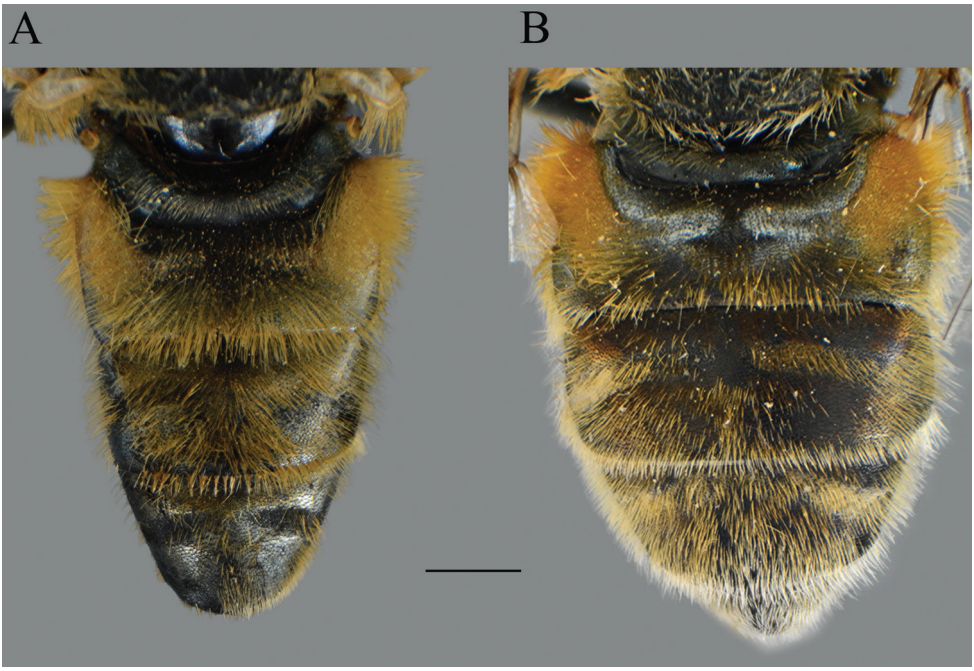

Figure 24. *Merodon medium* sp. nov., abdomen, dorsal view. **A** male **B** female. Scale bar: 2 mm.

postero- and anteroventral surface short (Fig. 22D); terga pale yellow pilose at lateral sides, anterior two thirds of tergum 2 and all terga 4 and 5; terga 2 and 3 medially with short adpressed black pile; microtrichose fasciae on terga 3 and 4 broad (Fig. 24B).

Etymology. Medium (middle, center) refers to the species' distribution, being the only taxon of the group found on Crete, in the middle of Mediterranean Sea.

Distribution. *Merodon medium* sp. nov. is endemic to the Greek island of Crete (Fig. 7).

Ecology. Preferred environment: forest/open ground; evergreen oak forest, dry *Pinus* forest; scrub with *Pistacia lentiscus* L.; well-vegetated, unimproved grassland. Flowers visited: *Ornithogalum* spp., *Potentilla* spp. and *Thymus* spp. Flight period: May.

Type material. Holotype. Greece • ♂; Crete, Chania, Omalos plain; 35°19'21"N, 23°55'50"E; 28 May 2014; A. Vujić leg.; FSUNS 06729. Original label: "HOLOTYPE of *Merodon* / *medium* Vujić, Likov et / Radenković sp.n. 2019" [red label], "Greece, Crete, Chania, / Omalos plain / 28.05.2014. 35.322593 / 23.930496 Leg. Vujić", "AU298", "06729" (See Supplementary file 3: Figure 3). **Paratypes**. Greece • 1 ♀; Crete, Chania, Imbors; 35°15'08"N, 24°10'28"E; 27 May 2014; A. Vujić leg.; FSUNS 06706 • 1 ♂; Crete, Chania, Omalos plain; 35°19'06"N, 23°54'51"E; 28 May 2014; A. Vujić leg.; FSUNS 06723 • 1 ♂; Crete, Chania, Omalos plain; 35°19'21"N, 23°55'50"E; 28 May 2014; A. Vujić leg.; FSUNS 06731 • 1 ♀, Crete, Chania, Mescla, 35°24'05"N 23°56'26"E; 28 May 2014; A. Vujić leg.; FSUNS 06718.

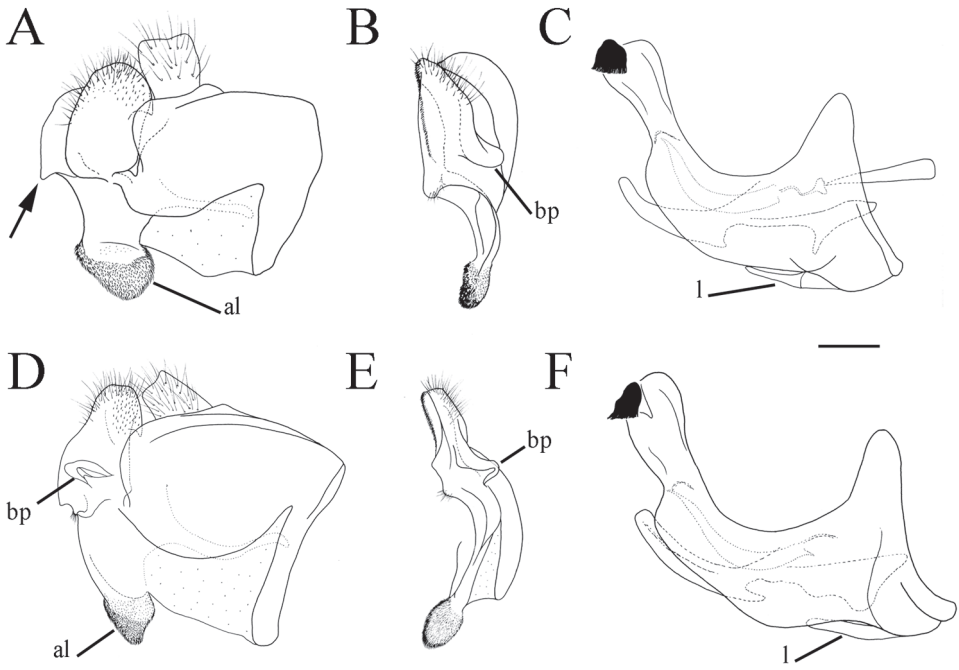

Figure 25. Male genitalia. **A** *Merodon medium* sp. nov., epandrium, lateral view **B** *Merodon medium* sp. nov., epandrium, ventral view **C** *Merodon medium* sp. nov., hypandrium, lateral view **D** *Merodon nigrocapillatus* sp. nov., epandrium, lateral view **E** *Merodon nigrocapillatus* sp. nov., epandrium, ventral view **F** *Merodon nigrocapillatus* sp. nov., hypandrium, lateral view. Abbreviations: al–anterior surstyle lobe, bp–basolateral protrusion, l–lingula; arrow marks the hook-like extension in **A**. Scale bar: 0.2 mm.

Merodon nigrocapillatus Vujić, Likov & Radenković sp. nov.

http://zoobank.org/09B368F3-6BCF-4CF1-95E1-8AC43C14B1D4
Figs 25D–F, 26A–D, 27A, 28C, D

Diagnosis. Medium sized (10.2–10.8 mm), black and shiny species, covered with mostly black pile on scutum, terga and legs in both sexes (Fig. 26); antennae dark; legs black; male dichoptic (Fig. 27A); basoflagellomere short, 1.3 times longer than wide (Fig. 28C); terga black, without pale lateral maculae on tergum 2; microtrichose fasciae on terga 2–4 very narrow or absent in males (Fig. 26A) and narrow in females (Fig. 26C).

Description. Male. Head. Antennae black; basoflagellomere short, 1.3 times as long as wide, and ca. two times as long as pedicel, with rounded apex; fossette dorsolateral; arista black and thickened at basal one third, covered with dense microtrichia, ca. two times as long as basoflagellomere (Fig. 28C); face and frons black with gray microtrichia, face covered with dense whitish gray or mixed black and whitish gray, and frons mostly with black pile; oral margin shiny, with lateral microtrichose area; lunule shiny black, bare; vertex isosceles, shiny black, except in front of anterior ocellus covered with microtrichia; vertex with long, black pile; ocellar triangle equilateral; eyes

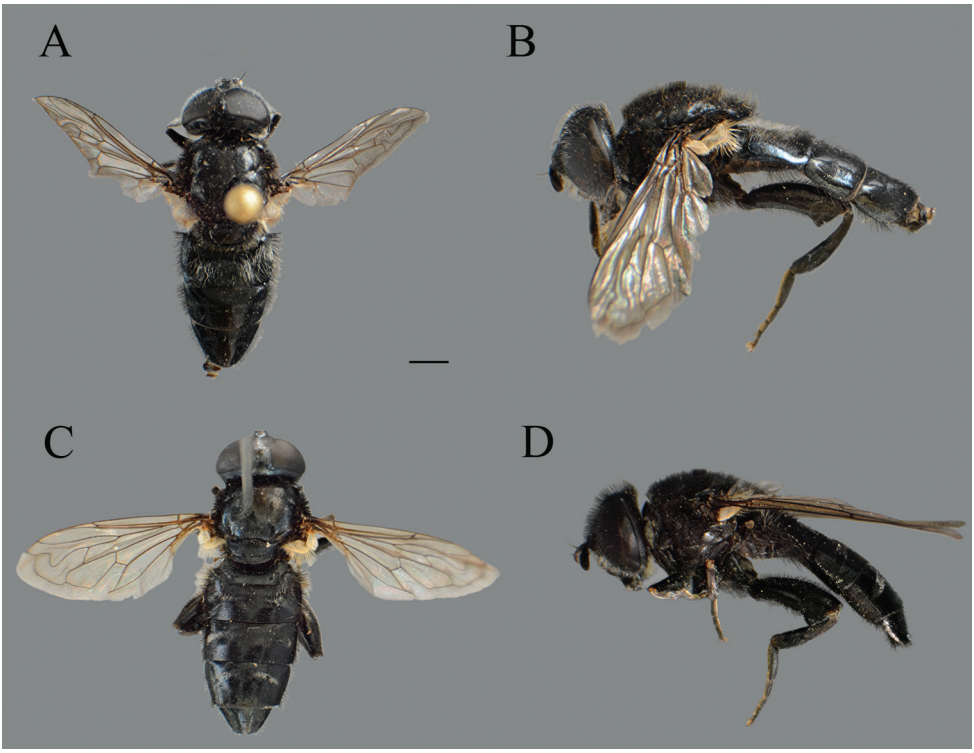

Figure 26. *Merodon nigrocapillatus* sp. nov., body parts. **A** dorsal view, male **B** lateral view, male **C** dorsal view, female **D** lateral view, female. Scale bar: 2 mm.

covered with dense whitish pile; occiput shiny covered with black pile in upper half, ventrally with gray-yellow pile and dense, gray microtrichia; eye dichoptic, separated by distance of three facets (Fig. 27A).

Thorax. Scutum and scutellum black, shiny, covered with dense, erect, black pile; scutum without microtrichose vittae (Fig. 26A); posterodorsal part of anterior anepisternum, posterior anepisternum (except anteroventral angle), anterior anepimeron, dorsomedial anepimeron, and posterodorsal and anteroventral parts of katepisternum with long, dark gray or black pile and grayish microtrichia; wings entirely covered with microtrichia, except bare area at basal one third; wing veins dark brown; calypteres gray; halteres blackish; legs black (Fig. 26B); pile on legs mostly black or dark gray; metafemur curved and medium incrassate, ca. four times longer than wide; pile on postero- and anteroventral surface ca. one third to half of width of metafemur, slightly shorter than pile dorsally.

Abdomen. Tapering, 1.2 times longer than mesonotum; terga completely dark; terga 3 and 4 without, or with indistinct pair of white microtrichose fasciae; pile on terga mostly black, except anteromedial part of tergum 2 partly covered with whitish pile (Fig. 26A); sterna dark brown to black, covered with long black and whitish pile.

Male genitalia. Apical part of anterior surstyle lobe rhomboid shape, ca. two times longer than wide, covered with dense, short pile (Fig. 25D: al); posterior surstyle lobe

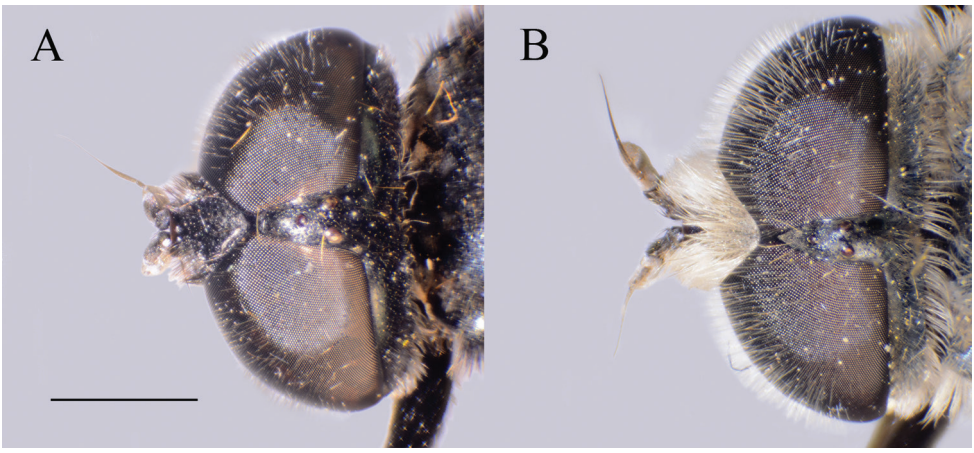

Figure 27. Head of male, dorsal view. **A** *Merodon nigrocapillatus* sp. nov. **B** *Merodon nigropunctum* sp. nov. Scale bar: 2 mm.

oval with basolateral protrusion (lateral hump) (Fig. 25D, E: bp); hypandrium sickle-shaped, without lateral projections; lingula large (Fig. 25F: l).

Female. Similar to the male except for normal sexual dimorphism and for the following characteristics: basoflagellomere 1.5 times longer than wide, fossette narrow (Fig. 28D); pile on face of variable color, from black to whitish; frons mostly microtrichose, covered with black pile; ocellar triangle covered with black pile; microtrichose fasciae on terga 2–4 narrow (Fig. 26C); thorax on lateral sides with variable pilosity color, from black to whitish.

Etymology. The name *nigrocapillatus* is derived from Latin adjective *niger* meaning black, dark and Latin noun *capillatus* meaning long-haired, referring to the long, black body pile of this species.

Distribution. *Merodon nigrocapillatus* sp. nov. has only been recorded in Tajikistan (Fig. 7).

Ecology. Preferred environment: open areas at high altitudes, unimproved grassland (Fig. 35D). Flowers visited: white Apiaceae. Flight period: June-July.

Type material. Holotype. Tajikistan • ♂; Varzob, Kalon; 39°03'36"N, 68°52'12"E; 2440 m a.s.l.; 1–4 Jul. 2017; A. Barkalov leg.; SZMN 22625. Original label: "HOLOTYPE of *Merodon* / *nigrocapillatus* Vujić, Likov / et Radenković sp.n. 2019" [red label], "Таджикистан, Варзобское / ущ., 3 км с.-в. кишлака / Калон, 2440м н.у.м. 39,06° / N, 68,87° 1-4.07.2017 / Сб.А. Баркалов", "*2017* / *sp. 1* / A. Barkalov det., 201" [label partly handwritten], "22625" (See Supplementary file 1: Figure 1B). **Paratypes**. Tajikistan • 1 ♀; Varzob, Kalon; 39°03'00"N, 68°52'48"E; 2484 m a.s.l.; 7–12 Jul. 2017; A. Barkalov leg.; SZMN 22626 • 1 ♀; 65km N of Dushanbe, S side ANZOP pass; 39°03'00"N, 68°19'12"E; 2380 m a.s.l.; 21 Jul. 2010; J. Dils, J. Faes leg.; G. V. W. coll. 10397 • 1 ♀; Iskanderkul kishlak, Sarytag; 39°03'00"N, 68°19'12"E; 2374 m a.s.l.; 14 Jun. 2018; A. Barkalov leg.; SZMN 24506 • 4 ♂♂; Varzob Canyon, 3 km N-E Kalon kishlak; 39°03'36"N, 68°52'12"E; 2440 m a.s.l.; A. Barkalov leg.; SZMN • 14 ♀♀; same data as for preceding; SZMN • 2 ♀♀; same

data as for preceding; 4 and 7 Jul. 2017; V. Zinchenko leg.; SZMN • 3 ♀♀; same data as for preceding; 4 and 7 Jul. 2018; SZMN • 1 ♀; Varzob Canyon, 3 km N-E Kalon kishlak; 39°03'36"N, 68°52'12"E; 2356 m a.s.l.; 5 Jul. 2018; A. Barkalov leg.; SZMN 24502 • 1 ♀; same data as for preceding; 7 Jun. 2018; SZMN 24505 • 1 ♀; same data as for preceding; ~2400 m a.s.l.; 28 Jun. 2018; V. Zinchenko leg.; SZMN 24503 • 1 ♀; same data as for preceding; 30 Jun. 2018; SZMN 24504 • 1 ♀; Varzob Canyon, 4 km N-E Kalon kishlak; 39°04'48"N, 68°51'36"E; 3375 m a.s.l.; A. Barkalov leg.; SZMN • 1 ♀; Iskanderkul, Zmeinoe Lake; 39°05'20"N, 68°22'08"E; ~2217 m a.s.l.; 16 Jun. 2018; V. Zinchenko leg.; SZMN 24507.

***Merodon nigropunctum* Vujić, Likov & Radenković sp. nov.**
http://zoobank.org/13F2CA9B-BD91-4FD6-B66A-B89DE0F13726
Figs 27B, 28A, B, 29A–C, 30A–C

Diagnosis. Medium sized (10.3 mm), bluish species (Fig. 29A, B) with dark macula on medial part of wing (Fig. 29C); basoflagellomere narrow and elongated, 1.8 times as long as wide, rounded at the tip (Fig. 28A, B); arista long, two times as long as basoflagellomere; body pile whitish; posterior half of scutum with square shaped area of black pile medially; terga 2–4 covered with black pile medially, except whitish pilosity on conspicuous silver microtrichose fasciae (Fig. 29A).

Description. Male. Head. Antennae black to dark brown; basoflagellomere narrow and elongated, 1.8 times as long as wide, and 2.5 times as long as pedicel, with rounded tip; large fossette dorsomedial and dorsolateral (Fig. 28A, B); arista dark and thickened at basal one third, covered with dense microtrichia; arista long, ca. two times as long as basoflagellomere (Fig. 28A, B); face and frons black covered with whitish pile; face covered with indistinct whitish gray microtrichia; frons with dense whitish microtrichia; lunule shiny black, bare; vertex isosceles, with long whitish pile and black pilosity on the ocellar triangle; ocellar triangle equilateral; eyes covered with long, dense, whitish pile (Fig. 27B); occiput with whitish pile, covered with a dense, silver microtrichia along eye margin; eye contiguity short, approximately five facets long; vertical triangle: eye contiguity: frons = 4.5 : 1 : 4.5.

Thorax. Scutum and scutellum black with bluish luster, covered with dense, erect, white pile including wing basis; posterior half of scutum with square shaped area of black pile medially; scutum with indistinct microtrichose vittae; posterodorsal part of anterior anepisternum, posterior anepisternum (except anteroventral angle), anterior anepimeron, dorsomedial anepimeron, and posterodorsal and anteroventral parts of katepisternum with long, whitish pile and grayish microtrichia; wings entirely covered with microtrichia; wing veins dark brown; wing with distinct dark area in apical half (Fig. 29C); calypteres whitish; halteres yellowish, with darker capitulum; legs mostly black, except dark brown tarsi ventrally; pile on legs mostly whitish mixed with black ones on femora; metafemur moderately incrassate, ca. three times longer than wide; pile on postero- and anteroventral surface very long, and ca. two thirds of width of metafemur, approximately the same length as pile on dorsal surface.

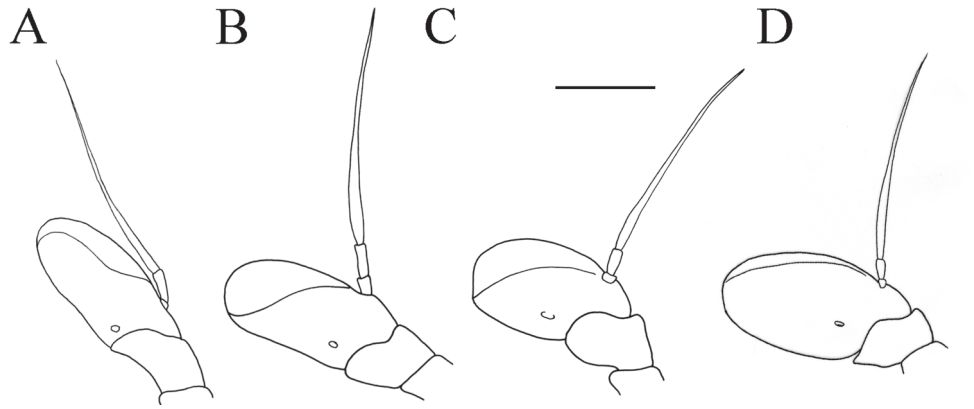

Figure 28. Antenna. **A** *Merodon nigropunctum* sp. nov., outer side lateral view, male **B** *Merodon nigropunctum* sp. nov., inner side, lateral view, male **C** *Merodon nigrocapillatus* sp. nov., outer side, lateral view, male **D** *Merodon nigrocapillatus* sp. nov., outer side, lateral view, female. Scale bar: 1 mm.

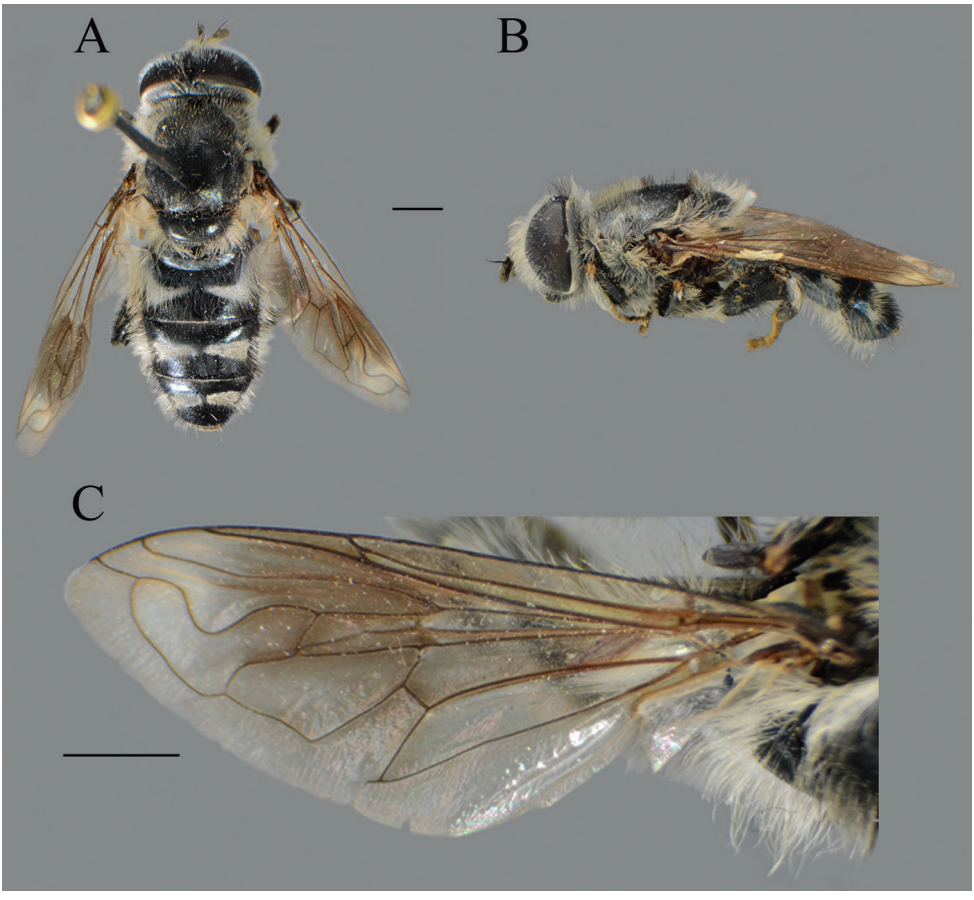

Figure 29. *Merodon nigropunctum* sp. nov., male. **A** body, dorsal view **B** body, lateral view **C** left wing, dorsal view. Scale bar: 2 mm.

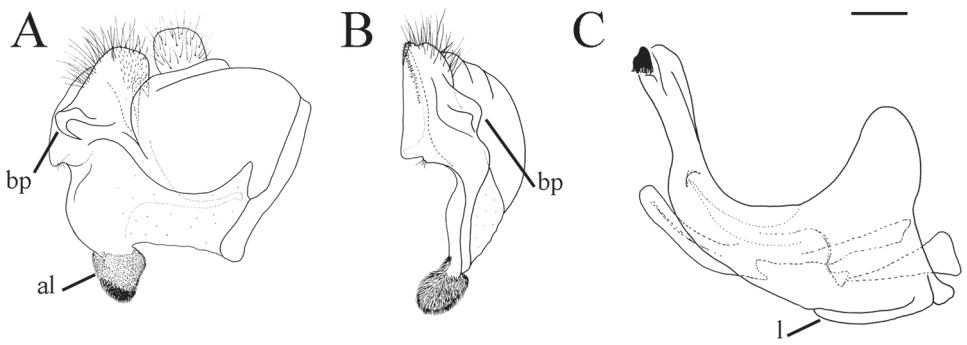

Figure 30. Male genitalia. **A** *Merodon nigropunctum* sp. nov., epandrium, lateral view **B** *Merodon nigropunctum* sp. nov., epandrium, ventral view **C** *Merodon nigropunctum* sp. nov., hypandrium, lateral view. Abbreviations: al–anterior surstyle lobe, bp–basolateral protrusion, l–lingula. Scale bar: 0.2 mm.

Abdomen. Tapering, 1.2 times longer than mesonotum; terga dark brown to black; terga 2–4 each with a pair of white microtrichose, wide, oblique fasciae (on tergum 2 triangular); pile on terga long, whitish laterally and at microtrichose fasciae, medially black (Fig. 29A); sterna dark brown, covered with long whitish pile.

Male genitalia. Apical part of anterior surstyle lobe rhomboid shape, 1.5 times longer than wide, covered with dense, short pile (Fig. 30A: al); posterior surstyle lobe oval with basolateral protrusion (lateral hump) (Fig. 30A, B: bp); hypandrium sickle-shaped, without lateral projections; lingula large (Fig. 30C: l).

Female. Unknown.

Etymology. The word *nigropunctum* is derived from the Latin words *niger* (black, dark whitish) and *punctum* (dot/spot) referring to the dark macula on the wing as an important diagnostic character of this new species.

Distribution. *Merodon nigropunctum* sp. nov. was recorded at only one locality in Uzbekistan (Fig. 7).

Ecology. Preferred environment: no data. Flowers visited: no data. Flight period: May.

Type material. Holotype. Uzbekistan • ♂; Kadamžai, S of Fergana; 40°20'00"N, 71°47'39"E; 21 May 1980; Z. Padr leg.; NMPC 18248. Original label: "HOLOTYPE of *Merodon* / *nigropunctum* Vujić, Likov / Radenković sp.n. 2019" [red label], "C.ASIA, Uzbekistan / Kadanžai, S of Fergana / 21.5.1980 leg.Z.Pádr", "18248" (See Supplementary file 4: Figure 4A).

Merodon opacus Vujić, Likov & Radenković sp. nov.

http://zoobank.org/256F1010-6AAF-406A-830B-4F4A1D95126A

Figs 12A–F, 13A, B, 14H–J, 20C, 21A–D, 31A, B, 32A–C

Diagnosis. Medium sized (7.2–10.6 mm), short pilose dark species with olive-brown reflection; antennae dark; legs mostly black; basoflagellomere elongated (1.8–2 times as long as wide) obviously concave dorsally; arista short 1.5 times as long as basoflagel-

lomere (Fig. 12A–F); terga dark (Fig. 21A, B); metafemur incrassate covered with very short pilosity (Fig. 13A, B); male genitalia: posterior surstyle lobe with small lateral hump (Fig. 14H, I: bp); apical part of anterior surstyle lobe rhomboid (Fig. 14H: al); lingula medium sized (Fig. 14J: l). Similar to *Merodon serrulatus* from which it differs in dark tergum 2 (in *M. serrulatus* with small pale lateral maculae). Related to *M. hirsutus* from which can be distinguished by frons covered with dense microtrichia (Fig. 20C) (mostly shiny in *M. hirsutus*), shorter dorsolateral and ventral pile on metafemur (Fig. 13A, B), and shorter and more adpressed pile on terga in females (Fig. 21D). Morphologically related to *M. defectus* sp. nov. from which can be distinguished by dark tergum 2 (in *M. defectus* sp. nov. tergum 2 with yellow-orange lateral maculae). Additionally, differs from *M. defectus* sp. nov. by posterior surstyle lobe with developed lateral hump (Fig. 14I: bp), reduced in *M. defectus* sp. nov. (Fig. 14B: bp).

Description. Male. Head. Antennae black to dark brown; basoflagellomere elongated 1.8–2 times as long as wide, and 2.3 times as long as pedicel, concave dorsally with acute apex; large fossette dorsomedial and dorsolateral (Fig. 12A–C); arista dark and thickened at basal one third, covered with dense microtrichia, 1.5 times as long as basoflagellomere; face and frons black with gray microtrichia, face covered with dense whitish gray, and frons with yellowish gray pile; oral margin microtrichose with shiny lateral areas; lunule shiny black, bare; vertex covered with microtrichia (Fig. 20C); vertex isosceles, with long, pale whitish yellow pile, in some cases mixed with few black pile on the ocellar triangle; ocellar triangle equilateral; eyes covered with dense pile; occiput with gray-yellow pile, covered with a dense, gray microtrichia; eye contiguity ca. 10–12 facets long; vertical triangle: eye contiguity: frons = 1.2 : 1 : 2.

Thorax. Scutum and scutellum black with bronze luster, covered with dense, erect, yellow pile; scutum at wing basis with short black pile; scutum with two or more microtrichose vittae, anteriorly connected and posteriorly reaching the scutellum; scutum dull; posterodorsal part of anterior anepisternum, posterior anepisternum (except anteroventral angle), anterior anepimeron, dorsomedial anepimeron, and posterodorsal and anteroventral parts of katepisternum with long, pale yellow pile and grayish microtrichia; wings entirely covered with microtrichia; wing veins brown; calypteres yellowish; halteres yellowish, in some specimens with darker capitulum; legs mostly black, except brown tarsi ventrally in some specimens; pile on legs pale yellow; metafemur moderately incrassate, 3.5 times longer than wide; pile on postero- and anteroventral surface very short with few sparse pile, and ca. as one fourth of width of metafemur, approximately the same length as pile on dorsal surface (Fig. 13A).

Abdomen. Tapering, 1.2 times longer than mesonotum; terga dark brown to black; terga 2–4 each with a pair of white microtrichose, wide, oblique fasciae (on tergum 2 more triangular); pile on terga all yellow (Fig. 21A, C); sterna dark brown, covered with long whitish yellow pile.

Male genitalia. Apical part of anterior surstyle lobe rhomboid in shape, 1.5 times longer than wide, covered with dense, short pile (Fig. 14H: al); posterior surstyle lobe oval with small basolateral protrusion (lateral hump) (Fig. 14H, I: bp); hypandrium sickle-shaped, without lateral projections; lingula medium sized (Fig. 14J: l).

Female. Similar to the male except for normal sexual dimorphism and for the following characteristics: antennae with rounded tip, basoflagellomere ca. two times longer than wide, fossette dorsal (Fig. 12D–F); frons with broad microtrichose vittae along eye margins; frons covered with pilosity of variable color, from mostly gray-yellow to predominantly black; ocellar triangle covered with black pile; terga pale pilose, in some specimens terga 2–4 medially with short adpressed black pile; microtrichose fasciae on terga 3 and 4 narrower (Fig. 21B, D).

Morphological description of the puparium (Fig. 31A). Length: 7.5 mm, width: 4 mm; light brown in color; sub-cylindrical; rough integument with larval segmentation persisting as transverse folds and wrinkles; integument covered with small domes and spicules; pronounced segmental sensilla, bearing seta. The dorsal surface of the prothorax with a pair of anterior spiracles, which are more than two times longer than broad at the base, sclerotized, cylindrical in shape, brown in color, apex with two linear spiracular openings (Fig. 32B). On the anal segment, two different pairs of lappets present: the ventro-lateral pair represented by fleshy papilla with one sensilla bearing a seta and the dorso-lateral pair with a very poorly developed basal papilla, apically divided bearing one sensilla with a long seta on top of each division. ***Cephalopharyngeal skeleton*** (Fig. 31B). Robust mandibles with dark highly sclerotized hooks, without accessory teeth, fused to the external mandibular lobes; the dorsal cornu narrowed, representing almost the whole length of the ventral cornu. Clypeal sclerite sclerotized, tentorium and intermediate sclerites highly sclerotized and apparently fused; ventral cornu elongated and narrow in profile view, wider and more heavily sclerotized at the posterior end, forming the grinding mill of pestle and mortar construction at the posterior end of the cibarium; cibarium at the base, with a clearly sclerotized end. ***Posterior respiratory process*** (Fig. 32A). Brownish, wider than long, very short (barely visible from dorsal view), button shape, base only slightly wider than apex; dorsal and lateral surface covered by a barely visible ornamentation resembling a network. The outline of the spiracular plate sub-elliptical and barely irregular. Spiracular plate with four pairs of sinuous spiracular openings (clearly separated from each other) around two central scars, first pair clearly shorter than the others; three or four very small circular nodules on each side of the surface of spiracular plate in the area of spiracular openings; four pairs of branched inter-spiracular setae emerging on the outward edges of the spiracular plate. ***Pupal spiracles*** (Fig. 32C). Sclerotized, brownish in color, stout, cylindrical in shape, almost as long as broad, slightly tapered, with not heavily rounded prominence at the end (length 0.3 mm) separated by a distance of ca. five times their length. Upper two-thirds of the lateral sides (except for the granularly surfaced apex) covered with irregularly-spaced, oval-shaped domed tubercles, leaving a more or less triangular central area free of tubercles on both ventral and dorsal surfaces; 3–7 radially-arranged spiracular openings on each tubercle. The whole spiracle surface (from the base to the apex) reticulated with a polygonal pattern, more irregular on ventral side, with polygons being noticeably smaller in the apical part. ***Material examined.*** Greece, Lesvos Island, Agiassos, C. Pérez-Bañón leg.: 1 larva (L3 instar) buried in the ground of a chestnut forest, 2 Mar 2006; reared, pupa 4 Mar 2006, adult emerged 21 Mar 2006.

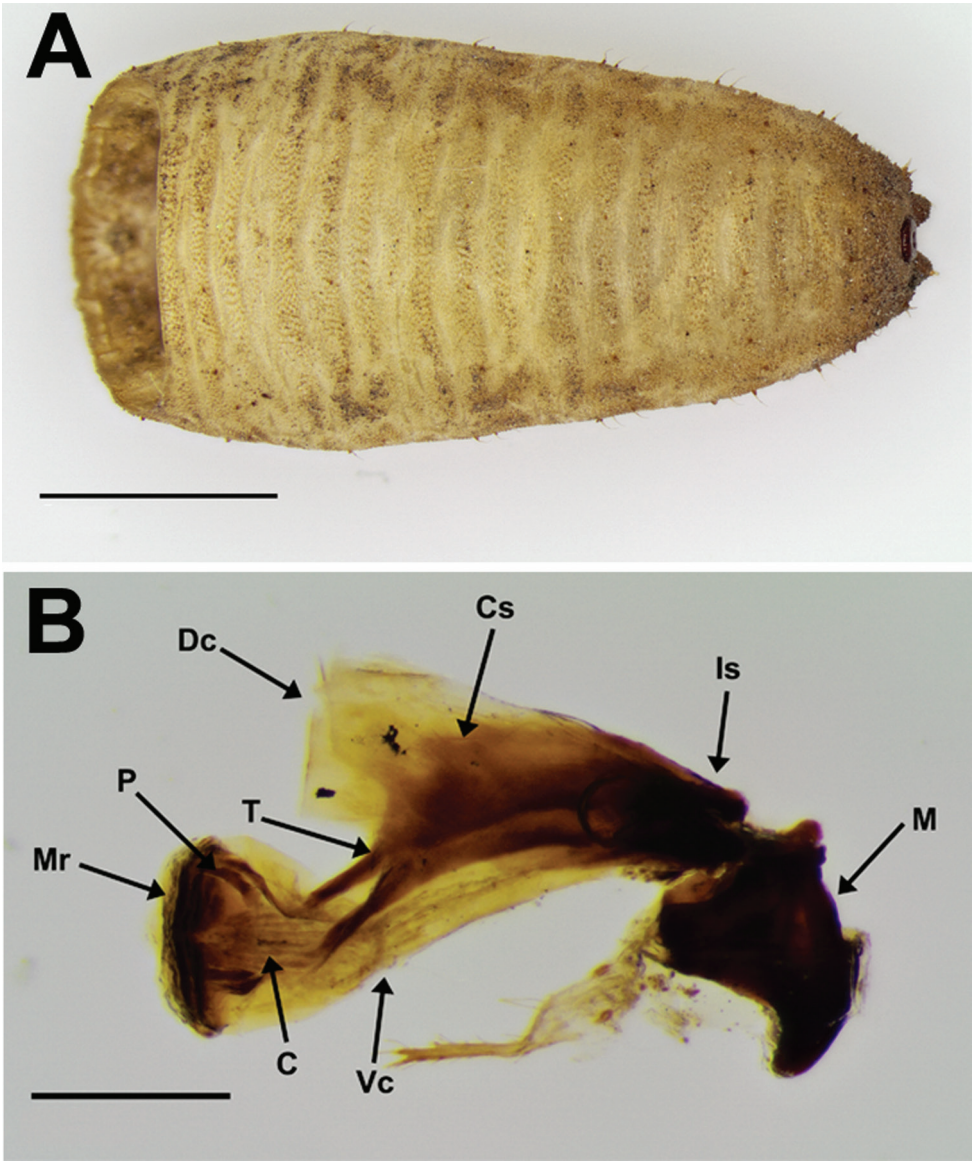

Figure 31. Light micrographs of *Merodon opacus* sp. nov. puparium. **A** puparium in dorsal view **B** cephalopharyngeal skeleton in lateral view. Abbreviations: C–cibarium, Cs–clypeal sclerite, Dc–dorsal cornu, Is–intermediate sclerite, M–mandibles, Mr–mortar, P–pestle, T–tentorium, Vc–ventral cornu. Scale bars: 3 mm (**A**); 500 μm (**B**).

Etymology. Latin adjective *opacus* (opaque, not transparent), pertains to the dark tergum 2, without reddish yellow lateral maculae.

Distribution. *Merodon opacus* sp. nov. has been recorded on the Greek island of Lesvos and in western Turkey (Fig. 7).

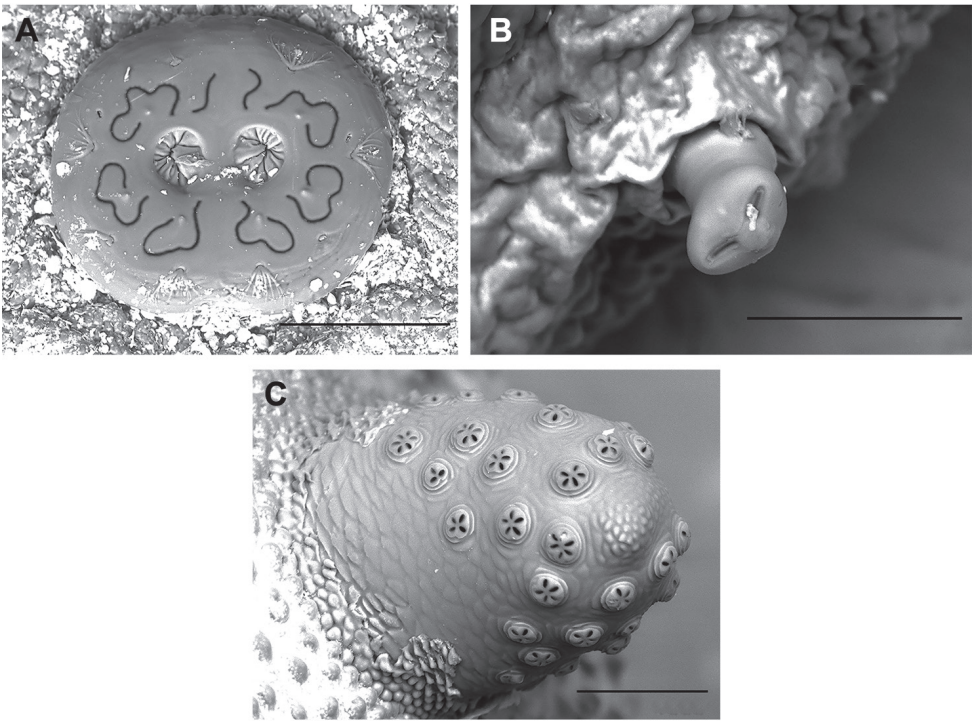

Figure 32. SEM micrographs of *Merodon opacus* sp. nov. puparium. **A** posterior respiratory process in polar view showing the spiracular plate **B** anterior spiracle **C** pupal spiracle. Scale bars: 200 μm (**A**); 100 μm (**B**, **C**).

Ecology. Preferred environment: forest/open ground; thermophilous and evergreen *Quercus* forest; *Castanea* forest, dry *Pinus* forest; unimproved grassland and tracksides (Fig. 35A). Flowers visited: *Ornithogalum* spp. and *Potentilla* spp. Flight period: March-September.

Type material. Holotype. Greece • ♂; Lesvos; Polichnitos; 39°05'02"N, 26°09'13"E; 30 Apr. 2008; A. Vujić leg.; FSUNS 03758. Original label: "HOLOTYPE of *Merodon* / *opacus* Vujić, Likov et / Radenković sp.n. 2019" [red label], "Greece, Lesvos, / Polichnitos 30.IV 2008. / Leg. A. Vujic", "03758" (See Supplementary file 4: Figure 4B). **Paratypes**. Greece, Lesvos • 1 ♂; Ag. Ermogenis; 39°01'07"N, 26°32'44"E; 2 May 2008; A. Vujić leg.; FSUNS 03760 • 1 ♂; Neochori II; 39°01'10"N, 26°20'02"E; 2 May 2016; A. Vujić, J. Ačanski leg.; FSUNS 11396 • 1 ♀; Agiassos; 39°03'00"N, 26°22'60"E; 6 Jun. 2004; M. Kapsali leg.; MAegean • 3 ♀♀; Agiassos; 39°03'00"N, 26°22'60"E; 23 May 2004; A. Kyriakopoulos leg.; MAegean • 1 ♂; same data as for preceding; 24 May 2001; MAegean • 1 ♀; same data as for preceding; MAegean • 1 ♂; Agiassos; 39°03'00"N, 26°22'60"E; Mar. 2006; C. Pérez-Bañón leg.; CEUA • 4 ♂♂; same data as for preceding; 11 Jun. 2005; CEUA • 4 ♂♂; same data as for preceding; 10 Jun. 2005; CEUA • 8 ♀♀; same data as for preceding; CEUA • 4 ♀♀; same data as for preceding; 6 Jun. 2005; CEUA • 4 ♂♂; same data as for preceding; CEUA • 1 ♂; Agiassos; 39°03'09"N, 26°22'57"E; 860 m

a.s.l.; 23 May 2004; M. Kapsali leg.; MAegean • 2 ♂♂; 3.5 km S Agiassos; 39°03'09"N, 26°22'57"E; 860 m a.s.l.; 23 May 2004; M. Kapsali leg.; FSUNS 02487, 02503 • 1 ♂; 3.5 km S Agiassos; 39°03'09"N, 26°22'57"E; 860 m a.s.l.; 23 May 2004; A. Kyriakopoulos leg.; FSUNS 03762 • 1 ♀; 3.5 km S Agiassos; 39°03'09"N, 26°22'57"E; 860 m a.s.l.; 23 May 2004; M. Kapsali leg.; FSUNS 03764 • 3 ♀♀; Agiassos; 39°03'17"N, 26°23'50"E; 760 m a.s.l.; 10 Jun. 2004; M. Kapsali leg.; MAegean • 1 ♂; same data as for preceding; 24 May 2004; MAegean • 2 ♂♂; same data as for preceding; A. Kyriakopoulos leg.; MAegean • 1 ♀; same data as for preceding; MAegean • 2 ♀♀; same data as for preceding; 10 Jun. 2004; MAegean • 1 ♀; 3.8 km SSE Agiassos; 39°03'17"N, 26°23'50"E; 760 m a.s.l., 10 Jun. 2004; A. Kyriakopoulos leg.; FSUNS 03763 • 1 ♀; Agiassos; 39°03'45"N, 26°23'30"E; 700 m a.s.l.; 20 May 2004; A. Kyriakopoulos leg.; MAegean • 1 ♀; same data as for preceding; 6 Jun. 2004; M. Kapsali leg.; MAegean • 1 ♂; Agiassos; 39°03'92"N, 26°22'87"E; 27 May 2009; M. Taylor leg.; MZH http://id.luomus.fi/GJ.1133 • 1 ♂; Agiassos; 39°04'09"N, 26°23'17"E; 600 m a.s.l.; 15 May 2004; T. Petanidou leg.; MAegean • 5 ♂♂; Agiassos; 39°04'17"N, 26°22'22"E; Sep. 2009; A. Vujić leg.; FSUNS Č64, Č65, Ž9 to Ž11 • 10 ♀♀; Agiassos; 39°04'17"N, 26°22'22"E; Sep. 2009; A. Vujić leg.; FSUNS Ž12 to Ž19, Ž28, Ž29 • 2 ♂♂; Agiassos; 39°04'17"N, 26°22'22"E; 8 Jun. 2009; G. Ståhls leg.; MZH GJ.1139, GJ.1141• 4 ♀♀; same data as for preceding; MZH GJ.1135 to GJ.1138 • 4 ♂♂; same data as for preceding; 25 May 2009; MZH GJ.1140, GJ.1142, GJ.1143, GJ.1145 • 1 ♂; Agiassos; 39°04'25"N, 26°22'35"E; 8 May 2007; G. Ståhls leg.; MZH GJ.1144 • 1 ♀; same data as for preceding; MZH GJ.1126 • 5 ♂♂; same data as for preceding; 30 May 2009; MZH GJ.1119 to GJ.1123 • 2 ♀♀; same data as for preceding; MZH GJ.1124, GJ.1125 • 1 ♂; same data as for preceding; 27 May 2009; MZH • 1 ♂; 39°10'17"N, 26°18'14"E; FSUNS 02504 • 1 ♀; 39°10'17"N, 26°18'14"E; FSUNS 02505 • 3 ♀♀; 39°10'17"N, 26°18'14"E; 4 Jun. 2012; A. Vujić, L. Likov leg.; FSUNS G1747 to G1749 • 1 ♂; Vatousa; 39°13'51"N, 26°01'23"E; 200 m a.s.l.; 28 May 2001; FSUNS • 1 ♀; 2.5 km S Gavathas; 39°14'54"N, 25°58'60"E; 28 Apr. 2010; M. Hull leg.; WML 05042 • 6 ♂♂; near Sikaminea; 39°21'14"N, 26°17'56"E; 11 May 2009; G. Ståhls leg.; MZH GJ.1127 to GJ.1129, GJ.1132, GJ.1134, GJ.1147 • 2 ♀♀; same data as for preceding; 2 Jun. 2009; MZH GJ.1130, GJ.1131 • 2 ♀♀; 5.7 km NW Mantamados; 39°21'19"N, 26°17'52"E; 600 m a.s.l.; 2–10 May 2001; FSUNS 02488, 02507 • 3 ♂♂; Mantamados; 39°21'19"N, 26°17'52"E; 600 m a.s.l.; 10 May 2001; FSUNS • 2 ♀♀; same data as for preceding; FSUNS • 3 ♂♂; same data as for preceding; 17 May 2001; FSUNS • 1 ♀; same data as for preceding; FSUNS • 1 ♂; same data as for preceding; 23 May 2001; FSUNS • 1 ♂; Sikaminia; 39°21'42"N, 26°17'47"E; 10 May 2001; C. Pérez-Bañón, S. Rojo leg.; CEUA • 3 ♂♂; same data as for preceding; 14 May 2001; CEUA • 15 ♂♂; same data as for preceding; 17 May 2001; CEUA • 1 ♀; same data as for preceding; CEUA • 2 ♂♂; Sikaminia; 39°21'44"N, 26°17'49"E; 3 May 2008; A. Vujić leg.; FSUNS 03757, 03759 • 1 ♂; Sikaminia; 39°21'44"N, 26°17'49"E; 2 May 2001; FSUNS 02506 • 1 ♀; Near Lepetimnos; 39°21'47"N, 26°16'32"E; 1 May 2016; A. Vujić, J. Ačanski leg.; FSUNS 11243.

Turkey • 3 ♀♀; 12 km SW of Muğla; 37°07'40"N, 28°16'28"E; 660 m a.s.l.; 23 May 2011; M. Bartak, Kubik leg.; M. B. coll. 17921 to 17923 • 26 ♂♂; Muğla, Uni-

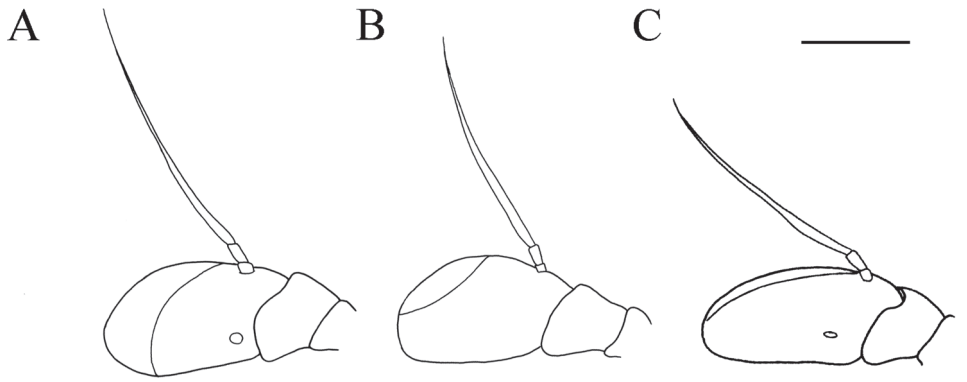

Figure 33. *Merodon trianguloculus* sp. nov., antenna, lateral view. **A** outer side, male **B** inner side, male outer side, female. Scale bar: 1 mm.

versity Campus; 37°09'42"N, 28°22'13"E; 700 m a.s.l.; 17–22 May 2011; M. Bartak, Kubik leg.; M. B. coll. 17927, 17928, 17930, 17931, 17937, 17938, 17940 to 17943, 17946, 17951, 17955 to 17960, 17965 to 17972 • 20 ♀♀; Muğla, University Campus; 37°09'42"N, 28°22'13"E; 700 m a.s.l.; 17–22 May 2011; M. Bartak, Kubik leg.; M. B. coll. 17929, 17932 to 17936, 17939, 17944, 17945, 17947 to 17950, 17952 to 17954, 17961 to 17964 • 1 ♀; Muğla, University campus; 37°09'42"N, 28°22'21"E; 700 m a.s.l.; Apr.–May 2014; O. Dursun leg.; M. B. coll. 10463 • 3 ♀♀; Muğla, 13 km NE pine wood; 37°14'50"N, 28°30'00"E; 1200 m a.s.l.; 23–27 Jun. 2015; M. Bartak, Kubik leg.; M. B. coll. 17924 to 17926 • 4 ♀♀; Bozdağ mountain, Near Bozdağ; 38°22'28"N, 28°04'38"E; 1140 m a.s.l.; 7 Jun. 2014; A. Vujić, J. Ačanski leg.; FSUNS 06945, 06946, 06948, 06951 • 2 ♂♂; Bozdağ mountain, Near Bozdağ; 38°22'28"N, 28°04'38"E; 1140 m a.s.l.; 7 Jun. 2014; A. Vujić, J. Ačanski leg.; FSUNS 06947, 06949.

Other material. Greece, Lesvos • 1 ♀; Agiassos; 39°03'00"N, 26°22'60"E; 28 May 2010; Horsfield leg.; NMS • 1 ♀; Agiassos; 39°03'00"N, 26°22'60"E; 3 Jun. 2010; Wilkinson leg.; NMS [published in Ricarte et al. (2012), as *Merodon serrulatus*] • 1 ♀; same data as for preceding; 8 Jun. 2010; NMS • 1 ♀; Agiassos; 39°03'00"N, 26°22'60"E; 1–8 Jun. 2010; Hancock leg.; GLAHM • 2 ♂♂; same data as for preceding; 28–29 May–Jun. 2010; GLAHM • 2 ♀; Agiassos; 39°03'36"N, 26°23'30"E; 1 Jun. 2010; Horsfield leg.; NMS [published in Ricarte et al. (2012), as *Merodon serrulatus*] • 1 ♀; Agiassos; 39°03'36"N, 26°23'30"E; 28 May 2010; Horsfield leg.; NMS • 1 ♂; 3.5 km S Agiassos; 39°04'15"N 26°22'17"E; 860 m a.s.l.; 8 Jun. 2004; M. Kapsali leg.; MZH • 1 ♂; Agiassos; 39°04'17"N, 26°22'22"E; 1910 m a.s.l.; 26 May 2003; C. J. Palmer leg.; WML 298/03 • 1 ♀; same data as for preceding; WML 310/03 • 1 ♂; SW from Agiassos; 39°04'35"N, 26°22'03"E; 24 May 1988; NBCN • 1 ♀; Potamia river; 39°13'36"N, 26°06'48"E; 1–8 Jun. 2010; Hancock leg.; GLAHM • 1 ♂; 2 km S Gavathas; 39°16'11"N, 25°58'33"E; 5 May 2005; M. Hull leg.; WML • 1 ♂; 5.7 km NW Mantamados; 39°21'19"N, 26°17'52"E; 31 May 2004; E. Lamborn leg.; MZH.

***Merodon sacki* (Paramonov, 1936)**
Figs 8C, 9D–F, 10C, D, 11D–F

Diagnosis. Large (9.5–11.6 mm) dark brown species with lack of microtrichose fasciae on terga 2–4 in males (Fig. 10C) and curved and very incrassate metafemur with long pile on ventral margin; the longest pile as long as half of width of metafemur (Fig. 8C). Similar to *Merodon bequaerti* but differs by strongly curved metafemur and generally longer body pile, clearly visible on tergum 4 (Fig. 10D).

Redescription (based on holotype and additional material from the type area, Spain). **Male.** Head. Antennae black to dark brown; basoflagellomere ca. two times as long as wide, and ca. two times as long as pedicel, concave dorsally; large fossette dorsolateral; arista dark and thickened at basal one third, covered with dense microtrichia, 1.6 times as long as basoflagellomere (Fig. 11D–F); face and frons black with gray microtrichia, face covered with dense whitish gray, and frons with yellowish gray pile; oral margin microtrichose with shiny lateral areas; lunule shiny black, bare; vertex covered with golden microtrichia around ocellar triangle; vertex isosceles, with long, pale whitish yellow pile mixed with black pile on the ocellar triangle; ocellar triangle equilateral; eyes covered with dense pile; occiput with gray-yellow pile, covered with a dense, gray microtrichia; eye contiguity 10–14 facets long.

Thorax. Scutum and scutellum black with bronze luster, covered with dense, erect, yellow pile; scutum at wing basis with short black pile; scutum with two or more microtrichose vittae, anteriorly connected and posteriorly reaching the scutellum; scutum dull; posterodorsal part of anterior anepisternum, posterior anepisternum (except anteroventral angle), anterior anepimeron, dorsomedial anepimeron, and posterodorsal and anteroventral parts of katepisternum with long, pale yellow pile and grayish microtrichia; wings entirely covered with microtrichia; wing veins brown; calypteres and halteres pale yellowish; legs mostly black, except brown tarsi ventrally in some specimens; pile on legs pale yellow, except black pile at apical one fourth of metafemur; metafemur curved and incrassate, approximately three to four times longer than wide; pile on postero- and anteroventral surface long, and ca. half of width of metafemur (Fig. 8C).

Abdomen. Broad, tapering, 1.2 times longer than mesonotum; terga dark brown to black, usually without microtrichose fasciae; tergum 2 with orange lateral maculae; pile on terga all yellow (Fig. 10C, D); sterna dark brown, covered with long whitish yellow pile.

Male genitalia. Apical part of anterior surstyle lobe rhomboid in shape, 1.5 times longer than wide, covered with dense, short pile (Fig. 9D: al); posterior surstyle lobe oval with basolateral protrusion (lateral hump) (Fig. 9D, E: bp); hypandrium sickle-shaped, without lateral projections; lingula large (Fig. 9F: l).

Female. Unknown.

Distribution. *Merodon sacki* is known only from Spain (Fig. 7).

Ecology. Preferred environment: forest/open ground; open areas in evergreen oak forest (*Quercus ilex* and *Q. suber*) and Mediterranean scrub. Flowers visited: no data. Flight period: April-July.

Type material. Holotype (original designation): male, "Holotypus Lampetia / sacki Paramononv, 1936 / G.V. POPOV des. 2007" [red label], "*Lampetia* / *sacki n. sp*. / ♂ *Typus* / *Paramonov d*." [pink label handwritten], "*Merodon* / *mir únbekannt*" [yellow label handwritten], "*14 VII 81*" "*Chiclana*" [handwritten on the back side] (SIZK) (See Supplementary file 6: Figure 6B) (studied).

Note (Popov pers. comm.). The species was described by examining a single male, with the type clearly indicated on the label by Paramonov (discovered and deposited in SIZK). The type specimen is considered lost (Liepa 1969). Hurkmans (1993: 178, 179) incorrectly considered *M. sacki* as a junior synonym of *M. clavipes* (Fabricius, 1781). Hurkmans (1993) also provided an incorrect year for the description of *Lampetia sacki* (1937 instead of the correct 1936), and also incorrectly designated the lectotype and paralectotype [Articles 73 and 74 of the ICZN (1999)] for two *M. clavipes* females with the same label "Chiklana", which are not syntypes [a violation of Articles 74.1 and 74.2 of ICZN (1999)]. The holotype was established by the original designation according to Article 73.1.1 of the ICZN (1999), as well as by a monotype according to Article 73.1.2 (ibid.).

Other material. Spain • 3 ♂♂; La Corte; 37°57'41"N, 6°49'09"W; 28 Apr. 2015; A. Vujić, D. Obreht leg.; FSUNS 09340, 09343, 09345.

***Merodon serrulatus* (Wiedemann in Meigen, 1822)**
Figs 1A–G, 2A–D, 3A–J, 4A–F, 5A–D, 6A–G, 14C

Merodon alexeji Paramonov, 1925: 155 – syn. published in Vujić et al. 2011: 84.
Merodon lusitanicus Hurkmans, 1993: 181 – syn. published in Marcos-García et al. 2007: 566.
Merodon tener Sack, 1913: 443 syn. nov.

Diagnosis. Medium sized (7.1–10.9 mm), short pilose dark species with olive-brown reflection; antennae dark brown; legs mostly black; body pile predominantly pale yellow, except black pile on vertex and scutum, terga 2–4 in some specimens and apical one third of femora in some specimens and populations; basoflagellomere elongated (1.7–2.2 times as long as wide) obviously concave dorsally, arista short (Fig. 3); tergum 2 usually with small pale orange-yellow lateral maculae (Fig. 2); metafemur incrassate, ca. three times longer than wide, with short pilosity, except few long pile on postero- and anteroventral surface of metafemur (Fig. 4); male genitalia: apical part of anterior surstyle lobe triangular (Fig. 1A: al, C, D); posterior surstyle lobe with lateral hump (Fig. 1A, B: lp); lingula large (Fig. 1E: l).

Redescription (based on the types and specimens from the type area of nominal taxon, Iberian Peninsula; variability includes populations from all of the range). **Male.** Head. Antennae black to dark brown; basoflagellomere (Fig. 3A–C, G–J) elongated, 1.7–2.2 times as long as wide, and 2.5–3 times as long as pedicel, concave dorsally, tapering to the apex; dorsolateral and dorsomedial (if present) fossette large with vari-

able shape (see variability) (as on Fig. 3); arista dark and thickened at basal one third, covered with dense microtrichia; arista short, 1.2–1.5 times as long as basoflagellomere (Fig. 3); face and frons black with gray microtrichia, face covered with dense whitish, and frons with yellowish gray pile; oral margin shiny, with small lateral microtrichose area; lunule shiny black, bare; eye contiguity 8–10 facets long; vertex isosceles, shiny black, except in front of anterior ocellus, covered with microtrichia; vertex with long, pale whitish yellow pile, in some cases mixed with few black pile on the ocellar triangle; ocellar triangle from equilateral to isosceles (see variability); occiput with gray-yellow pile, ventrally covered with a dense, gray microtrichia; eyes covered with dense whitish pile (Fig. 5A, B); ratio of length of vertical triangle: eye contiguity: frons = 3 : 1 : 3.

Thorax. Scutum and scutellum black with bronze luster, covered with dense, erect, usually yellow pile; scutum at wing basis in some specimens and populations with patch of black pile, or with fascia of black pile between wing basis; scutum usually with two or four microtrichose vittae (see variability), anteriorly connected and posteriorly reaching the scutellum (Fig. 2A); anterior half of scutum from dull until shiny black (see variability); posterodorsal part of anterior anepisternum, posterior anepisternum (except anteroventral angle), anterior anepimeron, dorsomedial anepimeron, and posterodorsal and anteroventral parts of katepisternum with long, dense pale yellow pile and grayish microtrichia; wings entirely covered with microtrichia; wing veins brown; calypteres pale yellow; halteres yellow, in some cases with dark capitulum; legs (Fig. 4) without spinae or other protuberances; legs mostly black, except brown tarsi ventrally in some specimens; pile on legs pale yellow, except black pile at apical one third of metafemur in some populations (see variability); metafemur moderately incrassate, ca. three times longer than wide; long pile on postero- and anteroventral surface sparse, and ca. one third to one fourth (see variability) of width of metafemur, approximately the same length as pile on dorsal surface (Fig. 4).

Abdomen. Tapering posteriorly, ca. 1.2 times longer than mesonotum; terga dark brown to black, except for a pair of pale yellow-orange, triangular, lateral maculae on tergum 2 (in some specimens less visible: see variability); terga 3 and 4 each with a pairs of white microtrichose, oblique fasciae (on tergum 2 triangular); color of pile on terga variable, from all yellow to specimens with many black pile on terga 2–4 (see variability) (Fig. 2C, D); sterna dark brown, covered with long whitish yellow pile.

Male genitalia. Apical part of anterior surstyle lobe triangular shape, 1.1–1.4 times longer than wide, covered with dense, short pile (Fig. 1A: al, C, D); posterior surstyle lobe oval with basolateral protrusion (lateral hump) (Fig. 1A, B: bp, 14C: bp); cercus rectangular (Fig. 1A: c); hypandrium sickle-shaped, without lateral projections; lingula large (Fig. 1E: l).

Female. Similar to the male except for normal sexual dimorphism and for the following characteristics: antennae with rounded tip, basoflagellomere ca. two times longer than wide, fossette dorsal (Fig. 3D–F); frons with microtrichose vittae along eye margins variable in shape and size (see variability); frons covered with variable color of pilosity, from mostly gray-yellow until predominately black (see variability) (Fig. 5C, D); ocellar triangle covered with black pile; lateral side of terga, anterior two third of

tergum 2 and all tergum 5 with yellow pile; central part of terga 2–4 with short adpressed black pile; microtrichose fasciae on terga 3 and 4 conspicuous (Fig. 2D).

Variability. There is some intra- and interpopulation variability in the morphological characters of *Merodon serrulatus*, which are summarized in Table 1.

Distribution. As shown in Fig. 7, this *Merodon* taxon is characterized by the greatest range, extending from Iberian Peninsula in the south-west, through Greece and eastern Turkey to the south, and eastward to Siberia and Mongolia (Doczkal pers. comm.).

Ecology. Preferred environment: forest/open ground; thermophilous *Quercus* forest; *Castanea* forest (Ståhls et al. 2009), evergreen oak forest (*Quercus ilex* L. and *Q. suber* L.), dry *Pinus* forest; lentisc scrub; dry, well-vegetated, calcareous and non-calcareous unimproved grassland and tracksides; hedgehog heath (Speight 2018); *Pinus*, *Picea,* and *Larix* forests (Siberia) (Fig. 35B). Flowers visited: Umbelliferae; *Cirsium* spp., *Helianthemum* spp., *Potentilla* spp., *Rosa* spp., *Thapsia* spp., and *Thymus* spp. (Speight 2018). Flight period: April-August.

Type material. Holotype of *Merodon serrulatus* [original designation in Meigen (1822: 360)]: Wiedemann in Meigen (1822) as *Lampetia serrulata*: "Portugal / Hoffmannsegg S." 1 ♀, (ZHMB) (studied).

Merodon alexeji: Described by Paramonov (1925) based on two specimens (male and female). Lectotype [designated by Marcos-García et al. (2007)]: male, "*Merodon* / *alexeji n. sp.* / Typus / Paramonov d.", "Kohanovka / Baltsk. u. / Odes. g. [in Cyrillic] 1.VI.24. Ucraina" (PC) (SIZK) (studied).

Merodon lusitanicus: Holotype [original designation by Hurkmans (1993: 181)]: female, "Portugal, Algarve, Quarteira 27.iv.1985, J.A.W. Lucas" (NBCN) (studied). Paratypes. Portugal • 1 ♀; Algarve, Quarteira; 37°03'29"N, 8°04'47"W; 27 Apr. 1985; NBCN • 1 ♀; Algarve, Vilamoura; 37°04'35"N, 8°07'46"W; 27 Apr. 1985; NBCN.

Merodon tener: Described by Sack (1913: 443) based on three male and three female syntypes. Lectotype [designated by Hurkmans (1993)]: female "Sarepta [= Krasnoarmeysk near Volgograd, after Peck 1988] / *M. tener* Sack det. Sack / coll. Lichtwardt / coll. D. E. I. Eberswalde" (ZHMB) (studied). Original label: "LECTOTYPE of / M. tener Sack / des. 1988 Hurkmans" [red label handwritten], "Sarepta" [yellow label handwritten], "M. tener Sack / ♀ det. Sack" [label partly handwritten], "Coll. DEI / Eberswalde", "Coll. Lichtwardt". (See Supplementary file 6: Figure 6A). Lectotype is conspecific with type of *M. serrulatus*, sharing the same morphological characters.

Other material. Croatia • 1 ♀; Velebit, Brušane; 44°29'55"N, 15°16'43"E; 600 m a.s.l.; 13 Jun. 1969; NBCN 02489.

France • 1 ♀; Languedoc-Roussillon, Corbieres, Carcassonne; 43°13'00"N, 2°21'00"E; 18 Jun. 1974; NBCN • 1 ♂; Provence Alpes Cote d'Azur, Saint-Maximin-la-Sainte-Baume; 43°25'23"N, 5°50'11"E; 17–20 Jun. 1951; M. Bequaert leg.; NBCN 02491 • 1 ♀; same data as for preceding; NBCN 02492 • 1 ♀; Source du Lez, Saint Clement; 43°43'05"N, 3°50'39"E; 24 May 1989; Maldes leg.; MNHN 22629 • 1 ♂; Provence Alpes Cote d'Azur, Montagne du Luberon, W from Bonnieux; 43°48'00"N, 5°22'00"E; 3 Jun. 1993; NBCN • 1 ♀; Feuilla, Route de Treilles, en face du village Panais;

43°53'53"N, 2°00'16"E; 7 Jun. 1988; J. Hamon leg.; MNHN 17973 • 3 ♂♂; Departement du Gard, Mas Mejean; 44°05'24"N, 3°35'26"E; 29 May 1952; NBCN • 2 ♂♂; P. N. Mercantour, Le Bor, on, Umgebung, mesophiles pot. Argent; 44°06'47"N, 7°16'42"E; 1380 m a.s.l.; 21 Jun. 2011; A. Ssymank leg.; A. S. coll. G1057 • 1 ♂; Causse de Sauveterre; 44°22'03"N, 3°13'49"E; 20 Jul. 1971; MNHN 22628 • 1 ♀; Larche (Basses Alpes); 44°26'59"N, 6°50'60"E; 22 Jul. 1925; R. Benoist leg.; MNHN PM0383 • 1 ♂; same data as for preceding; MNHN PM0429 • 1 ♂; same data as for preceding; 3 Jul. 1925; MNHN 22630 • 1 ♂; Provence Alpes Cote d'Azur, Larche; 44°26'59"N, 6°50'60"E; 22 Jul. 1923; NBCN • 1 ♂; Drome, La Chapelle en Vercors; 44°58'12"N, 5°23'39"E; 28 Jun. 1970; Roman Emile leg.; MNHN PM0377 • 2 ♂♂; Isere, Villars de Lans Pic st Michel hill top; 45°05'24"N, 5°37'12"E; 1970 m a.s.l.; 20 Jul. 2010; J. van Steenis leg.; J. v. S. coll. • 1 ♀; L'Arselle; 45°23'10"N, 7°04'19"E; 14 Jun. 1909; MNHN PM0357.

Greece • 2 ♀♀; Mountain Taygetos; 22 km SW Sparta; 36°58'60"N, 22°24'09"E; 6 May 1990; NBCN • 1 ♂; Mountain Taygetos; 37°05'20"N, 22°18'55"E; 950–1800 m a.s.l.; 15–19 May 1990; ZMUC 00513256 • 7 ♂♂; Laconia, Karyes, 25 km N from Sparta; 37°18'15"N, 22°25'16"E; 930 m a.s.l.; 23 May 2014; A. Vujić, J. Ačanski leg.; FSUNS 06535, 06542, 06547, 06549, 06556, 06563, 06560 • 6 ♀♀; Laconia, Karyes, 25 km N from Sparta; 37°18'15"N, 22°25'16"E; 930 m a.s.l.; 23 May 2014; A. Vujić, J. Ačanski leg.; FSUNS 06543, 06544, 06546, 06553, 06555, 06565 • 3 ♂♂; Chelmos, Kalavryta ski center; 38°00'25"N, 22°11'40"E; 6 Jun. 2017; A. Vujić, Z. Nedeljković, L. Likov, M. Miličić, T. Tot, leg.; FSUNS 15980 to 15982 • 2 ♀♀; Chelmos, Kalavryta ski center; 38°00'25"N, 22°11'40"E; 6 Jun. 2017; A. Vujić, Z. Nedeljković, L. Likov, M. Miličić, T. Tot leg.; FSUNS 15983, 15984 • 1 ♂; Achaia, Mountain Chelmos above Kalavryta; 38°00'31"N, 22°07'08"E; 1700 m a.s.l.; 17–19 Jun. 1982; B. Skule, S. Langemark leg.; ZMUC 00513264 • 3 ♀♀; Achaia, Mountain Chelmos above Kalavryta; 38°00'31"N, 22°07'08"E; 1700 m a.s.l.; 17–19 Jun. 1982; B. Skule, S. Langemark leg.; ZMUC 00513265, 00513273, 00513301 • 2 ♂♂; Corfu; 39°40'00"N, 19°45'00"E; NHMW 02485, 02486 • 2 ♂♂; Corfu; 39°40'00"N, 19°45'00"E; 1400 m a.s.l.; NHMW • 1 ♀; Peristeri mountain; 39°40'36"N, 21°07'06"E; 2030 m a.s.l.; 24–28 May 1994; V. Michelsen leg.; ZMUC 00513259; • 1 ♂; 15 km NO Metsovo; 39°47'19"N, 21°11'58"E; 4 Jun. 1994; M. Ohl leg.; ZHMB • 4 ♂♂; Mountain Pindos, Katara Pass; 39°47'46"N, 21°13'44"E; 20 May 1997; S. Radenković leg.; FSUNS • 3 ♂♂; same data as for preceding; S. Šimić leg.; FSUNS • 4 ♀♀; same data as for preceding; A. Vujić leg.; FSUNS • 6 ♂♂; Mountain Pindos, Katara Pass; 39°47'48"N, 21°13'45"E; 1700 m a.s.l.; 20 May 1997; FSUNS 01779, 01781 to 01785 • 3 ♀♀; same data as for preceding; FSUNS 01786, 01787, 01780 • 1 ♀; Mountain Pindos, Katara Pass; 39°54'00"N, 21°11'00"E; 13 Jul. 1979; M. C. D Day, G. R. Else, D. Morgan leg.; NHMUK • 1 ♂; Mountain Pindos, "Iznad Panagije" [Panagia]; 39°48'25"N, 21°19'44"E; 850 m a.s.l.; 15 May 2011; A. Vujić leg.; FSUNS H38 • 15 ♂♂; Mountain Olympos, Litochoras-Prionia 3, "proplanak pored puta"; 40°04'36"N, 22°00'46"E; 17 May 2012; A. Vujić leg.; FSUNS H82, H83, H86 to H90, H92, H93, H95 to H97, H99, I6, I7 • 1 ♂; Mountain Olympos, Litochoras-Prionia 3, "proplanak pored puta"; 40°04'36"N, 22°00'46"E; 17

May 2012; FSUNS H94 • 1 ♂; Mountain Olympos, Near Litochoro; 40°06'30"N, 22°28'41"E; 21 May 2014; A. Vujić, J. Ačanski leg.; FSUNS 06499 • 1 ♀; Mt Olympos, Litochoro; 40°06'41"N, 22°28'37"E; 650 m a.s.l.; 17 May 2016; A. Vujić, J. Ačanski, M. Miličić, Z. Nedeljković leg.; FSUNS 11679 • 8 ♂♂; Mountain Olympos, Litochoras-Prionia 4; 40°06'43"N, 22°28'08"E; 18 May 2011; A. Vujić leg.; FSUNS I11 to I14, I17, I20 to I22 • 2 ♀♀; same data as for preceding; FSUNS I15, I16.

Italy • 1 ♀; Sicily, Etna, Rifugio Filiciusa; 37°43'14"N, 15°02'51"E; 1400–1500 m a.s.l.; 22–28 Jul. 1961; V. S. van der Goot leg.; NBCN • 1 ♂; Toscana, Florence, Careggi; 43°48'45"N, 11°15'07"E; 19 May 1986; NBCN • 2 ♂♂; Piedmont, Colle di Sestrieres; 44°57'00"N, 6°52'60"E; 1800/2100 m a.s.l.; 23–31 Jul. 1837; Zerny leg.; NHMW.

MONTENEGRO • 1 ♂; Lovćen, Lovćen 1; 42°22'59"N, 18°53'54"E; 17 May 2018; A. Vujić, A. Šebić, M. Ranković leg.; FSUNS 19017 • 1 ♂; Boka Kotorska, Morinj; 42°29'25"N, 18°38'56"E; 16–18 May 1998; FSUNS 03600 • 1 ♂; same data as for preceding; 18–19 May 1998; FSUNS 03601 • 2 ♀♀; same data as for preceding; FSUNS 03602, 03603.

Kazakhstan • 1 ♀; East Kazakhstan, Markakol' District, 20 km N settlement Alekseevka, Souther slop of Matobaj Mountain range; 48°42'22"N, 85°57'00"E; 2318 m a.s.l.; 6 Jul. 1996; V. Zinchenko leg.; SZMN • 1 ♀; Kazakhstan, 9 km S settlement Karaoj, Kyzyl-Tass Mountain; 29 Jun. 1996; V. Zinchenko leg.; SZMN.

NORTH MACEDONIA • 1 ♂; Kožuf, Golema poljana; 41°10'54"N, 22°12'05"E; 15 Jun. 1955; FSUNS 00165 • 1 ♂; same data as for preceding; 18 Jun. 1956; FSUNS 00166 • 5 ♂♂; Kožuf, Golema poljana; 41°10'54"N, 22°12'05"E; 14 Jun. 1975; FSUNS 00154, 00156 to 00158, 00162 • 1 ♀; Kožuf, Golema poljana; 41°10'54"N, 22°12'05"E; 15 Jun. 1968; FSUNS 00167 • 2 ♀♀; same data as for preceding; 17 Jun. 1956; FSUNS 00168, 00169 • 6 ♀♀; Kožuf, Golema poljana; 41°10'54"N, 22°12'05"E; 14 Jun. 1975; FSUNS 00155, 00159 to 00161, 00163, 00164 • 2 ♀♀; Kožuf; 41°25'38"N, 21°30'45"E; 14 Jun. 1975; FSUNS 00152, 00153.

Russia • 1 ♂; Sarepta, "Russia, RUS, Sarepta, now a suburb of Volgograd city (Christoph)"; 48°31'40"N, 44°29'01"E; ZHMB 02501 • 4 ♀♀; same data as for preceding; ZHMB 02500, 02502, 02508, 02509 • 32 ♂♂; Altai, 10 km S-W of Katanda; 50°06'51"N, 86°07'21"E; 6 Jul. 1983; A. Barkalov leg.; SZMN • 9 ♀♀; same data as for preceding; SZMN • 1 ♂; SW Altai, Katun valley 10 km W Katanda; 50°09'46"N, 86°06'50"E; 7 Jul. 1983; H. Hippa leg.; MZH • 1 ♂; same data as for preceding; 22–27 Jun. 1983; MZH; "exp. Mikkola, Hippa et Jalava" • 1 ♂; Altai, Kurayskaya Step'; 50°12'00"N, 87°47'60"E; 1662 m a.s.l.; 9 Jul. 2006; A. Barkalov leg.; SZMN • 17 specimens; Altai, Terekta; 50°16'12"N, 85°58'12"E; 1098 m a.s.l.; Jun. 1973; SZMN • 1 ♂; Tuva, Erzin river; 50°19'12"N, 95°30'00"E; 1288 m a.s.l.; 27 Jun.–1. Jul. 1989; D. Logunov leg.; SZMN • 16 ♀♀; same data as for preceding; SZMN • 2 ♂♂; Tuva, Tere Khol' Lake; 50°42'11"N, 97°20'2"E; 27 Jun.–1 Jul. 1989; D. Logunov leg.; SZMN • 1 specimen; Altai, Tuyekta; 50°51'00"N, 85°49'48"E; 944 m a.s.l.; Jun. 1979; SZMN • 2 specimens; Tuva, Chagytay; 50°58'30"N, 94°38'47"E; 1963; SZMN • 1 specimen; Altai, Baragash; 51°16'48"N, 85°12'36"E; 927 m a.s.l.; Jun. 1973; SZMN • 2 ♀♀; Altaj, Erlagol; 51°22'21"N, 86°05'22"E; 27 Jun. 1995; FSUNS 00171, 00173 • 3 ♂♂; Altaj, Er-

lagol; 51°22'23"N, 86°05'29"E; 27 Jun. 1995; A. Tepavčević leg.; FSUNS 00170, 00172, 02476 • 1 ♀; same data as for preceding; FSUNS 02477 • 1 ♂; Gornyi Altai, Turochaksky r-n kordon Obogo; 51°35'47"N, 87°05'45"E; 950 m a.s.l.; 15 Jun. 2003; D. Kropačeva leg.; SZMN 22631 • 18 ♂♂; Altai mountains, Teletskoye Lake; 51°41'20"N, 87°33'43"E; 23–25 Jun. 2013; A. Vujić, S. Radenković leg.; FSUNS NJ56, NJ57, NJ59 to NJ62, NJ64 to NJ71, NJ73 to NJ75, NJ77 • 5 ♀♀; same data as for preceding; FSUNS NJ63, NJ72, NJ76, NJ78, NJ79 • 2 ♂♂; Altai, Turochaksky r-n, Teletskoe Lake, 14 km S of Iogach; 51°42'0"N, 87°17'60"E; 598 m a.s.l.; 27 Jun. 2006; V. Zinchenko leg.; SZMN • 2 ♀♀; same data as for preceding; SZMN • 1 ♀; Mountain Ural, Orenburg; 51°46'12"N, 54°59'53"E; ZHMB 02519 • 15 ♂♂; Siberia, Altaya, Teletskoe Lake; 51°46'60"N, 87°18'00"E; 24–19 Jun. 2006; A. Barkalov, V. Zinchenko leg.; SZMN • 6 ♀♀; same data as for preceding; SZMN • 2 ♂♂; same data as for preceding; 27 Jun. 2006; J. T. Smit leg.; FSUNS 03972, 03973 • 1 ♀; same data as for preceding; 24 Jun. 2006; FSUNS 03974 • 1 ♂; Siberia, Republic Alatai, Teletskoe lake, Artybash.; 51°47'57"N, 87°14'58"E; 25 Jun. 1990; G. Ståhls leg.; MZH • 8 ♂♂; Altai, Teletskoe Lake, Artibash; 51°47'57"N, 87°14'58"E; 12 Jun. 1990; A. Barkalov, Čekanov leg.; SZMN • 1 ♀; same data as for preceding; SZMN • 17 ♂♂; same data as for preceding; 11–25 Jun. 1990; SZMN • 8 ♀♀; same data as for preceding; SZMN • 13 ♂♂; same data as for preceding; 18–20 Jun. 1990; SZMN • 10 ♀♀; same data as for preceding; SZMN • 1 ♀; same data as for preceding; 23 Jul. 1979; SZMN • 82 specimens; same data as for preceding; Jun. 1979; SZMN • 1 ♂; Altaj, Gorno-Altaysk; 51°57'08"N, 85°57'19"E; 21 Jun. 1983; MZH; "exp. Mikkola, Hippa et Jalava" • 152 specimens; Altai, Gorno-Altaysk; 51°57'08"N, 85°57'19"E; Jun.–Jul. 1979; A. Barkalov leg.; SZMN • 2 ♂♂; same data as for preceding; 22 Jun. 1983; SZMN • 3 ♀♀; same data as for preceding; SZMN • 1 ♂; Altai Republic; 52°30'00"N, 83°00'00"E; 25 Jun. 1979; NBCN • 1 ♀; same data as for preceding; NBCN • 2 ♂♂; Sayan Mountains, Abaza; 52°41'17"N, 90°05'27"E; 30 May–11 Jun. 1981; A. Barkalov, T. Varlamova leg.; SZMN • 7 specimens; same data as for preceding; Jun. 1969; SZMN • 2 specimens; Novosibirsk; 55°06'56"N, 82°51'33"E; 1972–1974; SZMN • 1 specimen; Tuva, Sosnovka; 56°18'18"N, 51°14'44"E; 1949; SZMN.

Spain • 1 ♂; Sierra Nevada, second valley; 37°06'10"N, 3°27'19"W; 1430 m a.s.l.; 17 Jun. 2014; A. Vujić, S. Radenković, C. Pérez-Bañón leg.; FSUNS 07410 • 3 ♂♂; Sierra Nevada, Ski Centar Sierra Nevada; 37°06'45"N, 3°25'10"W; 2190 m a.s.l.; 16 Jun. 2014; A. Vujić, S. Radenković, C. Pérez-Bañón leg.; FSUNS 07275, 07287, 07302 • 1 ♂; prov. Granada Sierra Nevada ri. Valetta; 37°06'55"N, 3°29'32"W; 1 Jun. 1982; NBCN • 11 ♂♂; Sierra Nevada, First valley; 37°07'40"N, 3°26'44"W; 1630 m a.s.l.; 17 Jun. 2014; A. Vujić, S. Radenković, C. Pérez-Bañón leg.; FSUNS 07325, 07326, 07328, 07338, 07342, 07344, 07358, 07368, 07371, 07373, 07384 • 10 ♀♀; same data as for preceding; FSUNS 07324, 07340, 07341, 07343, 07355, 07375, 07381, 07385, 07392, 07401 • 4 ♂♂; Sierra Nevada, road to hotel Duque; 37°08'17"N 3°25'46"W; 16 Jun. 2014; A. Vujić, S. Radenković, C. Pérez-Bañón leg.; FSUNS 07248, 07251, 07255, 07256 • 3 ♀♀; same data as for preceding; FSUNS 07262, 07263, 07265 • 1 ♂; Sierra Nevada Lugros, Horcajo del Camarate; 37°11'50"N, 3°15'13"W; 1370 m a.s.l.; 18 Jun. 2014; A. Vujić, S. Radenković, C. Pérez-Bañón leg.; FSUNS 07428 • 1 ♂; Andalusia, Sierra de Baza, Prados del Roy; 37°22'33"N, 2°51'06"W; 2000/2100 m

Table 1. Inter- and intrapopulation variability of *Merodon serrulatus*.

Character	Variability (intra- and/or interpopulation)	Intra	Inter
color of antenna	from black to brown	+	-
length of basoflagellomere	1.7–2.2 times as long as wide	+	+ shorter in Balkans populations (1.7–1.9)
position of antennal fossette in male	dorsal to lateral or dorsal and medial (Fig. 3)	+	+ Iberian populations with medial fossette
length of arista	1.0–1.5 times as long as basoflagellomere	-	+ longer in Balkans populations (1.4)
ocellar triangle in male	equilateral or isosceles	+	-
microtrichose vittae on scutum	from 2–4, posterior half dull without microtrichia	+	-
black pile on scutum	few, or fascia of black pile between wing basis, or many black pile on scutum	+	-
color of pile on metafemur in male	all yellowish to whitish or with many black in apical one third	+	+ some Iberian populations with only pale pile
length of pile on metafemur in male	one third to one fifth of width of metafemur	+	+ in eastern populations (southern Russia to Siberia) longer, from one third to one fourth of width of metafemur
color of knees, apex of tibiae and tarsi	from black to brown	+	-
lateral maculae on tergum 2	distinct, indistinct, to almost absent	+	-
pile on terga 3–4 in male	from all pale yellow to many black	+	+ Balkans populations with more black pile
microtrichose vittae on frons in female	from narrow unconnected to broad and connected near ocellar triangle	+	-
color of pile on frons in female	almost all black to mostly whitish	+	-
male genitalia	the shape of surstyle and size of area covered with dense short marginal setulae on anterior surstyle lobe (Figs 1, 6)	+	+ in eastern populations (southern Russia to Siberia) basolateral protrusion less distinct (Fig. 6G)

a.s.l.; 9 Jun. 2003; D. Doczkal leg.; D. D. coll. 04805 • 1 ♀; same data as for preceding; D. D. coll. 04808 • 2 ♂♂; Andalusia, Sierra de Baza, Santa Barbara; 37°23'16"N, 2°50'43"W; 1890 m a.s.l.; 9 Jun. 2003; D. Doczkal leg.; D. D. coll. 04806, 04807 • 1 ♀; La Corte; 37°57'41"N, 6°49'09"W; 28 Apr. 2015; A. Vujić, D. Obreht leg.; FSUNS 09333 • 1 ♂; Alicante, Alcoy-Font Roja; 38°42'00"N, 00°28'00"W; 31 May 1994; P. M. Isidro leg.; FSUNS 02494 • 1 ♀; Valensija, Utiel; 39°34'13"N, 1°11'15"W; 9 May 1994; C. Pérez-Bañón leg.; FSUNS 02495 • 1 ♂; Val de Cabras; 40°09'23"N, 2°01'48"W; 10 Jun. 1980; H. G. M. Tenuissen leg.; NBCN • 1 ♂; between Leon and Oviedo, Puerto de Pajares; 43°00'00"N, 5°46'00"W; 12 Jul. 1972; NBCN.

Turkey • 5 ♂♂; "Kop Dağı geçidi" [Kop mountain pass], Bayburt; 40°15'00"N, 40°15'00"E; 16 Jul. 1992; NBCN.

Merodon sophron Hurkmans, 1993

Figs 8D, 9G–I, K, 11G–I

Diagnosis. Medium sized (7.8–9.2 mm), dark species with olive-brown reflection; antennae dark; legs mostly black; body pile predominantly pale, except few black pile

on vertex and scutum; basoflagellomere elongated (1.8 times as long as wide) obviously concave dorsally, arista 1.8 times as long as basoflagellomere (Fig. 11G–I); tergum 2 with pale lateral maculae; metafemur incrassate with medium long pile on ventral surface, length approximately one third of its width (Fig. 8D); male genitalia: posterior surstyle lobe with lateral hump; apical part of anterior surstyle lobe rhomboid; lingula medium size (Fig. 9G–I). Related to *Merodon serrulatus* from which differs in absence of medial fossette (Fig. 11H), present in geographically related Iberian populations of *M. serrulatus* (Fig. 3B), molecular data and distribution (Fig. 7). Related to *M. bequaerti*, but differs by shorter pile on ventral margin of metafemur in both sexes (Fig. 8D), narrower and oval to triangular apical part of anterior surstyle lobe (Fig. 9G), with rounded margin in *M. bequaerti* (Fig. 9A), and light yellow and less dense marginal pile on apical part of anterior surstyle lobe (Fig. 9G, K: al), dark brown and dense in *M. bequaerti* (Fig. 9A: al, J).

Redescription (based on the material from type locality, Middle Atlas, Azrou). **Male.** Head. Antennae black to dark brown; basoflagellomere elongated, ca. 1.8 times as long as wide, and ca. 2.5 times as long as pedicel, concave dorsally with acute apex; fossette dorsolateral; arista dark and thickened at basal one third, covered with dense microtrichia, ca. 1.8 times as long as basoflagellomere (Fig. 11G, H); face and frons black with gray microtrichia, face covered with dense whitish, and frons with yellowish gray pile; oral margin shiny, with small lateral microtrichose area; lunule shiny black, bare; vertex shiny black, except in front of anterior ocellus, covered with microtrichia; vertex isosceles, with long, pale whitish yellow pile, mixed with black pile on the ocellar triangle; ocellar triangle isosceles; eyes covered with dense pile; occiput with gray-yellow pile, ventrally covered with a dense, gray microtrichia; eye contiguity 8–11 facets long; vertical triangle: eye contiguity: frons = 3 : 1 : 3.

Thorax. Scutum and scutellum black with bronze luster, covered with dense, erect, usually yellow pile; sides of scutum at wing basis with patch of black pile or fascia of short black pile and few black pile between wing basis; scutum with two microtrichose vittae, anteriorly connected and posteriorly reaching the scutellum; anterior half of scutum dull; posterodorsal part of anterior anepisternum, posterior anepisternum (except anteroventral angle), anterior anepimeron, dorsomedial anepimeron, and posterodorsal and anteroventral parts of katepisternum with long, dense pale yellow pile and grayish microtrichia; wings entirely covered with microtrichia; wing veins brown; calypteres and halteres pale yellow; legs mostly black, except brown tarsi ventrally in some specimens; pile on legs pale yellow; metafemur moderately incrassate, ca. three times longer than wide; pile on postero- and anteroventral surface medium long, and ca. as one third of width of metafemur, approximately the same length as pile on dorsal surface (Fig. 8D).

Abdomen. Tapering, 1.2 times longer than mesonotum; terga dark, except for a pair of pale yellow-orange, triangular, lateral maculae on tergum 2; terga 3 and 4 each with a pair of white microtrichose and oblique fasciae (on tergum 2 triangular); pile on terga all yellow; sterna dark brown, covered with long whitish yellow pile.

Male genitalia. Apical part of anterior surstyle lobe rhomboid shape, ca. 1.5 times longer than wide, covered with dense, short pile (Fig. 9G, J: al); posterior surstyle lobe

oval with basolateral protrusion (lateral hump) (Fig. 9G, H: bp); hypandrium sickle-shaped, without lateral projections; lingula medium size (Fig. 9I: l).

Female. Similar to the male except for normal sexual dimorphism and for the following characteristics: antennae with rounded tip, basoflagellomere ca. two times longer than wide (Fig. 11I); frons with broad microtrichose vittae along eye margins; frons covered with variable pilosity, from mostly gray-yellow until predominantly black; ocellar triangle covered with black pile; lateral side of terga, anterior two thirds of tergum 2 and all of tergum 5 with yellow pile; terga 2–4 with short adpressed black pile.

Distribution. *Merodon sophron* is distributed in north-western Africa (Morocco) (Fig. 7).

Ecology. Preferred environment: forest/open ground; open areas in evergreen oak maquis, dry *Pinus* forest; unimproved grassland and tracksides (Fig. 35C). Flowers visited: no data. Flight period: May-June.

Type material. Holotype [original designation by Hurkmans (1993: 168)]. Morocco • ♂; Azrou; 33°25'00"N, 5°20'00"W; 29 May 1925; E. Hartert leg.; NHMUK (studied).

Other material. Morocco • 1 ♂; Azrou; 30°40'00"N, 7°30'00"W; 31 May 1953; G. L. Spoek leg.; NBCN • 2 ♂♂; Moyen Atlas, Azrou; 30°40'00"N, 7°30'00"W; 19 Jun. 1928; R. Benoist leg.; MNHN PM0344, PM0350 • 1 ♀; Moyen Atlas, Azrou; 30°40'00"N, 7°30'00"W; 16 Jun. 1928; R. Benoist leg.; MNHN PM0371 • 1 ♀; Middle Atlas, Azrou; 33°24'51"N, 5°11'36"W; 1789 m a.s.l.; 25–26 Jun. 2014; A. Vujić, S. Radenković, J. Ačanski, S. Veselić leg.; FSUNS 07044 • 1 ♂; Moyen Atlas, Azrou; 33°25'48"N, 5°12'36"W; 16 Jun. 1928, R. Benoist leg.; MNHN 22624 • 1 ♂; Middle Atlas, Maknes, Azrou; 33°25'48"N 5°12'36"W; 1800 m a.s.l.; 25 May 1995; C. Kassebeer leg.; FSUNS 02496.

Merodon trianguloculus Vujić, Likov & Radenković sp. nov.

http://zoobank.org/343FE864-04B3-4B5A-BC75-217DDEFA7CDE
Figs 23A–D, 33A–C, 34A–C

Diagnosis. Medium sized (7.5–11.6 mm), dark brown species with characteristic large silver microtrichose fasciae on terga 2–4 in males (Fig. 23C), and silver michrotrichose ornamentation on scutum in both sexes (Fig. 23A, B); basoflagellomere with rounded apex, 1.6–1.8 times longer than wide in male (Fig. 33A, B).

Description. Male. Head. Antennae black to dark brown; basoflagellomere rounded, 1.6–1.8 times as long as wide, and ca. 2.3 times as long as pedicel; large fossette dorsomedial and dorsolateral; arista brown and thickened at basal one third, covered with dense microtrichia, ca. 1.8 times as long as basoflagellomere (Fig. 33A, B); face and frons black with gray microtrichia, face covered with dense whitish gray, and frons with yellowish gray pile; oral margin shiny with microtrichose lateral areas; lunule shiny black, bare; vertex covered with gray microtrichia; vertex isosceles, with long, pale whitish yellow pile mixed with black pile on the ocellar triangle; ocellar triangle equilateral; eyes covered with dense pile; occiput with gray-yellow pile, covered with a dense, gray microtrichia; eye contiguity 8–12 facets long.

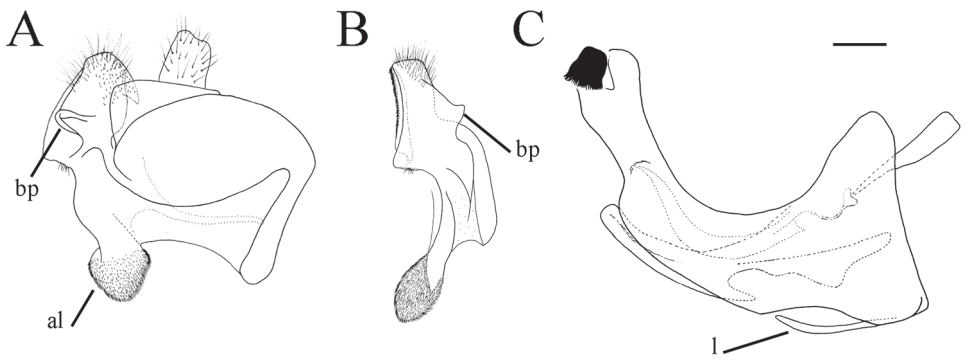

Figure 34. Male genitalia. **A** *Merodon trianguloculus* sp. nov., epandrium, lateral view **B** *Merodon trianguloculus* sp. nov., epandrium, ventral view **C** *Merodon trianguloculus* sp. nov., hypandrium, lateral view. Abbreviations: al–anterior surstyle lobe, bp–basolateral protrusion, l–lingula. Scale bar: 0.2 mm.

Thorax. Scutum and scutellum black with bronze luster, covered with dense, erect, yellow pile; scutum with conspicuous silver microtrichose ornamentation (Fig. 23A); posterodorsal part of anterior anepisternum, posterior anepisternum (except anteroventral angle), anterior anepimeron, dorsomedial anepimeron, and posterodorsal and anteroventral parts of katepisternum with long, pale yellow pile and grayish microtrichia; wings entirely covered with microtrichia; wing veins brown; calypteres and halteres pale yellow; legs mostly black, except yellowish tip of femora, basal and apical part of tibiae and brown tarsi ventrally; pile on legs pale yellow; metafemur moderately incrassate, ca. four times longer than wide; pile on metafemur long, and ca. half to two thirds of width of metafemur.

Abdomen. Tapering, 1.2 times longer than mesonotum; terga dark, with broad silver microtrichose fasciae; tergum 2 with pale orange lateral maculae; pile on terga all yellow (Fig. 23C); sterna dark brown, covered with long whitish yellow pile.

Male genitalia. Apical part of anterior surstyle lobe rhomboid shape, approximately as long as wide, covered with dense, short pile (Fig. 34A: al); posterior surstyle lobe oval with basolateral protrusion (lateral hump) (Fig. 34A, B: bp); hypandrium sickle-shaped, without lateral projections; lingula (Fig. 34C: l).

Female. Similar to the male except for normal sexual dimorphism and for the following characteristics: basoflagellomere ca. 1.8 times longer than wide, fossette dorsolateral (Fig. 33C); frons with microtrichose vittae along eye margins; frons covered with mostly gray-yellow pile mixed with black ones; ocellar triangle covered with black pile; ventral margin of metafemur with sparse pilosity, only individual pile longer; lateral side of terga, anterior two third of tergum 2 and all tergum 5 with whitish pile; terga 2–4 with short adpressed black pile medially; microtrichose fasciae on terga 3 and 4 narrower (Fig. 23D).

Etymology. The name *trianguloculus* derives from the Latin adjective *triangulus* (triangular) and Latin noun *loculus* (spot) and describes the distinctive triangular silver pollinose fasciae on the abdomen.

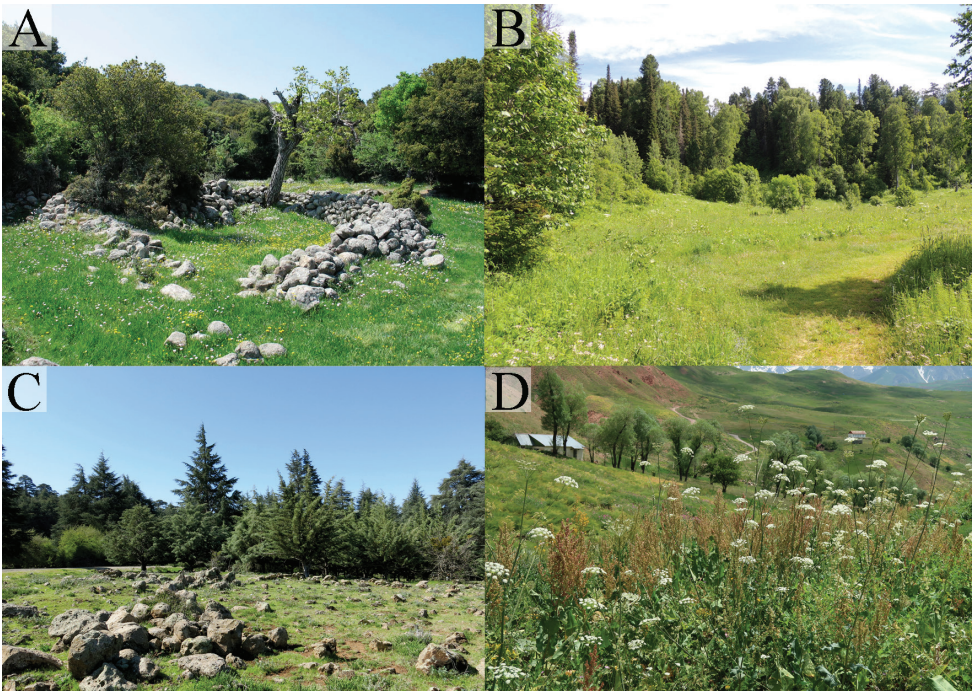

Figure 35. Different types of habitats of *Merodon serrulatus* species group. **A** Lesvos (Greece), habitat of *Merodon opacus* sp. nov., Photograph by Ante Vujić **B** Siberia, Teletskoye Lake (Russia), habitat of *Merodon serrulatus*, Photograph by Jeroen van Steenis **C** Morocco, habitat of *Merodon sophron*, Photograph by Ante Vujić **D** Tajikistan, habitat of *Merodon nigrocapillatus* sp. nov., Photograph by Anatolij Barkalov.

Distribution. *Merodon trianguloculus* sp. nov. was recorded only in Turkmenistan (Fig. 7).

Ecology. Preferred environment: open areas extending to the forest zone; unimproved grassland; adults resting on the stones and in flight between grasses at the top of Dushak Mountain. Flowers visited: no data. Flight period: May-June.

Type material. Holotype. Turkmenistan • ♂; 120 km SW Geok-Tepe town; 38°10'31"N, 57°58'01"E; 11 May 1988; A. Barkalov leg.; SZMN 05818. Original label: "HOLOTYPE of *Merodon* / *trianguloculus* Vujić, Likov / et Radenković sp.n. 2019" [red label], "Туркмения, 120 км / юз Геок–Тепе 11.У. 1988 / Сб.А. Баркалов", "05818" (See Supplementary file 5: Figure 5). **Paratypes.** Turkmenistan • 1 ♀; 15 km k-s pos. Firjuza settlement, Dushak Mountain; 18 May 1988; A. Barkalov leg.; SZMN 05819 • 1 ♀; same data as for preceding; SZMN 05837 • 1 ♀; Centr. Kopetdag g. Dušak; 2100–2300 m a.s.l.; 6 Jun. 1986; Dubatolov leg.; SZMN 05844 • 1 ♂; Firjuza settlement 15 km zap., Dushak Mountain; 16 May 1988; A. Barkalov leg.; SZMN 05816 • 1 ♂; same data as for preceding; 8 May 1987; SZMN 05840 • 1 ♂; 120 km SW Geok-Tepe town; 38°10'31"N, 57°58'01"E; 11 May 1988; A. Barkalov leg.; SZMN 05817.

Merodon trizonus (Szilády, 1940) *nomen dubium*

Remarks. The identity of *Merodon trizonus* remains unclear. The species was described based on two male and two female syntypes labelled "La Calle [el Kala], Algeria" and "Ain Draham, Tunisia", which were not examined. Originally, the syntypes were located in the Hungarian National Museum in Budapest, but the Diptera collection was destroyed by a fire in 1956. The description of Szilády (1940) is incomplete and based on a few differences from the related species *M. hirsutus*. The types of *M. trizonus* are assumed lost and the description is insufficiently accurate to associate name to one of these species. Currently, two species from the *M. serrulatus* species group, to which *M. hirsutus* belongs, occur in northern Africa, namely *M. bequaerti* and *M. sophron*. Therefore, we propose to leave the name *Merodon trizonus* (Szilády, 1940) as *nomen dubium*.

Key to the *Merodon serrulatus* species group

1 Posterior part of mid coxa without long pile (***Merodon avidus-nigritarsis* lineage**) **2**

– Posterior part of mid coxa with long pile ..... **other *Merodon* lineages**[*]

2 Taxa with characteristic basolateral protrusion (lateral hump) on posterior surstyle lobe (as on Figs 1, 6: bp). Species with dark scutum and usually whitish microtrichose fasciae on terga 2–4, at least in females (as on Fig. 15C); tergum 2 usually with a pair of reddish orange lateral maculae; abdomen elongated, usually narrow and tapering, slightly longer than scutum and scutellum together (as on Figs 26, 29); legs mostly black; metafemur incrassate (as on Fig. 4); tarsi black dorsally and dark brown ventrally; antennae usually dark; basoflagellomere usually obviously concave dorsally (as on Figs 11, 12); male genitalia: apical part of anterior surstyle lobe more or less of rhomboid to triangular shape, covered with dense short pile (as on Fig. 1: al); cercus rectangular, without prominences (as on Fig. 14A: c); hypandrium elongated and sickle-shaped (as on Fig. 1); lateral sclerite of aedeagus finger-like with basal thorn-like process (Fig. 1G: s); lingula usually present (as on Fig. 1E: l) (***Merodon serrulatus* group**) **3**

– Species without basolateral protrusion (lateral hump) on posterior surstyle lobe in males and with different combinations of characters in females..... ..**other species groups belonging to the *Merodon avidus-nigritarsis* lineage**[**]

3 Males **4**

– Females **19**

4 Eyes dichoptic (as on Figs 16B, 27A) **5**

– Eyes holoptic (as on Fig. 5B) **6**

[*] not treated here

[**] not treated here

5 Black species with predominantly black body pile, especially on thorax (Fig. 26A, B); terga 2–4 bare or with indistinct microtrichose fasciae (Fig. 26A); distribution: Tajikistan (Fig. 7) ..... ***Merodon nigrocapillatus* sp. nov.**

– Species with olive-brown reflection, predominantly covered with pale yellow pile; terga 2–4 with conspicuous lateral microtrichose fasciae (Fig. 15A); distribution: Kyrgyzstan and Kazakhstan (Fig. 7) ***.Merodon disjunctus* sp. nov.**

6 Bluish species (Fig. 29A) with dark macula on the medial part of the wing (Fig. 29C) and whitish pale body pile; distribution: Uzbekistan (Fig. 7) .... ***Merodon nigropunctum* sp. nov.**

– Dark brown species without dark macula on wings..... **7**

7 Tergum 2 entirely dark brown to black (as on Fig. 21A) **8**

– Tergum 2 with yellow-orange lateral maculae (at least small ones) (as on Fig. 23E) **10**

8 Scutum without black pile, except few black setae at wing basis in some specimens; terga 2–4 with a conspicuous microtrichose fasciae (as on Fig. 21A)... **9**

– Scutum with black pile, at least on fascia between wing basis; terga 2–4 with a less conspicuous microtrichose fasciae (as on Fig. 2A) .... ***Merodon serrulatus* (Wiedemann in Meigen, 1822) (part)**

9 Dorsolateral pile on metafemur dense and longer (Fig. 13C); terga with longer and erect pile (Fig. 21F); tergum 2 shiny; posterior surstyle lobe with big lateral hump, clearly visible in ventral view (Fig. 14E, F: bp); distribution: Syria, Israel and south-eastern Turkey (Fig. 7)..... ***Merodon hirsutus* Sack, 1913**

– Dorsolateral pile on metafemur shorter (Fig. 13A); terga with shorter pile, adpressed at tergum 4 (Fig. 21C); tergum 2 dull; posterior surstyle lobe with small lateral hump, less distinct in ventral view (Fig. 14H, I: bp); distribution: Lesvos Island (Greece) and western Turkey (Fig. 7)..... ..... ***Merodon opacus* sp. nov.**

10 Terga 3 and 4 with a pair of broad silver microtrichose maculae (Fig. 23C); scutum with characteristic silver microtrichose ornamentation (Fig. 23A); distribution: Turkmenistan (Fig. 7)..... ***Merodon triangulocullus* sp. nov.**

– Terga 3 and 4 without or with a less conspicuous pair of broad silver microtrichose fasciae (as on Fig. 10)..... **11**

11 Terga 3 and 4 without microtrichose fasciae..... **12**

– Terga 3 and 4 with a pair of white microtrichose, oblique fasciae (as on Fig. 23E) **13**

12 Metafemur strongly curved (Fig. 8C); body pile longer, clearly visible on tergum 4 (Fig. 10D); distribution: Iberian Peninsula (Fig. 7)..... ..... ***Merodon sacki* (Paramonov, 1936)**

– Metafemur less curved (Fig. 8A); body pile shorter, clearly visible on tergum 4 (Fig. 10B); distribution: north-west Africa (Fig. 7)..... ..... ***Merodon bequaerti* Hurkmans, 1993 (part)**

13 Antennae reddish yellow; basoflagellomere short and broad, ca. 1.2 times as long as wide, with large dorsal to dorsolateral fossette (Fig. 19E–G); tergum 2 with large reddish yellow lateral maculae (Fig. 23E); tergum 3 laterally reddish or brown; tibiae and tarsi partly reddish brown; metafemur incrassate with long pilosity as long as half of width of metafemur (Fig. 22A); distribution: Japan and China (Fig. 7) ..... ***Merodon kawamurae*** **Matsumura, 1916**

– Antennae dark brown/black; basoflagellomere elongated; legs mostly black **14**

14 Abdomen broad, tergum 2 at least 2.5 times wider than long (as on Fig. 24A); metafemur incrassate and curved (as on Fig. 8C) **15**

– Abdomen narrower, tergum 2 ca. two times wider than long (as on Fig. 2); metafemur less incrassate and with almost straight lateral margin (as on Fig. 4) **16**

15 Pile on ventral margin of metafemur very short (Fig. 22C); distribution: Crete Island (Greece) (Fig. 7) ..... ***Merodon medium*** **sp. nov.**

– Pile on ventral margin of metafemur long and dense (Fig. 8A); distribution: north-west Africa (Fig. 7)..... ***Merodon bequaerti*** **Hurkmans, 1993 (part)**

16 Male genitalia: basolateral protrusion (lateral hump) on posterior surstyle lobe reduced (Fig. 14A: bp); distribution: western Turkey (Fig. 7) ..... ***Merodon defectus*** **sp. nov.**

– Male genitalia: basolateral protrusion (lateral hump) on posterior surstyle lobe well developed (as on Fig. 1, 6: bp), visible at least from ventral view (Fig. 14C: bp) **17**

17 Medial fossette absent (as on Fig. 11H) **18**

– Medial fossette present (Fig. 3B) ..... ***Merodon serrulatus*** **(Wiedemann in Meigen, 1822)**[*]

18 GenBank acc. no. MN623564-MN623581; distribution: Palaearctic, extending from France in the west to Turkey in the south-east, and to Siberia toward north-east (Fig. 7) ..... ***Merodon serrulatus*** **(Wiedemann in Meigen, 1822) (part)**

– GenBank acc. no. MN623540; distribution: north-west Africa (Fig. 7) ..... ***Merodon sophron*** **Hurkmans, 1993**

19 Tergum 2 dark (as on Fig. 26C, D) ..... **20**[**]

– Tergum 2 with reddish lateral maculae (as on Fig. 23F) **22**

20 Black species (Fig. 26C, D); body covered with predominantly black pilosity, especially on thorax; distribution: Tajikistan (Fig. 7) ..... ***Merodon nigrocapillatus*** **sp. nov.**

– Species with olive-brown reflection, predominantly covered with pale pile **21**

21 Pile on dorsolateral margin of metafemur long (Fig. 13D); distribution: Syria and south-east Turkey (Fig. 7)..... ***Merodon hirsutus*** **Sack, 1913**

– Pile on dorsolateral margin of metafemur short (Fig. 13B); distribution: Lesvos Island (Greece) and western Turkey (Fig. 7) .... ***Merodon opacus*** **sp. nov.**

---

[*] part: Iberian populations

[**] unknown female of *Merodon nigropunctum* sp. nov. probably keys out here

22 Metafemur with long pile on the entire surface of ventral margin (as on 22B) (unknown female of *Merodon sacki* (Paramonov 1936), probably keys out here) **23**

– Metafemur with mostly short pile on ventral margin (as on Fig. 4C) **27**

23 Scutum with characteristic silver microtrichose ornamentation (Fig. 23B); terga 3 and 4 with broad lateral microtrichose fasciae; distribution: Turkmenistan (Fig. 7)..... ***Merodon triangulocullus* sp. nov.**

– Scutum with indistinct microtrichose vittae; terga 3 and 4 with narrower lateral microtrichose fasciae..... **24**

24 Scutum at wing basis with only yellowish pilosity; metafemur with long, dense dorsal pile (as on Fig. 22B)..... **25**

– Scutum at wing basis with short black pile; metafemur with sparse dorsal pile (as on Fig. 8B) **26**

25 Blackish species; terga 3 and 4 with broad lateral microtrichose fasciae; basoflagellomere dark brown to black; distribution: Kyrgyzstan and Kazakhstan (Fig. 7)..... ***Merodon disjunctus* sp. nov.**

– Brownish species; terga 3 and 4 with narrower lateral microtrichose fasciae (Fig. 23F); basoflagellomere yellowish; distribution: Japan and China (Fig. 7)..... ***Merodon kawamurae* Matsumura, 1916**

26 Distribution: north-west Africa (Fig. 7) ..... ***Merodon bequaerti* Hurkmans ,1993**

– Distribution: France ..... ***Merodon serrulatus* (Wiedemann in Meigen, 1822) (part)**

27 Females of these three species can be separated by distribution and genetic data:

– GenBank acc. no. MN623540. Distribution: North-west Africa (Fig. 7) ..... ***Merodon sophron* Hurkmans, 1993**

– GenBank acc. no. MN623564-MN623581. Distribution: Palaearctic, extending from Iberian Peninsula in the west to Turkey in the south-east and toward Siberia in the north-east (Fig. 7)..... ***Merodon serrulatus* (Wiedemann in Meigen, 1822) (part)**

– Distribution: western Turkey (Fig. 7)..... ***Merodon defectus* sp. nov.**

Molecular inference

The final aligned and pruned dataset including two-gene data matrix (COI+28S rRNA) comprised 1,859 nucleotide characters (421 parsimony informative sites) pertaining to 81 specimens (79 in-group specimens of the studied genus *Merodon* lineages along with two outgroups). The final number of aligned sites for COI gene (concatenated 3' and 5' fragments of the gene) included 1,273 nucleotides, while 586 nucleotide characters (with gaps) were included in analyses for the D2–3 region of the 28S rRNA gene.

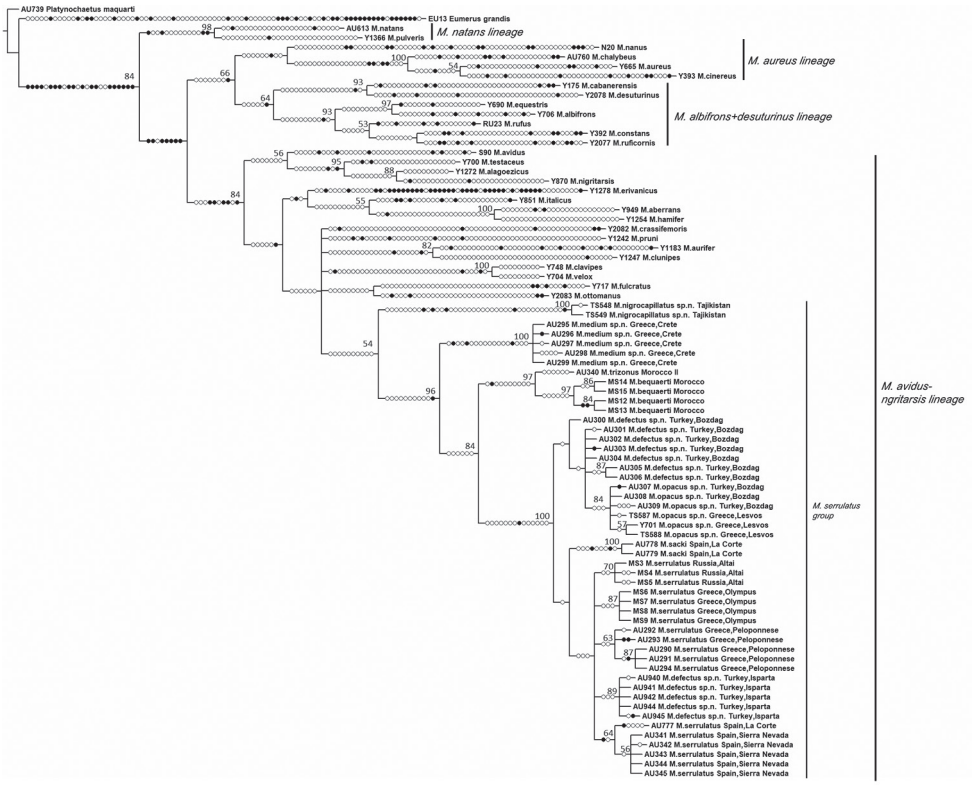

Figure 36. Strict consensus tree of 41 most parsimonious trees from the analysis of combined COI mitochondrial and 28S nuclear genes sequences. Length 2093 steps, Consistency Index (CI) 37, Retention Index (RI) 65. Bootstrap support values are depicted near nodes (≥ 50). Filled circles represent non-homoplasious changes and open circles are homoplasious changes. Four lineages observed in the genus *Merodon*, as well as the *M. serrulatus* group, are marked on the tree.

Both obtained phylogenetic trees (Maximum Parsimony, Fig. 36 and Maximum Likelihood, Supplementary file 7: Figure 7) resolved the four previously described lineages as clades, while the *M. serrulatus* species group was recovered as monophyletic within the *Merodon avidus-nigritarsis* lineage (MP = 54, ML = 75). Within the *serrulatus* species group, specimens belonging to *M. nigrocapillatus* sp. nov., *M. medium* sp. nov., *M. bequaerti* and *M. sacki* were clearly grouped together with high bootstrap support (MP = 100, ML = 100; MP = 100, ML = 100; MP = 97, ML = 94; MP = 100, ML = 100, respectively). The single sequenced specimen of *M. sophron* was resolved as sister taxon of *M. bequaerti*. Unfortunately, although morphologically differentiated, specimens identified as *M. defectus* sp. nov. clustered with *M. serrulatus* in a clade without support, but also with *M. opacus* sp. nov. in another clade without support. These three species together with *M. sacki* were resolved in a group with high support value. High level of inter-population molecular variability within *M. serrulatus* species was also detected.

Discussion

Taxon delimitation and integrative taxonomy

Likov et al. (2019) reported the monophyly of the *Merodon avidus-nigritarsis* lineage. Within this lineage, the *Merodon serrulatus* species group is supported in our phylogenetic analyses.

The *M. serrulatus* species group comprises six already described species (*Merodon bequaerti*, *M. hirsutus*, *M. kawamurae*, *M. sacki*, *M. serrulatus*, and *M. sophron*) and seven new species described here. Based on the present results, six species of this group, namely *M. disjunctus* sp. nov., *M. kawamurae*, *M. medium* sp. nov., *M. nigrocapillatus* sp. nov., *M. nigropunctum* sp. nov., and *M. triangulocculus* sp. nov., are delimited on differences of morphological characters. Moreover, two pairs of very similar species can be separated from other species of the group by some distinct characters, but the distinction between the species in each pair is based on characters with more subtle differences. These two pairs are *M. bequaerti* / *M. sacki*, with the metafemur incrassate and long pile on postero- and anteroventral surface of the metafemur, and *M. hirsutus* / *M. opacus* sp. nov., with tergum 2 dark, without yellow-orange lateral maculae in both sexes.

The remaining three species within the *M. serrulatus* species group are morphologically very similar to each other. *Merodon defectus* sp. nov. has subtle, but stable differences in structures of the male genitalia serving as diagnostic characters (lateral hump on posterior surstyle lobe reduced). Closely related and very similar, *M. serrulatus* and *M. sophron* are distinguished by molecular data, in addition to a clear morphological diagnostic character in males (presence or absence of medial antennal fossette).

Using different methodologies to assess various aspects of the diversity of the genus *Merodon*, previous authors (Mengual et al. 2006; Marcos-García et al. 2007, 2011; Ståhls et al. 2009; Radenković et al. 2011; Vujić et al. 2012, 2013, 2015) have shown the potential of the integrative taxonomy to indicate cryptic taxa, to define new species and to point out different evolutionary lineages. The integration of multiple data sources, combining different molecular (Popović et al. 2014, 2015; Ačanski et al. 2016; Šašić et al. 2016; Kočiš Tubić et al. 2018; Radenković et al. 2018a), morphological (Popović et al. 2015), distributional (Radenković et al. 2018a), and environmental (Popović et al. 2015; Vujić et al. 2015; Šašić et al. 2016) information, has proven to be significant in re-evaluating taxonomic delimitations within the *Merodon* genus. Although results of this integrative approach have not been always congruent (Mengual et al. 2006; Ståhls et al. 2009; Popović et al. 2015; Radenković et al. 2018a).

In the present study we applied this integrative approach, i.e., to combine morphology, genetic data, and distribution, to support the taxonomic status and systematic decisions made for the *M. serrulatus* species group. For example, the species *M. sophron* and *M. serrulatus*, although morphologically similar, are conspicuously separated from each other based on molecular data. The same situation is found between *M. bequaerti* and *M. sacki*. In contrast, the morphologically distinct species *M. defectus* sp. nov., *M. serrulatus*, and *M. opacus* sp. nov. cluster together in the molecular analysis. Discord-

ance between morphological and molecular data has been observed in some previous studies concerning closely related taxa within the family Syrphidae (e.g., Ståhls et al. 2009; Francuski et al. 2014; Haarto and Ståhls 2014), as well as in recently conducted studies on *Merodon* species groups (Likov et al. 2019). In the present study the molecular data for *M. defectus* sp. nov. show some interpopulation differentiation: while the specimens from Bozdag (Turkey) were resolved in the same cluster with *M. opacus* sp. nov., the specimens of *M. defectus* sp. nov. from Isparta (Turkey) and *M. serrulatus* were resolved in another cluster. Unfortunately, these two clades do not have support and the whole cluster, including *M. sacki*, could be resolved in a large polytomy when collapsing nodes without high support. Different molecular profile of different populations of one species was also detected by Likov et al. (2019). The suggested reasons for the low COI divergence between these species are retained polymorphism or mitochondrial introgression between the taxa, as it has been hypothesized in previous studies (e.g., Ståhls et al. 2009; Francuski et al. 2014; Haarto and Ståhls 2014).

It is important to do further taxonomic research with the populations of *Merodon serrulatus* with high inter-population morphological and genetic variability. These populations may be also geographically isolated and are posited to exhibit low genetic flow. The very wide distributional range of *M. serrulatus*, extending from Iberian Peninsula to Mongolia, is highly unusual in the genus *Merodon*, thus exemplifying a complex population structure that might contain evolutionary units at different levels of speciation.

Immature stages

One of the main reasons for the gap in extant knowledge on the immature stages of *Merodon* species is the difficulty of finding specimens in the field, since host plants, the larval food-plants and the breeding and oviposition sites, have not been recorded for the great majority of *Merodon* species (Hurkmans 1993; Rotheray 1993; Speight 2018). The description of the puparium of *Merodon opacus* sp. nov. in this work is based on a single specimen reared from the larva found in the soil near the bulbs of *Fritillaria*, *Gagea*, *Muscari*, and *Ornithogalum*. In extant studies, the immature stages of *Merodon* species were linked to bulbous geophytes, mostly belonging to plant families Asparagaceae (Ricarte et al. 2008; Andrić et al. 2014; Preradović et al. 2018), Iridaceae (Stuckenberg 1956) and Amaryllidaceae (Heiss 1938; Ricarte et al. 2017).

The morphology of the puparium of *M. opacus* sp. nov. shows similarities with the puparium of *M. avidus* in terms of the morphology of the posterior respiratory process (prp) and ornamentation of pupal spiracles (Preradović et al. 2018). In fact, these species share the button-shaped prp and the poorly defined outline of the spiracular plate, whereas the spiracular openings of *M. opacus* sp. nov. are less convoluted than those in *M. avidus*. The pupal spiracles are stout in shape (almost as long as broad) and are clearly shorter than in *M. avidus*, but share the reticulated ornamentation (polygonal pattern).

A single larva of *Merodon opacus* sp. nov. was found in the ground surrounded with bulbs of different plant genera (*Fritillaria*, *Gagea*, *Muscari*, *Ornithogalum*). Recent

larval records suggest that groups of related *Merodon* species could have the same plant genus as a host. These close relationships could be suspected between: *M. constans* species group and *Galanthus* L. (Amaryllidaceae) [Popov and Mishustin (pers. comm) confirmed that eight species of the *constans* species group feed on bulbs of eleven snowdrop species], *M. aureus* species group and *Crocus* L. (Iridaceae) [Speight 2018; Popov pers. comm.], and *M. geniculatus* species group and *Narcissus* L. (Amaryllidaceae) [i.e., *M. eques* (Fabricius, 1805) (see Pehlivan and Akbulut 1991), *M. geniculatus* Strobl, 1909 (see Ricarte et al. 2017), and *M. neofasciatus* Ståhls & Vujić, 2018 (see Vujić et al. 2018)]. Based on these findings, we suggest that the host plant for the members of the *M. serrulatus* species group should be a plant genus present on its large range, extending from North Africa, throughout the entire Palaearctic region to Japan. Two bulb genera with native ranges (WCSP 2019) fitting this distribution, *Gagea* and *Fritillaria* (Liliaceae), might be the larval food-plants. Future research in this field could thus focus on more detailed field work in areas characterized by numerous populations of species from the *M. serrulatus* species group.

Distribution and species diversity

Being distributed from the Iberian Peninsula in the south-west, along the Mediterranean and Balkan Peninsula, through Turkey and southern Russia to Siberia and Mongolia in the north-east, *Merodon serrulatus* is the species of the genus *Merodon* with the largest distributional range. Other species of the *M. serrulatus* species group can be found at the edges of this distributional range, albeit with a much more restricted distribution. For example, *M. sacki* has been found in southern Spain, *M. medium* sp. nov. is endemic to Crete Island, whereas *M. defectus* sp. nov. and *M. opacus* sp. nov. have been recorded in western Turkey, with the latter species also being found on Lesvos Island, and *M. hirsutus* found in south-eastern Turkey, Israel and Syria. The *M. serrulatus* species group includes two North-African species, i.e., *M. sophron* restricted to Morocco, and *M. bequaerti* more widely distributed along the Mediterranean coast of the African continent. Only one species of the group, *M. kawamurae*, is found in the Far East of the Palearctic region, i.e., in central and south-eastern China and Japan. It is worth noting that four of the seven newly described species are distributed in Central Asia, the central and somewhat isolated part of the distribution range of the *M. serrulatus* species group. *Merodon disjunctus* sp. nov. is found in Kyrgyzstan and Kazakhstan, *M. nigrocapillatus* sp. nov. has been collected in Tajikistan, whereas *M. nigropunctum* sp. nov. and *M. triangulocullus* sp. nov. are found in Uzbekistan and Turkmenistan, respectively.

The genus *Merodon* is known to be widespread in regions such as the Mediterranean Basin, with high diversity of geophytes, whereby underground storage organs serve as larval food sources for *Merodon* species (Ricarte et al. 2008, 2017). Such potential for the development of a high diversity of *Merodon* taxa might explain their current geographical distributions (Vujić et al. 2011, 2013). The highest number of *Merodon* species and

the greatest endemicity level in the Mediterranean Basin was noted for the Anatolian region (Vujić et al. 2011), which represents the main center of *Merodon* diversity within the Palaearctic region, along with the Iberian Peninsula (Marcos-García et al. 2007). The high number of endemic species in the eastern Mediterranean Basin has been suggested to be related to the intense orogenic activity favoring isolation and allopatric speciation (Vujić et al. 2011). The biologically diverse Anatolian region, characterized by a rich geological history, comprises of an extensive system of high mountain chains and closed basins, thus providing a wide range of habitats. Throughout history, different parts of this topographically complex area, connecting diverse geographic regions of Asia and Europe, have served not only as natural barriers but also as highly important refugia and corridors providing passages for species spreading (Vujić et al. 2013, 2015).

Central Asia is characterized by many mountains exceeding 6,500 m in elevation, as well as by major desert basins, which have thus far remained understudied. This is particularly the case for the alpine areas, and especially in terms of the invertebrate fauna (CEPF 2017). The very diverse flora of this region harbors a large number of endemics, including many bulbous plants (CEPF 2017) which can support high diversity of *Merodon* taxa, including the four endemic species of the *M. serrulatus* species group described here. Major mountain ranges located in Central Asia represent an extensive zone for faunistic evolution and differentiation, not only ecologically, but also orographically and biogeographically (Mani 1968). Heterogeneous topography with various isolated habitats along altitudinal gradients fosters high rates of speciation, species diversity and endemism. Climatic fluctuations and tectonic processes throughout the complex geological history of this region have contributed to its unique climate and have promoted high levels of floristic diversification and alpine endemism, while also affecting the distributions and structure of many taxa (e.g., Djamali et al. 2012; Zinenko et al. 2015). Having a long history as the crossroads between east and west, this region has historically been subjected to high levels of anthropogenic disturbance that continue to the present day, and populations of many species have declined due to habitat modifications (Djamali et al. 2012; CEPF 2017). The results yielded by the present study confirm previous conclusions emphasizing the importance of such underexplored regions as centers of endemicity, hosting habitats potentially harboring hidden diversity within the genus *Merodon* (Vujić et al. 2019).

Acknowledgments

We thank the curators of the museums listed in the Materials and methods for facilitating visits and loans for the study of specimens in their care. We are also indebted to our professional English language editor for linguistic revision and editing of the manuscript. This work was funded by the Ministry of Education, Science and Technological Development of the Republic of Serbia, Grant Nos. OI173002 and III43002, the Provincial Secretariat for Science and Technological Development (0601-504/3), the H2020 Project "ANTARES" (664387) and the Scientific and Technological Research Council of Turkey (TÜBİTAK, project number: 213O243). The work of A.V.

Barkalov was supported by the Russian Foundation for Basic Research. The authors confirm that no competing interests exist.

Permission to collect biological specimens in protected areas was provided by the competent authorities. The Greek material was collected under a permit issued by Greek Ministry of Environment, Energy and Climate change (130276/1222), in Turkey by TÜBİTAK, and in Spain with permission N. Ref.: ENSN/FJSG/IMJ (232) (Junta de Andalucia, Consejería de Medio Ambiente y Ordenación del Territorio).

Roles of authors: AV, LL, SRad, CPB, AB, RH, GS and SRojo performed the sampling; AV, LL, SRad, NKT and MD conceived and designed the study; AV, LL, SRad, NKT, MD, CPB, SR, AA, GS performed the experimental analysis, while AV, LL, SRad, NKT, MD, AŠ, CPB, AB, RH, SRojo, AA, GS participated in data analyses. All authors took part in draft preparation, contributed to discussions during preparation of the paper, as well as read, commented on, and approved the final version of the manuscript.

References

Ačanski J, Vujić A, Djan M, Obreht-Vidaković D, Ståhls G, Radenković S (2016) Defining species boundaries in the *Merodon avidus* complex (Diptera, Syrphidae) using integrative taxonomy, with the description of a new species. European Journal of Taxonomy 237: 1–25. https://doi.org/10.5852/ejt.2016.237

Andrić A, Šikoparija B, Obreht D, Đan M, Preradović J, Radenković S, Pérez-Bañón C, Vujić A (2014) DNA barcoding applied: identifying the larva of *Merodon avidus* (Diptera: Syrphidae). Acta Entomologica Musei Nationalis Pragae 54(2): 741–757. https://biotaxa.org/AEMNP/article/view/9167/10927

Belshaw R, Lopez-Vaamonde C, Degerli N, Quicke DLJ (2001) Paraphyletic taxa and taxonomic chaining: evaluating the classification of braconine wasps (Hymenoptera: Braconidae) using 28S D2-3 rDNA sequences and morphological characters. Biological Journal of the Linnean Society 73(4): 411–424. https://doi.org/10.1006/bijl.2001.0539

CEPF (2017) Ecosystem Profile: Mountains of Central Asia Biodiversity Hotspot. On behalf of The Critical Ecosystem Partnership Fund (CEPF). https://www.cepf.net/our-work/biodiversity-hotspots/mountains-central-asia [Accessed on 30.03.2019]

Chen H, Rangasamy M, Tan SY, Wang H, Siegfried BD (2010) Evaluation of five methods for total DNA extraction from western corn rootworm beetles. PLoS ONE 5 (8): e11963. https://doi.org/10.1371/journal.pone.0011963

Czerny L, Strobl PG (1909) Spanische Dipteren. III. Verhandlungen der Zoologisch-Botanischen Gesellschaft in Wien 59: 121–301.

Djamali M, Brewer S, Breckle SW, Jackson ST (2012) Climatic determinism in phytogeographic regionalization: A test from the Irano-Turanian region, SW and Central Asia. Flora 207(4): 237–249. https://doi.org/10.1016/j.flora.2012.01.009

Doczkal D, Pape T (2009) *Lyneborgimyia magnifica* gen. et sp. n. (Diptera: Syrphidae) from Tanzania, with a phylogenetic analysis of the Eumerini using new morphological characters. Systematic Entomology 34(3): 559–573. http://dx.doi.org/10.1111/j.1365-3113.2009.00478.x

Fabricius JC (1781) Species insectorum, exhibentes eorum differentias specificas, synonyma auctorum, loca natalia, metamorphosin, adjectis observationibus, descriptionibus. Vol. 1. impensis CE Bohnii, Hamburgi et Kilonii, 494 pp.

Fabricius JC (1805) Systema antliatorum secundum ordines, genera, species, adiectis synonymis, locis, observationibus, descriptionibus. Apud Carolum Reichard, Brunswick, 372 + 30 pp.

Francuski L, Djurakic M, Ludoški J, Hurtado P, Pérez-Bañón C, Ståhls G, Rojo S, Milankov V (2014) Shift in phenotypic variation coupled with rapid loss of genetic diversity in captive populations of *Eristalis tenax* (Diptera: Syrphidae): consequences for rearing and potential commercial use. Journal of Economic Entomology 107: 821–832. https://doi.org/10.1603/EC13243

Folmer O, Black M, Hoeh W, Lutz R, Vrijenhoek R (1994) DNA primers for amplification of mitochondrial cytochrome c oxidase subunit I from diverse metazoan invertebrates. Molecular Marine Biology and Biotechnology 3(5): 294–299. https://www.ncbi.nlm.nih.gov/pubmed/7881515

Goloboff PA (1999) NONA computer program. Version 2.0. Tucuman (Argentina). https://www.softpedia.com/get/Scienece-CAD/NONA.shtml [Accessed on 22.01.2019]

Haarto A, Ståhls G (2014) When mtDNA COI is misleading: congruent signal of ITS2 molecular marker and morphology for North European *Melanostoma* Schiner, 1860 (Diptera, Syrphidae). ZooKeys 431: 93–134. https://doi.org/10.3897/zookeys.431.7207

Hadley A (2006) CombineZ, Version 5. Published by the author. http://www.hadleyweb.pwp.blueyonder.co.uk/CZ5/combinez5.htm [Accessed on 21.11.2006]

Hall TA (1999) BioEdit: a user-friendly biological sequence alignment editor and analysis program for Windows 95/98/ NT. Nucleic Acids Symposium Series 41: 95–98. http://brownlab.mbio.ncsu.edu/JWB/papers/1999Hall1.pdf

Hartley JC (1963) The cephalopharyngeal apparatus of syrphid larvae and its relationship to other Diptera. Proceedings of the Zoological Society of London 141(2): 261–280. https://doi.org/10.1111/j.1469-7998.1963.tb01612.x

Heiss EM (1938) A classification of the larvae and puparia of the Syrphidae of Illinois exclusive of aquatic forms. In: Buchholz JT, Tanner FW, van Cleave HT (Eds) Illinois Biological Monographs Vol. 16(4). The University of Illinois, Urbana, 1–142. https://doi.org/10.5962/bhl.title.50277

Hervé-Basin J (1929) Un nouveau *Lampetia* (*Merodon*) de Chine (Dipt. Syrphidae). Bulletin de la Société Entomologique de France 69: 111–115.

Hurkmans W (1993) A monograph of *Merodon* (Diptera: Syrphidae). Part 1. Tijdschrift Voor Entomologie 136: 147–234.

ICZN [International Commission on Zoological Nomenclature] (1999) International Code of Zoological Nomenclature, Fourth Edition. London: The International Trust for Zoological Nomenclature. https://www.iczn.org/the-code/the-international-code-of-zoological-nomenclature/the-code-online/

Katoh K, Standley DM (2013) MAFFT multiple sequence alignment software version 7: improvements in performance and us-ability. Molecular Biology and Evolution 30(4): 772–780. https://doi.org/10.1093/molbev/mst010

Katoh K, Asimenos G, Toh H (2009) Multiple alignment of DNA sequences with MAFFT. In: Posada D (Ed.) Bioinformatics for DNA Sequence Analysis. Methods in Molecular Biology (Methods and Protocols) Vol. 537. Humana Press, New York, 39–64. https://doi.org/10.1007/978-1-59745-251-9_3

Katoh K, Kuma K, Toh H, Miyata T (2005) MAFFT version 5: improvement in accuracy of multiple sequence alignment. Nucleic Acids Research 33(2): 511–518. https://doi.org/10.1093/nar/gki198

Kočiš Tubić N, Ståhls G, Ačanski J, Djan M, Obreht Vidaković D, Hayat R, Khaghaninia S, Vujić A, Radenković S (2018) An integrative approach in the assessment of species delimitation and structure of the *Merodon nanus* species group (Diptera: Syrphidae). Organisms Diversity & Evolution 18(4): 479–497. https://doi.org/10.1007/s13127-018-0381-7

Kumar S, Stecher G, Tamura K (2016) MEGA7: Molecular Evolutionary Genetics Analysis version 7.0 for bigger datasets. Molecular Biology and Evolution 33(7): 1870–1874. https://doi:10.1093/molbev/msw054

Liepa ZR (1969) Lists of the scientific works and described species of the late Dr. S. J. Paramonov, with locations of types. The Journal of the Entomological Society of Australia (New South Wales) 5: 3–22.

Likov L, Vujić A, Kočiš Tubić N, Đan M, Veličković N, Rojo S, Pérez-Bañón C, Veselić S, Barkalov A, Hayat R, Radenković S (2019) Systematic position and composition of *Merodon nigritarsis* and *M. avidus* groups (Diptera, Syrphidae) with a description of four new species. Contributions to Zoology. https://doi.org/10.1163/18759866-20191414

Loew H (1862) Sechs neue europaische Dipteren. Wiener Entomologische Monatsschrift 6: 294–300

Mani MS (1968) The Alai-Pamirs and the Tien Shan. In: Mani MS (Ed.) Ecology and Biogeography of High Altitude Insects. Series Entomologica Vol. 4. Springer, Dordrecht, 229–274. https://doi.org/10.1007/978-94-017-1339-9_10

Marcos-García MÁ, Vujić A, Mengual X (2007) Revision of Iberian species of the genus *Merodon* (Diptera: Syrphidae). European Journal of Entomology 104(3): 531–572. https://doi.org/10.14411/eje.2007.073

Marcos-García MÁ, Vujić A, Ricarte A, Ståhls G (2011) Towards an integrated taxonomy of the *Merodon equestris* species complex (Diptera: Syrphidae) including description of a new species, with additional data on Iberian *Merodon*. The Canadian Entomologist 143(4): 332–348. https://doi.org/10.4039/n11-013

Matsumura S (1916) Thousand insects of Japan. Additamenta Vol. 2 (Diptera). Keisei-sha, Tokyo, 185–474. [In Japanese]

Meigen JW (1803) Versuch einer neuen Gattungs-Eintheilung der europäischen zweiflügligen Insekten. Magazin für Insektenkunde 2: 259–281.

Meigen JW (1822) Systematische Beschreibung der bekannten europäischen zweiflügeligen Insekten. Dritter Theil. Schulz-Wundermann, Hamm, x + 416 pp.

Mengual X, Ståhls G, Vujić A, Marcos-García MA (2006) Integrative taxonomy of Iberian *Merodon* species (Diptera: Syrphidae). Zootaxa 1377: 1–26. http://www.eje.cz/scripts/viewabstract.php?abstract=1262

Miller MA, Pfeiffer W, Schwartz T (2010) Creating the CIPRES Science Gateway for inference of large phylogenetic trees. In: Proceedings of the Gateway Computing Environments Workshop (GCE), New Orleans, Louisiana (USA), November 2010. Institute of Electrical and Electronics Engineers, Piscataway, New Jersey (USA), 1–8. https://doi.org/10.1109/GCE.2010.5676129

Nedeljković Z, Ačanski J, Đan M, Obreht-Vidaković D, Ricarte A, Vujić A (2015) An integrated approach to delimiting species borders in the genus *Chrysotoxum* Meigen, 1803 (Diptera: Syrphidae), with description of two new species. Contributions to Zoology 84(4): 285–304. https://doi.org/10.1163/18759866-08404002

Nedeljković Z, Ačanski J, Vujić A, Obreht D, Đan M, Ståhls G, Radenković S (2013) Taxonomy of *Chrysotoxum festivum* Linnaeus, 1758 (Diptera: Syrphidae) – an integrative approach. Zoological Journal of the Linnean Society 169(1): 84–102. https://doi.org/10.1111/zoj.12052

Nixon KC (2008) ASADO, version 1.85 TNT-MrBayes Slaver version 2; mxram 200 (vl 5.30). Made available through the author (previously named WinClada, version 1.00.08 (2002). Available from http://www.diversityoflife.org/winclada [Accessed on 22.01.2019]

Paramonov SJ (1925) Zur Kenntnis der Gattung Merodon. Encyclopédie Entomologique (B II) Diptera 2(1): 143–160.

Paramonov SJ (1936) Матерыали до монографп роду *Lampetia* (*Merodon* olim) (Diptera, Syrphidae) (Beitrage zur Monographie der Gattung Lampetia (*Merodon* olim). Syrphidae, Diptera). Збірка наукових праць Зоологічному музей та Институт зоологй и біологй АН УРСР 17: 3–13. [in Ukrainan, with German summary]

Parks DH, Mankowski T, Zangooei S, Porter MS, Armanini DG, Baird DJ, Langille MGI, Beiko RG (2013) GenGIS 2: Geospatial analysis of traditional and genetic biodiversity, with new gradient algorithms and an extensible plugin framework. PLoS ONE 8(7): e69885. https://doi.org/10.1371/journal.pone.0069885

Pehlivan E, Akbulut N (1991) Some investigations on the syrphid species attacking on *Narcissus* in Karaburun (Izmir) and the biology and control measures of *Merodon eques* (F.) (Diptera). Turkish Journal of Agriculture and Forestry 15: 47–81.

Popović D, Djan M, Šašić Lj, Šnjegota D, Obreht D, Vujić A (2014) Usage of Different Molecular Markers in Delimitation of Cryptic Taxa of *Merodon avidus* species complex (Diptera: Syrphidae). Acta Zoologica Bulgarica Suppl. 7: 33–38. http://acta-zoologica-bulgarica.eu/downloads/acta-zoologica-bulgarica/2014/supplement-7-33-38.pdf

Popović D, Ačanski J, Đan M, Obreht D, Vujić A, Radenković S (2015) Sibling species delimitation and nomenclature of the *Merodon avidus* complex (Diptera: Syrphidae). European Journal of Entomology 112(4): 790–809. https://doi.org/10.14411/eje.2015.100

Preradović J, Andrić A, Radenković S, Šašić Zorić Lj, Pérez-Bañón C, Campoy A, Vujić A (2018) Pupal stages of three species of the phytophagous genus *Merodon* Meigen (Diptera: Syrphidae). Zootaxa 4420(2): 229–242. https://doi.org/10.11646/zootaxa.4420.2.5

Radenković S, Vujić A, Ståhls G, Pérez-Bañón C, Rojo S, Petanidou T, Šimić S (2011) Three new cryptic species of the genus *Merodon* Meigen (Diptera: Syrphidae) from the island of Lesvos (Greece). Zootaxa 2735: 35–56. https://www.researchgate.net/publication/229041969

Radenković S, Šašić Zorić Lj, Đan M, Obreht Vidaković D, Ačanski J, Ståhls G, Veličković N, Markov Z, Petanidou T, Kočiš Tubić N, Vujić A (2018a) Cryptic speciation in the

Merodon luteomaculatus complex (Diptera: Syrphidae) from the eastern Mediterranean. Journal of Zoological Systematics and Evolutionary Research 56(2): 170–191. https://doi.org/10.1111/jzs.12193

Radenković S, Veličković N, Ssymank A, Obreht Vidaković D, Djan M, Ståhls G, Veselić S, Vujić A (2018b) Close relatives of Mediterranean endemo-relict hoverflies (Diptera, Syrphidae) in South Africa: Morphological and molecular evidence in the *Merodon melanocerus* subgroup. PLoS ONE 13(7): e0200805. https://doi.org/10.1371/journal.pone.0200805.

Reemer M, Smit JT (2007) Some hoverfly records from Turkey (Diptera, Syrphidae). Volucella 8: 135–146.

Ricarte A, Marcos-García MÁ, Rotheray GE (2008) The early stages and life histories of three *Eumerus* and two *Merodon* species (Diptera: Syrphidae) from the Mediterranean region. Entomologica Fennica 19(3): 129–141. http://www.entomologicafennica.org/Volume19/EF_19_3/1Ricarte.pdf

Ricarte A, Souba-Dols GJ, Hauser M, Marcos-García MÁ (2017) A review of the early stages and host plants of the genera *Eumerus* and *Merodon* (Diptera: Syrphidae), with new data on four species. PLoS ONE 12(12): e0189852. https://doi.org/10.1371/journal.pone.0189852

Ricarte A, Nedeljković Z, Rotheray G, Lyszkowski RM, Hancock EG, Watt K, Hewitt SM, Horsfield D, Wilkinson G (2012) Syrphidae (Diptera) from the Greek island of Lesvos, with description of two new species. Zootaxa 3175: 1–23. http://dx.doi.org/10.11646/zootaxa.3175.1.1

Rodríguez FJLOJ, Oliver JL, Marín A, Medina JR (1990) The general stochastic model of nucleotide substitution. Journal of Theoretical Biology 142(4): 485–501. https://doi.org/10.1016/S0022-5193(05)80104-3

Rotheray GE (1993) Color guide to hoverfly larvae (Diptera, Syrphidae) in Britain and Europe. Dipterist Digest 9: 1–156. http://www.dipteristsforum.org.uk/documents/DD/df_1_9_Colour_Guide_to%20Hoverfly_Larvae.pdf

Rotheray GE, Gilbert FS (1999) Phylogeny of Palaearctic Syrphidae (Diptera): evidence from larval stages. Zoological Journal of the Linnean Society 127(1): 1–112. https://doi.org/10.1006/zjls.1998.0156

Sack P (1913) Die Gattung *Merodon* Meigen (*Lampetia* Meig. olim). Abhandlungen der Senckenbergischen Naturforschenden Gesellschaft 31(4): 427–462.

Šašić Lj, Ačanski J, Vujić A, Ståhls G, Radenković S, Milić D, Obreht-Vidaković D, Đan M (2016) Molecular and morphological inference of three cryptic species within the *Merodon aureus* species group (Diptera: Syrphidae). PLoS ONE 11(8): e0160001. https://doi.org/10.1371/journal.pone.0160001

Schiner IR (1860) Vorlaufiger Commentar zum dipterologischen Theile der 'Fauna Austriaca', mit einer naheren Begrundung der in derselben aufgenommenen neuen Dipteren-Gattungen. II. Wiener Entomologische Monatsschrift 4: 208–216.

Simon C, Frati F, Beckenbach A, Crespi B, Liu H, Flook P (1994) Evolution, weighting, and phylogenetic utility of mitochondrial gene sequences and a compilation of conserved polymerase chain reaction primers. Annals of the Entomological Society of America 87(6): 651–701. https://doi.org/10.1093/aesa/87.6.651

Speight MCD (2018) Species Accounts of European Syrphidae, 2018. Syrph the Net, the Database of European Syrphidae (Diptera) Vol. 103. Syrph the Net publications, Dublin, 302 pp.

Ståhls G, Vujić A, Pérez-Bañón C, Radenković S, Rojo S, Petanidou T (2009) COI barcodes for identification of *Merodon* hoverflies (Diptera, Syrphidae) of Lesvos Island, Greece. Molecular Ecology Resources 9(6): 1431–1438. https://doi.org/10.1111/j.1755-0998.2009.02592.x

Stamatakis A (2014) RAxML version 8: a tool for phylogenetic analysis and post-analysis of large phylogenies. Bioinformatics 30(9): 1312–1313. https://doi.org/10.1093/bioinformatics/btu033

Stuckenberg BR (1956) The immature stages of *Merodon bombiformis* Hull, a potential pest of bulbs in South Africa. Journal of Entomological Society of South Africa 19(2): 219–224. https://journals.co.za/content/JESSA/19/2/AJA00128789_4333

Szilády L (1940) Über Paläarktische Syrphiden. Annales Musei Nationalis Hungarici 33: 34–70.

Thompson FC (1999) A key to the genera of the flower flies (Diptera: Syrphidae) of the Neotropical Region including descriptions of new genera and species and a glossary of taxonomic terms used. Contributions on Entomology, International 3: 321–378.

Thompson JD, Higgins DG, Gibson TJ (1994) Clustal W: improving the sensitivity of progressive multiple sequence alignment through sequence weighting, position-specific gap penalties and weight matrix choice. Nucleic Acids Research 22(22): 4673–4680. https://doi.org/10.1093/nar/22.22.4673

Veselić S, Vujić A, Radenković S (2017) Three new Eastern-Mediterranean endemic species of the *Merodon aureus* group (Diptera: Syrphidae). Zootaxa 4254(4): 401–434. https://doi.org/10.11646/zootaxa.4254.4.1

Vujić A, Marcos-García MÁ, Sarıbıyık S, Ricarte A (2011) New data on the *Merodon* Meigen, 1803 fauna (Diptera: Syrphidae) of Turkey, including description of a new species and changes in the nomenclatural status of several taxa. Annales de la Société entomologique de France (N.S.) 47(1–2): 78–88. https://doi.org/10.1080/00379271.2011.10697699

Vujić A, Radenković S, Likov L, Trifunov S, Nikolić T (2013) Three new species of the *Merodon nigritarsis* group (Diptera: Syrphidae) from the Middle East. Zootaxa 3640(3): 442–464. https://doi.org/10.11646/zootaxa.3640.3.7

Vujić A, Ståhls G, Ačanski J, Rojo S, Pérez-Bañon C, Radenković S (2018) Review of the *Merodon albifasciatus* Macquart species complex (Diptera: Syrphidae): the nomenclatural type located and its provenance discussed. Zootaxa 4374(1): 25–48. http://dx.doi.org/10.11646/zootaxa.4374.1.2

Vujić A, Radenković S, Likov L, Andrić A, Gilasian E, Barkalov A (2019) Two new enigmatic species of the genus *Merodon* Miegen (Diptera: Syrphidae) from the north-eastern Middle East. Zootaxa 4555(2): 187–208. http://dx.doi.org/10.11646/zootaxa.4555.2.2

Vujić A, Radenković S, Ačanski J, Grković A, Taylor M, Senol GS, Hayat R (2015) Revision of the species of the *Merodon nanus* group (Diptera: Syrphidae) including three new species. Zootaxa 4006(3): 439–462. http://dx.doi.org/10.11646/zootaxa.4006.3.2

Vujić A, Radenković S, Ståhls G, Ačanski J, Stefanović A, Veselić S, Andrić A, Hayat R (2012) Systematics and taxonomy of the *ruficornis* group of genus *Merodon* (Diptera: Syrphidae). Systematic Entomology 37(3): 578–602. https://doi.org/10.1111/j.1365-3113.2012.00631.x

WCSP (2019) World Checklist of Selected Plant Families. Facilitated by the Royal Botanic Gardens, Kew. Published on the Internet: http://wcsp.science.kew.org [Accessed on 01.08.2019]

Zinenko O, Stümpel N, Mazanaeva L, Bakiev A, Shiryaev K, Pavlov A, Kotenko T, Kukushkin O, Chikin Y, Duisebayeva T, Nilson G, Orlovm NL, Tuniyev S, Ananjevam NB, Murphy RW, Joger U (2015) Mitochondrial phylogeny shows multiple independent ecological transitions and northern dispersion despite of Pleistocene glaciations in meadow and steppe vipers (*Vipera ursinii* and *Vipera renardi*). Molecular Phylogenetics and Evolution 84: 85–100. https://doi.org/10.1016/j.ympev.2014.12.005

Supplementary material 1

Figure S1

Authors: Ante Vujić, Laura Likov, Snežana Radenković, Nataša Kočiš Tubić, Mihajla Djan, Anja Šebić, Celeste Pérez-Bañón, Anatolij Barkalov, Rüstem Hayat, Santos Rojo, Andrijana Andrić, Gunilla Ståhls

Data type: type specimens' data

Explanation note: **A** *Merodon bequaerti*, holotype and labels **B** *Merodon nigrocapillatus* sp. nov., holotype and labels.

Link: https://doi.org/10.3897/zookeys.909.46838.suppl1

Supplementary material 2

Figure S2

Authors: Ante Vujić, Laura Likov, Snežana Radenković, Nataša Kočiš Tubić, Mihajla Djan, Anja Šebić, Celeste Pérez-Bañón, Anatolij Barkalov, Rüstem Hayat, Santos Rojo, Andrijana Andrić, Gunilla Ståhls

Data type: type specimens' data

Explanation note: **A** *Merodon defectus* sp. nov., holotype and labels **B** *Merodon disjunctus* sp. nov., holotype and labels.

Link: https://doi.org/10.3897/zookeys.909.46838.suppl2

Supplementary material 3

Figure S3. *Merodon medium* sp. nov., holotype and labels

Authors: Ante Vujić, Laura Likov, Snežana Radenković, Nataša Kočiš Tubić, Mihajla Djan, Anja Šebić, Celeste Pérez-Bañón, Anatolij Barkalov, Rüstem Hayat, Santos Rojo, Andrijana Andrić, Gunilla Ståhls

Data type: type specimens' data

Explanation note: *Merodon medium* sp. nov., holotype and labels.

Link: https://doi.org/10.3897/zookeys.909.46838.suppl3

Supplementary material 4

Figure S4

Authors: Ante Vujić, Laura Likov, Snežana Radenković, Nataša Kočiš Tubić, Mihajla Djan, Anja Šebić, Celeste Pérez-Bañón, Anatolij Barkalov, Rüstem Hayat, Santos Rojo, Andrijana Andrić, Gunilla Ståhls

Data type: type specimens' data

Explanation note: **A** *Merodon nigropunctum* sp. nov., holotype and labels **B** *Merodon opacus* sp. nov., holotype and labels

Link: https://doi.org/10.3897/zookeys.909.46838.suppl4

Supplementary material 5

Figure S5. *Merodon triangulocul*us sp. nov., holotype and labels

Authors: Ante Vujić, Laura Likov, Snežana Radenković, Nataša Kočiš Tubić, Mihajla Djan, Anja Šebić, Celeste Pérez-Bañón, Anatolij Barkalov, Rüstem Hayat, Santos Rojo, Andrijana Andrić, Gunilla Ståhls

Data type: type specimens' data

Link: https://doi.org/10.3897/zookeys.909.46838.suppl5

Supplementary material 6

Figure S6

Authors: Ante Vujić, Laura Likov, Snežana Radenković, Nataša Kočiš Tubić, Mihajla Djan, Anja Šebić, Celeste Pérez-Bañón, Anatolij Barkalov, Rüstem Hayat, Santos Rojo, Andrijana Andrić, Gunilla Ståhls

Data type: type specimens' data

Explanation note: **A** *Merodon tener*, lectotype and labels **B** *Merodon sacki*, holotype and labels.

Link: https://doi.org/10.3897/zookeys.909.46838.suppl6

Supplementary material 7

Figure S7

Authors: Ante Vujić, Laura Likov, Snežana Radenković, Nataša Kočiš Tubić, Mihajla Djan, Anja Šebić, Celeste Pérez-Bañón, Anatolij Barkalov, Rüstem Hayat, Santos Rojo, Andrijana Andrić, Gunilla Ståhls

Data type: phylogenetic data

Explanation note: Maximum likelihood tree based on analysis of combined COI mitochondrial and 28S nuclear genes sequences. Bootstrap support values of the main clades of the analysed *Merodon serrulatus* group of species are depicted near nodes (≥ 50).

Link: https://doi.org/10.3897/zookeys.909.46838.suppl7

Supplementary material 8

Table S1. Data for the specimens used in the molecular analysis, including GenBank accession numbers

Authors: Ante Vujić, Laura Likov, Snežana Radenković, Nataša Kočiš Tubić, Mihajla Djan, Anja Šebić, Celeste Pérez-Bañón, Anatolij Barkalov, Rüstem Hayat, Santos Rojo, Andrijana Andrić, Gunilla Ståhls

Data type: molecular specimens' dataset

Link: https://doi.org/10.3897/zookeys.909.46838.suppl8